Chemistry of microbial players in the microcosmos of leaf-cutting ants

Dissertation

for obtaining the degree of Doctor of Natural Sciences

(Dr.rer.nat.)

submitted by

Basanta Dhodary

at the

Faculty of Sciences

Department of Biology

Konstanz, 2020

Date of oral examination: 20.07.2020

1. Referee: Prof. Dr. Dieter Spiteller
2. Referee: Prof. Dr. Bernhard Schink
3. Referee: Prof. Dr. David Schleheck

Table of contents

Summary

Leaf-cutting ants and their symbionts comprise a fascinating example of the diverse interactions between insects and microorganisms. Leaf-cutting ants cultivate their garden fungus *Leucoagaricus gongylophorus* with leaf material. In return, the ants use *L. gongylophorus* as their major food source. However, the ant-cultivated fungus is frequently attacked by filamentous fungi of the genus *Escovopsis* and threats the survival of the whole ant nest. To control *Escovopsis*, the ants clean their garden fungus and make use of antibiotic-producing *Actinomycetes* symbionts.

In my doctoral thesis, I studied the chemical basis of the interactions in the microcosmos of leaf-cutting ants in order to understand in detail how *Escovopsis* attacks and how the ants and their symbionts defend against it.

Toxins from *Escovopsis weberi* and their effect in the nest of leaf-cutting ants

E. weberi produces a variety of shearinine-type indole triterpenoids including two novel derivatives shearinine L and shearinine M. In addition, *E. weberi* produces the polyketides emodin and cycloarthropsone. Emodin and cycloarthropsone are toxic for the garden fungus *L. gongylophorus*. Shearinines did not inhibit *L. gongylophorus* but shearinine L turned out to be avoided by *A. octospinosus* ants in dual choice behavioral assays after a learning phase of 2d. This experiment suggested that shearinine L is either toxic for the ants or the ants recognize that it is bad for their garden fungus.

Upon *E. weberi* infection *L. gongylophorus* releases 3-octanone that induces cleaning behavior of leaf-cutting ants

For leaf-cutting ants, it is crucial to recognize infection by *E. weberi.* Mimicking the infection of *L. gongylophorus* with *E. weberi* on agar plates revealed that *E. weberi* stresses *L. gongylophorus* causing the release of the volatile C-8 oxylipin, 3-octanone. 3-octanone is most likely a lipid peroxidation product of linoleic acid from attacked membrane lipids. Behavioral assays with *A. octospinosus* leaf-cutting ant mini-subcolonies indicated that the ants recognize 3-octanone as they reacted with increased hygiene behavior. Interestingly, 3-octanone has been previously

characterized as an alarm signal of leaf-cutting ants. Thus, *L. gongylophorus* makes use of the same signal molecule as the ants to alarm the ants.

Ammonia from the symbiont *Streptomyces* sp. Av25_4 strongly inhibits *E. weberi* growth

In the last years a variety of higher molecular weight secondary metabolites have been identified from *Actinomycetes* symbionts of leaf-cutting ants that inhibit the growth of the parasite *E. weberi*. *Streptomyces* sp. Av25_4, previously isolated from *Acromyremx volcanus* ants inhibited *E. weberi* over long distances, even with a physical barrier between the cultures by producing antifungal volatiles. Although *Streptomyces* sp. Av25_4 produces antifungal organic volatiles, such as nonanal and benzaldehyde, the key volatile compound to inhibit *E. weberi* turned out to be ammonia. Ammonia comprises a highly efficient antifungal. Because of its simple structure, its biosynthesis is expected to be much less costly as that of complex secondary metabolites. Ammonia causes alkalinisation of the medium that is most likely the reason for the growth inhibition as alkalinisation of the medium by other inorganic bases caused the same growth inhibition.

Antibiotic peptides from *Pseudomonas* sp. Al1 associated with *Atta laevigata*

So far, no secondary metabolites have been characterized from *Atta* leaf-cutting ants. In contrast to *Acromyrmex*, *Atta* ants do not exhibit clearly visible bacterial biofims on their integument. I isolated *Pseudomonas* sp. Al1 from *A. laevigata,* which is in line with previous findings of *Pseudomonas* strains from *Atta* ants. *Pseudomonas* sp. Al1 produced peptides were identified using mass spectrometry, chemical degradation as well as secondary metabolite gene cluster analysis of its sequenced genome. The peptides were cyclic lipopeptides: WLIP (white line-inducing principle), massetolide H, massetolide E, and the siderophore: pyoverdine Pf 1547. For pyoverdine Pf 1547 that has been previously identified from a *Pseudomonas* strain collected from Thailand, I identified the so far lacking stereochemistry of the amino acids in the peptide chain. In addition, I identified the pyoverdine Pf 1547 gene cluster. Future experiments are

needed to characterize the ecological role of the identified peptides in the context of *Atta* leaf-cutting ants.

My findings contribute to reveal the chemistry shaping the complex interactions between the diverse partners in the microcosmos of leaf-cutting ants.

Zusammenfassung

Blattschneiderameisen und ihre Symbionten sind ein faszinierendes Beispiel für die vielfältigen Interaktionen zwischen Insekten und Mikroorganismen. Blattschneiderameisen kultivieren den Pilz *Leucoagaricus gongylophorus* mit Blattmaterial. Im Gegenzug ernähren sich die Ameisen von ihrem Futterpilz. Der *L. gongylophorus* kann durch pathogene Pilze der Art *Escovopsis* angegriffen werden und das Überleben des gesamten Ameisennestes bedrohen. Um *Escovopsis* in Schach zu halten, reinigen die Blattschneiderameisen den Futterpilz kontinuierlich und nutzen Antibiotika-produzierende Actinomyceten als Helfer.

In meiner Doktorarbeit habe ich die Chemie der Interaktionen im Mikrokosmos der Blattschneiderameisen studiert, um im Detail zu verstehen, wie *Escovopsis* angreift und wie sich die Ameisen und ihre mikrobiellen Symbionten dagegen zur Wehr setzen.

Toxine von *Escovopsis weberi* und ihre Wirkung im Nest der Blattschneiderameisen

E. weberi produziert eine Reihe von Sekundämetaboliten wie Shearinine (Indoltriterpenoide). Zwei neue Shearinin derivate Shearinine L und Shearinine M konnten identifiziert werden. Außerdem produziert *E. weberi* die Polyketide Emodin und Cycloarthropson. Emodin und Cycloarthropson sind toxisch für *L. gongylophorus*. Die Shearinine zeigten dagegen keine Wirkung gegen *L. gongylophorus*. In Wahlversuchen mit *Acromyrmex octospinosus* Blattschneiderameisen Minisubkolonien mieden die Ameisen Shearinine L nach einer Lernphase von 2 d. Dies legt nahe, dass die Verbindungen entweder giftig für die Ameisen sind oder der Futterpilz den Ameisen signalisiert, Substrat mit Shearinin L nicht in den Pilzgarten zu bringen.

Bei Infektion durch *E. weberi* produziert *L. gongylophorus* 3-Oktanon, welches das Reinigungsverhalten der Blattschneiderameisen induziert

Für Blattschneiderameisen ist es essentiell, die Infektion durch *E. weberi* zu erkennen. Der Befall durch *E. weberi* wurde imitiert, indem L*. gongylophorus* auf PDA Agarplatten mit *E. weberi* infiziert wurde.*L. gongylophorus* reagiert auf den Angriff durch *E. weberi*

mit der Produktion von 3-Octanon, das höchstwahrscheinlich ein Lipid peroxidations produkt der Linolsäure von den geschädigten Lipid membranen darstellt.
Verhaltensversuche mit *A. octospinosus* Blattschneiderameisen Mini-Subkolonien zeigten, dass die Ameisen auf 3-Octanon mit verstärktem Reinigungsverhalten reagieren. Interessanterweise wurde 3-Octanon als Alarmpheromon der Blattschneider-ameisen beschrieben. *L. gongylophorus* nutzt demnach dasselbe Signal wie diese selbst, um die Ameisen zu alarmieren.

Ammoniak vom Symbionten *Streptomyces* sp. Av25_4 hemmt stark das Wachstum von *E. weberi*

In den letzten Jahren wurde eine Reihe von höhermolekularen Sekundärmetaboliten von Actinomyceten-Symbionten von Blattschneiderameisen identifiziert, die das Wachstum von *E. weberi* hemmen. Der Symbiont *Streptomyces* sp. Av25_4, der zuvor von der Blattschneiderameise *A. volcanus* isoliert worden ist, hemmte *E. weberi* auch über große Entfernungen, sogar wenn eine Wand die Agarmedien von *Streptomyces* sp. Av25_4 und *E. weberi* trennte und nur noch Austausch über den Gasraum möglich war. Obwohl *Streptomyces* sp. Av25_4 einige flüchtige organischen Verbindungen wie Dekanal und Benzaldehyd herstellt, die *E. weberi* hemmen können, erwies sich Ammoniak als die entscheidende Verbindung im Duft von *Streptomyces* sp. Av25_4. Ammoniak hemmt das Wachstum von *E. weberi* sehr stark. Mit seiner einfachen Struktur stellt Ammoniak ein effizientes Mittel gegen *E. weberi* dar, das im Vergleich zu komplexen Polyketiden mit wesentlich weniger metabolischen Kosten produziert werden kann. Ammoniak führt zu einem basischen pH im Medium, was höchstwahrscheinlich die Hemmwirkung darstellt, da auch andere anorganische Basen das Wachstum von *E. weberi* vergleichbar hemmten.

Antibiotisch wirksame Peptide vom *Pseudomonas* sp. Al1, einem Symbionten der Blattschneiderameise *Atta laevigata*

Bisher sind noch keine Sekundär metaboliten von *Atta* Blattschneiderameisen identifiziert worden. Im Gegensatz zu *Acromyrmex* haben *Atta* Blattschneiderameisen keine sichtbaren bakteriellen Beläge auf ihrer Kutikula. Ich habe *Pseudomonas* sp. Al1

von *A. laevigata* isoliert. Dies passt zu Versuchen, bei denen Pseudomonaden bei Atta gefunden wurden. Durch Kombination von Massenspektrometrie, Abbaureaktionen, Derivatisierung und Genclusteranalyse konnte ich vom *Pseudomonas* sp. Al1 eine Reihe von Peptiden identifizieren: WLIP(white line-inducing principle), Massetolid H, Massetolid E und das Siderophor Pyoverdin Pf 1547. Beim Pyoverdin Pf 1547, dessen Struktur bereits zuvor von einem Pseudomonaden aus Taiwan aufgeklärt wurde, konnte ich die bisher nicht geklärte Stereochemie der Aminosäuren bestimmen. Außerdem habe ich durch genome mining des Genoms von *Pseudomonas* sp. Al1 den Gencluster für die Biosynthese des Pyoverdin Pf 1547 identifizieren können. Weitere Versuche sind notwendig, um die Funktion der Peptide im Kontext der *Atta* Blattschneiderameisen zu studieren.

Meine Versuchsergebnisse haben dazu beigetragen, wesentlich besser zu verstehen, wie, - durch welche Metaboliten -, die unterschiedlichen Organismen im Mikrokosomos der Blattschneiderameisen mit einander interagieren.

Chapter 1: Introduction

General introduction

In nature there exist several fascinating examples of mutualistic symbiotic interaction between insect and microbes.[1] Leaf-cutting ant is a well-known example of such mutualistic symbiosis, wherein ants grow the fungus as like humans farm the crops for their food. In return, leaf-cutting ants provide plant material as a growth substrate for the fungus and also protect the fungus against parasites and foreign competitors.[2] The fungus garden of leaf-cutting ants is frequently attacked by the specialized fungal parasite of the genus *Escovopsis*.[3] Leaf-cutting ants cultivate *Actinomycetes* symbionts on the integument of their body that produce antibiotics to control infections, e. g. by *Escovopsis*.[4, 5] The details of individual players, - the leaf-cutting ants, the cultivated fungus, *Actinomycetes* symbionts, and pathogens, such as *Escovopsis* -, and their dynamic association in the leaf-cutting ant microcosmos will be discussed in the following chapter.

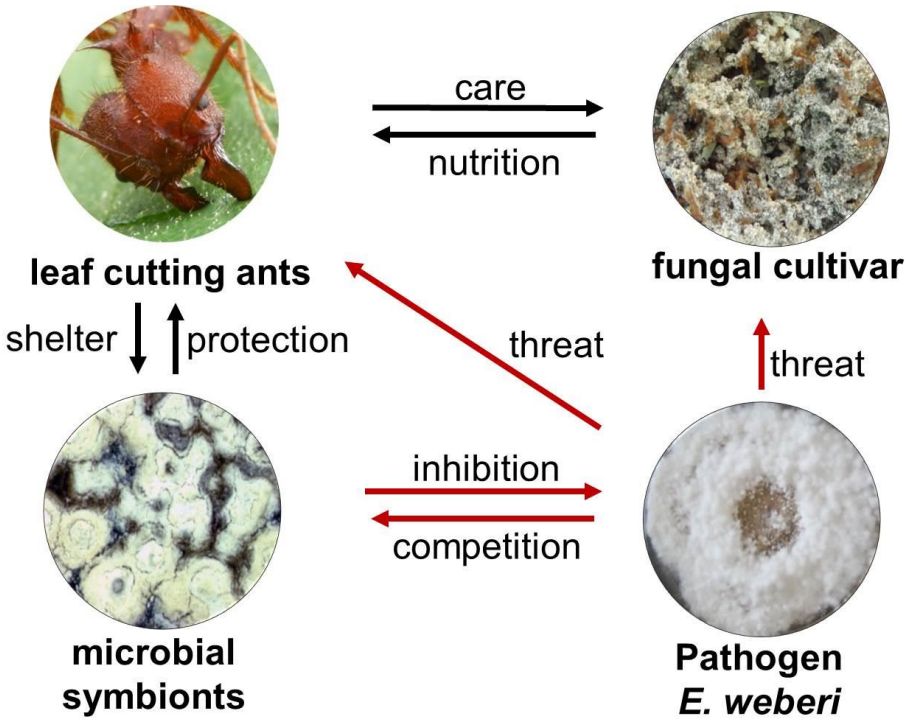

Figure 1.1: Interaction between different partners of the microcosmos of leaf-cutting ants.

Leaf-cutting ants

Ants of the tribe *Attini* (subfamily *Myrmicinae*) comprise 17 genera with more than 270 species, exclusively distributed in tropical South and Central America.[6, 7] Attine ants are cultivating a fungus for more than 50 million years as their primary food source.[8, 9] The primitive genera *Apterostigma, Myrmicocrypta, Mycocepurus, Mycetosoritis, Mycetophylax*, *Cyphomyrmex,* and *Mycetarotes* feed organic detritus to their symbiotic fungus.[10] The most evolved genera of fungus-growing ants, the genera *Atta* and *Acromyrmex*, cut and process the fresh leaves and flowers as main food substrate for their cultivated fungus.[11] *Atta* and *Acromyrmex* as typical leaf-cutting ants use their mandibles to cut plant material and can carry up to twenty times their body weight.[12]

Leaf-cutting ants vary in appearance from orange to brown to red to black. The workers' lengths vary from 0.3 to 1.3 cm whereas the queen is over 2.5 cm long. Like other insects, leaf-cutting ants have three body parts namely head, thorax and abdomen, six jointed legs, a pair of antennae, and a hard outer covering exoskeleton (**Figure 1.2**). The exoskeleton protects against dangers. Spines on the back of the thorax help the workers to carry leaf fragments on their back.[13] *Acromyrmex* ants have four pairs of spines on their relatively rough exoskeletons whereas the closely related *Atta* have three pairs of spines and comparatively smooth exoskeletons.[13]

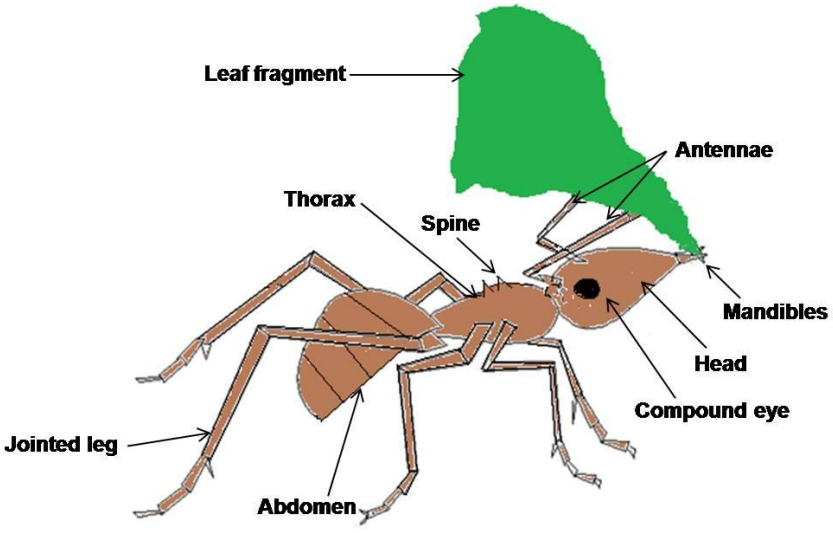

Figure 1.2: Anatomy of a leaf-cutting ant.

Life cycle of leaf-cutting ants

A leaf-cutting ant colony consists of workers of different castes of different body size that fulfill different tasks.The nests of *Atta* and *Acromyrmex* ants show the highest degree of biological polymorphism. Their nests contain four different castes namely majors (also called as soldiers), mediae, minors and minims.[13] Soldiers are protecting the nest from intruders, removing the big debris from foraging trails, and carry heavy material to nest. Mediae act as the general foragers, cut plant material and bring it into the nest. Minors are abundant in the nest and defend the foraging ants against any attack. Minims are the smallest workers and take care of the brood as well as fungus garden. Their head width is less than 1 mm.[13]

Mature nests of leaf-cutting ants produce every year a number of winged females and males. These ants fly off for the nuptial flight. The queens mate with multiple males in order to accumulate 300 million sperms to establish new colonies.[14] The queens lose her wings and begin to dig a nest chamber in order to establish their new colony. Only 2.5% of the young queens manage to establish a long surviving colony. In order to start a new colony the new queen took a piece of the garden fungus in her infrabuccal pocket of her oral cavity.[15]

Mutualistic symbiosis between leaf-cutting ants and their garden fungus

Compared to lower attines, leaf-cutting ants are highly evolved. Leaf-cutting ants develop larger colonies compared to ancestral fungus cultivators, their workers are bigger in size and exhibit a pronounced biological polymorphism. Leaf-cutting ants cultivate their fungus inoculating it with freshly collected leaves, stems, and flowers. Most of the cultivated symbiotic fungi belong to Lepiotaceae.[2]

Fungus gardens of leaf-cutting ants are sponge-like structures from the monoculture of the symbiotic fungus *Leucoagaricus gongylophorus* together with the harvested leaf fragments (**Figure 1.3B**).[16] Unlike free-living *Leucoagaricus*, leaf-cutting ant-associated fungal gardens lack the sexual and asexual reproductive stages because of the continuous pruning of the mycelium by ant workers. However, in absence of ant care, disturbance in the nest by digging, or death of the queen may facilitate the formation of basidiomata.[17] Basidiomata are club-shaped spore producing structures that grow from

the mycelium.[18] The founding of new attine colonies is based on the clonal propagation in which mycelium is periodically sub-cultured from the isolates carried by gardening ants. Moreover, the most derived attine ants have propagated the same lineage for at least 23 million years.[8] In sum, it implies that this symbiotic association promoted the mutual dependency. The fungus in spite of lacking reproductive stages propagates asexually through the ants. In turn, leaf-cutting ants feed on fungus produced swollen starch rich hyphal tips, known as gongylidia.[19] Leaf-cutting ant larvae are exclusively raised on fungal diet however adult ants may also get nutrients from the sap of the collected leaves or from leaves themselves.[18, 20]

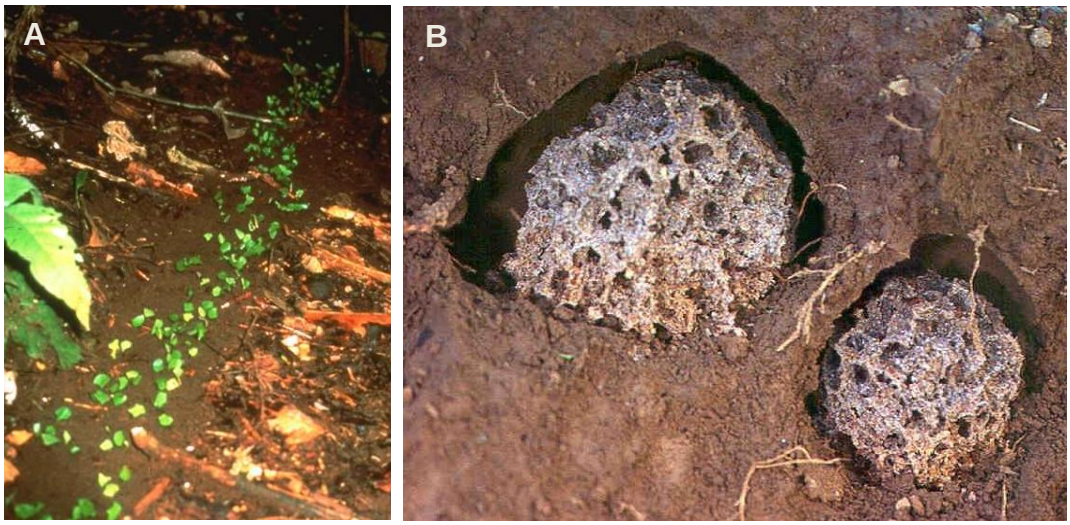

Figure 1.3: A) Leaf-cutting ants foraging leaves in the forest. **B**) Fungus garden cultivated by leaf-cutting ants (Picture credit: Hubert Herz).

Biodegradation of plant materials in fungus garden

Leaf-cutting ants follow several processing steps to convert the collected leaf material into a nutrient rich substrate. In the beginning, the collected leaf fragments are extensively sanitized by a scratching action of the mouthpart. Subsequently, the cleaned leaf fragments are cut into smaller fragments and the edges of each leaf fragment is squeezed by mandibles until they are darker than the center part of the leaf

fragments.[21] Such processed plant material is supplied together with ant fecal droplets into the top strata of the fungus garden.[22] The plant material progressively degrades as it moves into the lower layers of fungus garden. Moreover, on the top layer of the fungus garden, various polymers, plant toxins, and other compounds are degraded from fresh biomass whereas nutrient deficient partially degraded biomass accumulates in the bottom layer of the garden. The latter is removed and disposed as refuse by gardening ants. Thus, continuous biodegradation of plant biomass in a vertical gradient occurs in the fungus garden (**Figure 1.4**).[22]

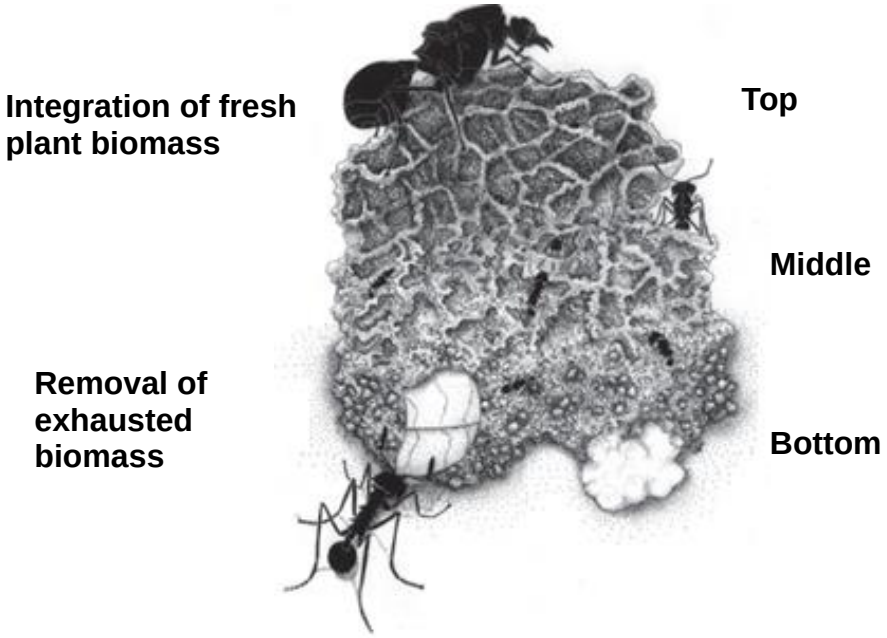

Figure 1.4: Vertical gradient of biodegradation in the fungus garden of leaf-cutting ants. Fresh plant biomass is integrated on the top layer and undergoes progressive degradation (Picture credit: Cara Gibson).

Plant biomass collected by leaf-cutting ants is a large reservoir of recalcitrant polymers which the ants cannot utilize themselves. Leaf-cutting ants make use of their symbiotic fungus to access the nutrients present in the plant material. The fungus has 145

lignocelluloses including several pectinases, amylases, xylanases, and cellulases that enable it to degrade complex polysaccharides such as pectin, xylane and cellulose present in the plant biomass.[22] There is evidence for the vertical distribution of enzymatic activity of fungal xylanases and cellulases in the fungal garden. Their enzymatic activity is highest in the lower layer, modest in the middle, and intermediate in the top newly established strata.[19] In sum, the fungal garden is essential to supply leaf-cutting ants with nutrients in the form of lipids and carbohydrates stored in the hyphal swellings, gongylidia.

Maintainance of the garden fungus by leaf-cutting ants

A drawback of social animals living together in complex communities is easy transmission of diseases between individuals. The accumulation of waste/refuse in the garden is a source of various harmful pathogenic microorganisms and hazardous toxins.[23] Moreover, the extensive foraging behavior of leaf-cutting ants may introduce various foreign microorganisms from the surrounding environment holding the capacity to invade or overgrow the ant cultivated fungus. Particularly, several species of microfungi and yeasts[24-26] as well as bacteria such as gamma proteobacteria[27, 28] have been frequently identified from the fungus garden habitat. Since the fungus garden is the sole source of food for the brood, leaf-cutting ants have to control such co-existing foreign invaders and maintain the purity of the fungus garden.

Therefore, leaf-cutting ants together with their cultivated fungus adapted several prophylactic and defensive measures. Leaf-cutting ants perform efficient waste management in their nests using sanitation behaviour and antimicrobial secretions. What more is the leaf-cutting ant joined alliance with actinomyetes bacteria. Metapleural glands secreted antifungal compounds and antibiotics from symbiotic *Actinomycetes* biofilms acts as the defensive measures.[4, 29]

Waste management

Leaf-cutting ants efficiently remove their waste in order to avoid spreading of pathogens. The nest waste is concentrated and disposed in one or few particular locations at a safe distance from the colony. *Atta* species mostly dispose their waste in

underground refuse chambers or rarely as a single dump heap above ground.[23] The transmission of pathogens between individuals in the nest is prevented by avoiding contact of workers which are involved in waste management with other workers in the nest. Moreover, leaf-cutting ants follow the task partitioning strategy to transport the waste to the refuse chamber.[23] For instance, *Atta* workers transport the waste from the fungus garden and deposit it on a cache outside the dump. Then, the waste is further transported and disposed by specialised dump workers that only work in the refuse chamber.[30] The partitioning of the work depends on the age of the ants. Young leaf-cutting ants work in the fungus garden whereas the older workers stay in the refuse chamber. As a result, the chance of infection is restricted to specific age group and the reproductive center of the colony is majorly protected from harmful pathogens.[23]

Hygienic behaviors

Besides the efficient waste management, leaf-cutting ants perform several other special hygienic behaviors in order to control the introduction of foreign invaders in their colony. The leaf-cutting ants perform licking behavior, in which ants process all the freshly cut plant materials through the filtering infrabuccal pocket in order to remove microbes and harmful debris. This material is later disposed as a pellet in the refuse chamber. Leaf-cutting ants practice fungal grooming to remove alien spores from the fungus garden by using their mouthparts and storing them in their infrabuccal cavity. In addition, leaf-cutting ants weed the fungus garden first loosening the infected pieces of fungal garden using their mandibles and then they remove the suspicious material from the colony.[31] Minor workers from the colony mostly perform the fungus grooming whereas removal of the infected fungus material is exclusively performed by stronger major workers.[32]

Antimicrobial compounds from the metapleural gland

The metapleural glands are located on the posterior lateral end of the metathorax. The metapleural glands continuously secrete a mixture of compounds.[33] The glandular secretions contain plenty of hydroxy acids, like myrmicacin, and indole acetic acid, which inhibit bacterial and fungal growth as well as their spore germination.[29] Moreover, several other compounds including fatty acids and alcohols having a wide range of

antimicrobial properties have been identified from the metapleural glandular secretion.[29, 34] In addition, the acidic nature of the metapleural gland secretion helps to maintain a low pH environment suitable for fungal cultivar whereas unfavorable for spread of other unwanted microbes in the fungus garden.[34] Leaf-cutting ants spread their metapleural gland secretion in the fungus garden as required by the level of harmful microbial burden in the garden.

Antimicrobial compounds from symbiotic *Actinomycetes*

On the integument of many fungus growing ants a naked eye visible whitish-grey crust of filamentous *Actinomycetes* bacteria mostly of genus *Pseudonocardia* and *Streptomyces* exist (**Figure 1.5A**).[4, 5] *Actinomycetes* are common in soil and are most well-known for their invaluable secondary metabolites that often exhibit antibacterial and antifungal properties. Approximately, 55 % of pharmaceutically used antibiotics are derived from *Streptomycetes* strains.[35] The *Actinomycetes* associated with leaf-cutting ant workers can produce diverse antibiotics. *Pseudonocardia* associated with various leaf-cutting ant workers produce antifungal gerumycins (dentigerumycin, gerumycin A-C), polyenes (Nystatin P1, selvamicin), and pseudonocardones (**Figure 1.5B**).[36, 37] *Pseudonocardia* symbionts are transmitted by older workers of the colony to the newly hatched workers within 24 h preserving the mutualistic microbial symbionts between the generations.[38] *Streptomycetes* derived from leaf-cutting ant colonies produce candicidin, antimycins, and valinomycin (**Figure 1.5B**).[39, 40] All those antifungal metabolites inhibit the growth of the most vulnerable and harmful specialized fungal pathogen of leaf-cutting ant microcosmos, namely *Escovopsis* and some other generalized pathogens too. These defensive compounds are vital to protect the fungal garden against different possible infections.

A

B

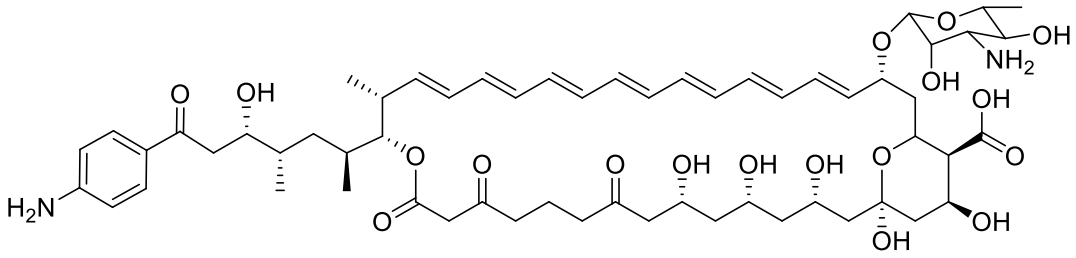

Candicidin D

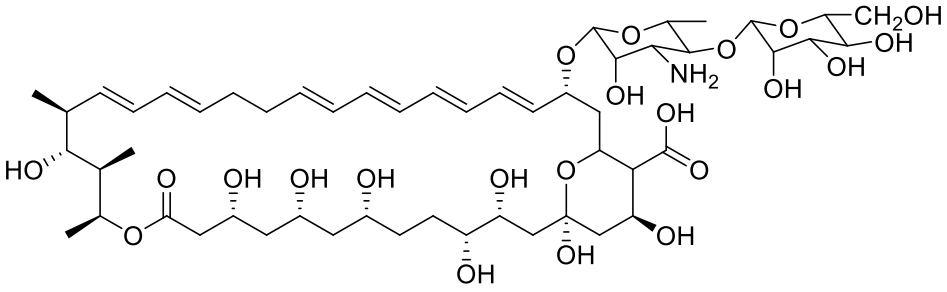

Nystatin P1

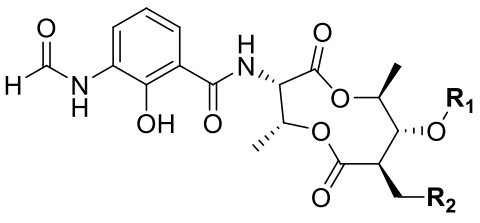

Antimycin A1: $\mathbf{R_1}$ = $COCH(CH_3)CH_2CH_3$ $\mathbf{R_2}$ = $(CH_2)_4CH_3$
Antimycin A2: $\mathbf{R_1}$ = $COCH(CH_3)_2$ $\mathbf{R_2}$ = $(CH_2)_4CH_3$
Antimycin A3: $\mathbf{R_1}$ = $COCH_2CH(CH_3)_2$ $\mathbf{R_2}$ = $(CH_2)_2CH_3$
Antimycin A4: $\mathbf{R_1}$ = $COCH(CH_3)_2$ $\mathbf{R_2}$ = $(CH_2)_2CH_3$

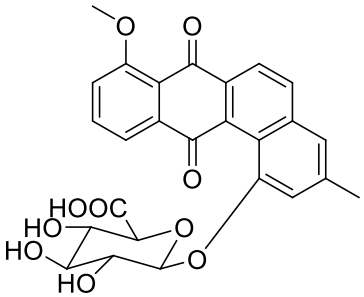

Pseudonocardone B

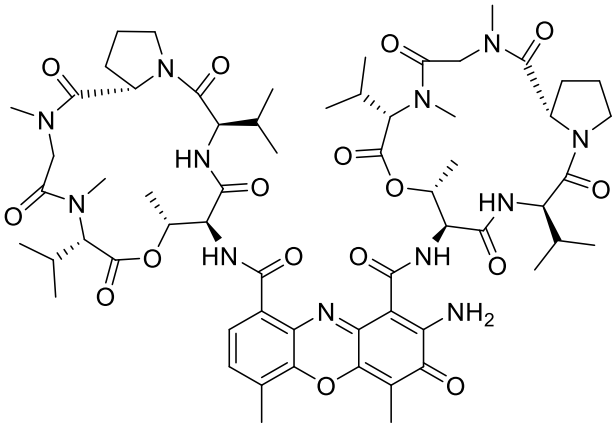

Actinomycin D

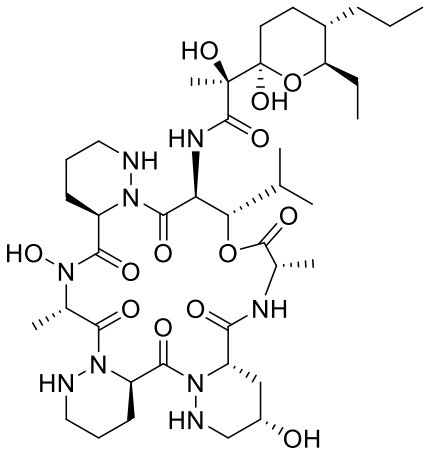

Dentigerumycin

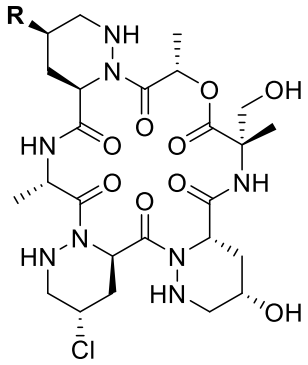

Gerumycin A: **R** = H
Gerumycin C: **R** = OH

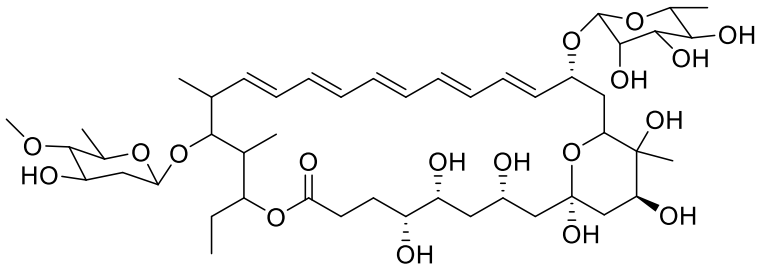

Selvamicin

Figure 1.5: A) *Actinomycetes* biofilm on the integument of a leaf-cutting ant (Picture credit: Dieter Spiteller). **B**) Structures of antimicrobial compounds produced by *Actinomycetes* symbionts associated with leaf-cutting ants.

Microbial parasites in the microcosmos of leaf-cutting ants

In spite of multiple strategies to prevent the spreading of pathogens, the leaf-cutting ant colonies are known to suffer from the infections of a variety of filamentous fungi, yeasts, and bacteria prevalent in the nest. Among the pathogenic microbes, asexual fungi of the genus *Escovopsis* (Ascomycota: Hypocreales) are specialized parasites of the ants' cultivated fungus.[4] *Escovopsis* are known to evolve together with attine ants and their mutualistic fungus.[41] Different species of *Escovopsis* can infect the garden fungus causing detrimental effects on the fungus garden health. Eventually, *Escovopsis* threats the survival of whole ant colonies.[3, 42] Moreover, so far *Escovopsis* was only isolated from leaf-cutting ant associated environment.[11, 43] *Escovopsis* has a reduced genome size as compared to other closer unspecialized fungal relatives due to loss of genes involved in plant material metabolism. However, the genome retains the genes necessary for production of toxins as well as unlocking nutrients present in its natural host, *L. gongylophorus*.[44]

Besides *Escovopsis*, a fungus of genus *Phialophora*, so called black yeast, was detected on the cuticle of leaf-cutting ants together with *Actinomycetes* symbionts. Such black yeasts associated with leaf-cutting ants are known to parasitize the *Pseudonocardia* symbionts by outcompeting them for the nutrients. Consequently, it compromises the defense associated with *Psedonocardia* and makes leaf-cutting ant colonies more vulnerable for *Escovopsis* infection.[45] In addition, the generalist pathogenic fungi like *Fusarium*, *Tricoderma*, and *Syncephalastrum* are also found in the colonies due to foraging behavior of leaf-cutting ants.[46] Those generalist pathogens can also overgrow and destroy the garden fungus.

Motivation and aim of dissertation

Insects comprise the most diverse group of animals in nature. 1-10 % of their body biomass accounts for associated microorganisms.[47] Insects are known to interact with microbes ranging from mutualistic to parasitic relationships. Mutualistic microbial symbionts provide their hosts with essential nutrients, such as amino acids and vitamins or digestive enzymes.[48] As defensive mutualists, microorganisms protect their host against parasites, pathogens and predators.[49] The detailed study of defensive compounds, their ecological function, and their genetic origin allows us to understand the symbiontic relationships in detail. Moreover, the molecular understanding of symbioses may provide novel compounds for drug discovery from little explored sources.

The leaf-cutting ant ecosystem is a unique, complex multiplayer symbiotic system. The understanding of the chemical basis of direct and indirect interactions between the microbial players in the leaf-cutting ant ecological context is necessary to fully decode the complexity of its microcosmos.

In my dissertation I aimed to gain insights into the chemical basis of interactions between *Leucoagaricus gongylophorus* and the pathogen *Escovopsis*. In order to explore that, the compounds produced by *Escovopsis* should be isolated by using different chromatographic techniques and characterized by NMR and mass spectroscopy. The possible role of those compounds in the ants' microenvironment should be evaluated. Moreover, I planned to investigate the possible induction of secondary metabolites during *Escovopsis* infection by *L. gongylophorus* using techniques like LC-MS and SPME-GC-MS. The volatile blends produced by antibiotic producing *Actinomycetes* symbionts will be investigated by GC-MS analysis and their ecological function in the respective ecological context will be addressed. In addition, i should provide further insights into the microbial community associated with *Atta* ants. The microbes associated with *Atta* should be isolated and identified by 16*S* or 18*S* rRNA sequencing. Chemical analysis as well as genome mining approaches should be applied to characterize bioactive compounds produced by microorganisms. Their ecological role should be investigated in bioassays.

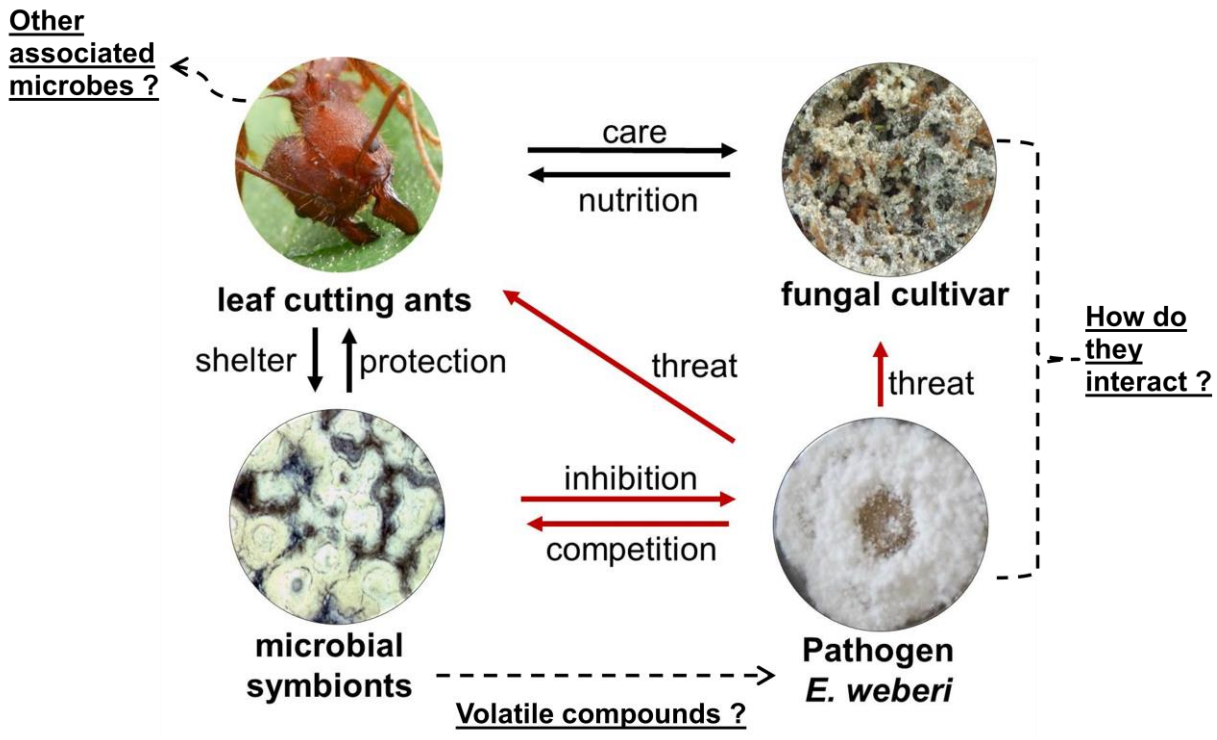

Figure 1.6: Interactions between different partners in the microcosmos of leaf-cutting ants.

Chapter 2: Secondary metabolites from *Escovopsis weberi* and their role in attacking the garden fungus *Leucoagaricus gongylophorus* of leaf-cutting ants

Secondary metabolites from *Escovopsis weberi* and their role in attacking the garden fungus *Leucoagaricus gongylophorus* of leaf-cutting ants

Basanta Dhodary[1], Michele Schilg[2], Rainer Wirth[2], and Dieter Spiteller[1*]

[1]*Chemical Ecology/Biological Chemistry, University of Konstanz, Universitätstrasse 10, D-78457 Konstanz, Germany.*
[2]*Plant Ecology and Systematics, Technical University Kaiserslautern, Erwin-Schrödingerstraße 13,* 67653 Kaiserslautern*, Germany.*

Abstract

The specialized, fungal pathogen *Escovopsis weberi* threatens the mutualistic symbiosis between leaf-cutting ants and their garden fungus (*Leucoagaricus gongylophorus*). Because *E. weberi* can overwhelm *L. gongylophorus* without direct contact, it was suspected to secrete toxins. Using NMR and mass spectrometry, we identified several secondary metabolites produced by *E. weberi*. *E. weberi* produces five shearinine-type indole triterpenoids including two novel derivatives, shearinine L and shearinine M, as well as the polyketides, emodin and cycloarthropsone. Cycloarthropsone and emodin strongly inhibited the growth of the garden fungus *L. gongylophorous* at 0.8 and 0.7 µmol, respectively. Emodin was also active against *Streptomyces* microbial symbionts (0.3 µmol) of leaf-cutting ants. Shearinine L instead did not affect the growth of *L. gongylophorus* in agar diffusion assays. However, in dual choice behavioral assays *Acromyrmex octospinosus* ants clearly avoided substrate treated with shearinine L for the garden fungus after a 2 d learning period, indicating that the ants quickly learn to avoid shearinine L.

Keywords: antibiotics, cycloarthropsone, emodin, natural products, shearinine.

Introduction

Attine ants (subfamily Myrmicinae, tribe Attini) evolved the practice to cultivate the fungus *Leucoagaricus gongylophorus* (Agaricales: Leucocoprineae). Among attine ants, the genera *Acromyrmex* and *Atta* are unique because they provide their fungal symbiont with fresh plant material as growth substrate. In turn the fungus serves the ants as primary food source.[2]

Microbial pathogens from the surrounding soil of the nest and microorganisms brought into the nest because of the foraging behavior[26] of the leaf-cutting ants potentially threaten the garden fungus as well as the leaf-cutting ants' survival.[50] Therefore, leaf-cutting ants control the growth of adverse microbes in their fungus gardens by chemical treatment[51] and weeding behaviour.[31] In addition, antibiotic-producing *Actinomyces* symbionts support leaf-cutting ants in the defense against noxious invaders.[11, 39, 52] Even so, a broad variety of detrimental bacteria, filamentous fungi and yeasts occur in the nests of leaf-cutting ants.[3, 53, 54] In particular, the specialized fungal parasite *Escovopsis* (Ascomycota, Pezizomycotina: anamorphic Hypocreales) attacks the fungus garden of leaf-cutting ants.[3] *Escovopsis* fungi have never been isolated outside of the fungus-growing ants' ecosystem and have been established to have co-evolved in association with fungus growing ants and their cultivated fungi.[11] In comparison to their closest known relatives, *Escovopsis* adapted to the mycoparasitic lifestyle, e.g. by loss of genes coding for plant material degrading enzymes.[44] Moreover, different *Escovopsis* strains can destroy the fungus gardens of *Atta* and *Acromyrmex* leaf-cutting ants.[43, 55]

Reynolds and Currie established in 2004 that *Escovopsis weberi* does not compete for the plant material brought into the nest by the leaf-cutting ants to feed *L. gongylophorus* but it directly consumes the mutualistic fungus.[56] *E. weberi* degrades the hyphae of *L. gongylophorus* before direct physical interaction, suggesting that the pathogen secretes toxins and/or enzymes that can break down host mycelium before contact occurs.[56] The recently sequenced *E. weberi* genome encodes for a variety of secondary metabolite biosynthesis gene clusters.[44] Some of these gene clusters including polyketide synthase gene clusters were significantly up-regulated when growing with *L. gongylophorus*.[44] Moreover, crude extracts of several *Escovopsis* species were reported to inhibit the

growth of *L. gongylophorus*.[57] In a co-cultivation study of *E. weberi* with microbial symbionts of leaf-cutting ants, Férnandez-Marín *et al.* discovered that *E. weberi* produces several shearinines.[58]

However, until now, no other secondary metabolites from *E. weberi* have been identified and it has not been established which compounds from *E. weberi* contribute to overpower the mutualistic fungus of leaf-cutting ants.[57, 58] Here, we present the isolation and identification of secondary metabolites from *E. weberi* and evaluate their biological function, in particular their impact on *L. gongylophorus* and *A. octospinosus* leaf-cutting ants.

Materials and Methods

General

Chemicals were purchased from Sigma Aldrich. IR detection was conducted on a ALPHA FT-IR spectrometer (Bruker, Germany). NMR spectra were recorded with a Bruker AVANCE AV-600 NMR spectrometer or a Bruker AV-600 NMR spectrometer fitted with a TCI cryoprobe (Bruker, Karlsruhe, Germany). Chemical shifts δ (ppm) were referenced to the solvent signals (^{1}H-NMR CD_3OD: 3.31, ^{13}C-NMR CD_3OD: 49.00, ^{1}H-NMR acetone-d6: 2.05, ^{13}C-NMR acetone-d6: 29.84). HR-ESI-MS were acquired using a Bruker Impact II (Bruker, Daltonics, Germany). UV-VIS spectra were recorded using an Implennanophotometer. For column chromatography silica gel (40-63 mesh, Macherey-Nagel, Germany) and Sephadex LH-20 (GE Healthcare, Upssala, Sweden) were used. Spots were detected under UV light and visualized by spraying with 5% H_2SO_4 in EtOH (v/v), followed by heating the plates. Silica GF254 (Merck KGaA, Germany) was used for analytical thin-layer chromatography. High performance liquid chromatography (HPLC) was performed on an Agilent 1100 liquid chromatography system fitted with a Phenomenex polar-RP column (250 x 2 mm, 4µm or 250 x 4.6 mm, 4µm) hyphenated to a Gilson FC204 fraction collector. LC-MS measurements were conducted with an Agilent 1100 HPLC connected to a Finnigan MAT LCQ. For GC-MS analysis, a Thermofisher Trace GC Ultra hyphenated with an ISQ was used.

Fungal and microbial cultures

E. weberi CBS 110660 and *E. aspergilloides* CBS 423.93 were obtained from the Westerdijk Fungal Biodiversity Institute (Utrecht, the Netherlands). *F. equiseti* FSU 5459 was from the Jena Microbial Resource Collection (JMRC, Jena, Germany). *P. fastigiata* DSM 2692 originated from the German Collection of Microorganisms and Cell Cultures (Braunschweig, Germany). The *Streptomyces* and *Pseudonocardia* strains used for bioassays were isolates from *A. volcanus*, *A. octospinosus*, and *A. echinatior* leaf-cutting ants. *L. gongylophorus* was isolated from an *A. octospinosus* nest maintained at University of Kaiserslautern by Dr. Rainer Wirth and verified by 18S rDNA sequencing (**SI**). *L. gongylophorus* was grown on potato dextrose agar medium (PDA) purchased

from Sigma Aldrich at 30 °C. All other strains were cultivated on soy flour medium (SFM) agar plates (20 g soy flour, 20 g mannitol, 15 g agar, 1L ddH_2O) at 28 °C.

A. octospinosus leaf-cutting ants

The *A. octospinosus* ants originated from Paratebueno, Medina, Colombia (4°23'38.4''N 73°16'07.5''W). The ants were kept as laboratory culture at the Technical University Kaiserslautern at 25 °C under a 12 h:12 h light:dark regime. The ants were offered fresh blackberry leaves as substrate for *L. gongylophorus*.

Extraction and isolation of secondary metabolites from *E. weberi*

Secondary metabolites were isolated from *E. weberi* grown on SFM agar plates at 28 °C for 14 d. 20 SFM agar plates (9 cm) were cut in pieces and extracted with ethyl acetate (500 mL) for 2 h twice. After filtration, the combined solvent extracts were dried *in vacuo*. The crude extract (0.459 g) was subjected to silica gel column chromatography (column dimension 3 x 25 cm) eluting with n-hexane and ethyl acetate (7:1, 5:1, 3:1, 2:1, 1:1, 1:3, 1:6, 0:1 v/v, 200 ml each) to give six fractions (Fr1- Fr6). Fr2 (11.3 mg) was passed three times through a Sephadex LH-20 column with 90 % MeOH to give pure compound **7** (3.1 mg). Likewise, Fr3 (16 mg) was subjected to Sephadex LH-20 column chromatography with 90 % MeOH and further purified by HPLC using a Phenomenex polar RP column (250 mm x 4.6 mm, 4 µm) at a flow rate of 0.8 mL/min eluting the compounds with a gradient of solvent A (H_2O 0.1 % acetic acid) and solvent B (MeOH 0.1 % acetic acid). HPLC conditions: 2 min 15 % B, in 28 min to 100 % B, 5 min 100 % B. Compound **1** (1.90 mg) and compound **3** (1.45 mg) were obtained. A similar fractionation procedure was used for Fr4 (31.0 mg) to yield compounds **4** (1.3 mg), **5** (1.25 mg) and **6** (3.2 mg). Furthermore, Fr5 (6.5 mg) was directly purified by HPLC with a gradient of solvent A (H_2O 0.1 % acetic acid) and solvent B (MeOH 0.1 % acetic acid): HPLC conditions: (2 min 50 % B, in 28 min to 100 % B, 5 min 100 % B) to yield compound **2**.

Spectroscopic data of shearinine L (1)

1.9 mg, white amorphous powder; IR (KBr):ν_{max}3441, 2971, 2617, 2343, 2051, 1668, 1462, 1365, 1253, 1149 (cm^{-1}); UV (CH_3OH) λ_{max} 255, 329 nm; ^{1}H-NMR (600 MHz, MeOD-d4) δ_H: 7.35 (1H, s, H-30), 7.16 (1H, s, H-20), 5.95 (1H, d, *J*=2.96, H-27), 5.93 (1H, brs, H-11), 5.72 (1H, dt, *J*=6.3, *J*=2.2, H-6), 4.12 (1H, s, H-9), 3.14 (1H, d, *J*= 18.5, H-5), 3.09 (1H, dd, *J*=15.3, *J*=9.2, H-22), 2.86-2.91 (1H, m, H-23), 2.67 (1H, dd, *J*=12.5, *J*=6.2, H-17), 2.60-2.64 (1H, m, H-22), 2.52-2.59 (1H, m, H-16), 2.30-2.35 (1H, m, H-17), 2.27-2.31 (m, H-5), 1.96-2.02 (1H, m, H-15), 1.89 (1H, d, *J*=13.6, H-14), 1.66-1.73 (1H, m, H-14), 1.61 (1H, d, *J*= 12.2, H-15), 1.38 (3H, s, H-40), 1.30-1.36 (12H, m, H-32, H-36, H-37, H-39), 1.27 (3H, s, H-35), 1.13 (3H, s, H38), 0.94 (3H, brs, H-33); ^{13}C-NMR (150 MHz, MeOD-d4) δ_C: 197.6 (C-10), 156.8 (C-7), 155.1 (C-2), 146.5 (C-12), 141.9 (C-31), 141.5 (C-29), 137.0 (C-28), 133.7 (C-21), 128.1 (C-19), 119.4 (C-27), 117.1 (C-11), 117.0 (C-18), 114.3 (C-20), 113.3 (C-6), 104.1 (C-30), 87.1 (C-9), 76.3 (C-24), 76.1 (C-13), 74.6 (C-34), 74.4 (C-26), 52.1 (C-3), 50.7 (C-16), 50.3 (C-23), 44.3 (C-4), 34.0 (C-22), 33.4 (C-14), 32.4 (C-5), 32.2 (C-39), 30.6 (C-40) 30.2 (C37), 28.0 (C-17), 26.8 (C-36), 26.7 (C-35), 22.7 (C-15), 22.3 (C-38), 21.3 (C-33), 16.6 (C-32); HR-ESI-MS: $[M-H]^-$ measured: 582.32053, calc.: 582.32250, $C_{37}H_{44}NO_5$.

Spectroscopic data of shearinine M (2)

0.98 mg, white amorphous powder; IR (KBr) ν_{max}3409, 3297, 2987, 2369, 2183, 1668, 1476, 1386, 1309, 1186cm^{-1}; UV (CH_3OH) λ_{max} 259, 328nm; ^{1}H-NMR (600 MHz, MeOD-d4) δ_H: 7.37 (1H, s, H-30), 7.36 (1H, s, H-20), 5.99 (1H, d, *J*=3.0, H-27), 5.94 (1H, brs, H-11), 5.72-5.75 (1H, m, H-6), 4.90 (1H, brd, *J*=5.7, H-22), 4.12 (1H, s, H-9), 3.16 (1H, d, *J*= 18.4, H-5), 2.69 (1H, dd, *J*=12.5, *J*=6.2, H-17), 2.67 (1H, dd, *J*=5.7, *J*=2.8, H-23), 2.65-2.67 (1H, m, H-16), 2.36-2.41 (1H, m, H-17), 2.30-2.36 (1H, m, H-5), 1.99-2.06 (1H, m, H-15), 1.90-1.96 (1H, m, H-14), 1.76-1.83 (1H, m, H-14), 1.67 (1H, d, *J*=12.3, H-15), 1.46 (3H, s, H-37), 1.37 (3H, s, H-40), 1.34 (3H, s, H32), 1.32-1.34 (6H, s, H-36, H-39), 1.27 (3H, s, H-35), 1.15 (3H, s, H38), 0.99 (3H, s, H-33); ^{13}C-NMR (150 MHz, MeOD-d4) δ_C: 197.6 (C-10), 156.7 (C-7), 155.5 (C-2), 146.5 (C-12), 142.9 (C-31), 139.2 (C-29), 137.3 (C-28), 132.0 (C-21), 128.2 (C-19), 120.2 (C-27), 117.4 (C-18), 117.1 (C-11), 114.2 (C-20), 113.3 (C-6), 103.6 (C-30), 87.2 (C-9), 76.7 (C-22), 76.0 (C-13), 75.6 (C-

24), 74.7 (C-34), 74.1 (C-26), 60.3 (C-23), 52.2 (C-3), 50.7 (C-16), 44.3 (C-4), 33.4 (C-14), 32.3 (C-5), 32.2 (C-39), 30.4 (C-40), 30.3 (C-37), 28.0 (C-17), 26.8 (C-36), 26.7 (C-35), 23.7 (C-38), 22.4 (C-15), 21.2 (C-33), 16.6 (C-32); HR-ESI-MS: $[M-H]^-$ measured: 598.31763, calc.: 598.31741, $C_{37}H_{44}NO_6$.

Agar diffusion assays

L. gongylophorus, F. equiseti, *P. fastigiata, Streptomyces* sp. Av25_4*, Streptomyces* sp. 28_1*, Streptomyces* sp. 26_3 and *Pseudonocardia* sp. Ao19 were used as test organisms in the agar diffusion assays against the purified secondary metabolites or reference compounds. For the agar diffusion assays, 100 µL of mycelium suspensions of the test organisms were spread onto SFM or PDA agar plates (5.5 cm diameter). Holes (6 mm diameter) were cut into the agar plates into which 50 µL of the test solutions or solvent controls (MeOH) were applied. For paper disk diffusion assays, sterilized filter paper disks (6 mm diameter) were impregnated with the test compounds (0.3, 0.66, and 0.82 µmol). The test organisms were cultivated at 28 °C except *L. gongylophorus*, which was grown at 30 °C. The inhibition zones were monitored daily from day 3 to 18. All assays were performed at least in triplicate and were compared to equally prepared solvent controls.

Establishment of *A. octospinosus* subcolonies

Bioassays with *A. octospinosus* leaf-cutting ants were performed with subcolonies (3 treatments, 3 controls). The subcolonies were established by isolating ca. 400 cm^3 of fresh fungus garden from three large laboratory mother colonies. The subcolonies were kept in experimental nests, consisting of 3 plastic boxes (feeding box, fungus garden box, and refuse chamber) connected by plastic tubes. The *A. octospinosus* subcolonies were kept at 25 ˚C under a 12 h:12 h light:dark regime. All subcolonies were established at least 5 d before the dual choice experiment and supplied with fresh blackberry leaves.

Coating of oat flakes with shearinine L (1)

Oat flakes (Blüten-zarteFlocken, Kölln, Germany) of approximately equal size were used for the experiment. The flakes were impregnated with 10 µL of shearinine L (**1**) (1

mg/mL) dissolved in acetone and air-dried. Control flakes were prepared analogously applying 10 µL acetone.

Dual-choice bioassays[59] with *A. octospinosus* leaf-cutting ants

For the dual-choice preference tests, 10 treated and 10 control flakes were simultaneously placed 3 cm apart in the foraging chamber of *A. octospinosus* subcolonies. The subcolonies were monitored continuously and the number of flakes carried inside the nest was noted until 8 out of 10 control or shearinine L (**1**) treated flakes were picked up or 5 h had elapsed. All collected flakes were readily processed and incorporated into the fungus garden. The foraging preferences of each subcolony were monitored daily over 5 d. Starting from the second day of feeding preference tests, the number of dead ants (i.e., worker mortality) and the amount of waste deposited by the ants into the waste chamber were recorded daily for 10 d. The influence of shearinine L (**1**) on the choice behaviour of ants, their mortality, and waste deposition was statistically analyzed using general linear mixed models ($GLMM_{choice\ assay}$, $GLMM_{worker\ mortality}$, and $GLMM_{waste\ deposition}$, respectively) with treatment, day and their interaction as fixed factors and subcolony as random factor. Ant mortality was square-root transformed to achieve homogeneity of variance. Statistical tests were performed with Statistica software (Statistica 13, TIBCO Software Inc., Palo Alto, USA).

Results

Identification of secondary metabolites from *E. weberi*

Methanol extracts of *E. weberi* grown on SFM agar plates at 28 °C for 14 d were analysed by high performance liquid chromatography (HPLC) coupled to a diode array detector and a electrospray mass spectrometer (LC-DAD-ESI-MS). The base peak chromatogram and the UV chromatogram (254 nm) (**Figure 2.1** and **Figure S2.1**) revealed a series of intense peaks. The compounds causing the most prominent peaks **1**-**7** were purified by silica gel column chromatography (CC), Sephadex LH-20 CC and reversed phase HPLC coupled with a fraction collector in order to elucidate their structures by mass spectrometry and NMR. The purified secondary metabolites comprised five shearinines including two novel shearinines (**1** and **2**), cycloarthropsone (**6**) and emodin (**7**) (**Figure 2.1**).

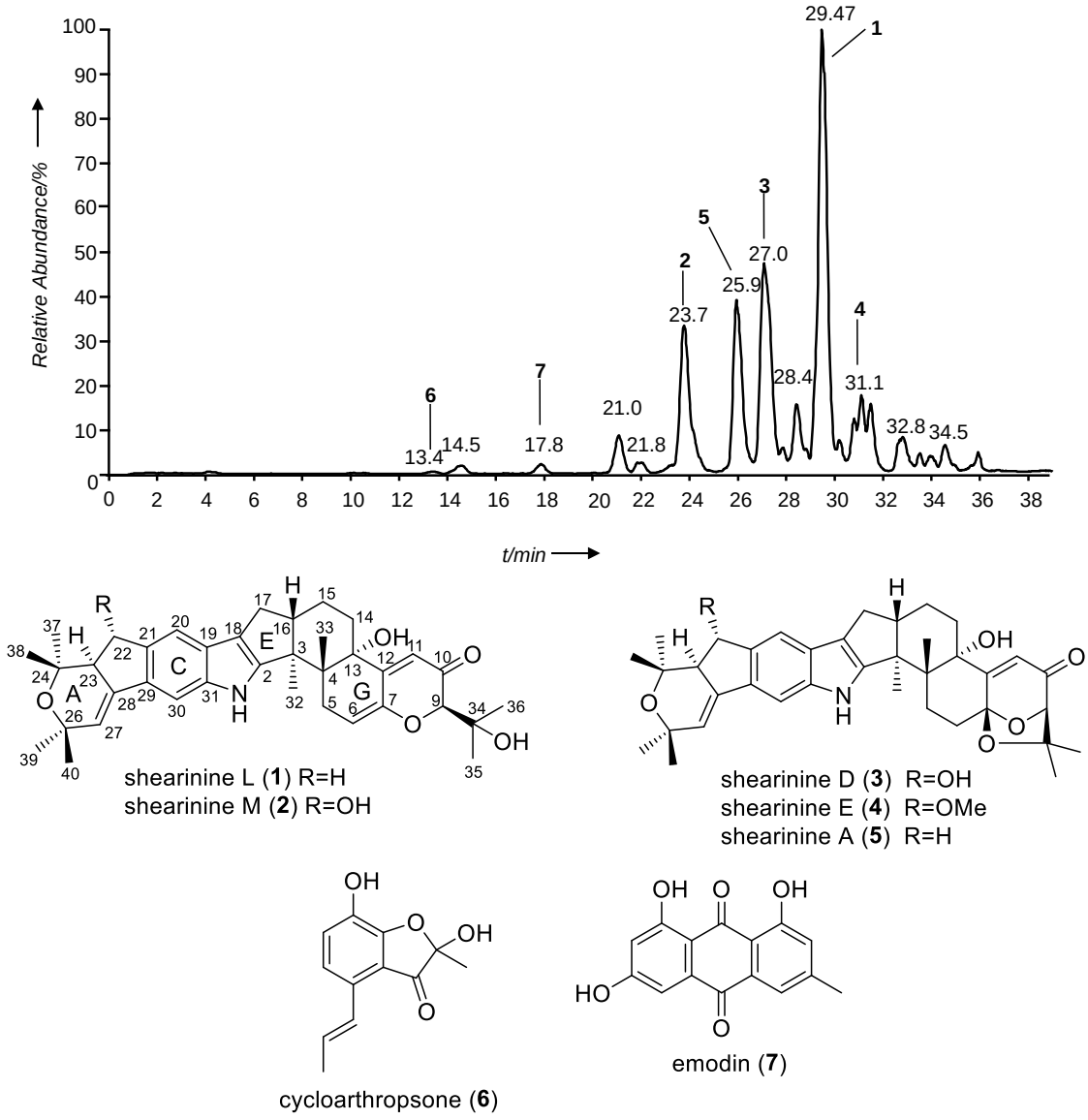

Figure 2.1: A) LC-negative-ESI-MS base peak chromatogram of a methanol extract of *E. weberi.* Labelled peaks were identified as shearinine L (**1**), shearinine M (**2**), shearinine D (**3**), shearinine E (**4**), shearinine A (**5**), cycloarthropsone (**6**), and emodin (**7**). **B**) Structures of the identified secondary metabolites from *E. weberi*.

Shearinines

Several shearinines have been recently identified as secondary metabolites from *E. weberi*.[58] However, we observed additional prominent peaks **1** and **2** in the LC-DAD-ESI-MS profile that turned out to be additional, novel shearinine derivatives.

Shearinines were detectable in SFM agar plates inoculated with *E. weberi* after 3 d at 28 °C. The amount of shearinines increased significantly with incubation time, reaching a maximum concentration of ca. 8 µg/mL SFM medium of **1** after day 9. Shearinine L (**1**) was obtained as a white amorphous powder. Its molecular formula was established to be $C_{37}H_{45}NO_5$ by HR-ESI-MS corresponding to 16 double bond equivalents (DBE).The ^{1}H-NMR spectrum (**Figure 2.2** and **Figure S2.3**) showed the presence of signals for eight aliphatic methyl singlets which are characteristic for a shearinine-type indole triterpenoid as well as two indicative aromatic proton singlets at δ_H 7.16 (H-20) and 7.35 (H-30). The ^{13}C-NMR spectrum (**Figure S2.4**) revealed 37 carbon resonances: eight methyl groups, five methylene groups, eight methine groups. Furthermore, among the 16 quaternary carbons, the signal at δ_C 197.6 (C-10) indicated the presence of an unsaturated keto group. The ^{1}H- and ^{13}C-NMR data together with HMBC correlation analysis, suggested that the structure of **1** is closely related to that of shearinine B.[60] Compound **1** and shearinine B[60] differ only in the ring G (**Figure 2.2**). Compound **1** bears a double bound between C-6 and C-7 that causes the appearance of one characteristic olefinic proton at δ_H 5.72 (H-6). The HMBC correlations between H-6 and C-4 (δ_C 44.3), C-7 (δ_C 156.8) and C-12 (δ_C 146.5) (**Figure 2.2B**, **Figure S2.7**) further confirmed the position of the double bond. Thus, **1** was determined as Δ6, 7-shearinine B and called shearinine L. The relative configuration of shearinine L (**1**) was clarified by NOESY spectrum analysis (**Figure S2.8**). The presence of NOE correlations between H_3-32 to H-17α and also between H-16 to H_3-33 indicated a trans-3,16-ring fusion. Moreover, NOE correlations between H_3-33 and H-14β as well as between H-11 and H-14α suggested the α-orientation of the hydroxy group at C-13 (**Figure S2.9**).

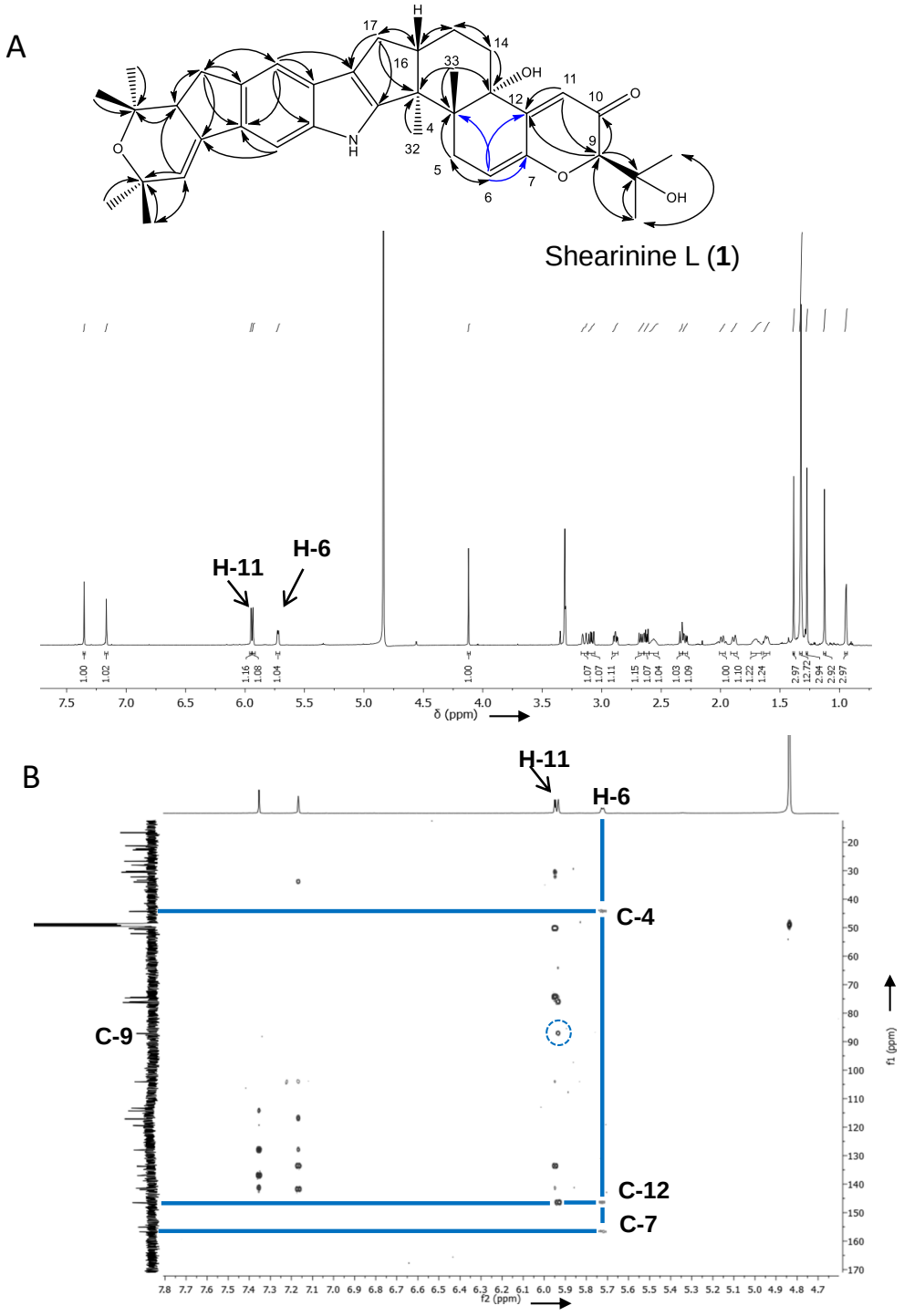

Figure 2.2: A) ^{1}H-NMR of shearinine L (**1**), **B**) key ^{1}H-^{1}H COSY and ^{1}H-^{13}C-HMBC correlations of shearinine L (**1**).

The HR-ESI-MS of compound **2** confirmed its molecular formula to be $C_{37}H_{45}NO_6$ (16 DBE). Thus, **2** contains one oxygen atom (16 amu) more compared to shearinine L (**1**). The ^{1}H and ^{13}C-NMR signals of **2** (**Figure S2.11** and **S2.12**) were similar with those of shearinine L (**1**) except for the presence of a single broad doublet signal at δ_H 4.90 (1H, *J*= 5.7 Hz, H-22) instead of the two signals δ_H 3.09 (1H, *J*= 15.3, 9.2 Hz, H-22), 2.60-2.64 (1H, m, H-22) in shearinine L (**1**) (**Figure S2.3** and **S2.11**). This suggested that compared to shearinine L (**1**) compound **2** contains a hydroxylated methine moiety at carbon C-22. The position of the hydroxy group at C-22 was further confirmed by HMBC correlations between H-22 and C-23 (δ_C 60.3), C-24 (δ_C 75.6), C-20 (δ_C 114.2), C-21 (δ_C 132.0), C-28 (δ_C 137.3) and C-29 (δ_C 139.2) (**Figure S2.15**). Thus, the structure of **2** was determined as 22-hydroxy-shearinine L. We named the new compound shearinine M. The NOESY spectrum exhibited correlations between H-22 and H_3-38 and between H-23 and H_3-37 (**Figure S2.16**), which implies that H-22 and H-23 are on opposite faces of ring B. The ^{1}H- and ^{13}C-NMR data at C-22 and C-23 of **2** were also in good agreement with those of shearinine D,[61] indicating the relative H-22β and H-23α configurations. The relative configuration of ring fusions in shearinine M (**2**) is identical to shearinine L (**1**) based on the NOESY correlations: H_3-32/H-17α, H-16/H_3-33, H_3-33/H-14β and H-11 and H-14α (**Figure S2.17**).

Compounds **3**-**5** were also identified as shearinine-type indole triterpenoids, namely shearinine D (**3**), shearinine E (**4**), and shearinineA (**5**), which have been characterized before from *Penicillium* species or its teleomorph *Eupenicillium* species.[60-62]

Cycloarthropsone (6)

3.2 mg (ca. 6 µg/mL SFM medium) were isolated of compound **6**. **6** was an aromatic compound with the molecular formula $C_{12}H_{12}O_4$ and seven DBE. Its ^{1}H-NMR spectrum exhibited two *ortho*-coupled aromatic protons, signals corresponding to an (*E*)-propenyl chain and a methyl singlet (**Figure S2.23**). The NMR data and MS/MS fragmentation (**Figure S2.25**) indicating loss of H_2O and CO suggested **6** to be a benzofuranone derivative. Moreover, GC-MS analysis after derivatization with *N*-Methyl-*N*-(trimethylsilyl) trifluoroacetamide (MSTFA) (**Figure S2.26**) exhibited a molecular ion at 364 (M + 2TMS), which pointed to the presence of two hydroxy groups. Thus,

compound **6** was identified as cycloarthropsone that had been identified previously from the fungus *Arthropsis truncate*.The reported NMR data matched perfectly with ours.[63]

Emodin (7)

Compound **7** was obtained as orange needles (ca. 6 µg/mL SFM medium). For the aromatic compound the molecular formula $C_{15}H_{10}O_5$ and 11 DBE were deduced. The UV spectrum of **7** in methanol (**Figure S2.30**) revealed four absorption maxima at 216, 256, 308 and 461 nm that are characteristic for anthraquinones. The ^{1}H-NMR spectrum exhibited four meta-coupled aromatic proton signals and a methyl singlet signal (**Figure S2.28**). Further analysis of the ^{13}C-NMR data (**Figure S2.29**) and comparison of the retention time with an authentic reference confirmed the compound to be emodin (**7**).

Comparison of secondary metabolite profiles from *E. weberi* with *Escovopsis aspergilloides*

E. apergilloides that has also been identified from nest of attine ants[64] is closely related to *E. weberi.* This parasitic fungus morphologically differs from *E. weberi* by its globose shaped, rather than clavate shaped phialide-vesicles.[65] However, the metabolite profiles of methanol extracts of both *Escovopsis* strains turned out to be very similar (**Figure S2.31**). Both strains produced shearinines (**1**-**5**), cycloarthropsone (**6**), and emodin (**7**). The amount of the compounds in both *Escovopsis* strains may slightly vary.

Antimicrobial activity of secondary metabolites from *E. weberi*

In order to evaluate the function of the identified secondary metabolites, cycloarthropsone (**6**), emodin (**7**), and shearinine L (**1**) were tested in agar diffusion assays against selected organisms present in the leaf-cutting ants' nests. In particular, the potential to overwhelm *L. gongylophorus* was addressed.

Cycloarthropsone (**6**) and emodin (**7**) inhibited the growth of *L. gongylophorus*,causing 14 and 10 mm inhibition zones, at 0.81 and 0.66 µmol, respectively (**Figure 2.3**, **Figure S2.34-36**). However, shearinine L (**1**) was not active at 0.31 µmol (**Figure S2.41**). 0.30 µmol emodin (**7**) inhibited the *Streptomyces* symbionts of leaf-cutting ants *Streptomyces* sp. 28_1 and *Streptomyces* sp. 26_1 causing inhibition zones of 10 mm and 7 mm,

respectively (**Figure S2.32-S33**). Moreover, none of the compounds tested showed activity against *Pseudonocardia* sp. Ao19, *Fusarium equiseti*, and *Phialophora fastigiata*.[66]

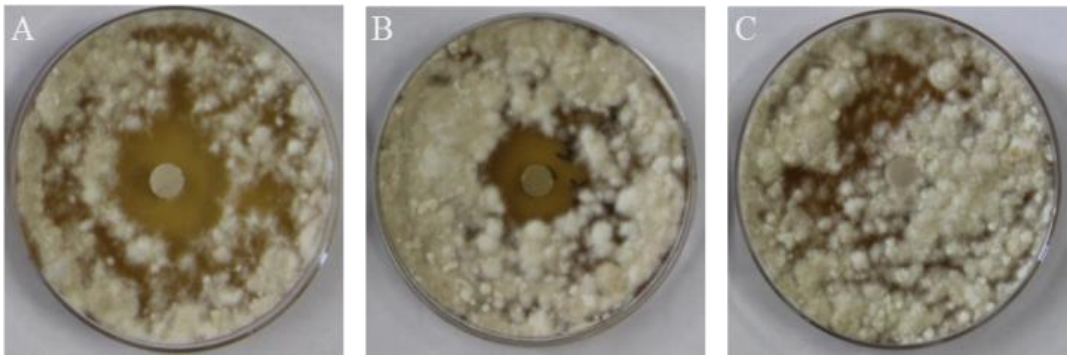

Figure 2.3: Agar diffusion assays against *L. gongylophorous*, on PDA agar plates (5.5 cm diameter) after 18 d of growth: **A**) 0.82 µmol cycloarthropsone (**6**) on paper disk; **B**) 0.66 µmol emodin (**7**) on paper disk, and **C**) control.

Response of *A. octospinosus* ants to shearinine L (1)

A. octospinosus ants from subcolonies were offered oat flakes as a substrate for their garden fungus. These flakes were either impregnated with shearinine L (**1**) (10 µg/flake) or control flakes in a dual-choice assay.[59] The oat flakes were transported by *A. octospinosus* workers into the subcolonies and processed into small pieces that were incorporated across the garden to cultivate *L. gongylophorus*. Oat flake choice by *A. octospinosus* workers was strongly influenced by the shearinine L (**1**) treatment (**Figure 2.4**, $GLMM_{choice\ assay}$, effect of treatment: $F_{1,18} = 19.59$; $p<0.001$) but preference reversed during the course of the assay ($GLMM_{choice\ assay}$, effect of day x treatment: $F_{4,18} = 20.93$; $p<0.001$). On day one the ants significantly preferred treated over control flakes (ca. 70 % versus 30 %). Reversely, from day 3 onwards, shearinine L treated oat flakes were strongly rejected (ca. 25% vs. 75 % on days 3, 4, and 5). This switch in preference occurred on day 2, with no significant difference in removal rates (42 % vs. 58 %). Both

subcolony and day had not significant effect on oat flake choice ($GLMM_{choice\ assay}$, effect of subcolony: $F_{2,18} = 0.00$; $p>0.05$; effect of day: $F_{4,18} = 0.00$; $p>0.05$).

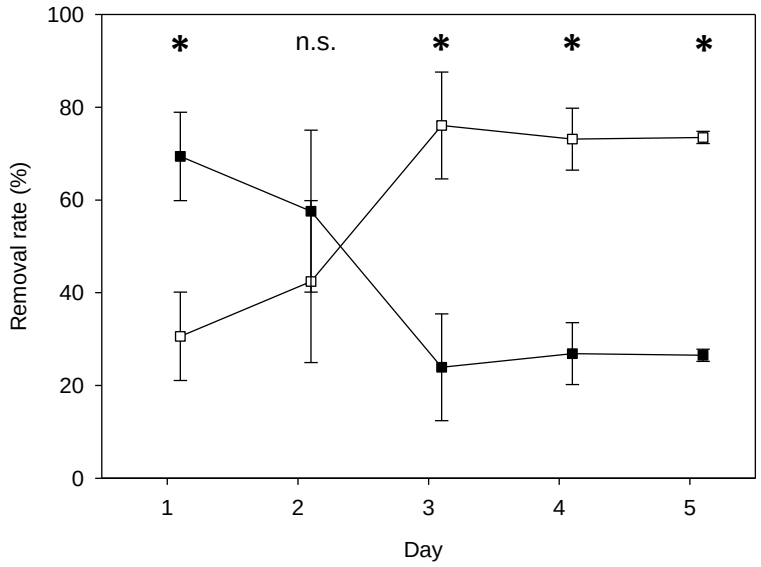

Figure 2.4: Dual choice assays with *A. octospinosus* leaf-cutting ants.The removal rate of shearinine L (**1**) treated oat flakes versus untreated flakes is shown. Black squares (shearinine L (**1**) treated flakes) and white squares (untreated flakes) represent the mean values, error bars indicate the standard deviation of 3 replicates. Star: statistically significant, n.s. not significant.

Leaf-cutting ant performance in shearinine L (**1**) treated versus control subcolonies was investigated for 10 days, starting on day 2 of the choice assay, by determining the daily amount of waste deposition (fresh weight) and worker mortality (number of dead ants). Subcolonies treated with shearinine L (**1**) revealed similar worker mortality and waste deposition as control subcolonies, and both measures of colony performance remained constant throughout the 10 d experiment ($GLMM_{waste\ deposition}$, effect of treatment: $F_{1,38} = 0.000036$; $p>0.05$; effect of day: $F_{9,38} = 1.37$; $p>0.05$; effect of day x treatment: $F_{9,38} = 0.62$; $p>0.05$; effect of subcolony: $F_{2,38} = 1.99$; $p>0.05$; $GLMM_{worker\ mortality}$, effect of treatment: $F_{1,38} = 0.34$; $p>0.05$; effect of day: $F_{9,38} = 8.42$; $p>0.05$; effect of day x treatment: $F_{9,38} = 0.62$; $p>0.05$; effect of subcolony: $F_{2,38} = 8.42$; $p<0.001$).

Discussion

How the major pathogen of leaf-cutting ants, *E. weberi*, overwhelms *L. gongylophorus* and thus threatens survival of the ants has not been addressed in detail so far. Using metabolite profiling by LC-DAD-MS of *E. weberi* extracts, we identified seven of the major compounds produced by both *E. weberi* and *E. aspergilloides* (**Figure 2.1** and **Figure S2.1**, **Figure S2.31**) as shearinines (**1-5**), cycloarthropsone (**6**), and emodin (**7**) (**Figure 2.1**). The finding of shearinines is in line with Boya *et al.*, who recently observed shearinines D, F, and J in a co-cultivation experiment with mutualistic Streptomyces symbionts of *Acromyrmex echinatior* leaf-cutting ants against *E. weberi TZ49*.[58] Also, genome mining using antismash[67] revealed that the *E. weberi* genome[44] comprises genes involved in indole terpenoid biosynthesis fitting to the formation of shearinines.

However, our *Escovopsis* strains mainly released two novel shearinines L (**1**) and M (**2**) alongside the known shearinines D (**3**), E (**4**) and A (**5**) with maximal production after 9-12 d of growth on SFM agar plates (**Figure 2.1**). Shearinines have been originally identified from *Eupenicillium shearii*.[60] Shearinines exhibit anticancer activities;[61] they block large-conductance calcium-activated potassium channels,[62] and are known to act against insects.[60] Furthermore, shearinines have been found to suppress *Candida albicans* biofilm formation and potentiate the antifungal activity of the polyene macrolide antifungal amphotericin B.[68] However, in agar diffusion assays against *L. gonglyophorus* 0.3 µmol shearinine L (**1**) did not stop the growth of *L. gongylophorus*.

Due to the reported activity of shearinines against insects,[60] they may rather act against the leaf-cutting ants and thus indirectly weaken the fitness of the garden fungus. In order to address how shearinines may affect the leaf-cutting ants' colony we investigated how *A. octospinosus* subcolonies responded to the major component shearinine L (**1**). Shearinine L (**1**) impregnated oat flakes and control oat flakes were offered to *A. octospinosus*. Initially, *A. octospinosus* accepted both treated and untreated flakes even preferring the shearinine L (**1**) treated flakes. Consequently, the ants did not immediately recognize shearinine L (**1**) as detrimental. However, the ants clearly rejected shearinine L treated flakes as substrate for *L. gongylophorus* from day 3 onwards (**Figure 2.4**). Thus, *A. octospinosus* ants quickly learned to avoid shearinine L (**1**) treated oat flakes. However, when we evaluated the state of the subcolonies (daily

waste production) as well as the death rate of *A. octospinosus* workers no clear signs of a direct toxicity of shearinine L (**1**) could be observed indicating that shearinine L (**1**) does not quickly kill *A. octospinosus* workers. Still after 2 d, *A. octospinosus* ants strongly rejected the substrate treated with shearinine L (**1**).

Currently, it remains elusive how *A. octospinosus* workers learn to avoid shearinine L (**1**) a major compound of their major pathogen. It is conceivable that the avoidance is induced due to a signal by *L. gongylophorus* indicating a detrimental substrate. Alternatively, the ants recognize themselves, e.g. during the processing of the flakes into small pieces for their garden fungus, that shearinine L (**1**) is noxious.

A similar delayed avoidance behaviour - likely induced by *L. gongylophorus* - has been observed previously with antifungal (cycloheximide) treated plant substrate[69, 70] as well as defense-induced plant material.[59]

In contrast to shearinine L (**1**), both cycloarthropsone (**6**) and emodin (**7**) strongly inhibited the growth of *L. gongylophorus* in agar diffusion assays (**Figure 2.3**) suggesting that *Escovopsis* fungi can make use of these polyketides to overpower *L. gongylophorus*. Cycloarthropsone (**6**) has been identified from *Arthropsis truncata*.[63] However, its biological activity has not been evaluated so far. In contrast, emodin (**7**), that is produced by plants and microorganisms, is well known for its wide range of pharmacological activities, such as antibacterial (against *Bacillus subtilis*),[71] antifungal (against *Alternaria*, *Fusarium*, *Fomesannosus* etc.),[72] antiviral,[73] anticancer,[74] anti-inflammatory,[75] and anti-ulcerogenic properties.[76] Thus, emodin (**7**) may help *Escovopsis* to outcompete other fungi that are known to occur in the leaf-cutting ants' nests.[46] However, our test strain for alternative pathogens, *Fusarium esquiseti*, was not clearly inhibited in our agar diffusion assays (0.3 µmol, **Figure S34**). Emodin (**7**) (0.3 µmol) strongly inhibited some Actinomyces symbionts of leaf-cutting ants (**Figure S2.32** and **S2.33**) indicating its use to fight against the protectors of the fungus garden.

Conclusions

With the production of diverse secondary metabolites such as the shearinines, emodin (**7**) and cycloarthropsone (**6**) *E. weberi* is well equipped to overpower its prey *L. gongylophorus* as well as to fight against the defenders, in particular the mutualistic actinomyces symbionts.

However, *A. octospinosus* leaf-cutting ants - probably communicated by *L. gongylophorus* - can quickly recognize shearinine L (**1**) and thus can initiate countermeasures against the pathogen demonstrating the arms race between the organisms.

With a multitude of organisms - the ants, their garden fungus, the mutualistic microbial symbionts, and pathogens, in particular *E. weberi*, - comprising the leaf-cutting ants' ecosystem, a detailed picture of the complex interactions can only be obtained if the involved chemicals, signaling compounds, toxins and antimicrobials, of the different partners are identified and their ecological function is addressed. In addition to straightforward *in vitro* bioassays, (behavioural) studies under close to natural conditions can help to reveal a more complete picture of the interactions and the diverse functions of the involved metabolites - as observed in the case of shearinines L (**1**).

Acknowledgements

We thank Prof. Peter Spiteller and Dr. Thomas Dülcks for HR-ESI-MS measurements and Natalie Kunz for advice in statistical analysis. Language editing and helpful comments by Dr. Anthony Farlow are gratefully acknowledged. We thank Christian Ziegler for the *A. octospinosus* photo. We greatly indepted to the Konstanz Research School Chemical Biology funded by the Deutsche Forschungsgemeinschaft for financial support and a doctoral fellowship to BD.

Chapter 3: Upon attack by the pathogen *Escovopsis weberi* the garden fungus of leaf-cutting ants *Leucoagaricus gongylophorus* releases 3-octanone that stimulates the ants' hygienic behavior

Upon attack by the pathogen *Escovopsis weberi* the garden fungus of leaf-cutting ants *Leucoagaricus gongylophorus* releases 3-octanone that stimulates the ants' hygienic behavior

Basanta Dhodary[1], Benjamin Feth[2], Julia Schulz[2], Rainer Wirth[2], Dieter Spiteller[1]*

[1]Chemical Ecology/Biological Chemistry, University of Konstanz, Universitätsstrasse 10, 78457 Konstanz, Germany.
[2]Plant Ecology and Systematics, Technical University Kaiserslautern, Erwin-Schrödingerstraße 13, 67653 Kaiserslautern, Germany

Abstract

Leaf-cutting ants, such as *Acromyrmex octospinosus*, cultivate the fungus *Leucoagaricus gongylophorus* with plant material in garden chambers inside their nest because they depend on *L. gongylophorus* as food source. Their mutualistic symbiosis is threatened by pathogens, in particular the specialized parasitic fungus *Escovopsis weberi*. For the ants, it is crucial to recognize infections in order to fight them. Mimicking infection by co-cultivating *L. gongylophorus* and *E. weberi* on agar plates and analysis of the emitted volatiles revealed that *L. gongylophorus* specifically induces 3-octanone release upon attack. 3-octanone is not present in the volatile profile of *L. gongylophorus* when there is no attack.

Using mini-subcolonies of *A. octospinosus*, the ants' cleaning behavior was studied in behavioral assays. The presence of 3-octanone contributed to the triggering of hygienic behavior *in A. octospinosus*. Precisely, 3-octanone led to a strong induction of fungus-tending. Fungus grooming was only slightly increased and removing behavior remained unchanged. We suggest that 3-octanone serves as volatile alarm cue for cross-kingdom communication, in which *L. gongylophorus* stimulates the ants to help against *E. weberi*.

Key words: volatiles, signals, interspecies interactions, lipid peroxidation, symbiosis.

Introduction

Atta and *Acromyrmex* leaf-cutting ants (Attini) live in mutualistic symbiosis with their garden fungus *Leucoagaricus gongylophorus* (Agaricales: Leucocoprineae) that they grow in chambers of their nests.[77, 78] Leaf-cutting ants cultivate *L. gongylophorus* with plant material collected from their foraging grounds and processed into small pieces. *L. gongylophorus* degrades the recalcitrant plant polymers and thus makes the nutrients available for the leaf-cutting ants that use the garden fungus as food source.[22]

However, this partnership can be threatened by pathogens that infect the leaf-cutting ants' nests and can challenge the survival of the garden fungus as well as the viability of the whole ant nest.[3,79,53] In order to keep pathogens under control, leaf-cutting ants invest great care into the maintenance of their fungus gardens: specific workers continuously clean the fungus garden and remove suspicious material into waste chambers.[23]

The ants combine behavioral strategies with the use of chemical treatment. Compounds such as 3-hydroxydecanoic acid[80] from their metapleural glands exhibit antimicrobial properties.[29] In addition, the ants joined forces with microbial symbionts.[3] *Actinomycetes* that grow on the integument of the ants produce powerful antifungal compounds, such as candicidin[39], dentigerumycin[81], gerumycin[82], antimycin[40], actinomycin[40] or nystatin P[83], and thus contribute to control infections in the fungus garden. Nevertheless, a broad variety of noxious bacteria, filamentous fungi and yeasts occur in leaf-cutting ant nests.[3, 53, 79] In particular, the specialized fungi of the genus *Escovopsis* (Ascomycota, Pezizomycotina: anamorphic Hypocreales) consume *L. gongylophorus. Escovopsis* pathogens co-evolved with leaf-cutting ants and their garden fungus.[3] *Escovopsis* fungi produce several toxins that target *L. gongylophorus,* the ants' microbial symbionts as well as the ants themselves. Shearinines (indole triterpenoids)[58, 84], emodin[84] and cycloarthropsone[84] are used to overpower *L. gongylophorus*. Upon infection, *Escovopsis* upregulates the production of shearinine D and melinacidin IV, which inhibit the antibiotic-producing *Pseudonocardia* symbionts as well as reduce the ants' behavioral defenses.[85]

Although we have gained some important insights into the chemical ecology of the complex symbiotic leaf-cutting ant microcosmos, we still have limited knowledge about

how the mutualistic partners, the ants, *L. gongylophorus,* and *Actinomycetes* symbionts*,* interact or even actively communicate in order to defend against threats such as *E. weberi*.[86]

Here, we investigated whether volatile cues that could act as cross-kingdom signals between leaf-cutting ants and their garden fungus in order to induce defense reactions upon infection by *E. weberi*.

Materials and Methods

Chemical and instruments

3-octanone, 1-octen-3-ol and potato dextrose medium (PDA) were purchased from Sigma-Aldrich (82024 Taufkirchen, Germany). Mannitol and agar agar Kobe I were obtained from Carl Roth (76185 Karlsruhe, Germany). Soy flour (Hensel Bio-Voll-Soja) was obtained from W. Schoenenberger GmBH Co. KG (71106 Magstadt, Germany).

All solvents used were HPLC grade solvents or distilled prior to use. Polydimethylsiloxane solid phase microextraction fibers SPME Arrow (100μm, 1.1 mm diameter) were purchased from Restek (61348 Bad Homburg, Germany). Closed loop stripping pumps were made by the workshop of the University of Konstanz.

Thermofisher ISQ connected to a Thermofisher Trace GC Ultra (63303 Dreieich, Germany) was used for the GC-MS analysis.

Fungal strains and cultivation conditions

E. weberi CBS 110660 was obtained from Westerdijk Fungal Biodiversity Institute (Utrecht, the Netherlands) and *Fusarium equiseti* FSU 5459 was from Jena Microbial Resource Collection (JMRC. Jena, Germany). *L. gongylophorus* was isolated from *A. octospinosus* nest maintained at University of Kaiserslautern origin. *E. weberi* and *L. gongylophorus* were cultivated on potato dextrose agar medium (PDA) agar plates at 30 °C, 50-60 % humidity in the dark. *F. equiseti* was cultivated on SFM agar plates (20 g mannitol, 20 g soy flour, 20 g agar, 1 L distilled water).[87]

Origin and rearing of *A. octospinosus* leaf-cutting ants

A. octospinosus ants were collected from Paratebueno (Medina, Colombia) as one year old colony in June 2015. *A. octospinosus* ants were reared as laboratory culture in plastic boxes (fungus/brood chamber, foraging chamber and waste chamber, 19x19x9 cm) connected with PVC tubes at 25 °C, 50-55 % humidity, under a 12 h:12 h light:dark cycle at the animal house of the Technical University Kaiserslautern. The ants were offered fresh blackberry leaves as growth substrate for their *L. gongylophorus* fungus daily. For the behavioral experiments, a subcolony (fungus/brood chamber, foraging

chamber and waste chamber, 10 x 10 x 6.5 cm) was established by isolating ca. 400 cm^3 of fresh fungus garden, including ca. 600–800 workers.[59]

Growth curve of *E. weberi* and *E. weberi*/*L. gongylophorus* co-culture

200 µl of mycelium suspension (ca. 95 mg mycelium in 1.5 mL water) of *L. gongylophorus* was spread onto PDA agar plates (9.5 cm diameter) and grown for 14 d at 30 °C before starting the experiments. *E. weberi* was grown on PDA agar plates for 4 d at 28 °C. At day 15, *E. weberi* fungal mycelium (6 mm in diameter) was added into the middle of *L. gongylophorus* agar plates. As control *L. gongylophorus* on PDA plates grown alone and *E. weberi* mycelium pieces (6 mm in diameter) on PDA agar plates were cultivated. The plates were wrapped with parafilm in order to accumulate any volatiles formed and to avoid potential contamination by volatiles emitted into the incubator.

The growth of *E. weberi* in co-culture samples and the control samples was recorded daily by measuring the diameter of area covered by *E. weberi*. The experiment was terminated when *L. gongylophorus* agar plates challenged by *E. weberi* were completely covered by *E. weberi*. The volatiles produced by single cultures and co-cultures were analyzed by SPME-GC-MS daily for 10 d. At least three replicates were measured for each cultivation condition.

SPME-GC-MS analysis of volatiles

The volatiles from each individual monoculture and co-culture were collected by SPME using a polydimethylsiloxane SPME arrow fiber. After drilling a small hole with a sterile cannula in the plastic side of the Petri dish, the SPME fiber was inserted into the Petri dish and the fiber was released to collect the volatiles for 15 min at room temperature. After the sampling, the SPME fiber was injected into the GC injector of the GC-MS and analysed. The GC-MS conditions were: inlet temperature 280 °C, splitless injection, helium served as carrier gas (1 ml/min). A Macherey-Nagel Optima 5 MS column (30 m x 0.25 mm, 0.25 µm) was used for the separation of the compounds. Volatile metabolite profiles were measured using the following temperature program: 50 °C 3 min isotherm,

heating rate 6 °C/min to 200 °C, heating rate 20 °C/min to 260 °C, 260 °C 1 min. The mass spectrometer was operated in electron impact ionization mode at 70 eV.

Freezing-thawing *L. gongylophorus* and *E. weberi* mycelium

Ca. 5 mg of 12 d grown *L. gongylophorus* or 5 d grown *E. weberi* mycelium was removed from the agar plate and transferred into 4 ml vial. The vials containing the fungus were tightly sealed and frozen for 30 min at -20°C followed by thawing at room temperature for 10 min. The volatile profiles were collected before and after freeze-thawing by SPME at room temperature for 15 min.The samples were analyzed by GC-MS (see above). All samples were at least analyzed in triplicate.

Testing of potential antifungal activity of 3-octanone against *E. weberi*

The antifungal activity of 3-octanone was evaluated using three compartment Petri dishes divided by a plastic barrier. The first compartment contained PDA medium (10 mL).

A *E. weberi* disc (6 mm in diameter) from an actively growing PDA plate was introduced in the center of the first compartment whereas into the second compartment a sterile filter paper piece (1.5 cm in diameter) impregnated with 6.2 µmol 3-octanone dissolved in 20 µL methanol or just 20 µL methanol as control was inserted. The third compartment was left empty.

The plates were sealed with parafilm and incubated for 5 d at 28 °C. Fungal growth was monitored daily for 5 d. Each treatment was performed in at least three replicates.

Behavioral experiments with *A. octospinosus* leaf-cutting ant workers

In order to study whether and how *A. octospinosus* respond to 3-octanone, behavioral experiments were performed. From the *A. octospinosus* subcolony ca. 2 cm^3 of fungus garden including 10-15 worker ants was removed by filling a standardized cardboard ring and transferring it onto a moisturized cellulose paper into a Petri dish (5.2 cm diameter). This experimental setup was considered as mini-subcolony.

The transferred ants were allowed to recover from the disturbance and repair any possible damage for 30 min. For each experiment all material was cleaned with ethanol

and allowed to dry. Different forceps were used to apply the control or the treated filter paper discs.

1 µL of a 3-octanone solution (100 nmol, 10 nmol, 1 nmol) in acetone or acetone as control were loaded onto a filter paper disc (ca. 0.1 cm^2) and introduced into the stabilized mini-subcolony. The filter paper discs were prepared in a separate room and transported to the behavioral assay in a closed Petri dish within 30 s. In a pairwise experimental design, the mini-subcolonies were first exposed to control filter discs for 30 min and the behavioral responses were video recorded using a Nikon D600 camera equipped with a macro objective AF-S Micro Nikkor fixed on a tripod (automatic iso settings, exposure time 1/30s, aperture F16) (**Figure S3.6**). Then the control experiment was stopped and the control filter disc was replaced with a 3-octanone-treated disc in the same mini-subcolony and video recording was resumed for another 30 min. The behavior of the individual ants was assessed in ten 5 s intervals by viewing the video always 5 s before 2, 4, 6, 8, 10, 12, 14, 16, 18 and 20 min, and counting the frequencies of the below-described behaviors (**Table 3.1**).

Only ants that were clearly visible and performed a specific hygiene or defense-related behavior were considered. E.g. if ants were covered by the fungus they were not evaluated. The behavioral categories that were studied were: tending, grooming, removal, freezing and ant grooming. For a definition of the different behaviors see the detailed description in **Table 3.1**. Hygienic behavior was defined as sum of fungus grooming, tending and removal.

Table 3.1: Behavioral responses examined in *A. octospinosus*, including their function and detection criteria

Behavior	**Function**	**Detection criteria**
Fungus grooming[32],[23]	Removal of pathogenic spores with mandibles, storage in infrabuccal pocket	• Antennae parallel to mandibles, stand still • Body stands still for >25 s • Head movement
Tending[88]	Treatment of the fungus surface with mouth parts	• Antennae point to fungus, move freely • Noticeable mandible movement

		• Licking fungus • Ants > 5 s at same position
Removal	Use of mandibles to remove infected fungus pieces	• Opening and closing of mandibles • Fungus material between mandibles • Loosening and dividing of fungus garden with mandibles
Freezing[89, 90]	Defensive posture and/or predator escape behavior	• Ants remain immobile, i.e., body stands still > 15 s • Freely moving antennae • Legs are spread and have contact to surface
Ant grooming[91, 92] Self-grooming Allo-grooming	Self-cleaning or cleaning each other	 • Freely moving antennae • Rubbing of legs against antennae and other legs • Front legs are moved through mandibles • Antennae point to body parts being cleaned • Mandibles contact the body of other ants

The frequency of occurrence of the different behaviors was calculated using the formula: frequency of a behavior in % = 100 times number of ants showing a particular behavior divided by the total number of ants in the mini-subcolony. For each mini-subcolony we determined an overall score by averaging the frequencies of all ten observation intervals. Then the mean behavioral response (± standard deviation) was calculated over 5 to 10 replicates per treatment.

The obtained data were analyzed using Statistica (Version 9.0, Statsoft). The collected data for the hygienic behaviors were tested for normal distribution by the Shapiro-Wilks-test. The effect of 3-octanone on the frequency of hygienic ant behaviors was evaluated by comparing treatment and control scores using a paired T-test.

Results

Co-cultivation of *E. weberi* and *L. gongylophorus*

In order to study how *L. gongylophorus* reacts to the attack by *E. weberi*, we co-cultivated both fungi on potato dextrose (PDA) agar plates. Because of its slow growth, *L. gongylophorus* was cultivated on agar plates for 14 d alone. Then, the well-grown *L. gongylophorus* was infected with *E. weberi*. After 2 d of growth *E. weberi* did not grow significantly faster on the co-culture plate than when it was cultivated alone. However, from the third day onwards, *E. weberi* grew 1.5 to 2 times faster on plates with *L. gongylophorous* present compared to when it grew alone (**Figure S3.1**). *E. weberi* completely overgrew *L. gongylophorus* by the fifth day.

Identification of an induced volatile in *E. weberi/L. gongylophorus* co-culture

To screen for potential signals from *L. gongylophorus* as response to the infection by *E. weberi*, we analyzed the volatile profile of single cultures and the co-culture for 10 d. The volatiles were collected by solid phase microextraction (SPME) and samples were subsequently analyzed by a gas chromatograph connected to a mass spectrometer (GC-MS). *L. gongylophorus* constitutively produced a large amount of diverse sesquiterpenes that account for its characteristic smell (**Figure 3.1A**). Apart from the sesquiterpenes, *L. gongylophorus* did not produce other GC-detectable volatile organic compounds above trace amount level. *E. weberi* did not release any volatile organic compounds in substantial amounts (**Figure 3.1B**).

When *L. gongylophorus* was infected with *E. weberi* in the co-cultivation scenario, a gradual reduction of the sesquiterpenes was observed (ca. 25 fold), that goes along with the decrease in biomass of *L. gongylophorus*. However, after ca. 4 d, a new volatile compound was detected by GC-MS in the volatile profiles of the co-culture at 8.5 min (**Figure 3.1C**). The compound exhibited a base peak ion at m/z 58 and a weak molecular ion at m/z 128. We identified the compound as 3-octanone based on its EI-mass spectrum and the comparison with an authentic 3-octanone reference compound (**Figure 3.2**).

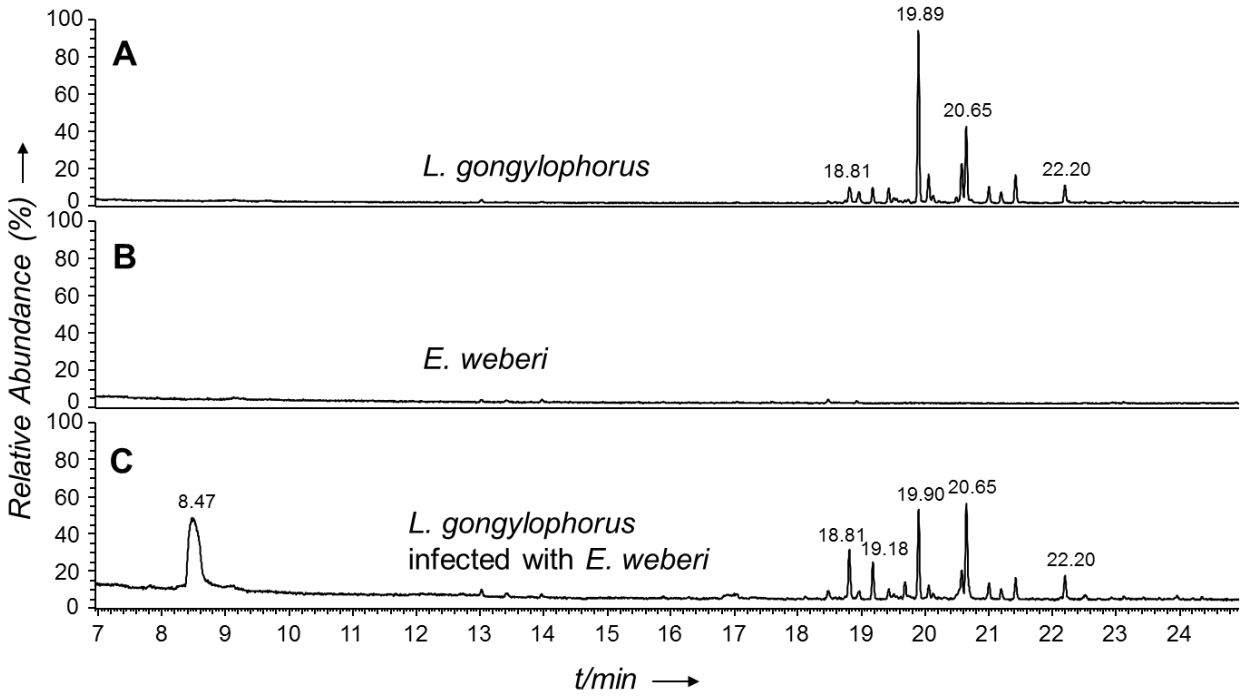

Figure 3.1: GC-MS profile of volatiles emitted by **A**) the 20 d old *L. gongylophorus*, **B**) 6 d grown *E. weberi*, and **C**) a 20 d grown *L. gongylophorus*/6 d grown *E. weberi* co-culture on PDA plates.

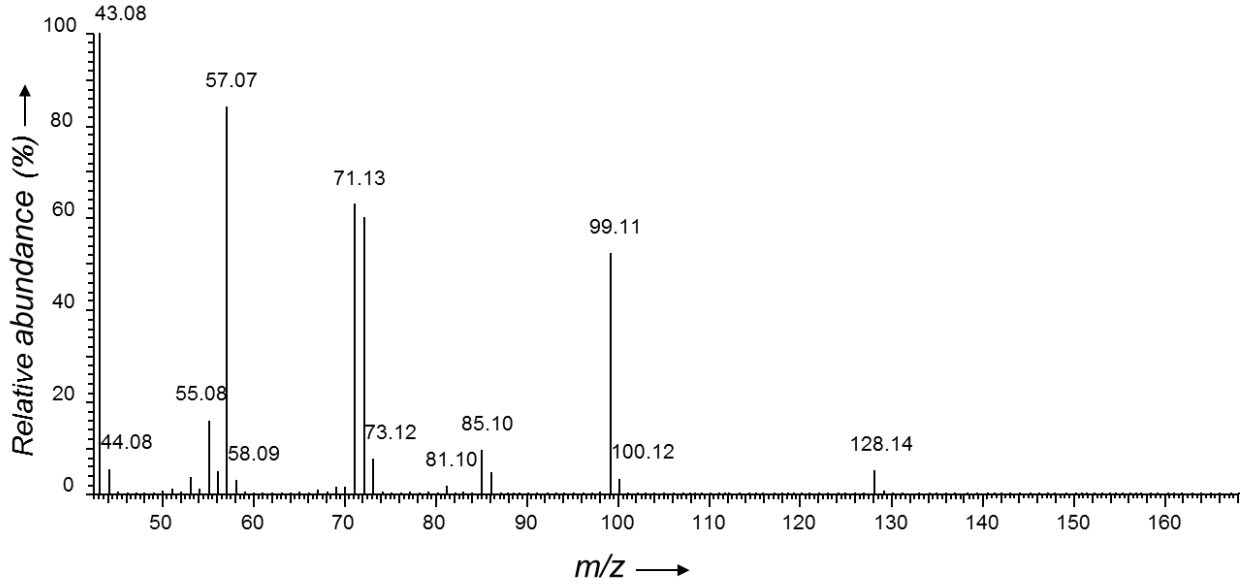

Figure 3.2: EI-MS (70 eV) of the induced volatile compound, 3-octanone, in *L. gongylophorus*/*E. weberi* co-culture.

Origin of 3-octanone

In order to investigate which organism produces 3-octanone, *L. gongylophorus* or *E. weberi*, we performed experiments with single cultures. Because we suspected 3-octanone to originate from peroxidation of linolenic acid from membrane lipids both fungi were exposed to freeze and thawing stress that can induce lipid peroxidation (**Figure S3.2**).[93]

After freezing and thawing, *L. gongylophorus* released 3-octanone in large amount (**Figure S3.2A**). When *E. weberi* was treated in the same way, it did not form any 3-octanone but it produced 1-octen-3-ol in large amount (**Figure S3.3**).

Biological function of 3-octanone

Antifungal properties of 3-octanone against *E. weberi*

To assess if 3-octanone could directly act against the attacking *E. weberi*, a bioassay was performed: 3-octanone (6.3 µmol per plate) was applied on a filter paper disk in one compartment of a three compartment Petri dish and *E. weberi* was inoculated onto SFM medium in another compartment. The growth of *E. weberi* was monitored for 5 d and compared to control samples. *E. weberi* was not inhibited (**Figure S3.5**).

3-Octanone is recognized by *A. octospinosus* workers

Mini-subcolonies of *A. octospinosus* in a Petri dish were used in order to study how the ants respond to 100, 10, 1 nmol 3-octanone dissolved in acetone. For this, a mini-subcolony was exposed to 3-octanone applied onto a filter paper disc compared to an acetone treated control filter paper disc (for experimental setup see **Figure S3.6**). The ants' hygienic behavior was evaluated by analyzing video recordings of hygienic behavior and assessing ant behavioral responses including fungus grooming, tending, and removal at given time points. In addition, we examined whether the ants respond to 3-octanone with defensive behavior, namely freezing and self-grooming/allo-grooming.

When 100 nmol 3-octanone paper disks were introduced into the mini subcolony, the ants responded with a 1.8 times increase of the hygienic activities compared to the control filter paper disc. The sum parameter of all hygienic activities was statistically highly significant (mean treatment: 8.2 %, mean control: 4.6 %, df = 9, t = -4.643, p =

0.0012) (**Figure 3.3A**). Looking at the different hygienic behaviors, tending activity was induced by 3-octanone the most (mean treatment: 6.1 %, mean control: 3.2 %, df = 9, t = -4.161, p = 0.002). Fungus grooming was also significantly induced (mean treatment: 1.1 %, mean control: 0.2 %, df = 9, t =-3.067, p = 0.013). In contrast, for the removal a slight, non-significant decrease was observed for filter paper discs treated with 100 nmol 3-octanone compared to the paper filter disc controls (mean treatment: 1.0 %, mean control: 1.2 %, df = 9, t = 0.440, p = 0.669) (**Figure 3.3B**).

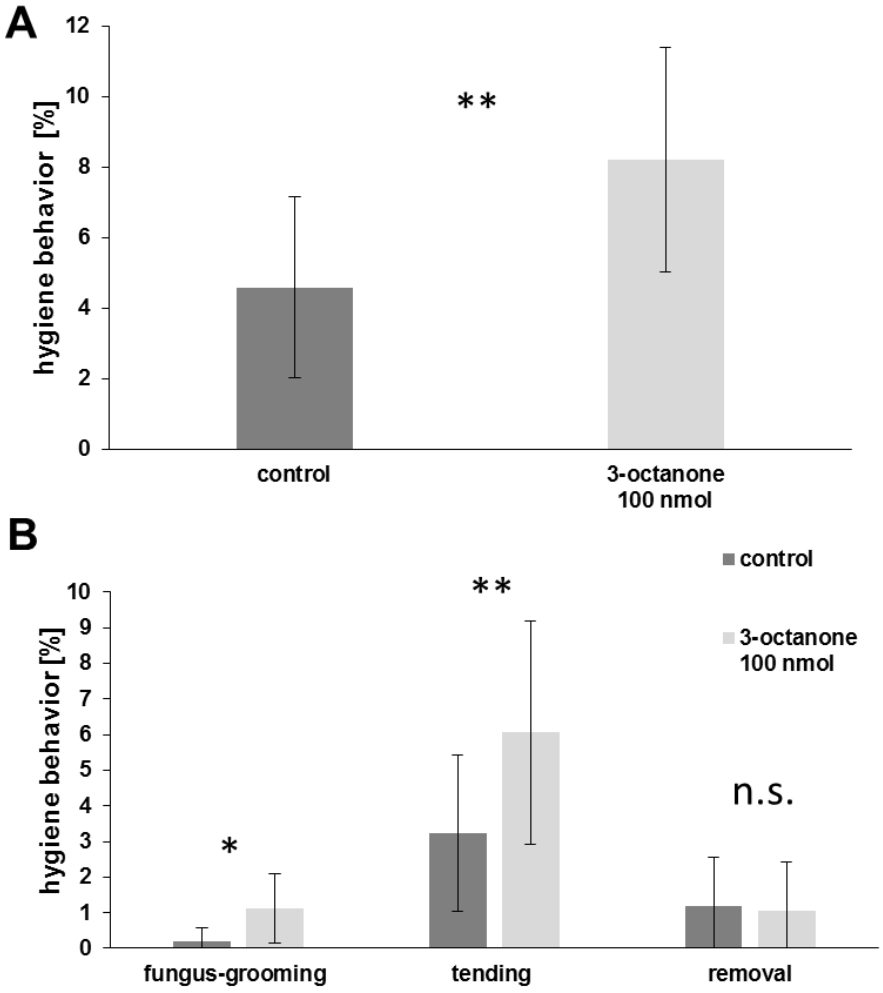

Figure 3.3: Hygienic behaviors of leaf-cutting ants in response to 3-octanone (100 nmol) **A**) hygienic behavior, **B**) tending fungus grooming and removal. Mean of the frequency of the ant workers behavior is given in %. Error bars reflect the standard variation, number of replicates n = 10, * p< 0.05, ** p< 0.01, n.s. not significant.

A decrease of the 3-octanone by factor 10, i.e. 10 nmol, still resulted in a significant 2.3 times increase of the sum of all hygienic behaviors compared to the control experiments (mean treatment: 6.3 %, mean control: 2.7 %, df = 4, t = -3.771, p = 0,019, **Figure 3.4A**). However, while the individual fungus cleaning behaviors increased at 10 nmol 3-octanone, the differences between treatment and control were not significant for fungus tending (mean treatment: 4.4 %, mean control: 1.9 %,df = 4, t = -2.218, p = 0.091), grooming (mean treatment: 0.6 %, mean control: 0%, df = 4, t = -1, p = 0.373) and removal (mean treatment: 1.4 %, mean control: 0.7 %, df = 4, t = -1.002, p = 0.372, **Figure 3.4B**). In a preliminary pilot experiment with 1 nmol 3-octanone, no statistically significant differences between control and 3-octanone treatments could be observed (data not shown).

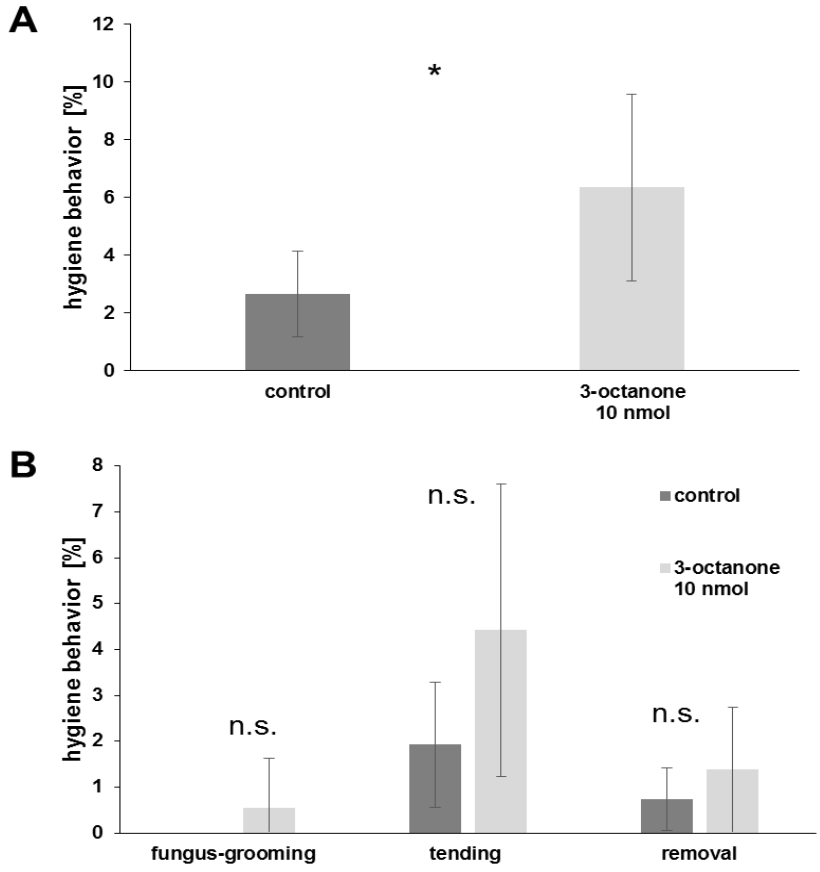

Figure 3.4: Hygienic behavior of leaf-cutting ants in response to 3-octanone (10 nmol) Mean of the frequency of the ant workers behavior is given in %. Error bars reflect the standard deviation, number of replicates n=5, * p< 0.05, n.s. not significant.

In addition to fungus hygienic behavior, we investigated the impact of 3-octanone on defensive responses of *A. octospinosus* ants: freezing and ant grooming (self-grooming and allo-grooming).

At 100 nmol 3-octanone freezing behavior did not change between control and treatment (mean treatment: 4.8 % mean control: 3.8 %, df = 9, t = 0.369, p = 0.720), whereas ant grooming activity increased but was not statistically significant (mean treatment: 6.4 %, mean control: 3.1 %, df = 9, t = -1.357, p = 0.207, **Figure 3.5**).

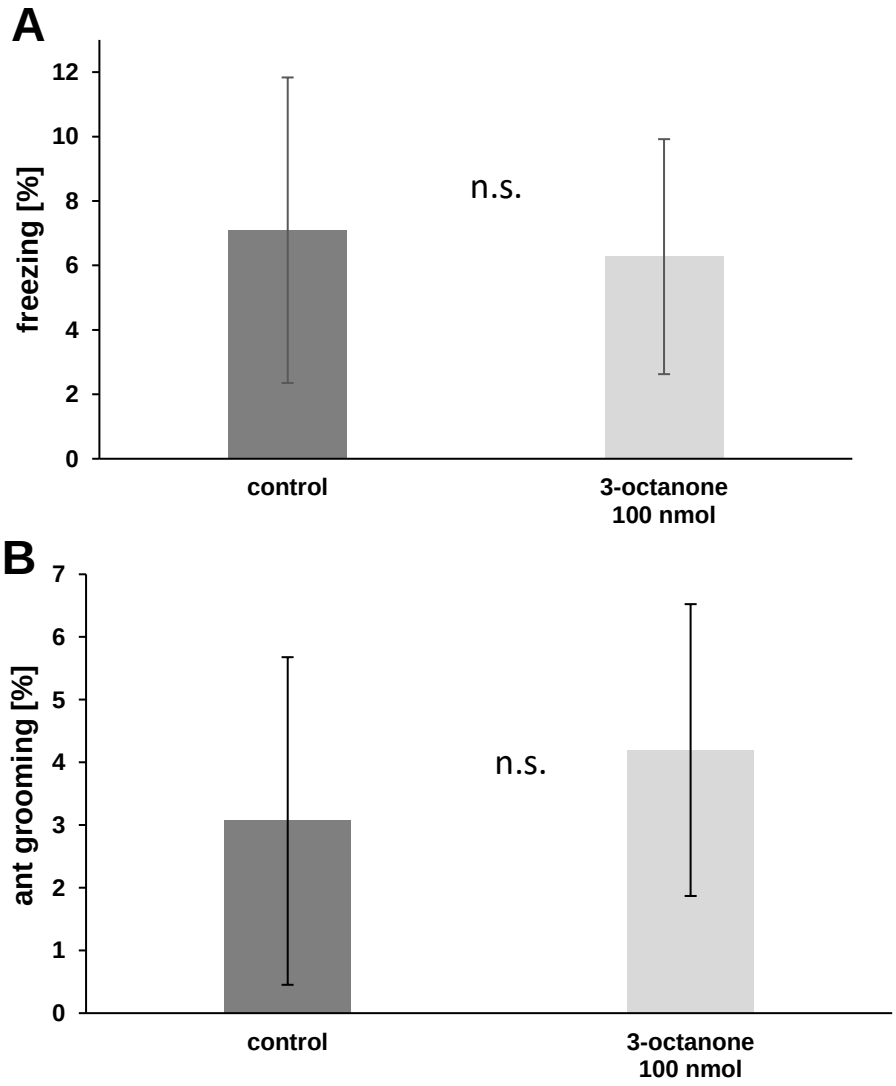

Figure 3.5: Influence of 3-octanone (100 nmol) on defense behaviors: **A**) freezing, and **B**) ant grooming. Mean of the frequency of ant workers showing the behavior in %. Error bars reflect the standard variation, number of replicates n=10, n.s. not significant.

Likewise, at 10 nmol, 3-octanone grooming intensity remained insignificant, although *A. octospinosus* workers engaged about twice as often in grooming as compared to the control, but with high standard deviation (ant grooming: mean treatment: 6.4 %, mean control: 3.1 %, df = 4, t = -2.001, p = 0.115, **Figure 3.5**). Freezing behavior in the presence of 10 nmol 3-octanone appeared to be not different between treatment and control experiments (mean treatment: 4.8 % mean control: 3.8 %, df = 4, t = -0.653, p = 0.549, **Figure 3.6**).

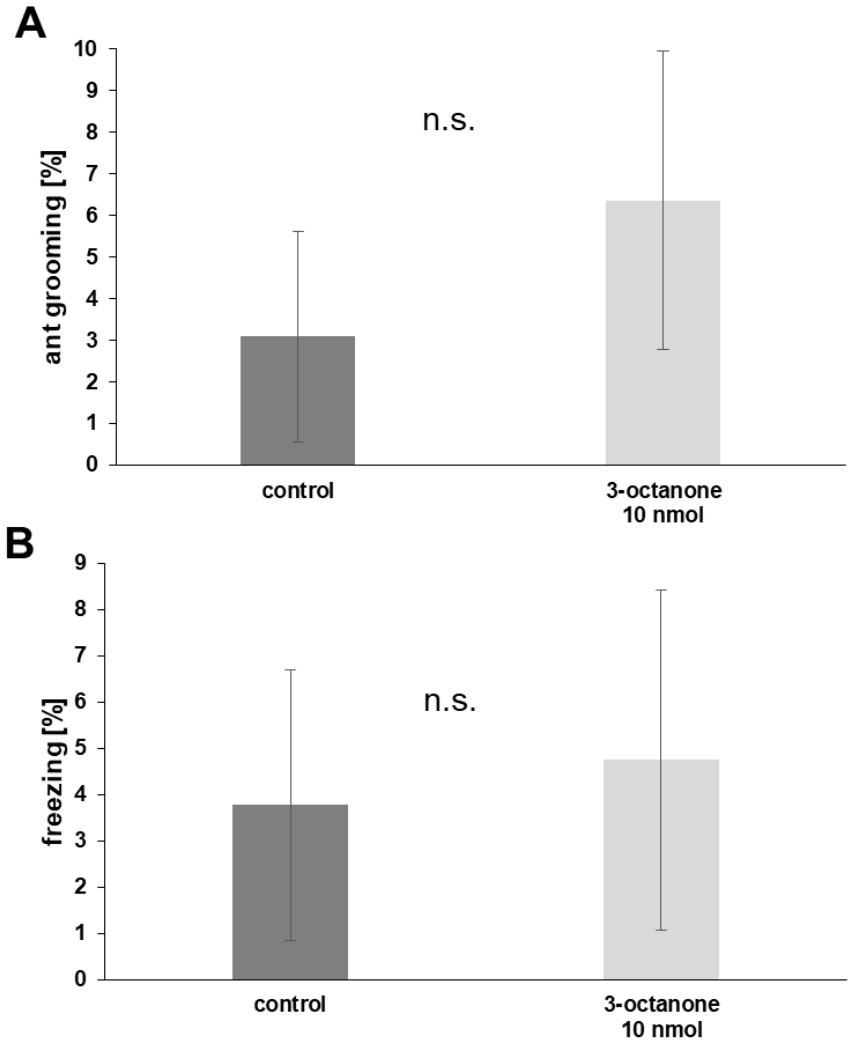

Figure 3.6: Influence of 3-octanone (10 nmol) on defense behaviors: **A**) freezing, and **B**) ant grooming. Mean of the frequency of ant workers showing the behavior in %. Error bars reflect the standard variation, number of replicates n=10, n.s. not significant.

Discussion

Leaf-cutting ants live in mutualistic symbiosis[41] with their garden fungus *L. gongylophorus*. This relationship established 50 million years ago[32] and both partners co-evolved and depend on each other as the ants maintain *L. gongylophorus* and depend on its enzymatic capabilities to supply them with accessible nutrients.[22] For such a partnership, it is evident that they need to exchange information.

However, little is known about how the partners may communicate. Still we know that leaf-cutting ants clearly recognize the needs of their garden fungus. For example, the ants maintain the ideal microclimate[94] and also select different food plants if the plant material is unsuitable for the fungus. The latter might be recognized due to a signal from the fungus.[69, 70] Pathogenic attack, in particular by the specialized *E. weberi*, comprises a major threat to both *L. gongylophorus* and the leaf-cutting ants. Clearly, the ants respond with specialized behavior and chemical treatment.[29, 31] How do the ants recognize *E. weberi* and are there signals from *L. gongylophorus* involved? When analyzing the reaction of *L. gongylophorus* to *E. weberi* attack using co-cultures 3-octanone was strongly induced within ca. 5 d, when *E. weberi* overgrows *L. gongylophorus* (**Figure S3.1**). In contrast, the terpenoids of the volatile signature of *L. gongylophorus* did not change in their relative peak ratio to each other despite decreasing in intensity.

3-Octanone has been already described in the context of *Acromyrmex* leaf-cutting ants as a component of the mandibular alarm pheromone.[95-97] This interesting coincidence suggests that the ants should be able to make use of 3-octanone from the garden fungus as signal. A similar observation was very recently made by Silva *et al*., who recognized that pyrazines that are known to act as trail- and alarm-pheromones of leaf-cutting ants are produced by their associated microbial symbionts.[98] However, the authors did not demonstrate if the microbially produced pyrazines induce a particular response in the respective leaf-cutting ants. Producing the same chemicals predestinates those compounds as potential interspecies signals of symbiotic partners. Still a problem occurs: how do the receivers react with the right response to an identical signal. This might depend on the context of the potential signal for example, when, where, and how it is released, and also which other compounds accompany it.[99]

A. octospinosus leaf-cutting ants react to 3-octanone with increased hygienic behavior. In particular, tending and also grooming activity was increased. At 10 nmol and 100 nmol, 3-octanone the total hygienic activities almost doubled (**Figure 3.3A/3.4A**), while the amount of 1 nmol was too low to observe a statistically significant difference.

While our bioassay with filter paper discs may not perfectly mimic an infected fungus, it clearly presents one of probably several cues to induce cleaning behavior. The observed clear, dose-dependent response of the ants to 3-octanone, suggests a decisive role in interspecies communication of leaf-cutting ants and their symbiotic garden fungus.

3-Octanone was emitted from *L. gongylophorus* without any traces of 3-octanol which was found to accompany 3-octanone in the alarm pheromone.[96] This may modulate different behavior as well as the additional sequiterpenoid volatiles in the blend of *L. gongylophorus*. We did not see strongly pronounced defensive behavior. More specifically, freezing was not induced, whereas ant-grooming was induced - although not statistically significant at - 10 and 100 nmol 3-octanone. Ant-grooming has been identified as an important defense mechanism against fungal parasites and thus contributes to avoid further contamination of the fungus garden with *E. weberi* (**Figure 3.5/3.6**).[92] Upon cell damage by *E. weberi*, *L. gongylophorus* releases 3-octanone. Any severe cell damage triggers lipid peroxidation. In fungi, linoleic acid from the lipid membranes is oxidized by a 10-Lipoxygenase to 10-hydroperoxyoctadecadienoic acid which undergoes breakdown to C-8 volatiles 3-octanone or 3-octen-1-ol (**FigureS3.4**).[93] The common fungus odor 3-octen-1-ol is formed by stressed *E. weberi* whereas 3-octanone is released by *L. gongylophorus,* which allowed us to assign the 3-octanone formation to *L. gongylophorus* in our co-cultivation experiment.

In summary, *L. gongylophorus* forms and releases 3-octanone when it is under attack by *E. weberi*. Leaf-cutting ants respond to it with increased nest hygiene. Thus, 3-octanone from *L. gongylophorus* can constitute a cry for help signal.

Clearly, 3-octanone will likely not be the only cue triggering the ants' hygienic behavior. We assume that 3-octanone in concert with other stimuli such as tactile cues of the pathogenic spores and/or additional (volatile) compounds, for example from the cleaning ant workers, are recognized by the ants and result in efficient nest hygiene. It

is unfortunately impossible to monitor this chemical communication directly in the microenvironment of the infected site in the nest due to instrumental detection limits and the complexity of the natural environment of the microcosmos of leaf-cutting ants. Future structure elucidation of other potential signals, e.g. the *L. gongylophorus* sesquiterpenes, improved bioassays considering and combining different aspects mimicking as good as possible the nest conditions will be needed to further uncover the fascinating communication within the microcosmos of leaf-cutting ants.

Acknowledgement

We gratefully acknowledge language editing and helpful comments by Dr. Anthony Farlow. We are greatly indebted to the Konstanz Research School Chemical Biology funded by the Deutsche Forschungsgemeinschaft for financial support and a doctoral fellowship to BD.

Chapter 4: Ammonia production by the *Streptomyces* sp. Av25_4 symbiont of the leaf-cutting ant *Acromyrmex volcanus* strongly inhibits the growth of the pathogenic fungus *Escovopsis weberi*

Ammonia production by the *Streptomyces* sp. Av25_4 symbiont of the leaf-cutting ant *Acromyrmex volcanus* strongly inhibits the growth of the pathogenic fungus *Escovopsis weberi*

Basanta Dhodary[1], Sören Radke[1], and Dieter Spiteller[1]*

[1]Chemical Ecology/Biological Chemistry, University of Konstanz, Universitätsstrasse 10, 78457 Konstanz, Germany.

Abstract

Acromyrmex volcanus leaf-cutting ants live in mutualistic symbiosis with their garden fungus *Leucoagaricus gongylophorus* that can be attacked by the specialized pathogenic fungus *Escovopsis weberi*. *Actinomyces* microbial symbionts from the integument of *A. volcanus* contribute to protect *L. gongylophorus* against pathogens. The symbiont *Streptomyces* sp. Av25_4 exhibited strong activity against *E. weberi* in co-cultivation assays. Experiments with agar plates physically separating *E. weberi* and *Streptomyces sp*. Av25_4 by a plastic barrier allowing only exchange of volatiles revealed that *Streptomyces* sp. Av25_4 produces volatile antifungals. Closed loop stripping and GC-MS analysis indicated that *Streptomyces* sp. Av25_4 produces nonanal and benzaldehyde that inhibit the growth of *E. weberi* rather at high concentration. During screening for volatiles that cannot be easily detected by GC-MS, ammonia produced by *Streptomyces* sp. Av25_4 (ca. 8 mM) was identified which completely inhibited the growth of *E. weberi* due to its strong basic pH. In contrast to metabolically complex and costly secondary metabolites, such as polyketides, *Streptomyces* symbionts that release simple ammonia in elevated quantities can contribute to the control of *E. weberi*.

Key words: antifungal, closed loop stripping, bioassay, nonanal, benzaldehyde, volatiles.

Introduction

Leaf-cutting ants, such as *Acromyrmex volcanus*, live in mutualistic symbiosis with the fungus *Leucoagaricus gongylophorus,* which the ants cultivate in their nests with leaf material they cut and process into small pieces. The garden fungus breaks down the plant material and serves the ants as a food source.[77, 78]

However, pathogens, in particular the specialized fungus *Escovopsis weberi*, can overgrow *L. gongylophorus* and thus threaten the survival of whole ant colonies.[3, 46, 100] Thus, in addition to own cleaning behavior and chemical treatment with compounds from the metapleural gland[29, 101, 102] *Acromyrmex* leaf-cutting ants are supported by microbial symbionts on their integument to fight with antifungals against *E. weberi*.[4] In the last years, a growing variety of polyketide and non-ribosomal peptide antifungals e.g. candicidin,[39] dentigerumycin,[82, 103] nystatin P1,[83] or antimycins,[40, 104] have been characterized from microbial symbionts of different leaf-cutting ant species.

Among the isolated *Actinomycetes* from the leaf-cutting ant *A. volcanus* we had obtained *Streptomyces* sp. Av25_4.[39] This strain exhibited pronounced activity against *E. weberi* when both were co-cultivated together on soy flour medium agar plates. Therefore, we got interested in how *Streptomyces* sp. Av25_4 inhibits the growth of *E. weberi*.

Here, we present our findings on the simple strategy *Streptomyces* sp. Av25_4 uses in contrast to many of the already studied microbial symbionts of leaf-cutting ants that rely on the production of complex secondary metabolites.

Materials and Methods

Chemicals

Activated charcoal, agar agar Kobe I, and mannitol were purchased from Carl Roth (76185 Karlsruhe, Germany). Soy flour (Hensel Bio-Voll-Soja) was from W. Schoenenberger GmBH Co. KG (71106 Magstadt, Germany).[87] HPLC grade methanol was purchased from VWR International GmbH (John-Deere-Str. 5, 76646 Bruchsal, Germany). Ethyl acetate was distilled before use. For preparation of media, double distilled water was used. All other chemicals were from Sigma-Aldrich (82024 Taufkirchen, Germany). Petri dishes were purchased from Greiner Bio-One GmbH (Maybachstraße 2, 72636 Frickenhausen, Germany).

Streptomyces symbionts, fungal strains and cultivation conditions

Streptomyces strains used in this work were isolated previously from *A. volcanus* and *A. echinatior* ants.[40] The microorganisms were cultivated on soy flour (SFM) agar plates (20 g soy flour, 20 g mannitol, 15 g agar 1L ddH_2O)[87] at 28 °C. *E. weberi* CBS 110660 was obtained from Westerdijk Fungal Biodiversity Institute (Utrecht, the Netherlands) and *Fusarium equiseti* FSU 5459 was from the Jena Microbial Resource Collection (JMRC, Jena, Germany). The fungal strains were cultivated at 28 °C on either SFM agar or potato dextrose agar (PDA) plates.

Screening *Streptomyces* symbionts for antifungal volatile compounds

Ten *Streptomyces* isolates (**Table S4.1**) from leaf-cutting ants were screened for their ability to produce antifungal volatiles using three compartment Petri dishes divided by a plastic barrier.

A *Streptomyces* symbiont was spread onto SFM medium in one compartment. The plates were wrapped by parafilm in order avoid potential contamination with external volatiles from other strains and incubated at 28 °C. After 3d, 80 µL of an *E. weberi* spore suspension was spread uniformly on the two remaining compartments of the divided plate containing SFM medium, and plates were again sealed with parafilm. As control, *E. weberi* was grown alone in the same way. The growth of *E. weberi* was monitored 5 d after inoculation of *E. weberi*. All bioassays were performed in triplicate per symbiont.

The strain *Streptomyces* sp. Av25_4 inhibited the growth of *E. weberi* mycelium completely and was therefore selected for detailed investigations.

Trapping volatiles released by *Streptomyces* sp. Av25_4 and evaluation of the consequences on *E. weberi* growth

Three compartment Petri dishes were used for the experiment (**Figure 4.1**). As a positive control, in the first compartment, *Streptomyces* sp. Av25_4 was spread on SFM medium whereas in the second compartment containing PDA medium *E. weberi* was introduced in the center on an agar plug (6 mm diameter). The agar plug originated from a PDA plate of actively growing *E. weberi*. The third compartment was left empty.

For the volatile trapping experiment, the third compartment was filled with 2 g of activated charcoal in order to adsorb the volatiles released by *Streptomyces* sp. Av25_4 and investigate their effect on the growth of *E. weberi*. The Petri dishes were sealed with parafilm after inoculation with *E. weberi* and further incubated for 5 d at 28 °C. As negative control, *E. weberi* was grown alone in the compartment containing PDA medium. The area of fungal growth was calculated by using image J 1.52a software. Each bioassay was at least performed in triplicate.

Closed loop stripping of volatiles and GC-MS analysis

Streptomyces sp. Av25_4 was cultivated on SFM medium at 28 °C for 7 d. Then the emitted volatiles were sampled. Through two holes in side of the agar plate a closed-loop stripping pump (3V power supply, Fürgut, 88459 Tannheim, Germany,) fitted with an activated charcoal filter (1.5 mg, CLSA, le Ruisseau de Montbrun, F-0935 Daumazan sur Arize, Frankreich) was inserted into the head space and the volatiles were collected for 1h.[105] The collected volatiles were eluted from the charcoal filter with ethyl acetate (3 x 25 µL). The extract was analyzed by GC-MS using a Trace GC Ultra hyphenated with an ISQ quadrupole mass spectrometer (Thermofisher, 63303 Dreieich, Germany). Separation was performed with an Optima 5 MS column (30 m x 0.25 mm, film 0.25 µm, Macherey-Nagel GmbH & Co. KG**,** Neumann Neander Strasse 6-8, D-52355 Düren, Germany). GC-MS conditions: inlet temperature 280 °C, splitless injection, hydrogen served as a carrier gas (0.7 mL/min). The volatile metabolite profiles were recorded

using the following temperature program: 50 °C isotherm for 3 min, 6 °C/min to 200 °C, 20 °C/min to 260 °C, 260 °C isotherm for 1 min. The mass spectrometer was operated in electron impact positive ionization mode at 70 eV. The EI mass spectra of the volatile compounds were analyzed and suspected compounds were identified by comparing their retention time and mass spectra with authentic reference compounds.

Antifungal volatile compounds produced by *Streptomyces* sp. Av25_4

Five compounds were identified in the GC-MS profile of *Streptomyces* sp. Av25_4 that we either suspected to inhibit or were present in the volatile profile in large amount were tested for their antifungal activity against *E. weberi*. For the bioassay, the three compartment Petri dish was used. In a preliminary screening, 10 µL of the respective test compound were dropped onto sterile filter paper discs (1.5 cm diameter) and placed in an empty compartment of divided agar plate. *E. weberi* agar plugs (6 mm diameter) were introduced onto the PDA medium-containing compartment of the divided Petri dish. The Petri dish was sealed tightly by parafilm. The growth of *E. weberi* was monitored daily for 5 d. In order to determine the minimal inhibitory concentration of benzaldehyde and nonanal as well as the mixture of both compounds they were tested at different concentrations (0.5 -14.5 µmol in methanol, see **Table S4.2** and **S4.3**). The growth of *E. weberi* in presence of the test compounds was followed for 5 d and compared to solvent controls. Each concentration was at least tested in triplicate.

Change of the pH upon growth of *Streptomyces* sp. Av25_4

The change of the pH in the growth medium was monitored by using phenol red as pH indicator. *Streptomyces* sp. Av25_4 was spread on the SFM medium of the first compartment. The other two compartments contained SFM medium with 0.002 % of phenol red as pH indicator. The plates were sealed with parafilm and the color change in the medium was recorded by taking pictures at 4, 7, and 10 d after incubation.

Detection of ammonia

Whether *Streptomyces* sp. Av25_4 produces ammonia or not was investigated by using ortho-phathaldialdehyde (OPA) derivatization and fluorescence detection of the

resulting derivative, as well as by ^{1}H NMR analysis.[106] The OPA derivatization reagent was prepared by mixing 10.5 mg OPA dissolved in 210 µL methanol and 10.5 mg of sodium sulfite dissolved in 630 µL of sodium phosphate buffer (100 mM, pH adjusted to 12.0 with 2M NaOH). *Streptomyces* sp. Av25_4 was grown for 7 d at 28 °C on SFM agar plates. Ten plates with fully-grown *Streptomyces* sp. Av25_4 were transferred into an exsiccator (2.5 L) that was closed with a septum. A CLS pump was used to directly transfer the volatiles released within 1 h by *Streptomyces* sp. Av25_4 from the exsiccator into the OPA derivatization solution (20 µL of OPA reagent in 500 µL of phosphate buffer) in a 4 mL glass vial (**Figure S4.7**).

Similarly, a CLS pump was used to directly transfer the volatiles released within 3 d by 6 days grown *Streptomyces* sp. Av25_4 from the exsiccator (size 2.5 L, 10 SFM agar plates) into the 250 mM HCl solution (500 µL prepared in ddH_2O) in a 4 mL glass vial. 10 % DMSO-d6 was added for calibration of the NMR spectrometer. ^{1}H-NMR spectra were recorded for the obtained solution of the collected volatiles, a solvent control and an equally prepared ammonium standard using a Bruker Avance III 600 spectrometer (Bruker BioSpin GmbH, 76287 Rheinstetten, Germany) with water suppression.

Quantification of ammonia produced by *Streptomyces* sp. Av25_4

From the *E. weberi*/*Streptomyces* sp. Av25_4 co-culture bioassays, where the strains were separated by a plastic barrier using the three compartment plates (see above), an agar plug (1 cm^2) was taken from the PDA agar compartment in which *E. weberi* was inoculated. The agar plugs were collected into 2 ml Eppendorf tubes at different time points (2 d, 4 d, 6 d, 8 d, 10 d, and 12 d) and stored at -20 °C. After freezing and thawing of the samples, the released liquid was collected by centrifugation at 16000 rpm for 3 min. 20 µL of the obtained liquid was diluted with 500 µL of 0.1 M phosphate buffer (pH 12.0) and derivatised with 20 µL of OPA reagent. The derivatised samples were kept in the dark for 30 min at room temperature and analyzed using a Dionex Ultimate 3000 UHPLC system connected to a Dionex RF 2000 fluorescence detector. UHPLC method: HPLC column: Thermo Scientific Accucore RP-MS column: 150 x 2.1, 1.5 µm); solvent A: H_2O 0.1 % acetic acid, solvent B: MeOH 0.1 % acetic acid; gradient elution: 35%-100% B in 20 min, 5 min 100 % B.

The fluorescence intensity of thus formed fluorescent product was measured at emission wavelength of 420 nm after excitation at 360 nm.[106]

Ammonia was quantified by comparison of the peak areas to an external calibration curve (2.5, 5, 7.5, 10 mM ammonia). All values where at least determined in triplicate.

Similarly, the amount of ammonia that accumulated in the PDA agar compartment with *E. weberi* in the bioassay where ammonia (5 mM, 7 mM, 9 mM, and 11 mM, see above) was supplied into one compartment of the three compartment agar plate was determined.

Influence of ammonia on the growth of *E. weberi*

In order to study how ammonia affects the growth of *E. weberi* the three compartment Petri dish was used. The first compartment containing PDA medium was inoculated with an *E. web*eri agar plug (6 mm diameter). The second compartment was supplemented with 5 mL of 5, 7, 9, 11 mM ammonia solution and the third compartment was left empty. The Petri dishes were sealed with parafilm and further incubated for 5 d at 28 °C. For the control plates, sterile water was added instead of the ammonia solution. Each concentration was at least tested three times. The area of fungal growth was calculated by using image J 1.52a software.

Influence of medium alkalinisation on the growth of *E. weberi*

The growth of *E. weberi* on SFM agar plates at pH 7.5, 8.0, and 8.5 was monitored. The SFM agar plates were inoculated with an *E. weberi* agar plug (6 mm diameter). The pH of SFM medium was adjusted by using 3 M sodium hydroxide solution. The growth of *E. weberi* was analyzed after 5 d of incubation. Each pH was at least reproduced three times.

Testing *Streptomyces* sp. Av25_4 for HCN production

In order to investigate whether *Streptomyces* sp. Av25_4 produces HCN or not, the method described by Castric and Castric[107] was used. Briefly, filter paper disks of 1.5 cm diameter were soaked in the reagent mixture containing 5 mg/mL of copper (II) ethyl acetoacetate and 4, 4'-methylenebis-(*N*, *N*-dimethylaniline) in chloroform. The paper

disks were dried and exposed to the volatiles produced by the *Streptomyces* sp. Av25_4 after 3 d to 13 d of growth.

Results

Streptomyces sp. Av25_4 produces antifungal volatiles

Streptomyces symbionts were screened for the production of volatile compounds that inhibit the growth of the pathogenic fungus *E. weberi* by using three compartment Petri dishes so that *E. weberi* and the *Streptomyces* isolates grow physically separated from each other by the plastic barrier. Only volatile compounds can be exchanged by both strains in this experimental design (**Figure S4.1** and **Table S4.1**). The volatile compounds of one of the tested strains, *Streptomyces sp.* Av25_4, completely inhibited the growth of *E. weberi* (**Figure 4.1**). Therefore, *Streptomyces* sp. Av25_4 was selected in order to reveal which compound(s) is/are responsible for the observed antifungal activity. By adding activated charcoal to the assay that adsorbs the volatiles from *Streptomyces* sp. Av25_4 to some extent, we observed a clear decrease of the antifungal effect against *E. weberi* leading to 42 ± 11 % increase in the area covered by *E. weberi* compared to the control (**Figure 4.2**).

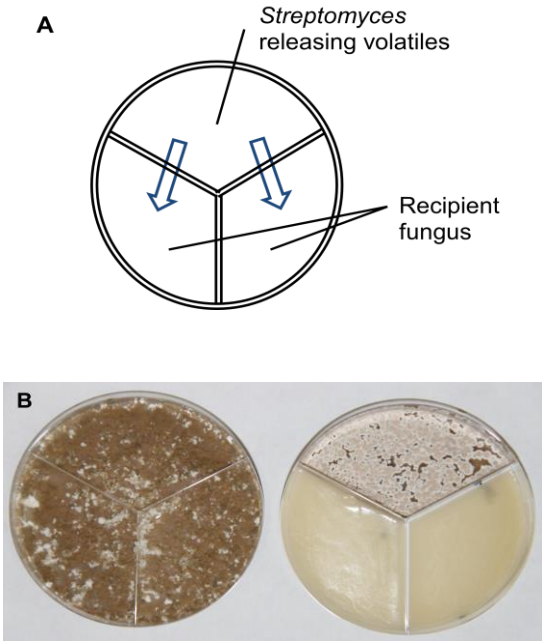

Figure 4.1: Screening *Streptomyces* symbionts of leaf-cutting ants for volatile antifungal compounds that inhibit *E. weberi.* **A**) Scheme of the experimental set-up in a three compartment Petri dish. **B**) Volatiles emitted by *Streptomyces* sp. Av25_4 completely inhibited the growth of *E. weberi.*

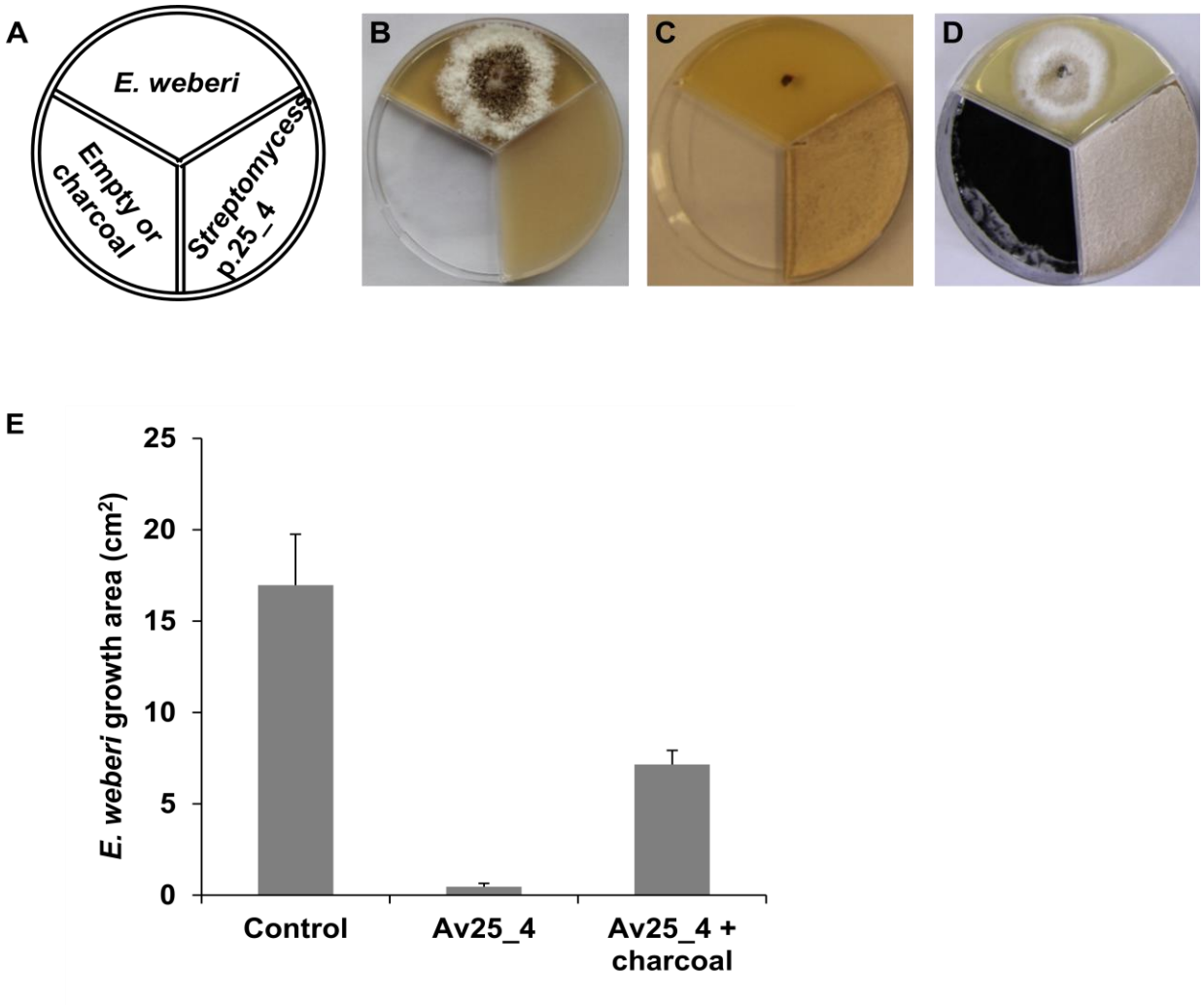

Figure 4.2: Antifungal activity of volatiles produced by *Streptomyces* sp. Av25_4 against *E. weberi* with and without activated charcoal in the third compartment. **A**) Scheme of the experimental setup. **B**) *E. weberi* grown for 4 d in the first compartment. **C**) *E. weberi* grown for 4 d in first compartment and *Streptomyces* sp. Av25_4 grown for 7 d in the second compartment. **D**) *E. weberi* grown for 4 d in the first compartment, *Streptomyces* sp. Av25_4 grown for 7 d in the second compartment and 2 g activated charcoal in the third compartment. **E**) Quantification of the *E. weberi* growth area analysed by image J 1.52a.

Analysis of volatiles from *Streptomyces* sp. Av25_4

In order to study the volatile compounds released by *Streptomyces* sp. Av25_4, the volatile compounds were collected using closed loop stripping (**Figure S4.3**). GC-MS analysis revealed a range of organic compounds, such as alcohols, ketones, aldehydes, terpenes, and lactones. Five compounds, namely geosmin, 2-methyl isoborneol, 2-phenyl ethanol, nonanal, and benzaldehyde were selected because they were both most abundant and some of them were also suspected to exert antifungal activity against *E. weberi* (**Figure 4.3**). Among the five compounds tested, only nonanal and benzaldehyde inhibited *E. weberi* growth. The minimum inhibitory concentration for benzaldehyde lay between 2 µmol/plate and 1 µmol/plate whereas for nonanal the minimum inhibitory concentration was between 3.5 µmol/plate and 1.7 µmol/plate (**Table S4.2** and **Table S4.3**).

Because nonanal and benzaldehyde are produced by *Streptomyces* sp. Av25_4 in the co-cultivation assay with *E. weberi* in ca. 0.22 and 0.04 nmol/plate respectively, these compounds can not account for the observed complete growth inhibition of *E. weberi* by volatiles from *Streptomyces* sp. Av25_4.

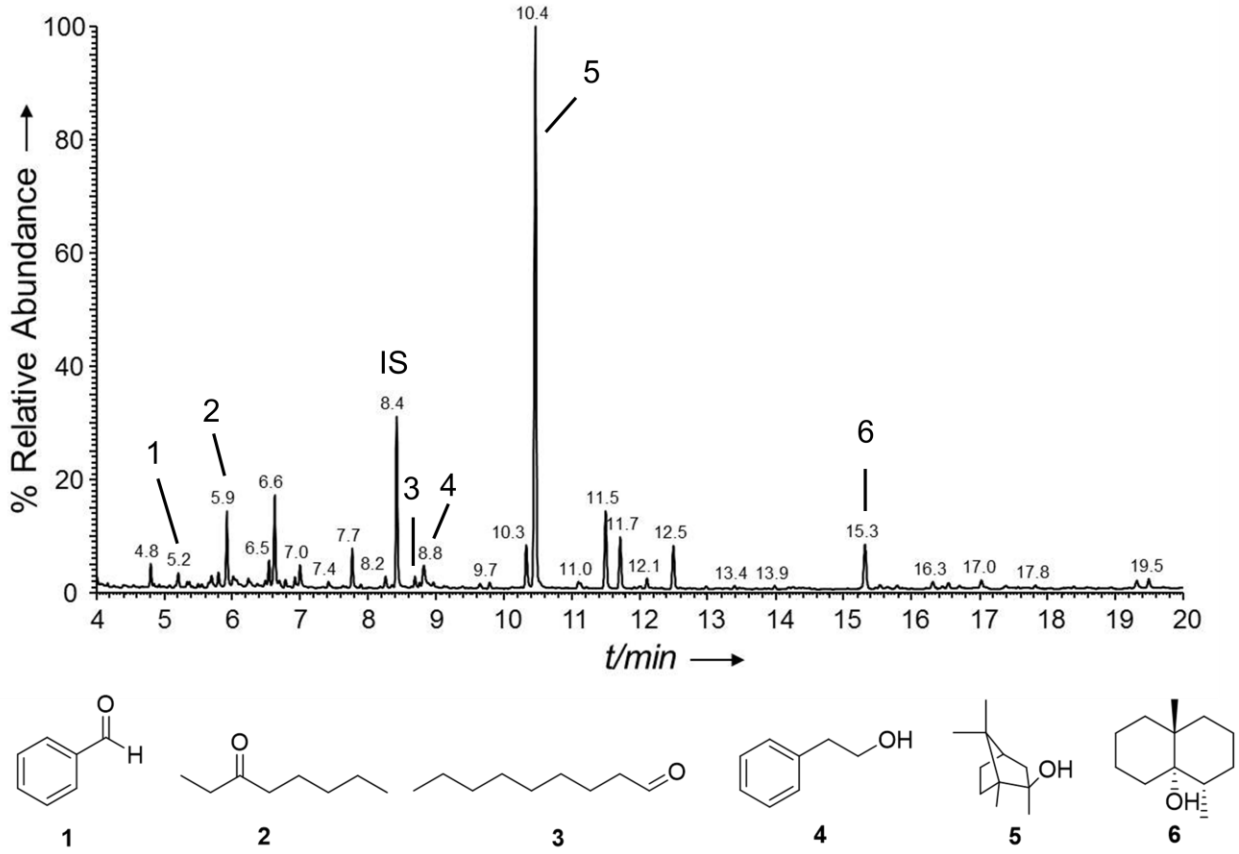

Figure 4.3: Collection of volatiles produced by *Streptomyces* sp. Av25_4 grown on SFM agar and their GC-MS analysis. TIC chromatogram of the volatiles produced by *Streptomyces* sp. Av25_4.

Alkalinisation of the growth medium

Because we suspected that *Streptomyces* sp. Av25_4 produces another volatile compound that is crucial for the inhibition of the growth of *E. weberi* than the identified aldehydes, we sought out to look for highly polar and volatile compounds, such as amines, that cannot be detected by standard GC-MS analysis.

In a first experiment, we investigated if volatiles from *Streptomyces* sp. Av25_4 alter the pH of the *E. weberi* growth medium using the three compartment Petri dish. To monitor any pH change, the medium was supplemented with the pH indicator phenol red.[108] Upon alkalinisation phenol red changes its color form pale yellow to bright pink. The pink colorization of the growth medium indicated that *Streptomyces* sp. Av25_4

produces a volatile compound that alkalizes the growth medium (**Figure 4.4**). At the beginning of the experiment, the pH increase was observed near *Streptomyces* sp. Av25_4. However, after 7 d the whole *E. weberi* growth medium appeared entirely pink, indicating the alkalinisation to pH 8.5 due to the volatile compound from *Streptomyces* sp. Av25_4 (**Figure 4.4**).

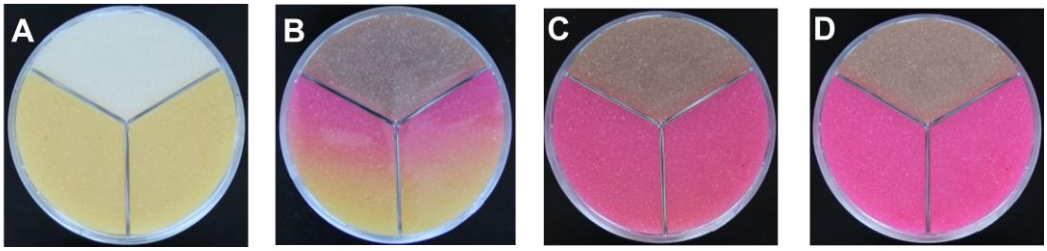

Figure 4.4: Ammonia from *Streptomyces* sp. Av25_4 grown in the first compartment of the three compartment Petri dish changes the pH via the headspace in the other compartments. The pH change in the second and third compartment of the Petri dish containing SFM medium is observed using the pH indicator phenol red.
A) Control plate with the first compartment with SFM medium, the second and third compartments with SFM medium containing 0.002 % of phenol red, **B**) 4d, **C**) 7d, **D**) 10d grown *Streptomyces* sp. Av25_4 in the first compartment with SFM medium, the second and third compartments with SFM medium contain 0.002 % of phenol red indicator.

Ammonia production of *Streptomyces* sp. Av25_4

Some *Streptomyces* strains can produce volatile amines such as ammonia[109] and trimethylamine.[110] As volatile bases, amines can alter the pH in the physically separated compartment with *E. weberi*. Therefore, we investigated if *Streptomyces* sp. Av25_4 produces volatile amines. The volatile amines were trapped in 250 mM HCl solution by using closed loop stripping. The resulting sample was analysed by ^{1}H-NMR spectroscopy using water suppression. The ^{1}H-NMR spectrum revealed an intense triplet signal at 7.01 ppm with a coupling constant of 51.6 Hz, proving that *Streptomyces*

sp. Av25_4 produces a high amount of ammonia (**Figure 4.5**).[109] Signals accounting for other volatile compounds were only detected in traces in the ^{1}H-NMR spectrum.

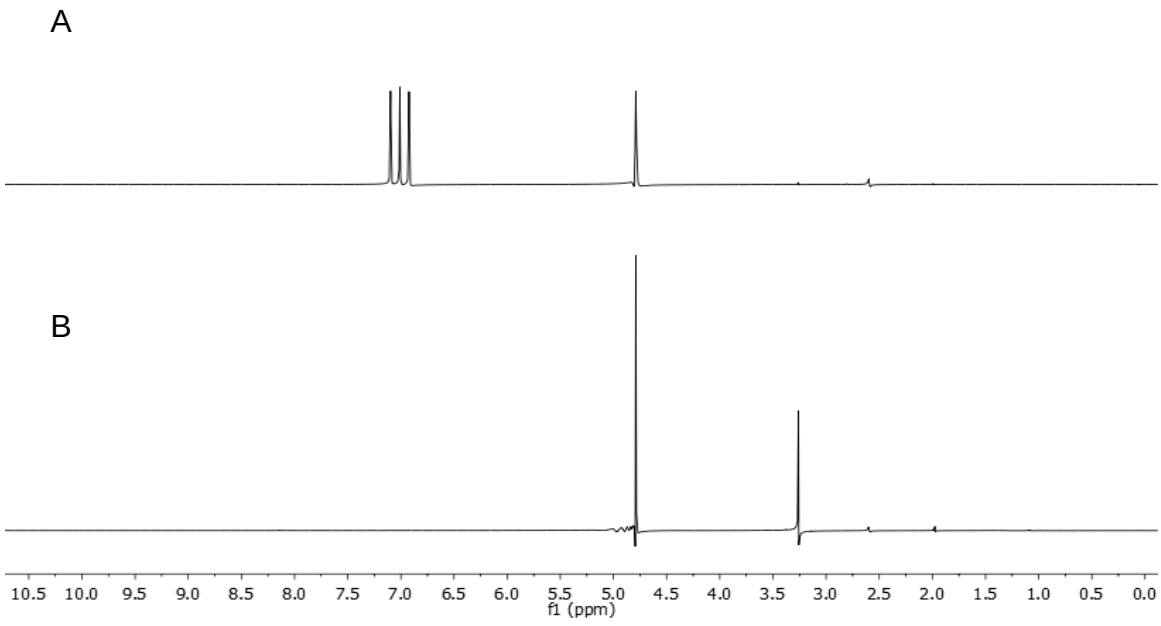

Figure 4.5: Identification of ammonia as the pH changing principle using ^{1}H-NMR spectroscopy.^{1}H-NMR spectra (600 MHz) of **A**) *Streptomyces* sp. Av25_4 produced volatiles exposed 250 mM HCl solution, **B**) SFM agar plates produced volatiles exposed 250 mM HCl solution as control.

Furthermore, the production of ammonia by *Streptomyces* sp. Av25_4 was quantified by derivatization with *ortho*-phthalaldehyde (OPA) and detection by HPLC hyphenated to a fluorescence detector. Initially, ammonia was detected by direct exposure of the headspace volatiles of *Streptomyces* sp. Av25_4 to the OPA reagent, leading to a reddish color caused by the formation of an isoindole derivative from ammonia and OPA. Thus, *Streptomyces* sp. Av25_4 appears to emit ammonia in large quantities comparison to other symbionts. HPLC analysis indicated that the retention time of the

fluorescent isoindole compound formed by OPA derivatization perfectly matched with the isoindole compound formed with the ammonia standard (**Figure S4.5**). Trimethylamine was not detected in the volatile blend of *Streptomyces* sp. Av25_4. In addition, we investigated if *Streptomyces* sp. Av25_4 produces hydrogen cyanide, because some *Streptomyces* strains are known to produce it.[111] However, we could not detect hydrogen cyanide in the volatile profile of *Streptomyces* sp. Av25_4 (**Figure S4.6**).

Ammonia from *Streptomyces* sp. Av25_4 strongly inhibits the growth of *E. weberi*

The growth inhibitory effect of ammonia against *E. weberi* was assessed by adding 5 mL of ammonia solutions (5, 7, 9, and 11 mM) into one compartment of a three compartment plate. An Ammonia concentration of 5, 7, and 9 mM respectively, inhibited 37 ± 9, 56 ± 4, and 77 ± 2 % of the *E. weberi* growth (**Figure 4.6**). 11 mM ammonia completely inhibited the growth of *E. weberi*.

In order to assess if the amount of ammonia necessary to inhibit *E. weberi* resembles the amount produced by *Streptomyces* sp. Av25_4, the ammonia concentration in the PDA agar compartment with *E weberi* was quantified after 2, 4, 6, 8, 10, and 12 d of *Streptomyces* sp. Av25_4 growth.

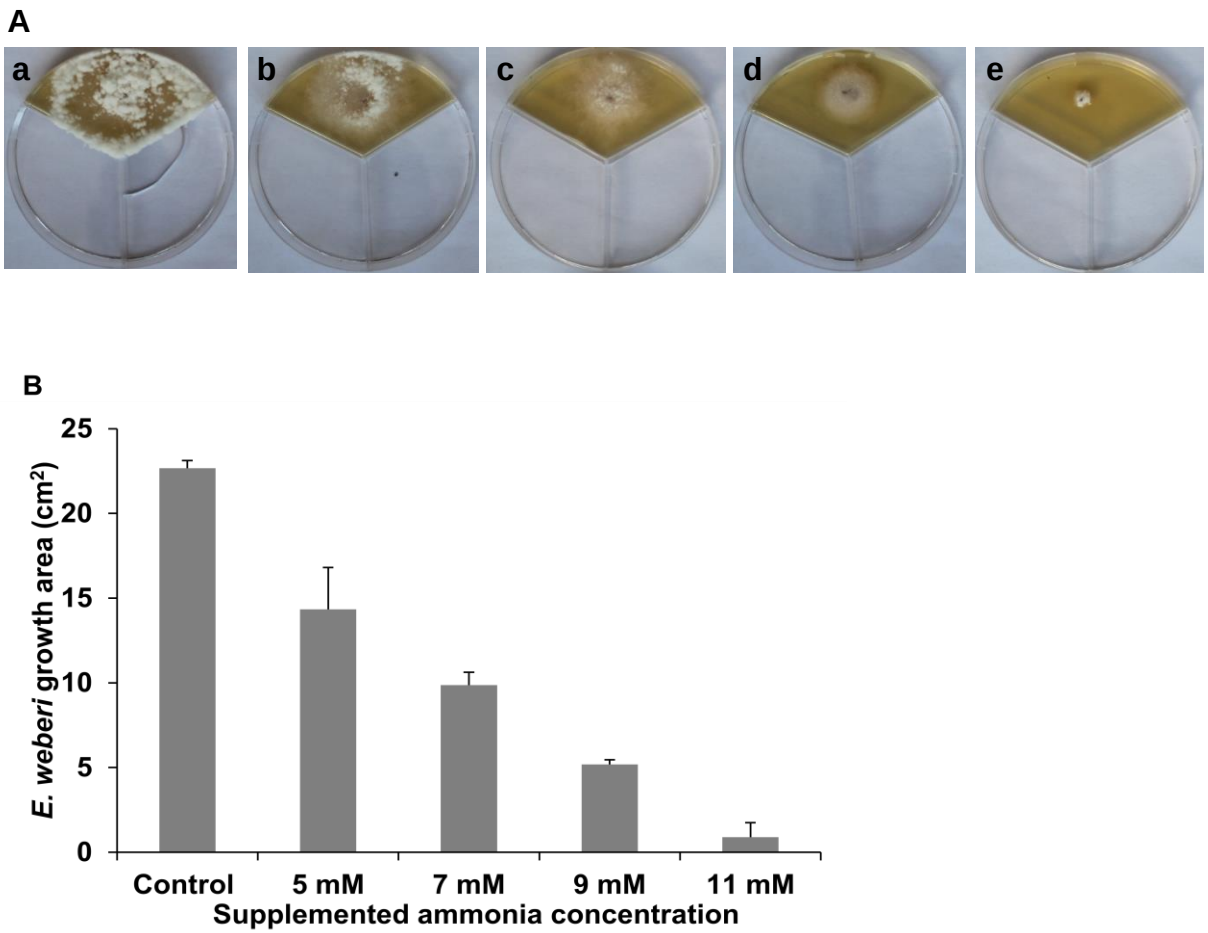

Figure 4.6: Effect of ammonia on *E. weberi* growth using the three compartment Petri dish assay. **A**) The first compartment contains *E. weberi* grown for 4 d, the second compartment contains 5 mL of sterile water or ammonia solutions in different concentrations: **a**) sterile water, **b**) 5 mM ammonia, **c**) 7 mM ammonia, **d**) 9 mM ammonia, and **e**) 11 mM ammonia. The third compartment is empty.
B) Quantification of *E. weberi* mycelium growth by analysis of the growth area using image J.

The ammonia concentration in PDA agar extracts of the *E. weberi* growth compartment was quantified by OPA derivatization and fluorescence detection in comparison to a standard ammonia reference curve ($y = 3136.8 x + 3578.6$, $R^2 = 0.999$). After 2 d of

growth, *Streptomyces* sp. Av25_4 caused an accumulation of ca. 4 mM ammonia in the PDA growth medium (**Figure 4.7**). After 10 d, the concentration of ammonia further increased to almost 8 mM.

The ammonia concentrations received in PDA agar extracts from the *E. weberi* compartment of the bioassay to which 5-11 mM ammonia was added (**Figure 4.6A**) are within the range of the ammonia concentration released by *Streptomyces* sp. Av25_4 to the *E. weberi* compartment. The ammonia concentrations of the PDA agar extract of the *Streptomyces* sp. Av25_4/*E. weberi* co-culture match to the concentration necessary to almost completely inhibit the growth of *E. weberi.*

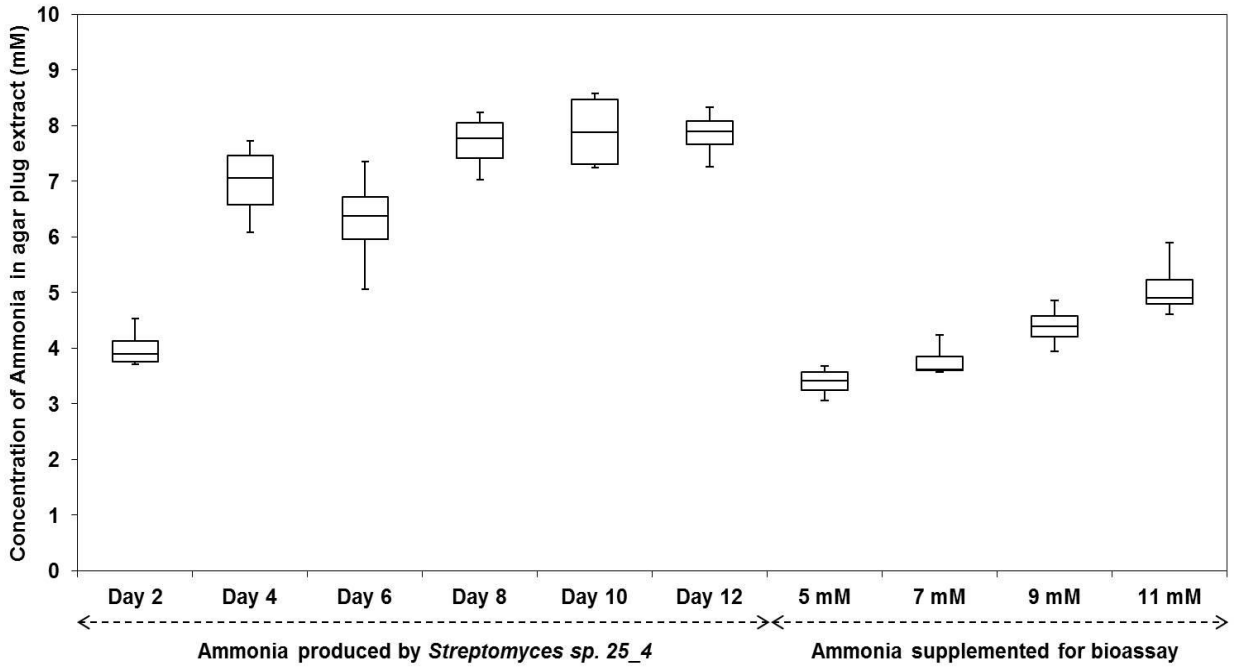

Figure 4.7: Box plot diagram showing the amount of ammonia released by *Streptomyces* sp. Av25_4 after 2, 4, 6, 8, 10, and 12 d in the agar plug of the PDA medium of the *E. weberi* compartment. Ammonia in the agar PDA plug of the *E. weberi* compartment after supplementation of ammonia (5, 7, 9, and 11 mM). The whiskers represent the minimum and maximum values and the segment inside the rectangle shows the median values (n = 4).

Alkalinisation of the medium and growth inhibition

Because the base ammonia was found to be sufficient to explain the observed growth inhibition of *E. weberi*, we studied if the alkalinisation of the medium is the reason for the growth inhibition. Therefore, the growth of *E. weberi* was monitored at pH 7.5, 8.0, and 8.5 adjusted with sodium hydroxide instead of ammonia. *E. weberi* was 90 ± 5 % inhibited at pH 7.5 (**Figure 4.8**). At pH 8.0 the growth of *E. weberi* was completely inhibited.

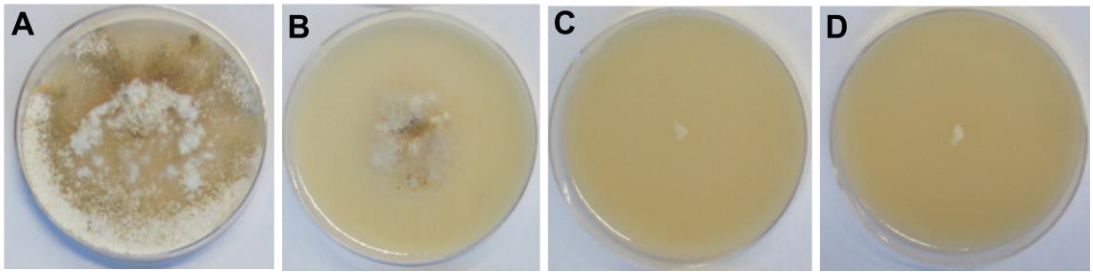

Figure 4.8: Growth of *E. weberi* on SFM agar plates at different pHs adjusted with sodium hydroxide. **A**) SFM medium without pH adjustment **B**) SFM medium adjusted to pH 7.5, **C**) SFM medium adjusted to pH 8.0, **D**) SFM medium adjusted to pH 8.5.

Discussion

It is well established that microorganisms, in particular *Actinomycetes*, often produce a large variety of volatile compounds. However, in contrast to volatiles from plants and animals the biological function of microbial volatiles, in particular in the ecological context, remained in most cases unknown. Because volatiles can diffuse over long distances they are ideally suited for communication as well as deterrence of competitors. For some microbial volatile compounds, e.g. the terpene albaflavenone[112] its antibiotic activity has been established. Recently, the biological role of volatile compounds from *Actinomycetes* gained interest among researchers interested in the chemical ecology of *Actinomycetes*.[113-115] In the context of leaf-cutting ants Sliva-Junior *et al.* recently pointed out the intriguing coincidence, that their *Actinomycetes* symbionts produce pyrazines[98] that the ants are known to use as infochemicals since a long time.[116-118] Based on the observation that *Streptomyces* sp. Av25_4, a symbiont from *A. volcanus* leaf-cutting ants, strongly inhibited the fungal pathogen *E. weberi* by its volatile compounds we started to identify the active compounds using a bioassay-guided approach. Although we could identify organic volatile compounds, namely nonanal and benzaldehyde, in the volatile bouquet of *Streptomyces* sp. Av25_4 these compounds likely occur in too low amount to explain the observed impressive antifungal effect (**Table S4.2** and **Table S4.3**). Therefore, we searched for additional compounds that are missed by standard GC-MS analysis of organic volatile compounds. Because we observed the strong alkalisation of the growth medium in the compartment of *E. weberi* of the three compartment plate (**Figure 4.4**) we suspected volatile amines to be released by *Streptomyces* sp. Av25_4, also because we previously established that ammonia released by *Streptomyces aburaviensis* induces droplet formation in *Streptomyces violaceoruber*.[109]

Using NMR and *ortho*-phthalaldehyde derivatisation we identified that *Streptomyces* sp. Av25_4 produces quite large amounts of ammonia ca 8 mM. The other *Streptomyces* symbionts that did not exhibit inhibition of *E. weberi* by volatile compounds (**Figure S4.1**) did not produce ammonia in comparable amount to *Streptomyces* sp. Av25_4.

8 mM of ammonia, as produced by *Streptomyces* sp. Av25_4 strongly inhibited the growth of the pathogen *E. weberi* perfectly explaining the observed inhibition of *E.*

weberi in co-culture with *Streptomyces* sp. Av25_4 separated by a plastic barrier using the compartment Petri dishes. Our results are perfectly in line with the recent, detailed mechanistic study by Avalos *et al*.[108] which nicely demonstrated that many *Streptomyces* produce ammonia that can serve them to inhibit potential microbial competitors. Clearly, volatile amines seem to play important physiological roles in some *Streptomyces* strains as trimethylamine was found to induce exploratory growth,[110] ammonia induces droplet production[109] and exerts antimicrobial[108] and antifungal effect.[119] In addition, ammonia potentiates the activity of antibiotic secondary metabolites.[108] This synergistic effect will also contribute in the nest of leaf-cutting ants to increase the antimicrobial and antifungal effect. Thus, it is important to identify and consider the variety of low and high molecular compounds present in the microcosmos of leaf-cutting ants to begin to understand their ecological functions in the complex interplay of the diverse compounds. Our experiments clearly demonstrate that the inhibition of *E. weberi* can be achieved by the pH change (**Figure 4.8**) that the volatile base ammonia can induce via the headspace. Still this does not completely exclude that additional modes of action may exist in particular if one would study very low doses in combination with other antifungal secondary metabolites.

Compared to the complex secondary metabolites, *Streptomyces* symbionts of leaf-cutting ants produce, e.g. the polyketide candicidin[39], ammonia is a very simple but remarkably efficient compound. As established by Avalos *et al*. ammonia production seems to be a highly efficient way to outcompete competitors because of its biosynthetic simplicity and thus metabolically low cost production. Streptomycetes often produce ammonia by degradation of amino acids like glycine.[108] Ammonia production only requires few enzymes in contrast to the huge mega-synthases needed for polyketide or non-ribosomal peptide production.

In summary, we demonstrated for the first time that in the microcosmos of leaf-cutting ants a microbial symbiont, *Streptomyces* sp. Av25_4, produces small, volatile compounds, in particular ammonia, that strongly inhibit the growth the fungal pathogen *E. weberi.* With this simple and metabolically efficient method, *Streptomyces* sp. Av25_4 contributes to support the leaf-cutting ants to protect their fungus garden from infections. Thus, ammonia from *Streptomyces* sp. Av25_4 comprises a nice example

that in nature not only complex, metabolically costly, high molecular secondary metabolites from *Actinomyces* symbionts can contribute to control infections but also simple, volatile molecules.

Acknowledgement

We thank Dr. Anthony Farlow for language editing. We are greatly indebted to the Konstanz Research School Chemical Biology funded by the Deutsche Forschungsgemeinschaft for financial support and a doctoral fellowship to BD.

Chapter 5: *Pseudomonas* sp. Al1 from *Atta laevigata* leaf-cutting ants produces a variety of antibiotic non-ribosomal peptides

Pseudomonas sp. Al1 from _Atta laevigata_ leaf-cutting ants produces a variety of antibiotic non-ribosomal peptides

Basanta Dhodary[1] and Dieter Spiteller[1]*

[1]Chemical Ecology/Biological Chemistry, University of Konstanz, Universitätsstrasse 10, 78457 Konstanz, Germany.

*corresponding author

Abstract

Atta leaf-cutting ants cultivate the fungus *Leucoagaricus gongylophorus* with leaf material because the fungus serves them as food source. Fungal pathogens, in particular *Escovopsis weberi*, can threaten the ants' survival as fungi can consume *L. gongylophorus.* Consequently, leaf-cutting ants fight against infections relying not only on own measures but antimicrobials from microbial symbionts. In contrast to *Acromyrmex* leaf-cutting ants that make use of antifungals from *Actinomycetes* the role of defensive microbial symbionts of *Atta* ants has remained less clear. We isolated microbes associated with *Atta laevigata* ants and that were screened for their potential to inhibit the growth of *E. weberi.* One strain that exhibited pronounced antifungal properties against *E. weberi* was designated as *Pseudomonas* sp. Al1 based on its 16*S* rDNA analysis. Using LC-MS profiling in combination with bioassays several antimicrobial, non-ribosomal peptides were purified from *Pseudomonas* sp. Al1. The lipopeptides WLIP, massetolide E, massetolide H, and the very large pyoverdine, pyoverdine Pf 1547, were identified using high resolution mass spectrometry, tandem mass spectrometry of the linearized peptides, and in the case of pyoverdine Pf 1547 in addition degradation reactions as well as gene cluster analysis of the sequenced genome of *Pseudomonas* sp. Al1.

The stereochemistry of the so far not assigned amino acids L-serine and D-serine of pyoverdine Pf 1547 were assigned by the Marfey method and analysis of the epimerase domains of the pyoverdine gene cluster. The lipopeptide WLIP (white line inducing

principle) was directly observed in extracts of *Atta laevigata* and *Atta sexdens* leaf-cutting ants and waste material, suggesting their possible ecological relevance.

Key words: *Escovopsis weberi*, pathogen, pyoverdine, secondary metabolite gene cluster, stereochemistry.

Introduction

Atta and *Acromyrmex* leaf-cutting ants live in mutualistic symbiosis with their garden fungus *Leucoagaricus gongylophorus.* Their relationship evolved about 50 million years ago.[2] The ants cultivate the fungus in chambers of their nest with leaf material that the ants harvest and bring into their nests. There the leaf material is processed and the garden fungus is inoculated with it. The fungus breaks down the polymers of the leaf material and makes nutrients accessible for the ants that dependent on the garden fungus as food source.[120] However, the garden fungus also comprises an ideal food source for pathogens, in particular the specialized fungal parasite *Escovopsis weberi.*[3] In addition generalist pathogens, such as *Fusarium*, *Tricoderma*, and *Syncephalastrum* can attack *L. gongylophorus*.[79] The parasites can overgrow *L. gongylophorus* and thus challenge the survival of whole colony.

Consequently, the leaf-cutting ants fight against infections by cleaning their nest combining hygienic behaviors with chemical treatment from their glands.[29, 101, 102, 121] The ants remove every suspicious material in waste chambers and continuously inspect their garden fungus. Moreover, *Acromyrmex* ants joined alliance with *Actinomycetes* symbionts. As discovered by Currie *et al*., *Acromyrmex* ants have visible whitish biofilms of *Actinomycetes* symbionts on their integument producing antifungals[3]. In the recent years more and more antifungal secondary metabolites have been characterized from leaf-cutting ants.[39, 81, 82, 122] In contrast, *Atta* leaf-cutting ants do not exhibit any visible biofilms and thus were suspected to rely on other defensive strategies such as metapleural gland secretions.[123]

Recently, the microbiota of *Atta* ants was studied using metagenomic and metaproteomic approaches revealing that *Atta* ant have rich microbiota that is very different to *Acromyrmex* leaf-cutting ants. Particularly, the *Pseudomonas*, *Enterobacter*, and *Rahnella* bacteria were found to constitute the microbial communities of *Atta* leaf-cutting ants.[28, 124] However, the chemical ecology of bacteria associated with *Atta* ants has not been addressed in detail.

Here, we report on the isolation of microbial symbionts of *Atta* leaf-cutting ants and the first characterization of antimicrobial secondary metabolites from the selected symbiont *Pseudomonas* sp. Al1 that strongly inhibited the growth of *E. weberi*.

Materials and Methods

Chemicals and instruments

Chemicals were purchased from Sigma Aldrich. NMR spectrum was recorded with a Bruker AVANCE III 400 NMR spectrometer (Bruker, Karlsruhe, Germany). Chemical shifts δ (ppm) were referenced to the solvent signals (^{1}H-NMR CD_3OD: 3.31). HR-ESI-MS were acquired using a Thermo Scientific Exative Orbitrap mass spectrometer. For column chromatography polygoprep C18 material (60-50 mesh, Macherey-Nagel, Germany) and Sephadex LH-20 (GE Healthcare, Upssala, Sweden) were used.

Organisms and cultivation conditions

E. weberi CBS 110660 was obtained from the Westerdijk Fungal Biodiversity Institute (Utrecht, the Netherlands). Microbial strains were cultivated on soy flour medium (SFM) (20 g soy flour, 20 g mannitol, 15 g agar, 1L ddH_2O) or YEME (3 g yeast extract, 3 g malt extract, 10 g glucose, 5 g peptone, 1L ddH_2O) or KB (20 g peptone, 1.5 g K_2HPO_4, 1.5 g $MgSO_4.7H_2O$, 10 mL glycerol, 15 g agar, 1L ddH_2O) solid agar plates or liquid broth without agar at 28 °C.

Atta laevigata leaf-cutting ants were either from Botucatu, Brazil or from the Catimbau National Park, Pernambuco, Northeastern Brazil. *Atta sexdens* originated from the Catimbau National Park, Pernambuco in Northeastern Brazil.

Isolation of microorganisms associated with *Atta laevigata*

Microorganisms were isolated from *Atta laevigata* leaf-cutting ants colony AL7 originated from Botucatu, Brazil (colony excavated in February 2017 by Luiz Forti) that were reared in the laboratory of Prof. Flavio Roces at the University of Würzburg, Würzburg, Germany. 20 ants were transferred into a 1.5 mL Eppendorf tube and 300 µL of a saline solution (0.9 % NaCl) containing 0.05 % Tween 80 was added. After, vortexing of the tubes for 1 min the supernatant was transferred to new tubes. The samples were diluted (1/10, 1/100) and 1 µL of the dilutions were streaked onto YEME (Yeast extract malt extract)[87] agar plates. The inoculated plates were incubated at 28 °C for 4 d. Each day the growth was monitored. Single colonies were picked using sterile

tooth picks and transferred to fresh YEME plates. Permanent stocks in 20 % glycerol of the isolates were prepared and stored at -80 °C.

Screening isolates for antifungal activity against *E. weberi* in confrontation bioassays

Isolated microorganisms were streaked in the middle of SFM[87], KB[125], YEME [87] agar plates and allowed to grow for 3 d at 28 °C. Then, 6 mm diameter *E. weberi* mycelium grown on SFM media for 5 d was inoculated in 1.5 cm distance from the test microorganism. The plates were incubated for seven more days and the growth of *E. weberi* was recorded by taking pictures.

DNA extraction and 16*S* rRNA sequencing

Genomic DNA was isolated from the bacterial strain and the 16*S* rDNA was amplified by PCR. The primers: (8F: 5'-AGAGTTTGATCCTGGCTCAG-3' and 1492R: 5'-CGGTTACCTTGTTACGACTT-3').[126]

The 50 µL of PCR reaction mixture contained 10 µL of phusion GC buffer (5X), 7.5 µl of dNTP's (10 mM), 1.25 µl of each of forward and reverse primers, 3 µL of $MgCl_2$ (50 mM), 1.5 µL of DMSO, 23 µL of double distilled water, 1 µL of phusion polymerase (2U/µL) and 1.5 µL of template genomic DNA (ca. 205 ng/µL).

The following touchdown PCR program was used: PCR program (initial denaturation: 2 min at 98 °C, 13 cycles of denaturation at 98 °C for 10 s, annealing at 65 °C and minus 1 °C per cycle for 20 s, extension at 72 °C for 45 s, followed by 20 cycles of denaturation at 98 °C for 10 s, annealing at 55 °C for 20 s, extension at 72 °C for 30 s, final extension at 72 °C for 10 min, and storage at 8 °C). The PCR product was purified by gel electrophoresis, and cloned into the pjet 2.1 vector using the CloneJET PCR cloning kit (Thermofisher). The purified plasmid was submitted for sequencing to Eurofins Genomics (85560 Ebersberg, Germany). Phylogenetic analysis was done by using Mega X[127].

Extraction and isolation of WLIP (1)

Pseudomonas sp. Al1 was grown in Erlenmeyer flasks (2L) containing 1L KB[125] medium in an orbital shaker at 28 °C at 160 rpm for 5 d. The grown culture was harvested by centrifugation for 15 min at 6000 rpm. The supernatant was collected and acidified to pH 4-5 with 2N HCl. The supernatant was extracted with the same volume of ethylacetate (1 times) and the organic layer was collected and concentrated *in vacuo*. The dried crude extract was purified using a Sephadex LH-20 column. With elution by methanol 10 fractions were collected. Fraction 3 and 4 contained a whitish precipitate.^{1}H-NMR of the precipitate suggested a mixture of peptides. The whitish precipitate was dissolved in methanol and further purified by HPLC using an Agilent 1100 HPLC system fitted with a Macherey-Nagel (52355 Düren, Germany) Nucleodur RP18 column (250 mm x 4.6 mm, 5 μm) hyphenated to a Gilson FC204 fraction collector. The peptides were purified by gradient elution. HPLC programme: solvents: solvent A water 0.1 % acetic acid, solvent B: methanol 0.1 % acetic acid, flow rate: 0.8 mL/min, gradient programme: 2 min 80 % B, in 30 min to 100 % B, 5 min 100 % B, fraction size: 1 min.

Alkaline hydrolysis of cyclic lipopeptides

0.2 mg of purified peptide was subjected to alkaline hydrolysis with 250 µL of 2N NaOH at 60 °C for 1 h. The hydrolyzed peptide sample was neutralized with 250 µL of 2N HCl and subjected to UPLC-ESI-HR-MS analysis.

The sample was analyzed by UPLC-ESI-HR-MS using an Acquity UPLC (Waters) hyphenated to a high resolution electrospray ionization mass spectrometer HR-ESI-MS (Thermofisher Exative Orbitrap). A Nucleodur Sphinx C18 column (100 mm x 2.1 mm, 1.8 μm) was used for the separation by gradient elution. UPLC conditions: A: methanol 0.1 % of acetic acid; B: water 0.1 % of acetic acid, flow rate: 0.4 ml/min, UPLC programme: 1 min 40 % B, in 9 min to 100 % B, 3 min100 % B.

Extraction and isolation of pyoverdine

Pseudomonas sp. Al1 was grown in 1L KB medium at 28 °C with shaking (160 rpm) for 7 d. The supernatant of the culture was separated by centrifugation (15 min) and

adjusted to pH 5. HP-20 resin (50 g/L) was added to the supernatant and incubated for 1 h. Then the liquid was removed and the collected HP-20 resin was washed with 500 mL of double distilled water. The resin was first eluted with 50 % of methanol and latter eluted by 100 % methanol. The first fraction eluted with 50 % methanol was dried and further purified using a Sephadex LH-20 open column with water as the eluting solvent. Afterwards, fraction 1 was purified by MPLC (Büchi sepacore with fraction collector C-660) using a packed RP18 column (Macherey Nagel Polygoprep 60-50 C18 resin) and gradient elution with solvent A: MeOH and solvent B: water at a flow rate of 15 mL/min. MPLC programme: 2 % - 45 % MeOH in 35 min, 45 % - 100 % MeOH from 35 min to 50 min, 100 % MeOH from 50 min to 60 min. Fractions 14 and 15 from the MPLC were combined based on LC-MS profile and further purified by HPLC using an Agilent 1100 HPLC system fitted with Phenomenex polar RP column (250 mm x 4.6 mm, 4 μm) connected to a Gilson FC204 fraction collector. Gradient elution with solvent A (H_2O 0.1 % acetic acid) and solvent B (MeOH 0.1 % acetic acid) at flow rate of 0.8 mL/min was applied. HPLC program: 2 min 5 % B, in 28 min to 40 % B, in 32 min to 100 % B, 7 min 100 % B.

Amino acid analysis of pyoverdine Pf 1547 (4) by Marfey's reagent[128]

0.2 mg of pyoverdine Pf 1547 (**4**) was dissolved in 300 µL of 6 N HCl in 1.5 ml vial. The sample was incubated at 99 °C for 18 h with shaking at 400 rpm. After that, the solvent was blown off in a nitrogen stream and the residue was dissolved in 100 µL of water. 200 µL of 1 % Marfey reagent prepared in acetone followed by 40 µL of 1 M aqueous sodium bicarbonate was added. The reaction mixture was shaken at 400 rpm for 2 h at 50 °C. The reaction mixture was neutralized with 20 µL of 2 N HCl and analyzed by LC-MS. HPLC conditions: Phenomenex Luna C18 column (250 mm x 4.6 mm, 5 μm), solvent A: H_2O 0.1 % acetic acid, solvent B: Acetonitrile 0.1 % acetic acid, flow rate: 0.8 mL/min, HPLC programme: 2 min 20 % B, in 40 min to 45 % B. A standard mix of D- and L-amino acids was derivatized using Marey’s reagent in same way for comparison (5 µmol).

Direct detection of peptides from *Pseudomonas* sp. Al1 WLIP[129] in *Atta* ants and their waste

Ant workers, fungus garden, and waste samples from *Atta laevigata*, and *Atta sexdens* were analyzed. 10 ants were killed at -20 °C and 500 µL of methanol was added. The samples were vortexed for 1 min and centrifuged at 14000 rpm for 2 min. The supernatant was concentrated *in vacuo*. The residue was re-dissolved in 50 µL of methanol and analyzed by LC-MS. For fungus garden and waste samples, ca. 5 g of samples were extracted with methanol by ultrasonication it for 2 min and mixing it for 1 min. After filtration, the filtrate was dried and dissolved in 1 mL methanol and analyzed by LC-MS.

Genome sequencing and secondary metabolite gene cluster analysis

The genome of *Pseudomonas* sp. Al1 was sequenced by Eurofins genomics (Konstanz, Germany) using Inview resequencing (10 M reads, 1.5 GB per sample). The DNA was isolated from a 2 d grown pellet of *Pseudomonas* sp. Al1 and a library for Illumina High Seq sequencing (2 x 150 bp paired end) was constructed by Eurofins. *De novo* assembly of the next generation sequences was performed by Eurofins genomics. 6144560 sequence reads with 56 contigs represented the draft genome. All the contigs were uploaded to antismash[130] in order to screen for secondary metabolite gene clusters encoded by the genome of *Pseudomonas* sp. Al1. Gene clusters were further inspected in detail by using Blast search.

Results

We isolated microorganisms from *A. laevigata* leaf-cutting ants. One of the isolated bacterial strains, Al1, strongly inhibited the growth of pathogenic fungus *E. weberi* when it was inoculated onto agar plates containing fully grown Al1 (**Figure S5.1**). 16*S* rRNA sequencing of strain Al1 revealed that it is 99.93 % identical to *Pseudomonas putida* (**Figure S5.2** and **Figure S5.3**).

The LC-MS profile of ethyl acetate soluble material of *Pseudomonas* sp. Al1 grown on KB medium revealed intense signals corresponding to cyclic lipopeptides. MS/MS- and NMR-analysis suggested that compounds are WLIP (**1**)[131], massetolide E (**2**)[132], and massetolide H (**3**)[132] (**Figure 5.1**). In addition to the lipopeptides, *Pseudomonas* sp. Al1 produced a pyoverdine-type siderophore: pyoverdine Pf 1547 (**4**)[133] (**Figure 5.1**).

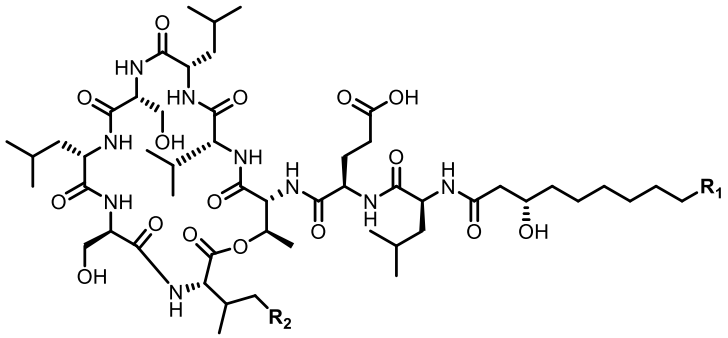

WLIP (**1**): $R_1 = CH_3$, $R_2 = CH_3$
Massetolide E (**2**): $R_1 = CH_3$, $R_2 = H$
Massetolide H (**3**): $R_1 = CH_2CH_2CH_3$, $R_2 = CH_3$

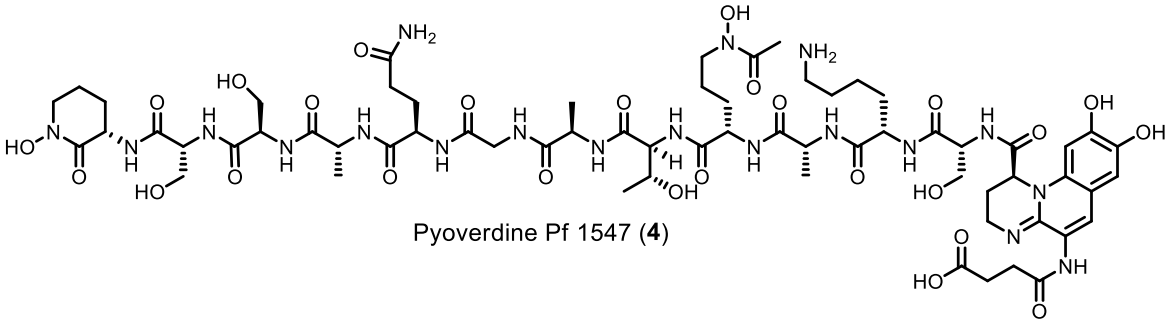

Pyoverdine Pf 1547 (**4**)

Figure 5.1: Structures of non-ribosomal peptides produced by *Pseudomonas* sp. Al1: WLIP (**1**)[129], massetolide E (**2**)[132], massetolide H (**3**)[132], and pyoverdine Pf 1547 (**4**)[133].

Characterization of lipopeptides from *Pseudomonas* sp. Al1

The highly produced WLIP (**1**)[129] was obtained as whitish powder, HR-ESI-MS gave a quasimolecular ion $[M+H]^+$ at m/z 1126.6927 (calculated: 1126.6969, -3.7 Δ ppm) suggesting a molecular formula of $C_{54}H_{95}N_9O_{16}$. The ^{1}H-NMR spectrum of WLIP (**1**) revealed resonances that were characteristic for a peptide namely the cluster of down fielded amide proton signals, the middle range α-proton resonances and upfield range side chain protons (**Figure S5.4**). Moreover, mild alkaline treatment of compound **1** shifted its quasimolecular ion by 18 Da to $[M+H]^+$ to m/z 1144.7063 (calculated: 1144.7075, -1.0 Δ ppm, molecular composition: $C_{54}H_{97}N_9O_{17}$), which suggested that **1** is a cyclic peptide. MS/MS analysis of the obtained linear peptide (**1a**) allowed to determine the amino acid sequence of **1** as well as indicated the presence of an *N*-terminal acyl residue (**Figure 5.2** and **Figure S5.5**). In addition, genome mining of *Pseudomonas* sp. Al1 indicated an NRPS gene cluster matching to WLIP (**1**). Particularly, bioinformatic prediction of the adenylation domain specificities matched well to the deduced amino acid sequence of WLIP (**1**). The starter condensation (C) domain analysis suggested the incorporation of an *N*-terminal acyl residue into WLIP (**1**).

Besides WLIP (**1**) there were two other related cyclic lipopetides with quasimolecular ions $[M+H]^+$ at m/z 1112.6785 (calculated for 1112.6813, -2.5 Δ ppm, molecular composition: $C_{53}H_{93}N_9O_{16}$) and 1154.7254 (calculated for 1154.7282, -2.4 Δ ppm, molecular composition: $C_{56}H_{99}N_9O_{16}$). Using the same purification protocol and MS/MS analysis of the linearized peptides, both compounds were identified as the cyclic lipopeptides massetolide E (**2**)[132] and massetolide H (**3**)[132], respectively (**Table S5.1** and **S5.2, Figure S5.6** and **S5.7**). Massetolide E differed in the structure with the WLIP by having valine as ninth amino acid instead of isoleucine whereas massetolide H contain longer fatty acid chain (- CH_2CH_2 -) than WLIP.

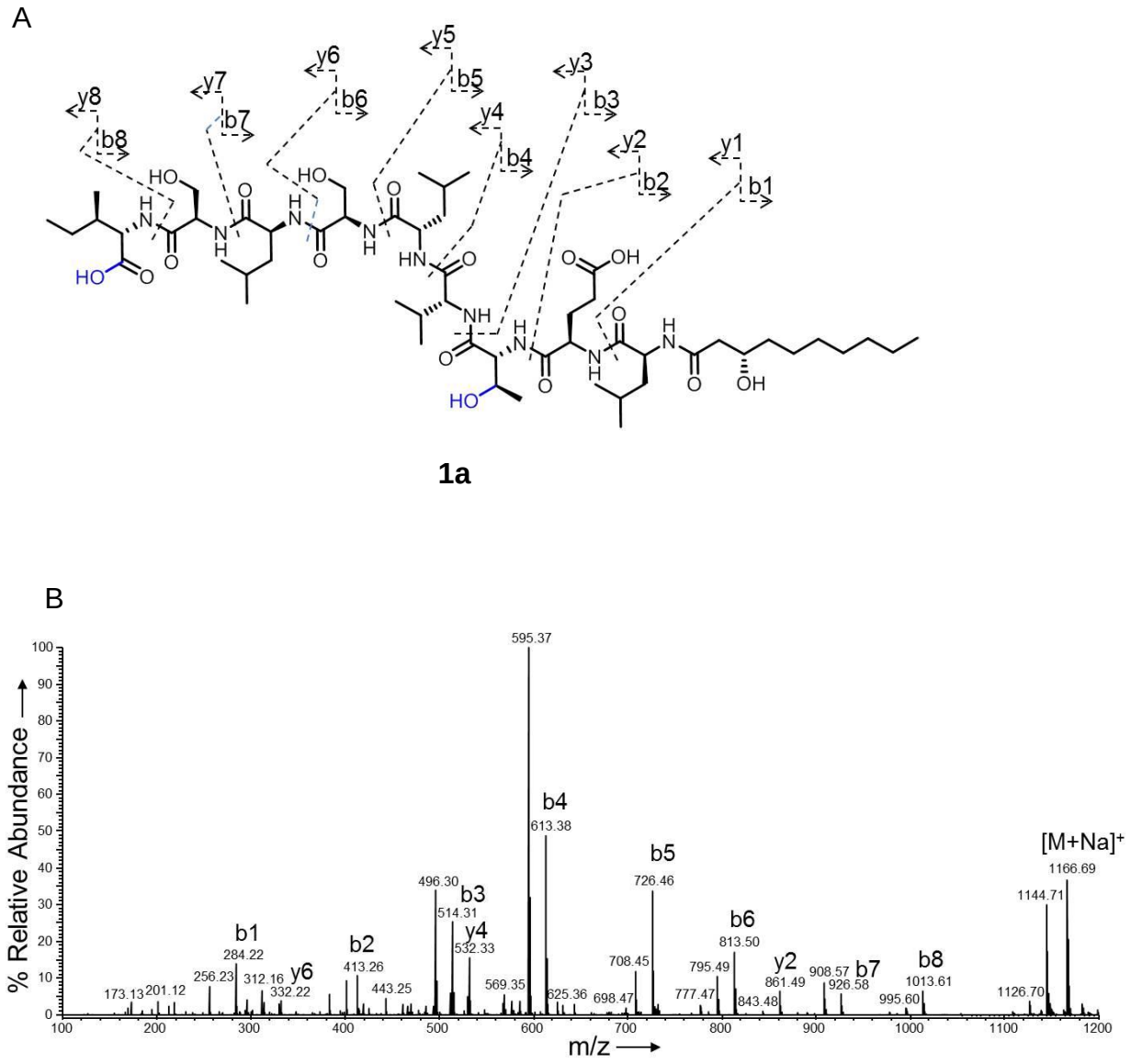

1a

Figure 5.2: A) Structure of linearized WLIP (**1a**).[129] The b and y fragments of the MS/MS of the quasimolecular ion $[M+Na]^+$ 1166.6 of WLIP (**1**) are shown. **B**) HR-ESI-MS/MS spectrum of linearized WILP (**1a**). The b and y peptide ion fragments are indicated above the peaks.

Identification of pyoverdine Pf 1547 (4)[133]

Pyoverdine Pf 1547 (**4**) was isolated as yellowish green water soluble fluorescent pigment with quasimolecular ion $[M+H]^+$ at m/z 1601.6039 in the HR-ESI-MS (calculated 1601.6034, 0.3 Δ ppm) fitting well to the molecular formula $C_{64}H_{95}FeN_{19}O_{26}$. The UV/VIS

spectrum of the compound exhibited absorption maxima at 362 nm and 378 nm wavelength, pointing to the presence of a quinoline chromophore in the structure (**Figure S5.8**).[134] Moreover, the MS/MS spectrum of the quasimolecular ion of **4** indicated a peptide structure due to the presence of b and y fragment ions (**Figure 5.3** and **Figure S5.10-S5.12**). The ion at m/z 358.1034 $[C_{17}H_{16}N_3O_6]^+$, suggested for the presence of succininc acid side chain in the quinolone chromophore. In addition the ion at m/z 445.1356 $[C_{20}H_{21}N_4O_8]^+$ corresponded to serine, the first amino acid attached to chromophore (Chr). Furthermore, ions at m/z 573.2305 $[C_{26}H_{33}N_6O_9]^+$, 644.2676 $[C_{29}H_{38}N_7O_{10}]^+$, and 816.3533 $[C_{36}H_{50}N_9O_{13}]^+$ suggested that the second, third and fourth amino acid were lysine, alanine and *N*-acetyl-*N*-hydroxy-ornithine (AcOHOrn), respectively (**Figure 5.3**).[133] The presence of the ion at *m/z* 131.0816 $[C_5H_{11}N_2O_2]^+$ indicated that there was an cyclo-hydroxy-ornithine (AcOHOrn) at the end of peptide chain (**Figure 5.3**).[133]

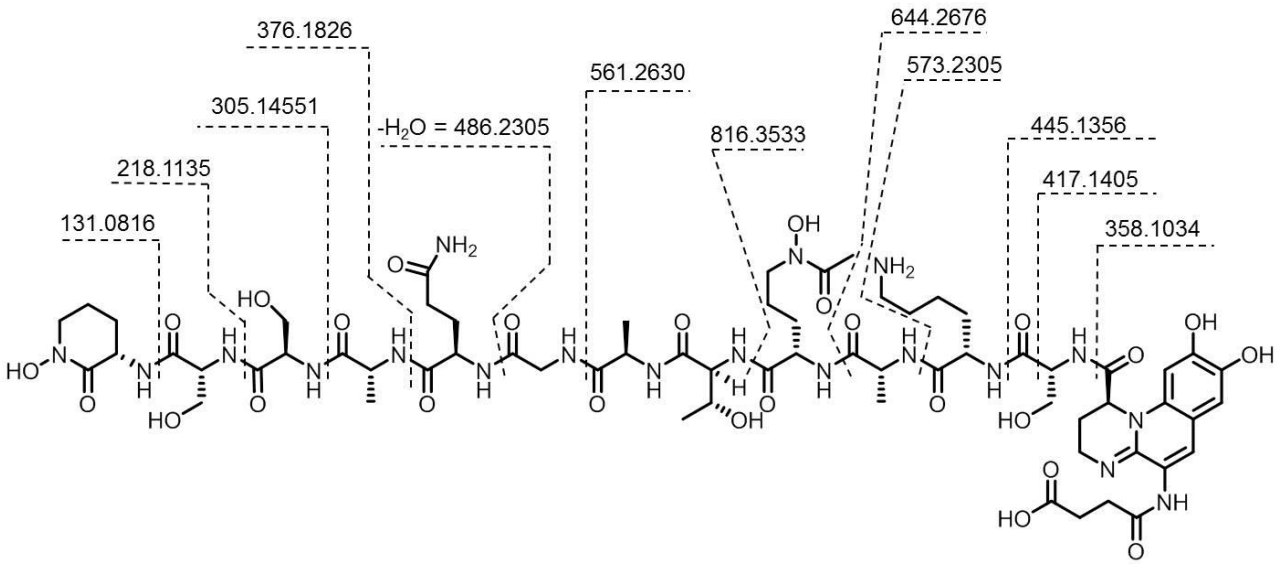

Figure 5.3: Structure of pyoverdine Pf 1547 (**4**)[133]. The b and y ion fragments are indicated in the structure of **4**.

Identification of the pyoverdine Pf 1547 biosynthetic gene cluster

Genome mining of *Pseudomonas* sp. Al1 genome using antiSMASH[130] revealed the non-ribosomal peptide biosynthetic gene cluster for the biosynthesis of pyoverdine Pf 1547 (**4**) (**Figure 5.4** and **Table S5.5**).

The pyoverdine Pf 1547 biosynthetic gene cluster of *Pseudomonas* sp. Al1 is present in two separate clusters found on two contigs. There is one NRPS gene encoding for the pyoverdine Pf 1547 chromophore in contig 6 and four adjacent NRPS genes in contig 7 which encoded for the amino acid chain (**Figure 5.4** and **Table S5.5**).

The amino acid chain encoding NRPSs gene cluster bears 12 adenylation (A) domains (**Figure 5.4**). Based on the bioinformatic analysis, the first adenylation domain in module 1 (M1) is predicted to be specific for the amino acid serine and the presence of a functional epimerase domain downstream to the adenylation domain suggested the D-configuration of serine. Likewise, third, fifth, sixth, seventh, eighth, ninth, tenth, and eleventh amino acids are predicted as D-Ala, L-Thr, D-Ala, Gly, D-Glu, D-Ala, L-Ser, and D-Ser. AntiSMASH analysis did not predict any clear annotation for the second, fourth and twelfth amino acid. However, the similarity of signature residues in the binding pockets (Stachelhaus code)[135] with other *Pseudomonas* strains suggested that substrates for second, fourth and twelfth modules are likely L-Lys (DGedhGtVVK), L-AcOHOrn (DGeacGgVtK), and L-cOHOrn (DGeccGgVtK) respectively.[136]

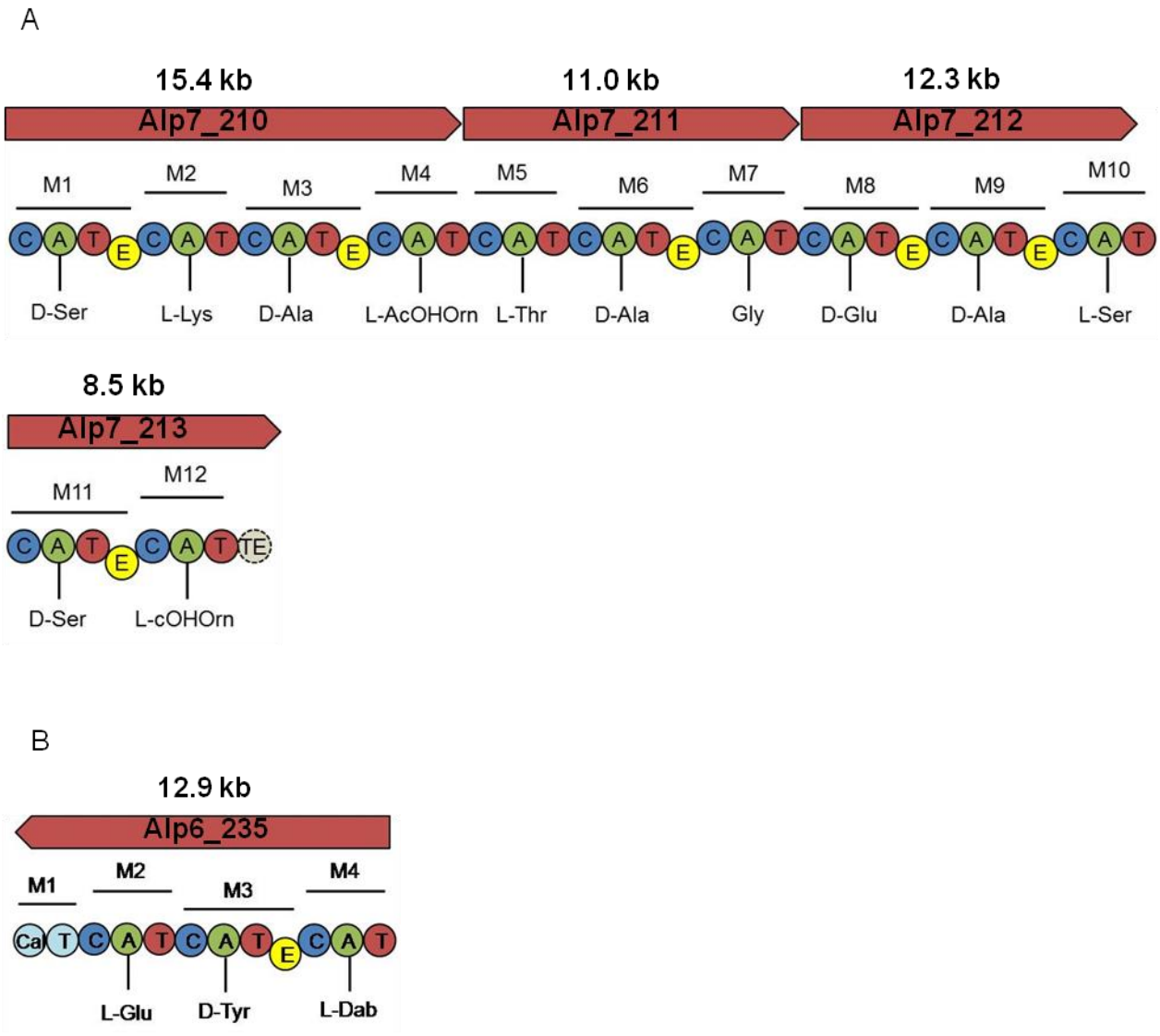

Figure 5.4: Biosynthetic gene cluster of pyoverdine Pf 1547 (**4**) from *Pseudomonas* sp. Al1. **A**) NRPS assembly line for the synthesis of the peptide chain. M represents different modules with condensation (C), adenylation (A), thiolation (T), epimerization (E), and thioesterase (TE) domains. The predicted amino acid specificity is indicated below the adenylation domain (A).
B) NRPS assembly line for the biosynthesis of pyoverdine chromophore.[137]

MS/MS analysis of compound **4** in combination with the detailed analysis of the adenylation (A) domain specificities of the pyoverdine NRPS gene cluster allowed to

fully establish the structure of compound **4** as pyoverdine Pf 1547 with the peptide sequence cOHOrn-Ser-Ser-Ala-Gln-Gly-Ala-Thr-AcOHOrn-Ala-Lys-Ser-Chr.

Stereochemistry of the amino acid residues in pyoverdine Pf 1547 (4)

The absolute configurations of amino acids were predicted based on the presence of functional epimerases downstream to the A domain of the pyoverdine Pf 1547 biosynthetic gene cluster. However, in some cases the prediction based on occurrence of functional epimerases can fail.[138] Therefore, we hydrolyzed pyoverdine Pf 1547 (**4**) and derivatized the obtained amino acids using Marfrey's reagent (1-fluoro-2,4-dinitrophenyl-5-L-alanine amide)[128] in order to confirm the amino acids and their respective absolute configuration. LC-MS analysis of the derivatized amino acid mixture revealed two D-Ser, one L-Ser, three D-Ala, one L-Thr, one D-Gln, and one Gly. The detection of two D-Ser, three D-Ala and one D-Gln matched to the predicted stereochemistry based on the analysis of the epimerase domains in the pyoverdine Pf 1547 biosynthetic gene cluster (**Table S5.3** and **Table S5.4**). Thus, the structure of compound **4** was established as pyoverdine Pf 1547 which was reported by Ruangviryachai *et al.* previously from a *Pseudomonas* strain originating from Taiwanese soil.[133]

Discussion

The microorganisms associated with *Atta* leaf-cutting ants strongly differ from those of *Acromyrmex*. Recent screenings of the symbionts from *Atta* ants revealed *Pseudomonas* and *Enterobacter* to occur in high abundance.[28, 124] Because of their potential to produce amino acids, B vitamins, and other nutrients these bacteria are expected to support the growth of *L. gongylophorus* and thus the fitness of the ants' nests.[28] However, whether microorganisms associated with *Atta* leaf-cutting ants contribute to protect *L. gonglyophorus* and their ant hosts against infections has not been addressed up to now.

Thus, we started to investigate if bacteria from *Atta laevigata* can inhibit the pathogen *E. weberi* and isolated *Pseudomonas* sp. Al1 which exhibited pronounced activity against *E. weberi* (**Figure S5.1**) and therefore caught our attention. The isolation of a *Pseudomonas* strain from *A. laevigata* is perfectly in line with the previous studies of their abundant presence in the microbiome of *Atta* ants [124, 139]. We identified several non-ribosomal peptide secondary metabolites, WLIP (**1**), massetolide E (**2**), massetolide H (**3**), and pyoverdine Pf 1547 (**4**) from *Pseudomonas* sp. Al1 by using mass spectrometry, NMR and genome mining. WLIP (**1**), massetolide E (**2**), massetolide H (**3**) belong to the viscosin-type non-ribosomal cyclic lipodepsipeptides that are common secondary metabolites of *Pseudomonas* strains (**Figure 5.1**).[140, 141]

For viscosin-type compounds antibiotic and antifungal activity has been reported[142-144] suggesting a similar role in the context of *Atta* leaf-cutting ants. *Atta* ants might directly benefit from the inhibitory potential of massetolides against plant pathogens such as *Phytophthora infestans*[145], because with the ants bringing leaf material into the fungus garden it is inevitable that plant pathogens are imported that are potentially also detrimental for the growth of the garden fungus. The nematode *Caenorhabditis elegans* is protected by massetolides from its *Pseudomonas* symbionts against pathogens.[146]

Recently, Martin *et al*. observed viscosin-like compounds produced by symbionts on the skin of frogs that exhibit antifungal activity against *Aspergillus*.[147] Also, leaf-cutting ants themselves are threatened by *Aspergillus* strains.[148] Thus, similarly the viscosin-type compounds **1**-**3** might serve the *Atta* ants to fight against *Aspergillus*.

In addition to the cyclic lipopeptides, *Pseudomonas* sp. Al1 produces the powerful siderophore pyoverdine Pf 1547 (**4**) (Km of pyoverdines ca. 10^{32} M^{-1})[149]. It has been reported first from a *Pseudomonas* strain collected from Thailand as an exceptionally large pyoverdine.[133] Because the absolute configuration of the serines attached to tenth and eleventh position of pyoverdine Pf 1547 (**4**) remained elusive[133] we studied the stereochemistry of the amino acids using both degradation and analysis of the amino acids by Marfey's method[128] and the analysis of the pyoverdine Pf 1547 biosynthetic gene cluster to determine the stereochemistry of all amino acids (**Figure 5.4**; position ten: L-Ser and position eleven: D-Ser). The biosynthetic gene cluster of pyoverdine Pf 1547 was identified for the first time and follows the NRPS logic as well as comprises highly similar genes for the quinolone chromophore as other well studied pyoverdine gene clusters.[137]

Pyoverdine siderophores are widespread among pseudomonads as these efficient siderophores allow pseudomonads to outcompete other bacteria and fungi by removing the essential iron ions from the environment.[150-153] All pyoverdines are composed of a quinolone chromophore, an acyl side chain attached to the chromophore and a variable peptide chain (6-14 amino acids).[154, 155] *Pseudomonas* strains produce different varieties of pyoverdines and so far more than 60 pyoverdines have been identified.[155-157]. In addition pyoverdines are involved in regulation of virulence [158, 159] and can remove toxic heavy metal ions.[160]

Because pseudomonads constitute abundant microorganisms in the microbiome of *Atta* leaf-cutting ants it is conceivable that they play an important role in the microcosmos of leaf-cutting ants, in particular support the *Atta* ants to be well defended against pathogens. Using mass spectrometry we could even directly observe WLIP on the body of *A. laevigata* as well as *A. sexdens* ants. Also, WLIP occurred in the waste of *Atta* ants. Consequently, it is obvious that the cyclic lipopeptides from *Pseudomonas* sp. Al1 are important antimicrobials in the context of leaf-cutting ants. Moreover, the compounds seem to be widespread among *Atta*, because we had two different *Atta laevigata* from different geographical collection sites and the compounds occur in different *Atta* species.

In summary, with the antimicrobial cyclic lipopeptides WLIP (**1**), massetolide E (**2**), massetolide H (**3**), and the very large pyoverdine Pf 1547 (**4**) we identified the first secondary metabolites from *Atta* associated microbe that are expected to protect the ants against pathogens also against *E. weberi*. In addition, we identified the pyoverdine Pf 1547 biosynthetic gene cluster and assigned all stereocenters of pyoverdine Pf 1547 (**4**).

Outlook

Pseudomonas sp. Al1 strongly inhibited the growth of *E. weberi*. Therefore, it was selected to identify its bioactive secondary metabolites. Having identified a series of non-ribosomal peptides from *Pseudomonas* sp. Al1, next we need to study their ecological function in the context of *Atta* leaf-cutting ants. The peptides should be tested against the specialized parasite *E. weberi*, generalist pathogens such as *Fusarium* and *Trichoderma*,[79] or the black yeast *Phialophora fastigiata*[66] as well as *Aspergillus*[148] pathogens infecting the leaf-cutting ants. The minimal inhibitory concentrations need to be determined and compared to the amounts found on ants or in the nest in order to estimate their function.

The pyoverdine siderohore serves most likely to compete for iron ions. Thus, we need to determine the iron concentrations in the nest: the waste and the fungus garden, so that we can evaluate its potential role. Also, agar diffusion assays against the test strains from the microcosmos of leaf-cutting ants need to be performed in case of pyoverdine Pf 1547 on iron ion-limiting and non-limiting media.

Moreover, it is worth to identify other secondary metabolites making use of the sequenced genome. To finally prove the suggested pyoverdine Pf 1547 gene cluster knock-out mutagenesis experiments should be undertaken.

Acknowledgement

We thank Dr. Rainer Wirth and Prof. Flavio Roces for samples of *Atta* ants. We are greatly indebted to the Konstanz Research School Chemical Biology funded by the Deutsche Forschungsgemeinschaft for financial support and a doctoral fellowship to BD.

Chapter 6: General discussion

General discussion

The microcosmos of leaf-cutting ants is an fascinating example of multiplayer symbiotic relationships that originated millions of years ago.[32] The understanding of the chemical basis of direct and indirect interactions between the microbial players is necessary to understand the complexity of symbiotic interactions. At the begining of my dissertation, most of the few available chemical studies have focused to unveil the contribution of secondary metabolites produced by *Actinomycetes* symbionts of leaf-cutting ants to control infection of the garden fungus *L. gongylophorus* by *Escovopsis*.[4, 39, 40, 82, 103] Very little was known how *Escovopsis* attacks *L. gongylophorus*, how the attack is recognized, how the ants respond. In my thesis, I addressed these questions.

In Chapters 2 of my thesis, i describe the toxins produced by *E. weberi* and their effects againsts different partners of ant's microcosmos. *E. weberi* released indole-terpenoids, - shearinines, and the polyketides, - cycloarthropsone and emodin. Among shearinines, *E. weberi* mainly released two unreported shearinine derivatives shearinine L and shearinine M as well as the known shearinine D, F and J. The detection of shearinines was in accordance with Boya *et al*. who observed shearinines D, F, and J in a co-cultivation experiment with *Streptomyces* associated with *A. echinatior* ants against *E. weberi* TZ49.[58] Also, the genome mining of *E. weberi* genome by antismash[67] revealed the genes encoding for indole terpenoid biosynthesis which confirmed the production of shearinines.[44] We did not observe any antimicrobial effect of shearinine L against the *L. gongylophorus* suggesting no direct effect of shearinines on *L. gongylophorus*. However, in a dual choice behavioral assay with the *A. octospinosus* ants, after learning for two days ants clearly rejected the oat flakes coated with shearinine L. In addition, shearinines have been reported to act against insects[60], so we suspect that they may rather target the ants and indirectly weaken the fitness of ant cultivated fungus. Cycloarthropsone and emodin inhibited the growth of *L. gongylophorus* in agar diffusion assays suggesting that *Escovopsis* uses these compounds to overpower *L. gongylophorus*. Moreover, Heine *et al*. reported - shortly after us - that in addition to shearinine derivatives and emodin, *Escovopsis* strains secreted melinacidin III, melinacidin IV, chetracin B and chetracin C as well.[85] Furthermore, their work revealed that upon infection *Escovopsis* upregulates the

production of shearinine D and melinacidin IV which inhibit the antibiotic producing *Pseudonocardia* symbionts as well as reduce the ants' behavioral defenses.[85] In sum, Escovopsis uses a variety of secondary metabolites to overpower *L. gongylophorus* and interfere with the defense of leaf-cutting ants and their *Actinomycetes* symbionts.

Consequently, the pathogen *Escovopsis* threatens the survival of both *L. gongylophorus* and the leaf-cutting ants.[3, 85] The ants defend against *Escovopsis* with specialized behavioral responses and chemical treatment.

How do leaf-cutting ants recognize *E. weberi* infection as well as other threats? Does *L. gongylophorus* alarm the ants? When we analyzed the reaction of *L. gongylophorus* to *E. weberi* attack using *in-vitro* infection experiments, a volatile signal 3-octanone was formed (Chapter 3). We found that 3-octanone was released by *L. gongylophorus* in response to *E. weberi* mediated cell damage and most likely as a lipid peroxidation product from linoleic acid of the lipid membranes that is also inevitably formed upon any intense enough stress.[93] In mini-subcolony assays, *A. octospinosus* leaf-cutting ants recognized the 3-octanone and reacted with increased hygienic behavior. In particular tending and to some extent grooming behavior of ants was increased. Moreover, 3-octanone has been already described in the context of *Acromyrmex* leaf-cutting ants as a component of the mandibular alarm pheromone.[96] This interesting coincidence further supported that the ants should be able to sense 3-octanone from the garden fungus as a signal. Thus, 3-octanone from *L. gongylophorus* can be regarded as a cry for help signal from stressed *L. gongylophorus*.

A variety of complex secondary metabolites are known from *Actinomyces* symbionts of leaf-cutting ants which can efficiently inhibit the growth of the parasite *E. weberi*.[37, 39, 40, 103] In addition to that, we demonstrated for the first time that in the microcosmos of leaf-cutting ants a microbial symbiont, *Streptomyces* sp. Av25_4, produces small, volatile compounds, in particular ammonia, that strongly inhibits the growth of *E. weberi* over long distances (Chapter 4). The result is perfectly in line with the recent, detailed mechanistic study by Avalos *et al.* that demonstrated that many *Streptomycetes* produce ammonia that can serve them to inhibit potential microbial competitors.[108] In addition, ammonia was found to potentiate the activity of antibiotic secondary metabolites.[108] This synergistic effect might also contribute in the nest of leaf-cutting

ants to increase the antimicrobial and antifungal effect of ammonia together with secondary metabolite antifungals. Thus, ammonia from *Streptomyces* sp. Av25_4 comprises a nice example that in nature not only complex, metabolically costly, high molecular secondary metabolites from *Actinomyces* symbionts can contribute to control infections but also simple, volatile molecules.

The microorganisms associated with *Atta* leaf-cutting ants and their secondary metabolite's potentials are so far much less studied compared to the symbionts of *Acromyrmex* ants. We isolated *Pseudomonas* sp. Al1 from *A. laevigata* which exhibited pronounced activity against *E. weberi*. The isolation of a *Pseudomonas* strain from *A. laevigata* is perfectly in line with the previous studies of their abundant presence in the microbiome of *Atta* ants [124, 139]. We identified several non-ribosomal peptide secondary metabolites, WLIP, massetolide E, massetolide H, and pyoverdine Pf 1547 from *Pseudomonas* sp. Al1 using mass spectrometry, NMR and genome mining (Chapter 5). WLIP, massetolide E, and massetolide H belong to the viscosin-type non-ribosomal cyclic lipodepsipeptides that are common secondary metabolites of *Pseudomonas* strains.[140, 141] For viscosin-type compounds antibiotic and antifungal activity has been reported[142-144] suggesting a similar role in the context of *Atta* leaf-cutting ants. In addition to the cyclic lipopeptides, *Pseudomonas* sp. Al1 produces the powerful siderophore pyoverdine Pf 1547. It has been reported first from a *Pseudomonas* strain collected from Thailand as an exceptionally large pyoverdine.[133] Furthermore, we identified the pyoverdine Pf 1547 biosynthetic gene cluster for the first time and assigned all stereocenters of pyoverdine Pf 1547. Pyoverdine siderophores are widespread among pseudomonads as these efficient siderophores allow pseudomonads to outcompete other bacteria and fungi by removing the essential iron ions from the environment.[150-153] However, the ecological functions of the identified non-ribosomal peptides from *Pseudomonas* sp. Al1 now need to be evaluated in the context of *Atta* leaf-cutting ants. Knock-out mutagenesis experiments should be performed in order to finally prove the function of the suggested pyoverdine Pf 1547 gene cluster.

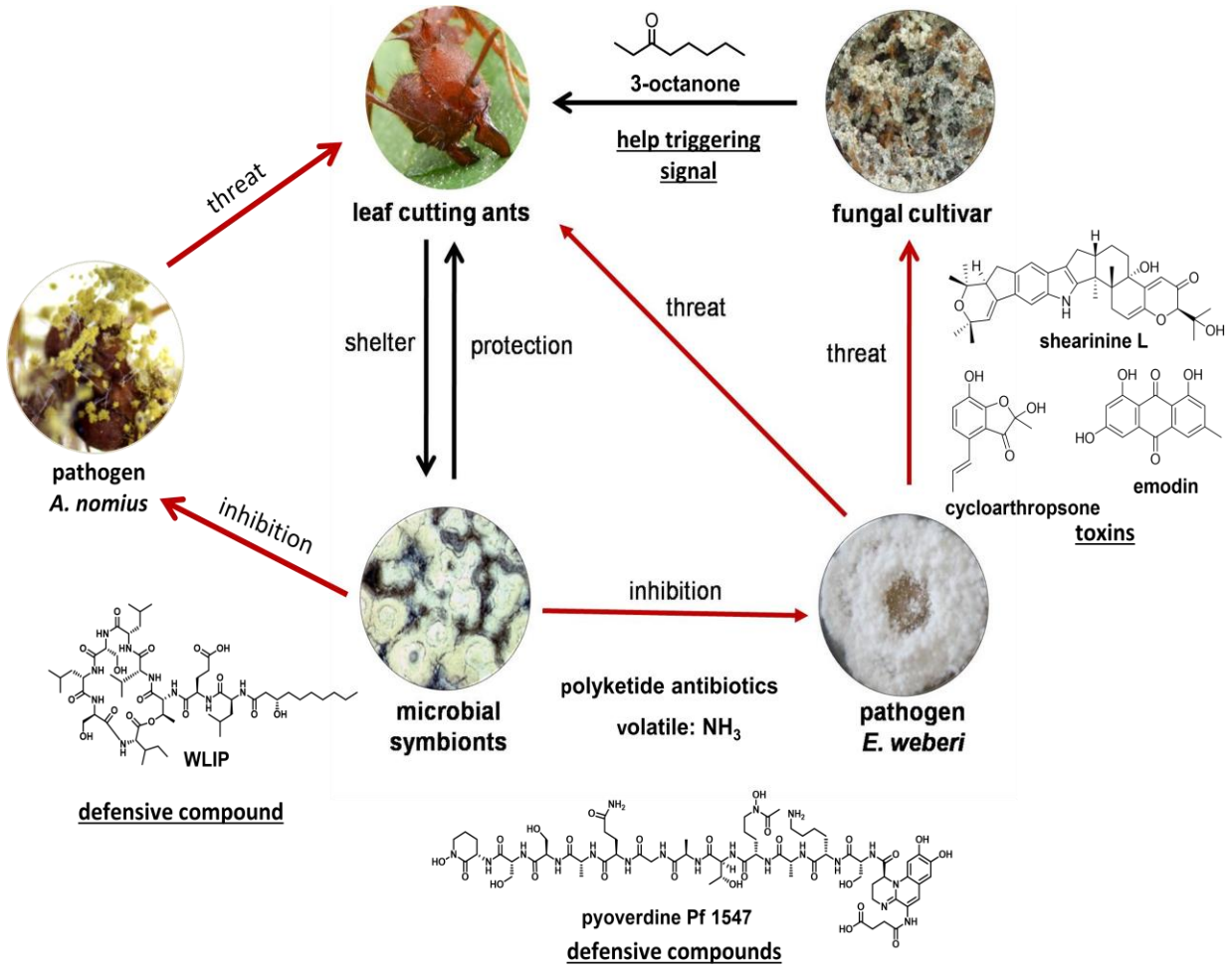

Figure 6.1: Complex interactions between different partners of the microcosmos of leaf-cutting ant's. *E. weberi* produced toxins threatening the survival of the fungal cultivar (*L. gongylophorus*) as well as ants. 3-octanone released by *E. weberi* attacked *L. gongylophorus* can be recognized by ants and reacts with enhanced hygiene behavior. Small volatile molecule like ammonia from *Streptomyces* symbiont has strength to control *E. weberi* pathogen. The compound WLIP is known for inhibiting *Aspergillus* and pyoverdines are reported to have antifungal effect. However, in our context their role needs to be verified.

In summary, the leaf-cutting ants' microcosmos comprises a crowd of organisms: the ants, their garden fungus, the mutualistic microbial symbionts, and pathogens. In order to understand the interactions in such a complex microcosmos more research should be directed towards the investigation of the chemicals - signaling compounds, toxins and antimicrobials - from the competing partners and their respective ecological functions. Moreover, investigation of the secondary metabolites from associated partners of such complex environment can lead to the identification of novel bioactive compounds as well as reveal new functions for known ones.

Author contributions

Chapter 2:

BD, DS and RW designed the experiments. BD performed purification, characterization, and agar diffusion assays of compounds. M.S and BD performed dual choice ant behavioral assays. BD, DS and RW analyzed the data. DS and BD wrote the manuscript.

(Published in Chemistry A European Journal)

Chapter 3:

BD, DS and RW designed the experiments. BD performed co-cultivation experiments and chemical analysis of volatiles. BF and JS performed the behavioral experiments. BD, DS, RW, BF and JS analyzed the data. DS and BD wrote the manuscript.

(Manuscript about to be submitted)

Chapter 4:

BD and DS designed the experiments. BD performed the experiments. SR performed bioassays with aldehydes. BD, DS and SR analyzed the data. D S and BD wrote the manuscript.

(Manuscript about to be submitted)

Chapter 5:

BD and DS designed the experiments. BD performed experiments. BD and DS analyzed the data. DS and B D wrote the manuscript.

(Manuscript close to final version, bioassays for evaluation of ecological role in progress)

List of abbreviations

A. echinatior	*Acromyrmex echinatior*
A. laevigata	*Atta laevigata*
A. octospinosus	*Acromyrmex octospinosus*
A. volcanus	*Acromyrmex volcanus*
AcOH	Acetic acid
AcOHOrn	Acetyl-hydroxy-ornithine
Ala	Alanine
Amu	Atomic mass unit
ACN	Acetonitrile
CC	Column chromatography
CD	Circular dichroism
Chr	Chromophore
CLS	Closed loop stripping
DAD	Diode array detector
DBE	Double bond equivalent
ddH_2O	Double distilled water
df	Degree of freedom
DNA	Deoxyribonucleic acid
E. aspergilloides	*Escovopsis aspergilloides*
E. weberi	*Escovopsis weberi*
EI	Electron impact
ESI	Electrospray ionization
EtOH	Ethanol
F. equiseti	*Fusarium equiseti*
FT-IR	Fourier transform infrared spectroscopy
GC-MS	Gas chromatography-mass spectrometry
GLMM	Generalized linear mixed model
Glu	Glutamine
Gly	Glycine
HCN	Hydrogen cyanide

HCOOH	Formic acid
KB	King's B
L. gongylophorus	*Leucoagaricus gongylophorus*
LCA	Leaf-cutting ant
LC-MS	Liquid chromatography-mass spectrometry
Lys	Lysine
m/z	Mass to charge ratio
MeOH	Methanol
MHz	Megahertz
MPLC	Medium pressure liquid chromatography
MSTFA	*N*-Methyl-*N*-(trimethylsilyl) trifluoroacetamide
n. s.	Not significant
NMR	Nuclear magnetic resonance
NOE	Nuclear Overhauser effect
NOESY	Nuclear Overhauser effect spectroscopy
NRPS	Non-ribosomal peptide synthetase
OPA	*o*-Phthalaldehyde
P. fastigiata	*Phialophora fastigiata*
PCR	Polymerase chain reaction
PDA	Potato dextrose agar
RNA	Ribonucleic acid
Ser	Serine
SFM	Soy flour mannitol medium
SPME	Solid phase microextraction
Thr	Threonine
TIC	Total ion chromatogram
UHPLC	Ultra high performance liquid chromatography
UPLC	Ultra performance liquid chromatography
UV	Ultra violet
VOCs	Volatile compounds
YEME	Yeast extract malt extract

List of publications

Included in this thesis:

- **B. Dhodary**, M. Schilg, R. Wirth, D. Spiteller (**2018**). Secondary Metabolites from *Escovopsis weberi* and Their Role in Attacking the Garden Fungus of Leaf-Cutting Ants. *Chemistry A European Journal*, 24 (17), 4445.

Not included in this thesis:

- H. J. Lee, **B. Dhodary**, J. Y. Lee, J. P. An, Y. K. Ryu, K. S. Kim, C. H. Lee, W. K. Oh (**2019**). Dereplication of Components Coupled with HPLC-qTOF-MS in the Active Fraction of *Humulus japonicas* and it's Protective Effects against Parkinson's Disease Mouse Model. *Molecules*, 24, 1435.
- Y. Qiang, W. F. Wang**, B. Dhodary**, J. L. Yang (**2017**). Zeolitic imidazolate framework 8 (ZIF-8) reinforced macroporous resin D101 for selective solid-phase extraction of 1-naphthol and 2-naphthol from phenol compounds. *Electrophoresis*, 38, 1685.
- J. L. Yang, T. K. Q. Ha**, B. Dhodary**, J. Y. Seo, H. Kim, J. Park, W. K. Oh (**2016**). 3, 4-seco-28-noroleanane triterpenes from *Camellia japonica* protect from neurotoxicity in a rotenone model of Parkinson's disease. *Tetrahedron*, 72, 3240.
- J. L. Yang[1], **B. Dhodary[1]**, T. K. Q. Ha, J. Kim, E. Kim, W. K. Oh (**2015**). Three new coumarins from *Saposnikovia divaricata* and their porcine epidemic diarrhea virus (PEDV) inhibitory activity. *Tetrahedron*, 71, 4651.
- J. L. Yang, T. K. Q. Ha, **B. Dhodary**, E. Pyo, N. Hieu, H. Cho, E. Kim, W. K. Oh (**2015**). Oleanane Triterpenes from the Flower of Camellia japonica Inhibit Porcine Epidemic Diarrhea Virus (PEDV) Replication. *Journal of Medicinal Chemistry*, 58, 1268.
- J. L. Yang, T. K. Q. Ha, **B. Dhodary**, K. H. Kim, J. Park, C. H. Lee, Y. C. Kim, W. K. Oh (**2014**). Dammarane Triterpenes as Potential SIRT1 Activators from the Leaves of *Panax ginseng*. *Journal of Natural Products,* 77, 1615.

Acknowledgement

Foremost, I am deeply grateful to my advisor, Prof. Dr. Dieter Spiteller for the continuous assistance and support for my PhD study and research. The guidance from professor helped me in my all aspects of research and writing of this dissertation. I could not have imagined having a better supervisor for my PhD degree. I am very thankful to my co-supervisor Prof. Dr. Bernhard Schink for his guidance.

Besides my supervisors, I would like to thank all lab members Karin Denger, Daniela Starke, Dr. Anthony Farlow, Dr. Darshani Rupasinghe, Kenechukwu Victor Iloabuchi, Dr. Khalid Naji, Alana Pereira and former lab members for their continuous support and kind cooperation. Also, I thank members of AG Schleck and AG Schink for letting me to join in several excursions and parties.

I thank Anke Friemel for NMR sample measurements.

Special thanks go to Dr. Rainer Wirth and his students Benjamin Feth and Julia Schulz, Plant Ecology and Systematics, Faculty of Biology, University of Kaiserslautern for providing mini-subcolonies of leaf-cutting ants and for performing the behavioral studies. I thank Prof. Dr. Flavio Roces, University of Würzburg for sending us leaf-cutting ants.

I would like to express my sincere gratitude to the Konstanz Research School Chemical Biology for providing funding for my research and offering lots of scientific and transferable skill courses. I am deeply indepted to the Welcome Center of the University of Konstanz for helping me in all the official matters and visa applications.

Last but not the least; I would like to thank my family and relatives for supporting me spiritually throughout my life.

Thank you all for your support and encouragement!

References

1. A. E. Douglas, *J. Mol. Biol.* 2014 **426**, 3830-3837.
2. T. R. Schultz and S. G. Brady, *Proc. Natl. Acad. Sci. USA* 2008, **105**, 5435-5440.
3. C. R. Currie, U. G. Mueller and D. Malloch, *Proc. Natl. Acad. Sci. USA* 1999, **96**, 7998-8002.
4. C. R. Currie, J. A. Scott, R. C. Summerbell and D. Malloch, *Nature* 1999, **398**, 701.
5. M. J. Cafaro and C. R. Currie, *C. J. Microbiol.* 2005, **51**, 441-446.
6. J. Sosa-Calvo, T. R. Schultz, C. R. Brandão, C. Klingenberg, R. M. Feitosa, C. Rabeling, M. Bacci Jr, C. T. Lopes and H. L. Vasconcelos, *PLoS One* 2013, **8**, e80498.
7. T. R. Schultz and R. Meier, *Syst. entomol.* 1995, **20**, 337-370.
8. I. H. Chapela, S. A. Rehner, T. R. Schultz and U. G. Mueller, *Sci.* 1994, **266**, 1691-1694.
9. U. G. Mueller, S. A. Rehner and T. R. Schultz, *Sci.* 1998, **281**, 2034-2038.
10. A. J. Mayhe-Nunes and K. Jaffé, *Ecotropicos* 1998, **11**, 45-54.
11. C. R. Currie, B. Wong, A. E. Stuart, T. R. Schultz, S. A. Rehner, U. G. Mueller, G.-H. Sung, J. W. Spatafora and N. A. Straus, *Sci.* 2003, **299**, 386-388.
12. http://cincinnatizoo.org/wp-content/uploads/2011/03/FactSheet-AntLeafCutter2010.pdf.
13. https://en.wikipedia.org/wiki/Acromyrmex.
14. R. Piper, *Extraordinary Animals: An Encyclopedia of Curious and Unusual Animals, Greenwood Press* 2007, 298.
15. N. A. Weber, *Gardening Ants, The Attines, The American Philosophical Society* 1972.
16. A. Rodrigues, C. D. Carletti, O. C. Bueno and F. C. Pagnocca, *Braz. J. Microbiol.* 2008, **39**, 64-67.
17. F. C. Pagnocca, M. Bacci, M. H. Fungaro, O. C. Bueno, M. J. Hebling, S. A. Ariovaldo and M. Capelari, *Mycol. Res.* 2001, **105**, 173-176.
18. P. Fisher, D. Stradling and D. Pegler, *Mycologist* 1994, **8**, 128-131.

19. M. Schiøtt, H. H. D. F. Licht, L. Lange and J. J. Boomsma, *BMC Microbiol.*, 2008, **8**, 40.
20. U. G. Mueller, T. R. Schultz, C. R. Currie, R. M. Adams and D. Malloch, *Q. Rev. Biol.* 2001, **76**, 169-197.
21. M. Littledyke and J. Cherrett, *Bull. Entomo. Res.* 1976, **66**, 205-217.
22. F. O. Aylward, K. E. Burnum-Johnson, S. G. Tringe, C. Teiling, D. M. Tremmel, J. A. Moeller, J. J. Scott, K. W. Barry, P. D. Piehowski and C. D. Nicora, *Appl. Environ. Microbiol.* 2013, **79**, 3770-3778.
23. A. N. Bot, C. R. Currie, A. G. Hart and J. J. Boomsma, *Ethol. Ecol. Evol.* 2001, **13**, 225-237.
24. A. Rodrigues, F. Pagnocca, O. Bueno, L. Pfenning and M. Bacci Jr, *Sociobiology* 2005, **46**, 329-334.
25. F. C. Pagnocca, A. Rodrigues, N. S. Nagamoto and M. Bacci, *Antonie van Leeuwenhoek* 2008, **94**, 517-526.
26. A. Rodrigues, M. Bacci Jr, U. G. Mueller, A. Ortiz and F. C. Pagnocca, *Microb. Ecol.* 2008, **56**, 604-614.
27. J. J. Scott, K. J. Budsberg, G. Suen, D. L. Wixon, T. C. Balser and C. R. Currie, *PloS one* 2010, **5**, e9922.
28. F. O. Aylward, K. E. Burnum, J. J. Scott, G. Suen, S. G. Tringe, S. M. Adams, K. W. Barry, C. D. Nicora, P. D. Piehowski and S. O. Purvine, *The ISME journal* 2012, **6**, 1688.
29. D. Ortius-Lechner, R. Maile, E. D. Morgan and J. J. Boomsma, *J. Chem. Ecol.* 2000, **26**, 1667-1683.
30. P. Schmid-Hempel, *Parasites in social insects*, Princeton University Press 1998.
31. C. R. Currie and A. E. Stuart, *Proc. R. Soc. B: Biol. Sci.* 2001, **268**, 1033-1039.
32. D. Abramowski, C. Currie and M. Poulsen, *Insectes Soc.* 2011, **58**, 65-75.
33. S. H. Yek and U. G. Mueller, *Biol. Rev.* 2011, **86**, 774-791.
34. A. N. Bot, D. Ortius-Lechner, K. Finster, R. Maile and J. J. Boomsma, *Insectes Soc.* 2002, **49**, 363-370.
35. S. B. Andersen, L. H. Hansen, P. Sapountzis, S. J. Sørensen and J. J. Boomsma, *Mol. Ecol.* 2013, **22**, 4307-4321.

36. C. Beemelmanns, H. Guo, M. Rischer and M. Poulsen, *Beilstein J. Org. Chem.* 2016, **12**, 314-327.
37. E. B. Van Arnam, A. C. Ruzzini, C. S. Sit, H. Horn, A. A. Pinto-Tomás, C. R. Currie and J. Clardy, *Proc. Natl. Acad. Sci. USA* 2016, **113**, 12940-12945.
38. S. E. Marsh, M. Poulsen, A. Pinto-Tomas and C. R. Currie, *PLoS One* 2014, **9**, e103269.
39. S. Haeder, R. Wirth, H. Herz and D. Spiteller, *Proc. Natl. Acad. Sci. USA* 2009, **106**, 4742-4746.
40. I. Schoenian, M. Spiteller, M. Ghaste, R. Wirth, H. Herz and D. Spiteller, *Proc. Natl. Acad. Sci. USA* 2011, **108**, 1955-1960.
41. C. R. Currie, A. N. Bot and J. J. Boomsma, *Oikos* 2003, **101**, 91-102.
42. C. R. Currie, *Oecologia* 2001, **128**, 99-106.
43. N. M. Gerardo, U. G. Mueller, S. L. Price and C. R. Currie, *Proc. R. Soc. B: Biol. Sci.* 2004, **271**, 1791-1798.
44. T. J. de Man, J. E. Stajich, C. P. Kubicek, C. Teiling, K. Chenthamara, L. Atanasova, I. S. Druzhinina, N. Levenkova, S. S. Birnbaum and S. M. Barribeau, *Proc. Natl. Acad. Sci. USA* 2016, **113**, 3567-3572.
45. A. E. Little and C. R. Currie, *Ecology* 2008, **89**, 1216-1222.
46. A. Rodrigues, F. Pagnocca, M. Bacci, M. Hebling, O. Bueno and L. Pfenning, *Folia Microbiol.* 2005, **50**, 421.
47. A. E. Douglas, *Ann. Rev. Entomol.* 2015, **60**, 17-34.
48. A. E. Douglas, *Funct. Ecol.* 2009, **23**, 38-47.
49. L. V. Flórez, P. H. Biedermann, T. Engl and M. Kaltenpoth, *Nat. Prod. Rep.* 2015, **32**, 904-936.
50. F. C. Pagnocca, V. E. Masiulionis and A. Rodrigues, *Psyche* 2012, **2012**.
51. A. Bot, D. Ortius-Lechner, K. Finster, R. Maile and J. Boomsma, *Insectes Soc* 2002.
52. A. V. Santos, R. J. Dillon, V. M. Dillon, S. E. Reynolds and R. I. Samuels, *FEMS Microbiol. Lett.* 2004, **239**, 319-323.
53. S. C. Carreiro, F. C. Pagnocca, O. C. Bueno, M. B. Júnior, M. J. A. Hebling and O. A. da Silva, *Antonie van Leeuwenhoek* 1997, **71**, 243-248.

54. G. Suen, J. J. Scott, F. O. Aylward, S. M. Adams, S. G. Tringe, A. A. Pinto-Tomás, C. E. Foster, M. Pauly, P. J. Weimer and K. W. Barry, *PLoS Genet.* 2010, **6**, e1001129.
55. N. M. Gerardo, S. R. Jacobs, C. R. Currie and U. G. Mueller, *PLoS biol.* 2006, **4**, e235.
56. H. T. Reynolds and C. R. Currie, *Mycologia* 2004, **96**, 955-959.
57. S. S. Varanda-Haifig, T. R. Albarici, P. H. Nunes, I. Haifig, P. C. Vieira and A. Rodrigues, *Antonie van Leeuwenhoek* 2017, **110**, 593-605.
58. C. P. Boya, H. Fernández-Marín, L. C. Mejía, C. Spadafora, P. C. Dorrestein and M. Gutiérrez, *Sci. Rep.* 2017, **7**, 5604-5604.
59. T. Thiele, C. Kost, F. Roces and R. Wirth, *J. Chem. Ecol.* 2014, **40**, 617-620.
60. G. N. Belofsky, J. B. Gloer, D. T. Wicklow and P. F. Dowd, *Tetrahedron* 1995, **51**, 3959-3968.
61. O. F. Smetanina, A. I. Kalinovsky, Y. V. Khudyakova, M. V. Pivkin, P. S. Dmitrenok, S. N. Fedorov, H. Ji, J.-Y. Kwak and T. A. Kuznetsova, *J. Nat. Prod.* 2007, **70**, 906-909.
62. M. Xu, G. Gessner, I. Groth, C. Lange, A. Christner, T. Bruhn, Z. Deng, X. Li, S. H. Heinemann and S. Grabley, *Tetrahedron* 2007, **63**, 435-444.
63. W. A. Ayer, P. A. Craw and J. Neary, *Can. J. Chem.* 1992, **70**, 1338-1347.
64. K. A. Seifert, R. A. Samson and I. H. Chapela, *Mycologia* 1995, **87**, 407-413.
65. L. A. Meirelles, Q. V. Montoya, S. E. Solomon and A. Rodrigues, *PloS one* 2015, **10**, e0112067.
66. A. E. Little and C. R. Currie, *Biol. Lett.* 2007, **3**, 501-504.
67. M. H. Medema, K. Blin, P. Cimermancic, V. de Jager, P. Zakrzewski, M. A. Fischbach, T. Weber, E. Takano and R. Breitling, *Nucleic Acids Res.* 2011, **39**, W339-W346.
68. J. You, L. Du, J. B. King, B. E. Hall and R. H. Cichewicz, *ACS Chem. Biol.* 2013, **8**, 840-848.
69. P. Ridley, P. Howse and C. Jackson, *Experientia* 1996, **52**, 631-635.
70. H. Herz, B. Hölldobler and F. Roces, *Behav. Ecol.* 2008, **19**, 575-582.

71. H. Levin, R. Hazenfratz, J. Friedman, D. Palevitch and M. Perl, *Phytother. Res.* 1988, **2**, 67-69.
72. I. Izhaki, *New Phytol.* 2002, **155**, 205-217.
73. D. L. Barnard, J. H. Huffman, J. L. Morris, S. G. Wood, B. G. Hughes and R. W. Sidwell, *Antiviral Res.* 1992, **17**, 63-77.
74. A. Liu, H. Chen, W. Wei, S. Ye, W. Liao, J. Gong, Z. Jiang, L. Wang and S. Lin, *Oncol. Rep.* 2011, **26**, 81-89.
75. M.-Y. Park, H.-J. Kwon and M.-K. Sung, *Biosci. Biotechnol. Biochem.* 2009, **73**, 828-832.
76. R. Goel, G. G. Das, S. Ram and V. Pandey, *Indian J. Exp. Biol.* 1991, **29**, 230-232.
77. B. Hölldobler and E. O. Wilson, *The ants*, Harvard University Press 1990.
78. R. Wirth, H. Herz, R. Ryel, W. Beyschlag and B. Hölldobler, 2003.
79. A. Rodrigues, F. Pagnocca, M. Bacci, M. Hebling, O. Bueno and L. Pfenning, *Folia microbiol.* 2005, **50**, 421-425.
80. A. J. Beattie, C. L. Turnbull, T. Hough and R. B. Knox, *Ann. Entomol. Soc. Am.* 1986, **79**, 448-450.
81. D.-C. Oh, M. Poulsen, C. R. Currie and J. Clardy, *Nat. Chem. Biol.* 2009, **5**, 391-393.
82. N. A. Holmes, T. M. Innocent, D. Heine, M. A. Bassam, S. F. Worsley, F. Trottmann, E. H. Patrick, D. W. Yu, J. C. Murrell and M. Schiøtt, *Front. Microbiol.* 2016, **7**, 2073.
83. J. Barke, R. F. Seipke, D. W. Yu and M. I. Hutchings, *Commun. Integr. Biol.* 2011, **4**, 41-43.
84. B. Dhodary, M. Schilg, R. Wirth and D. Spiteller, *Chem. Eur. J.* 2018, **24**, 4445-4452.
85. D. Heine, N. A. Holmes, S. F. Worsley, A. C. A. Santos, T. M. Innocent, K. Scherlach, E. H. Patrick, W. Y. Douglas, J. C. Murrell and P. C. Vieria, *Nat. Commun.* 2018, **9**, 2208.
86. D. Römer and F. Roces, *Sci. Nat.* 2019, **106**, 3.

87. M. J. B. T. E. Kieser, M. J. Buttner, K. F. Chater and D. A. Hopwood, *John Innes Foundation: Colney, England* 2000.
88. G. E. Julian and J. H. Fewell, *Anim. Behav.* 2004, **68**, 1-8.
89. S. D. Porter, R. K. V. Meer, M. A. Pesquero, S. Campiolo and H. G. Fowler, *Ann. Entomol. Soc. Am.* 1995, **88**, 570-575.
90. M. E. Whitehouse and K. Jaffe, *Anim. Behav.* 1996, **51**, 1207-1217.
91. M. Okuno, K. Tsuji, H. Sato and K. Fujisaki, *J. Ethol.* 2012, **30**, 23-27.
92. W. O. Hughes, J. Eilenberg and J. J. Boomsma, *Proc. R. Soc. B: Biol. Sci.* 2002, **269**, 1811-1819.
93. E. Combet, J. Henderson, D. C. Eastwood and K. S. Burton, *Mycoscience* 2006, **47**, 317-326.
94. C. Kleineidam and F. Roces, *Insectes Soc.* 2000, **47**, 241-248.
95. R. M. Adams, T. H. Jones, A. W. Jeter, H. Henrik, T. R. Schultz and D. R. Nash, *Biochem. Syst. Ecol.* 2012, **40**, 91-97.
96. V. C. Norman, T. Butterfield, F. Drijfhout, K. Tasman and W. O. Hughes, *J. Chem. Ecol.* 2017, **43**, 225-235.
97. R. M. Crewe and M. S. Blum, *J. Insect Physiol.* 1972, **18**, 31-42.
98. E. A. Silva-Junior, A. C. Ruzzini, C. R. Paludo, F. S. Nascimento, C. R. Currie, J. Clardy and M. T. Pupo, *Sci. Rep.* 2018, **8**, 2595.
99. L. Rasmussen, T. D. Lee, W. L. Roelofs, A. Zhang and G. D. Daves, *Nature* 1996, **379**, 684-684.
100. J. Muchovej and T. Della Lucia, *Mycotaxon* 1990.
101. H. Fernández-Marín, J. K. Zimmerman, S. A. Rehner and W. T. Wcislo, *Proc. R. Soc. B: Biol. Sci.* 2006, **273**, 1689-1695.
102. H. Fernández-Marín, D. R. Nash, S. Higginbotham, C. Estrada, J. S. van Zweden, P. d'Ettorre, W. T. Wcislo and J. J. Boomsma, *Proc. R. Soc. B: Biol. Sci.* 2015, **282**, 20150212.
103. D.-C. Oh, M. Poulsen, C. R. Currie and J. Clardy, *Nat. Chem. Biol.*, 2009 **5**, 391.
104. R. F. Seipke, J. Barke, C. Brearley, L. Hill, W. Y. Douglas, R. J. Goss and M. I. Hutchings, *PLoS one* 2011, **6**, e22028.
105. K. Grob, *J. Chromatogr. A* 1973, **84**, 255-273.

106. Z. Genfa and P. K. Dasgupta, *Anal. Chem.* 1989, **61**, 408-412.
107. K. F. Castric and P. A. Castric, *Appl. Environ. Microbiol.* 1983, **45**, 701-702.
108. M. Avalos, P. Garbeva, J. M. Raaijmakers and G. P. van Wezel, *The ISME journal* 2019, 1-15.
109. K. Schmidt and D. Spiteller, *J. Chem. Ecol.* 2017, **43**, 806-816.
110. S. E. Jones, L. Ho, C. A. Rees, J. E. Hill, J. R. Nodwell and M. A. Elliot, *Elife* 2017, **6**, e21738.
111. S. Anwar, B. Ali and I. Sajid, *Front. Microbiol.* 2016, **7**, 1334.
112. H. Gürtler, R. Pedersen, U. Anthoni, C. Christophersen, P. H. Nielsen, E. M. wellington, C. Pedersen and K. Bock, *J. Antibiot.* 1994, **47**, 434-439.
113. S. Schulz and J. S. Dickschat, *Nat. Prod. Rep.* 2007, **24**, 814-842.
114. R. Schmidt, V. Cordovez, W. De Boer, J. Raaijmakers and P. Garbeva, *The ISME journal* 2015, **9**, 2329.
115. M. Avalos, G. P. van Wezel, J. M. Raaijmakers and P. Garbeva, *Curr. Opin. Microbiol.* 2018, **45**, 84-91.
116. R. Evershed and E. Morgan, *Insect Biochem.* 1983, **13**, 469-474.
117. J. H. Cross, J. R. West, R. M. Silverstein, A. R. Jutsum and J. M. Cherrett, *J. Chem.Ecol.* 1982, **8**, 1119-1124.
118. J. de Oliveira, O. Martinez, N. Carnieri, E. Vilela and H. Reis, *Anais da Sociedade Entomológica do Brasil* 1990, **19**, 145-154.
119. P. Fiddaman and S. Rossall, *J. Appl. Bacteriol.* 1993, **74**, 119-126.
120. N. A. Weber, *Sci.* 1966, **153**, 587-604.
121. H. Schildknecht and K. Koob, *Ang. Chem. Int. Ed.* 1970, **9**, 173-173.
122. J. Barke, R. F. Seipke, S. Grüschow, D. Heavens, N. Drou, M. J. Bibb, R. J. Goss, W. Y. Douglas and M. I. Hutchings, *BMC Biol.* 2010, **8**, 109.
123. H. Fernández-Marín, J. K. Zimmerman, D. R. Nash, J. J. Boomsma and W. T. Wcislo, *Proc. R. Soc. B: Biol. Sci.* 2009, **276**, 2263-2269.
124. M. Zhukova, P. Sapountzis, M. Schiøtt and J. J. Boomsma, *Front. Microbiol.* 2017, **8**, 1942.
125. E. O. King, M. K. Ward and D. E. Raney, *J. Lab. Clin. Med.* 1954, **44**, 301-307.
126. C. Desai and D. Madamwar, *Bioresour. Technol.* 2007, **98**, 761-768.

127. K. Tamura, G. Stecher, D. Peterson, A. Filipski and S. Kumar, *Mol. Biol. Evol.* 2013, **30**, 2725-2729.
128. R. Bhushan and H. Brückner, *Amino acids* 2004, **27**, 231-247.
129. D. Sinnaeve and C. Michaux, *Tetrahedron* 2009, **65**, 4173-4181.
130. T. Weber, K. Blin, S. Duddela, D. Krug, H. U. Kim, R. Bruccoleri, S. Y. Lee, M. A. Fischbach, R. Müller and W. Wohlleben, *Nucleic Acids Res.* 2015, **43**, W237-W243.
131. M. Coraiola, P. L. Cantore, S. Lazzaroni, A. Evidente, N. Iacobellis and M. Dalla Serra, *Biochim. Biophys. Acta, Biomembr.* 2006, **1758**, 1713-1722.
132. J. Gerard, R. Lloyd, T. Barsby, P. Haden, M. T. Kelly and R. J. Andersen, *J. Nat. Prod.* 1997, **60**, 223-229.
133. C. Ruangviryachai, I. Barelmann, R. Fuchs and H. Budzikiewicz, *Z. Naturforsch. C* 2000, **55**, 323-327.
134. A. Deveau, H. Gross, B. Palin, S. Mehnaz, M. Schnepf, P. Leblond, P. C. Dorrestein and B. Aigle, *FEMS Microbiol. Ecol.* 2016, **92**.
135. T. Stachelhaus, H. D. Mootz and M. A. Marahiel, *Chem. Biol.* 1999, **6**, 493-505.
136. J. Y. Jang, S. Y. Yang, Y. C. Kim, C. W. Lee, M. S. Park, J. C. Kim and I. S. Kim, *J. Agr. Food Chem.* 2013, **61**, 6786-6791.
137. S. L. Hartney, S. Mazurier, M. K. Girard, S. Mehnaz, E. W. Davis, H. Gross, P. Lemanceau and J. E. Loper, *J. Bacteriol.* 2013, **195**, 765-776.
138. B. K. Scholz-Schroeder, J. D. Soule and D. C. Gross, *Mol. Plant Microbe In.* 2003, **16**, 271-280.
139. F. O. Aylward, G. Suen, P. H. Biedermann, A. S. Adams, J. J. Scott, S. A. Malfatti, T. G. del Rio, S. G. Tringe, M. Poulsen and K. F. Raffa, *MBio* 2014, **5**, e02077-02014.
140. J. M. Raaijmakers, I. De Bruijn, O. Nybroe and M. Ongena, *FEMS Microbiol. Rev.* 2010, **34**, 1037-1062.
141. N. Roongsawang, K. Washio and M. Morikawa, *Int. J. Mol. Sci.* 2011, **12**, 141-172.
142. J. C. Martins and N. Geudens, *Front. Microbiol.* 2018, **9**, 1867.

143. D. Sinnaeve, C. Michaux, J. Vandenkerckhove, E. Peys, F. A. Borremans, B. Sas, J. Wouters and J. C. Martins, *Tetrahedron* 2009, **65**, 4173-4181.
144. T. Nielsen, C. Christophersen, U. Anthoni and J. Sørensen, *J. Appl. Microbiol.* 1999, **87**, 80-90.
145. H. Tran, A. Ficke, T. Asiimwe, M. Höfte and J. M. Raaijmakers, *New Phytol.* 2007, **175**, 731-742.
146. K. A. Kissoyan, M. Drechsler, E.-L. Stange, J. Zimmermann, C. Kaleta, H. B. Bode and K. Dierking, *Curr. Biol.* 2019, **29**, 1030-1037. e1035.
147. R. Ibáñez, L.-F. Nothias, L. K. Reinert, L. A. Rollins-Smith, P. C. Dorrestein and M. Gutiérrez, *Sci. Rep.* 2019, **9**, 3019.
148. E. A. da Silva-Junior, C. R. Paludo, L. Valadares, N. P. Lopes, F. S. do Nascimento and M. T. Pupo, *Rev. Brasil. Farmacog.* 2017, **27**, 529-532.
149. A.-M. Albrecht-Gary, S. Blanc, N. Rochel, A. Z. Ocaktan and M. A. Abdallah, *Inorg. Chem.* 1994, **33**, 6391-6402.
150. P. Cornelis, *Appl. Microbiol. Biotechnol.* 2010, **86**, 1637-1645.
151. C. Kousser, C. Clark, S. Sherrington, K. Voelz and R. A. Hall, *Sci. Rep.* 2019, **9**, 5714.
152. E. Butaitė, M. Baumgartner, S. Wyder and R. Kümmerli, *Nat. Commun.* 2017, **8**, 414.
153. W.-J. Chen, T.-Y. Kuo, F.-C. Hsieh, P.-Y. Chen, C.-S. Wang, Y.-L. Shih, Y.-M. Lai, J.-R. Liu, Y.-L. Yang and M.-C. Shih, *Sci. Rep.* 2016, **6**, 32950.
154. P. Visca, F. Imperi and I. L. Lamont, *Trends Microbiol.* 2007, **15**, 22-30.
155. I. J. Schalk and L. Guillon, *Environ. Microbiol.* 2013, **15**, 1661-1673.
156. C. D. Moon, X.-X. Zhang, S. Matthijs, M. Schäfer, H. Budzikiewicz and P. B. Rainey, *BMC Microbiol.* 2008, **8**, 7.
157. F. Taguchi, T. Suzuki, Y. Inagaki, K. Toyoda, T. Shiraishi and Y. Ichinose, *J. Bacteriol.* 2010, **192**, 117-126.
158. I. L. Lamont, P. A. Beare, U. Ochsner, A. I. Vasil and M. L. Vasil, *Proc. Natl. Acad. Sci. USA* 2002, **99**, 7072-7077.
159. E. Banin, M. L. Vasil and E. P. Greenberg, *Proc. Natl. Acad. Sci. USA* 2005, **102**, 11076-11081.

160. S. O'Brien, D. J. Hodgson and A. Buckling, *Proc. R. Soc. B: Biol. Sci.* 2014, **281**, 20140858.

Supporting Information

Supporting Information

Chapter 2: Secondary metabolites from *Escovopsis weberi* and their role in attacking the garden fungus *Leucoagaricus gongylophorus* of leaf-cutting ants

Basanta Dhodary[1], Michele Schilg[2], Rainer Wirth[2], and Dieter Spiteller[1*]

[1]*Chemical Ecology/Biological Chemistry, University of Konstanz, Universitätstrasse 10, D-78457 Konstanz, Germany.*
[2]*Plant Ecology and Systematics, Technical University Kaiserslautern, Erwin-Schrödingerstraße 13,* 67653 Kaiserslautern*, Germany.*

Secondary metabolite profiling of *E. weberi*

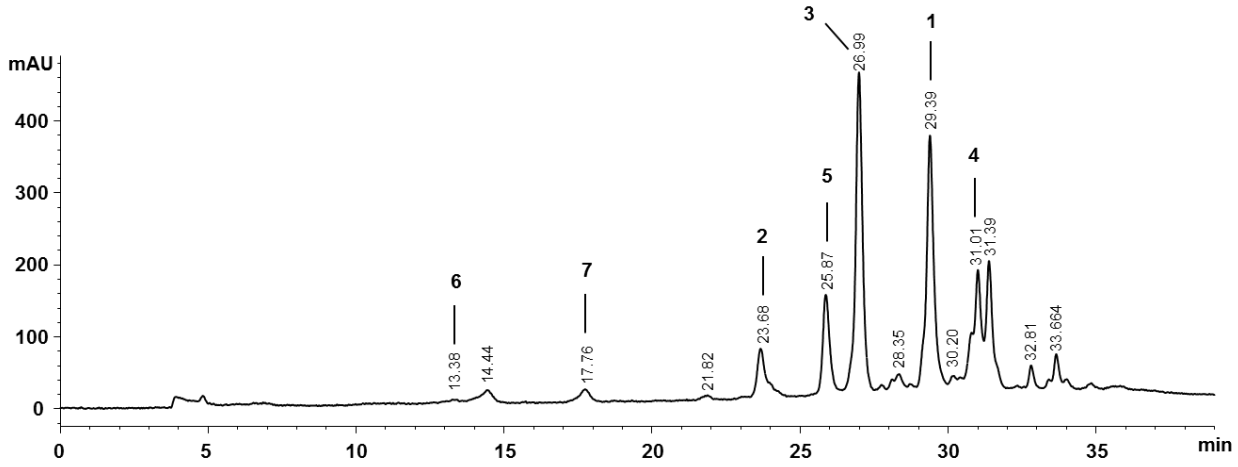

Figure S2.1: Reverse phase HPL-chromatogram of a methanol soluble extract of *E. weberi* analysed on a Phenomenex polar RP18 column with gradient elution; detected by diode array UV-visible detector at 254 nm wavelength.

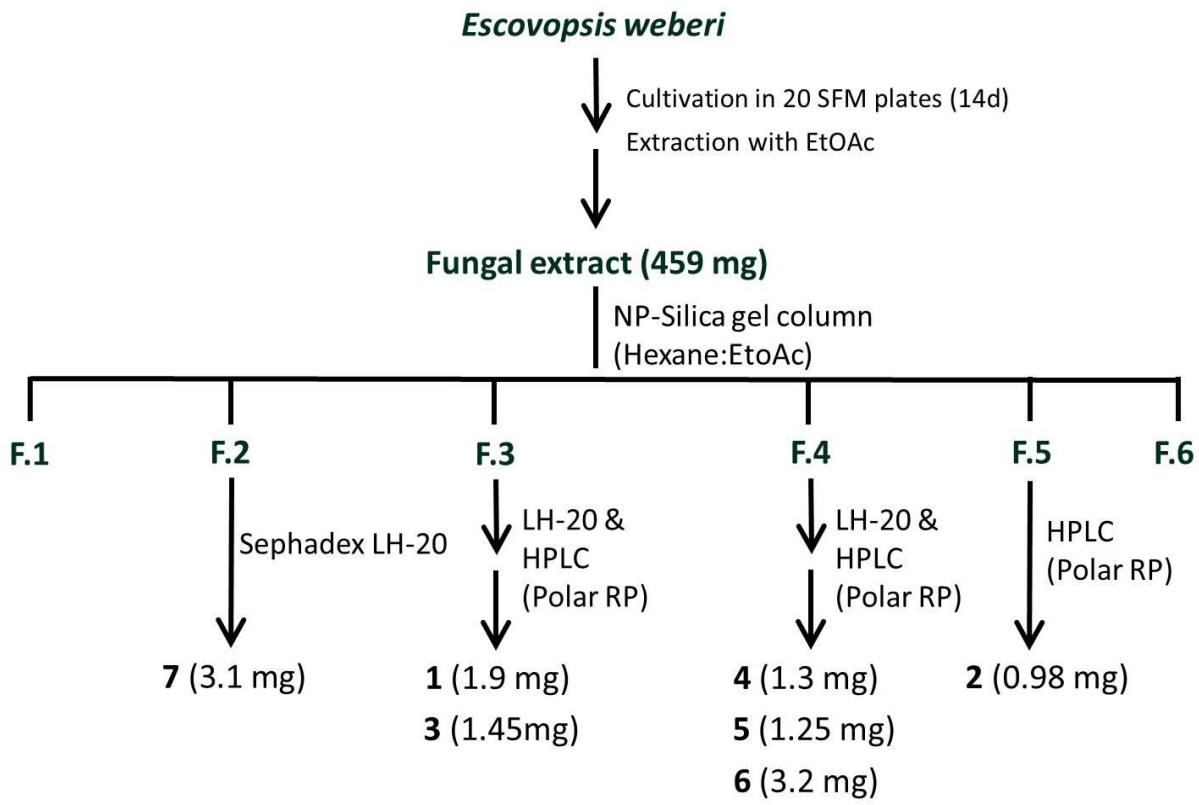

Figure S2.2: Flow chart of the isolation scheme of compounds (**1**-**7**) from *E. weberi*

Structure elucidation of shearinine L (1)

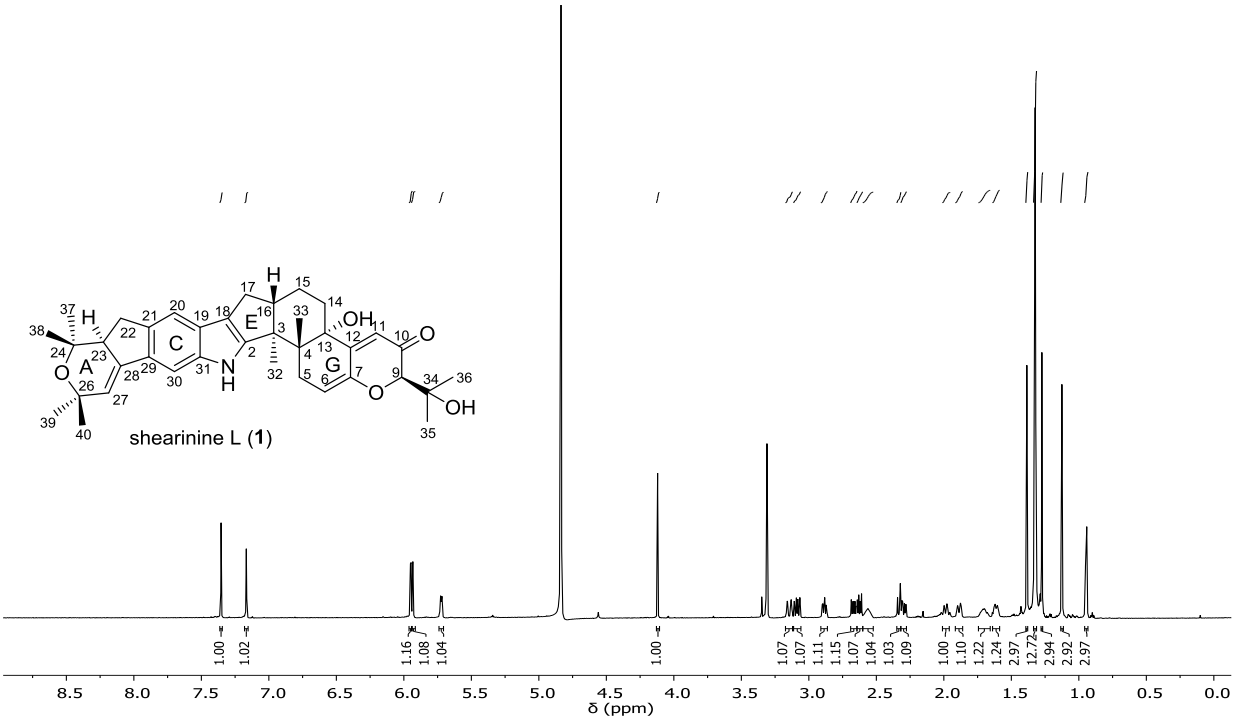

Figure S2.3. ^{1}H-NMR spectrum (600 MHz, MeOD-d_4) of shearinine L **(1)**

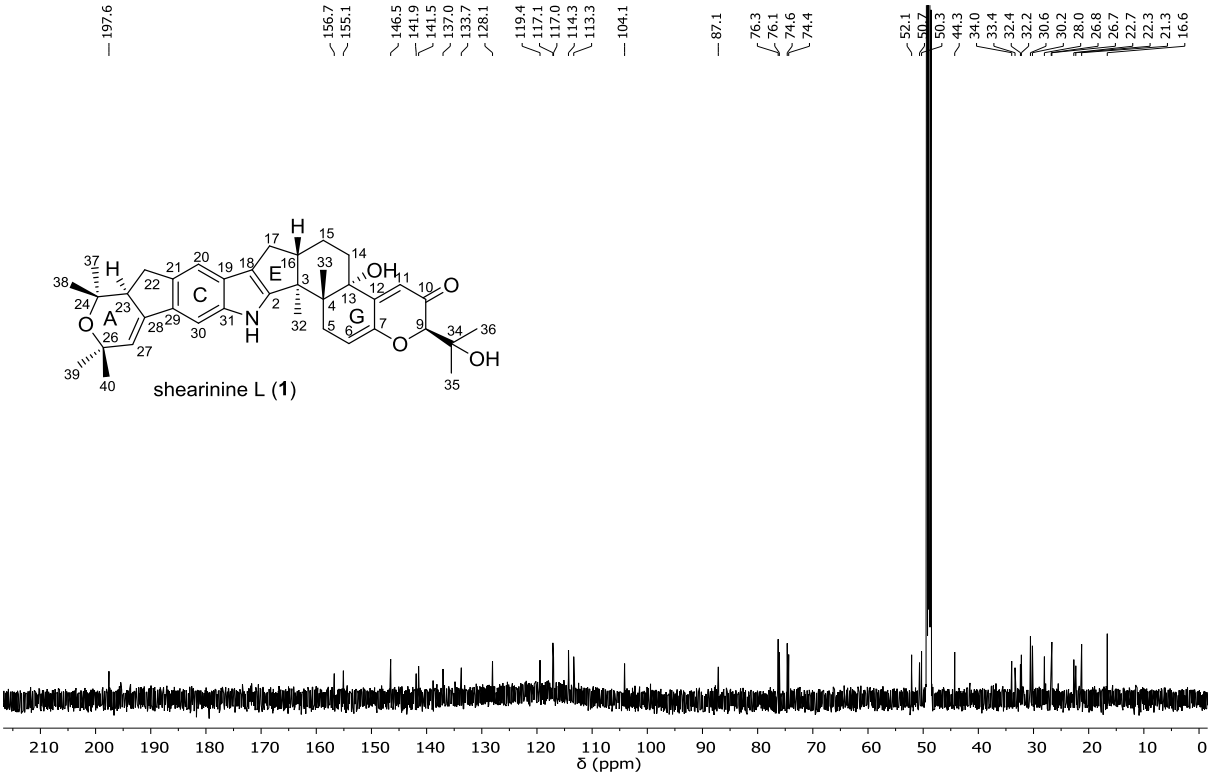

Figure S2.4. ^{13}C-NMR spectrum (150 MHz, MeOD-d_4) of shearinine L (**1**)

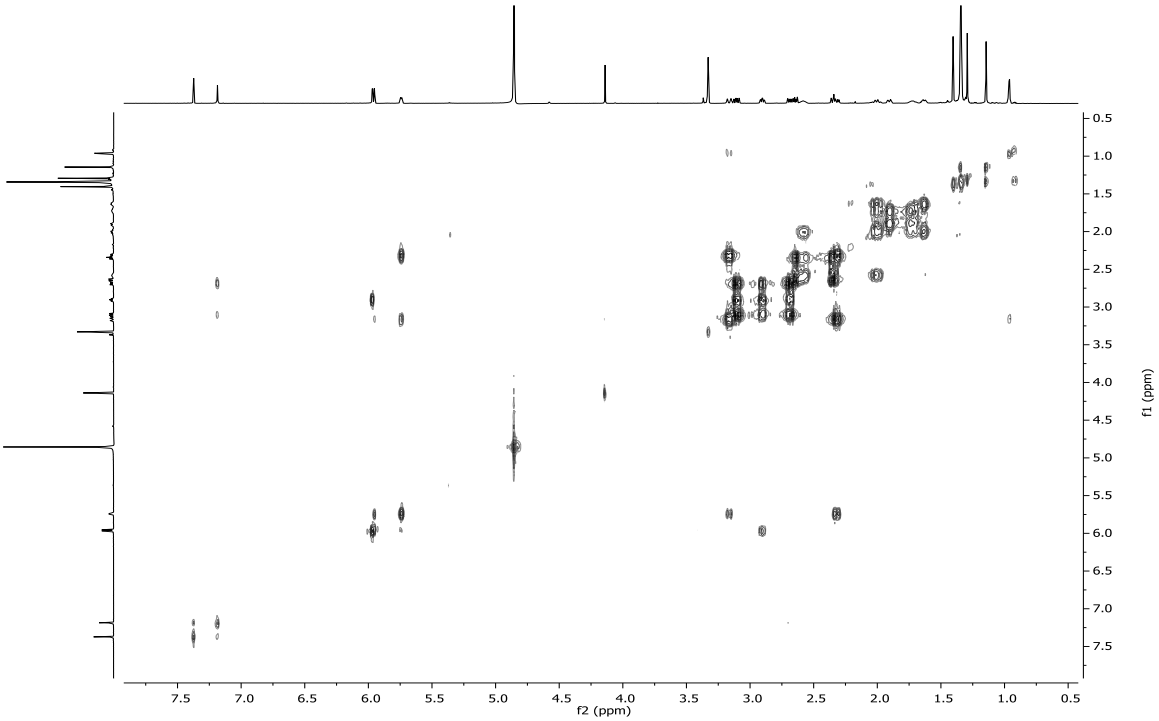

Figure S2.5. ^{1}H-^{1}H-COSY NMR spectrum (600 MHz, MeOD-d_4) of shearinine L (**1**)

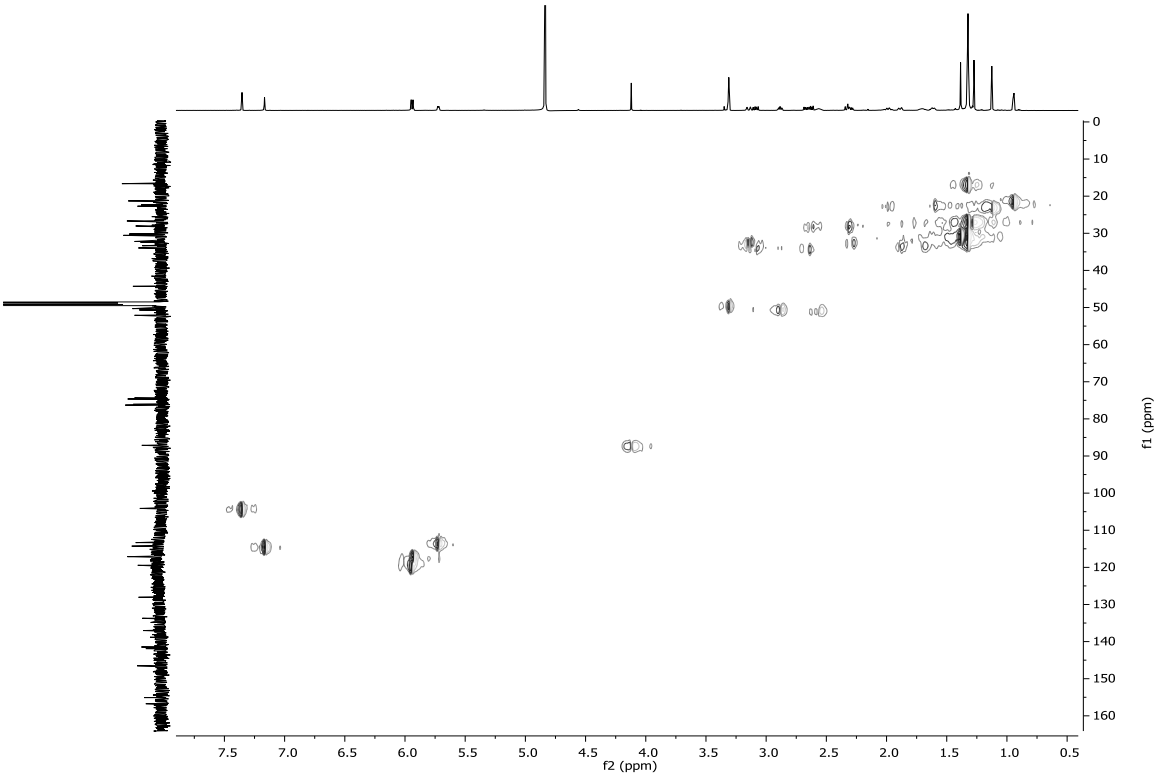

Figure S2.6. HSQC-NMR spectrum (600 MHz, MeOD-d_4) of shearinine L (**1**)

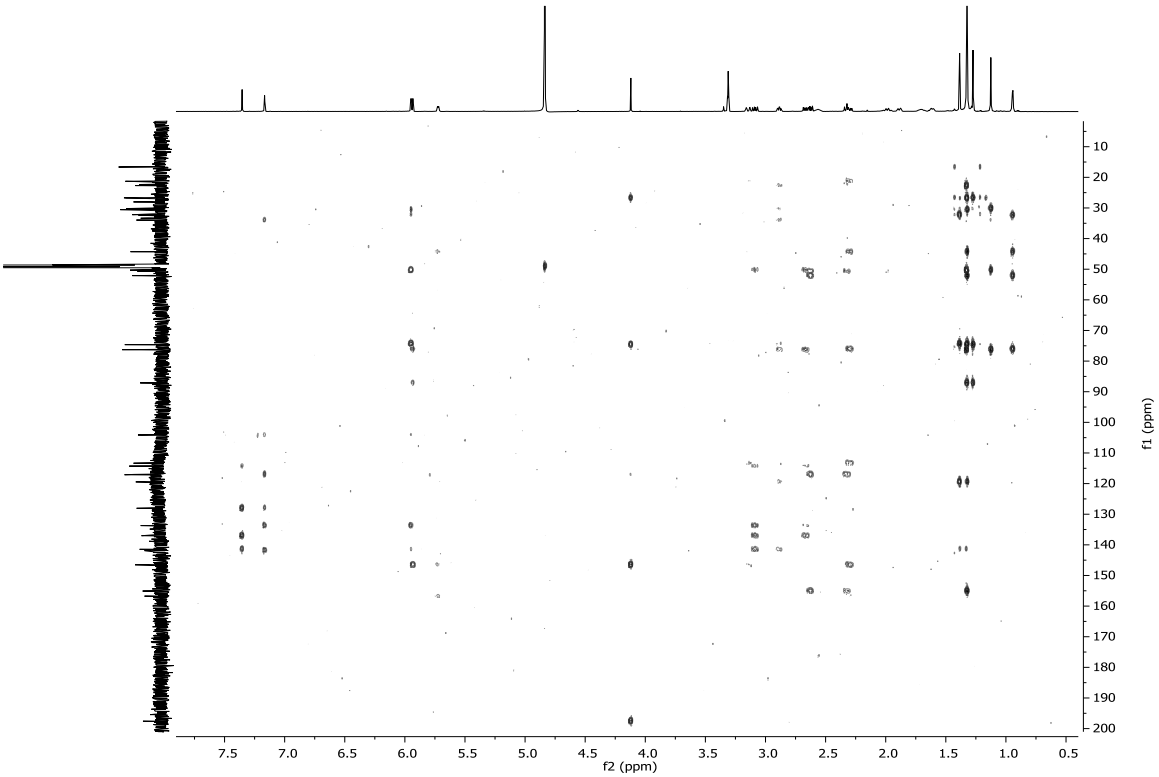

Figure S2.7. HMBC-NMR spectrum (600 MHz, MeOD-d_4) of shearinine L (**1**)

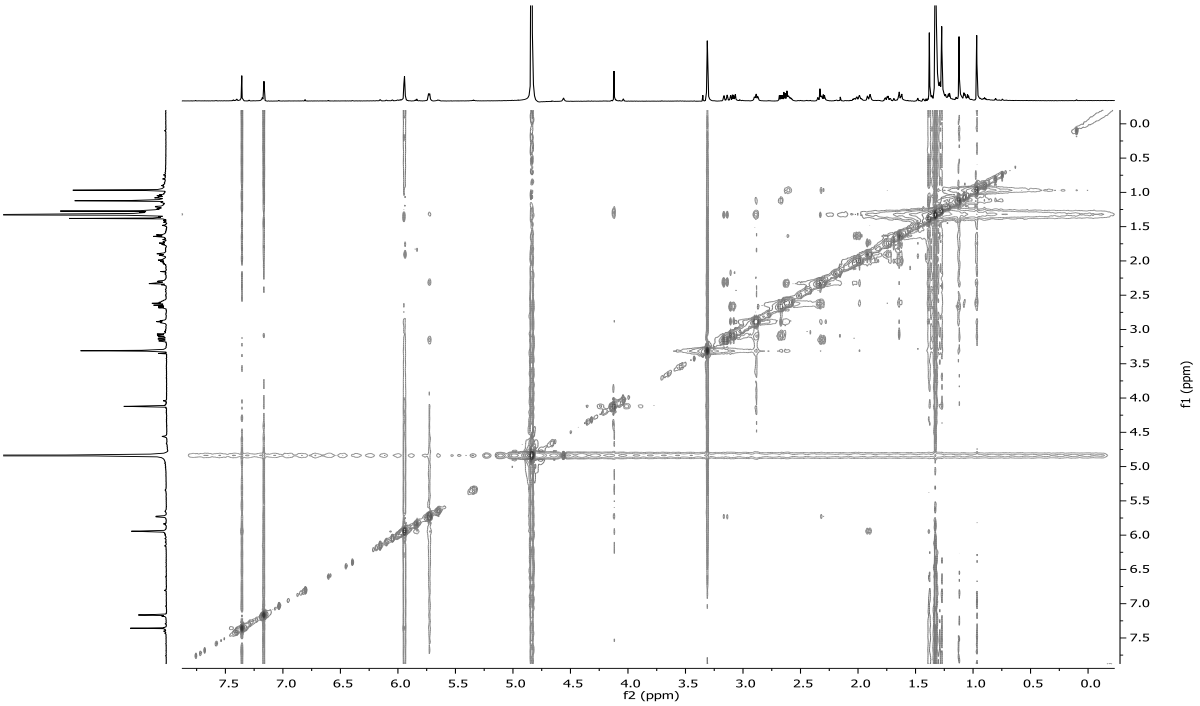

Figure S2.8. NOESY-NMR spectrum (600 MHz, MeOD-d_4) of shearinine L (**1**)

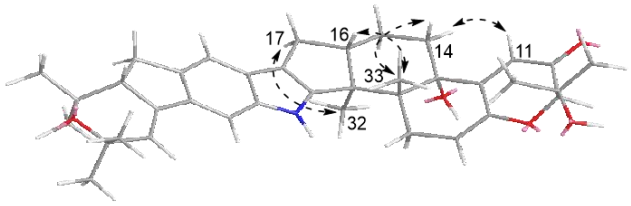

1

Figure S2.9. Key NOESY correlations of shearinine L (**1**).

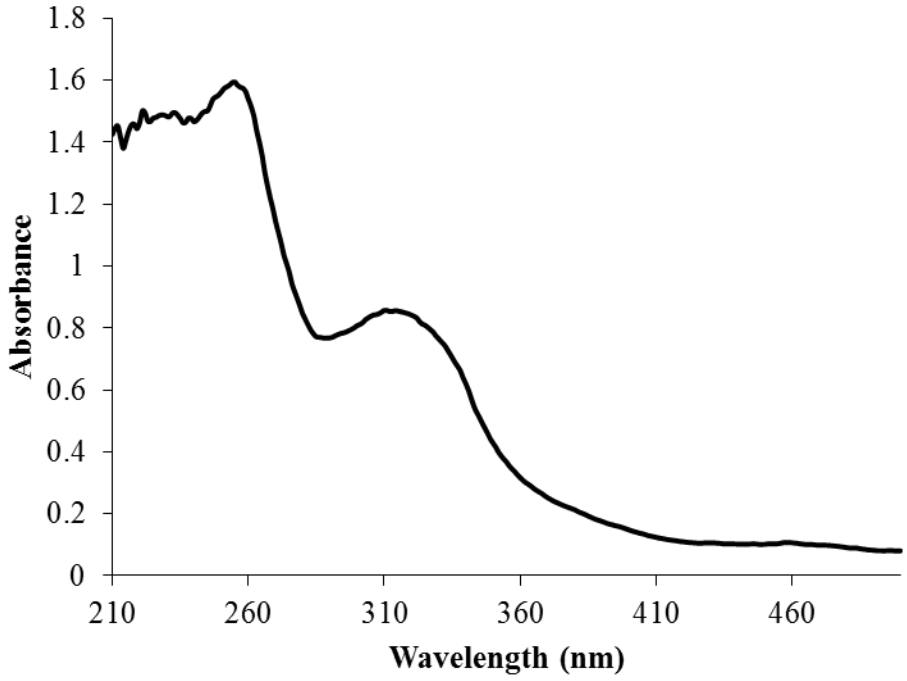

Figure S2.10. UV-Visible spectrum of the shearinine L (**1**) in methanol.

Structure elucidation of shearinine M (2)

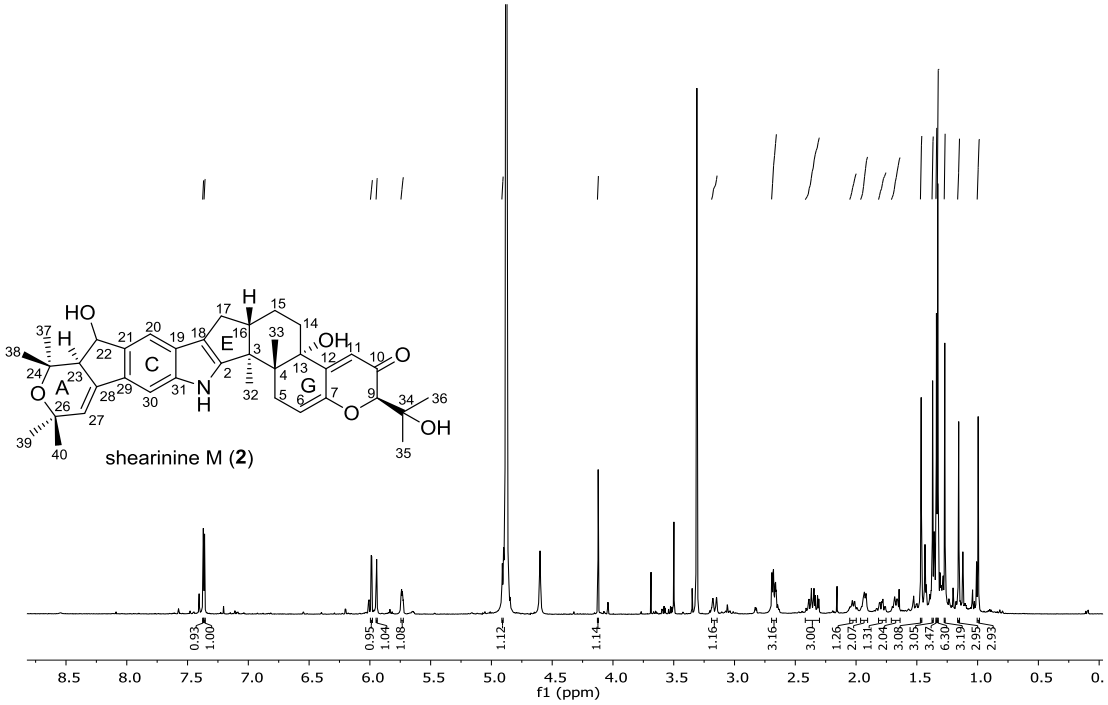

Figure S2.11. ^{1}H-NMR spectrum (600 MHz, MeOD-d_4) of shearinine M (**2**)

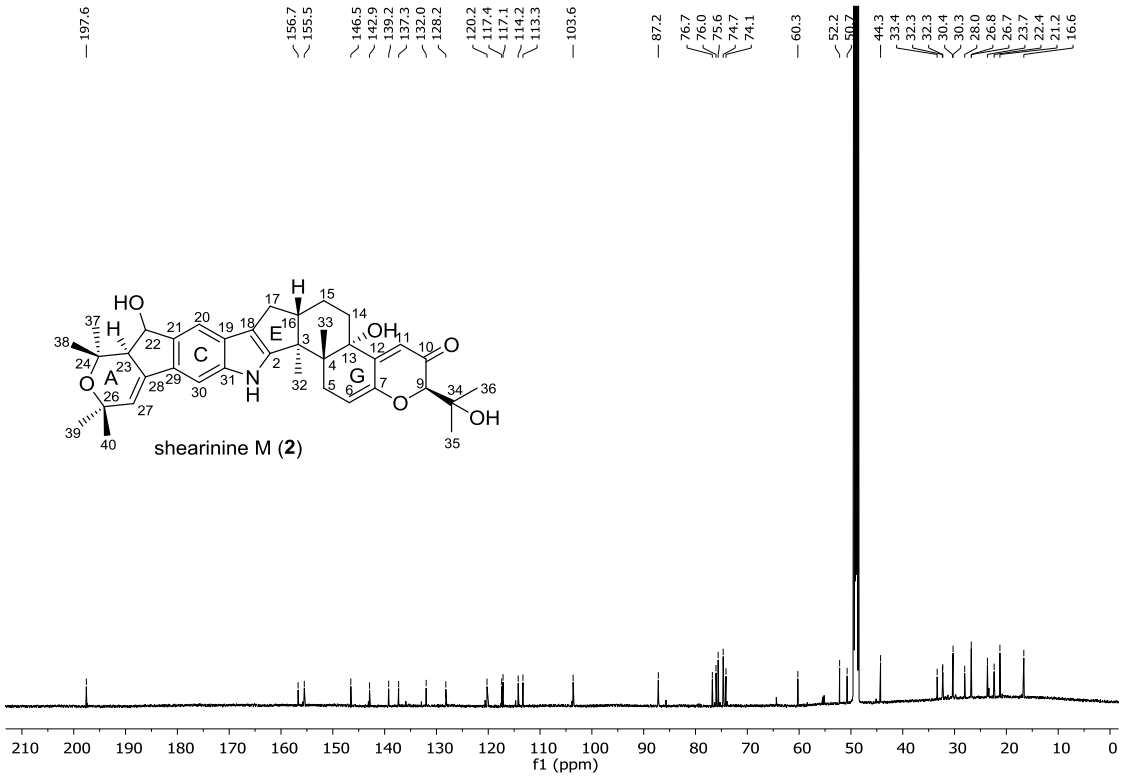

Figure S2.12. ^{13}C-NMR spectrum (150 MHz, MeOD-d_4) of shearinine M (**2**)

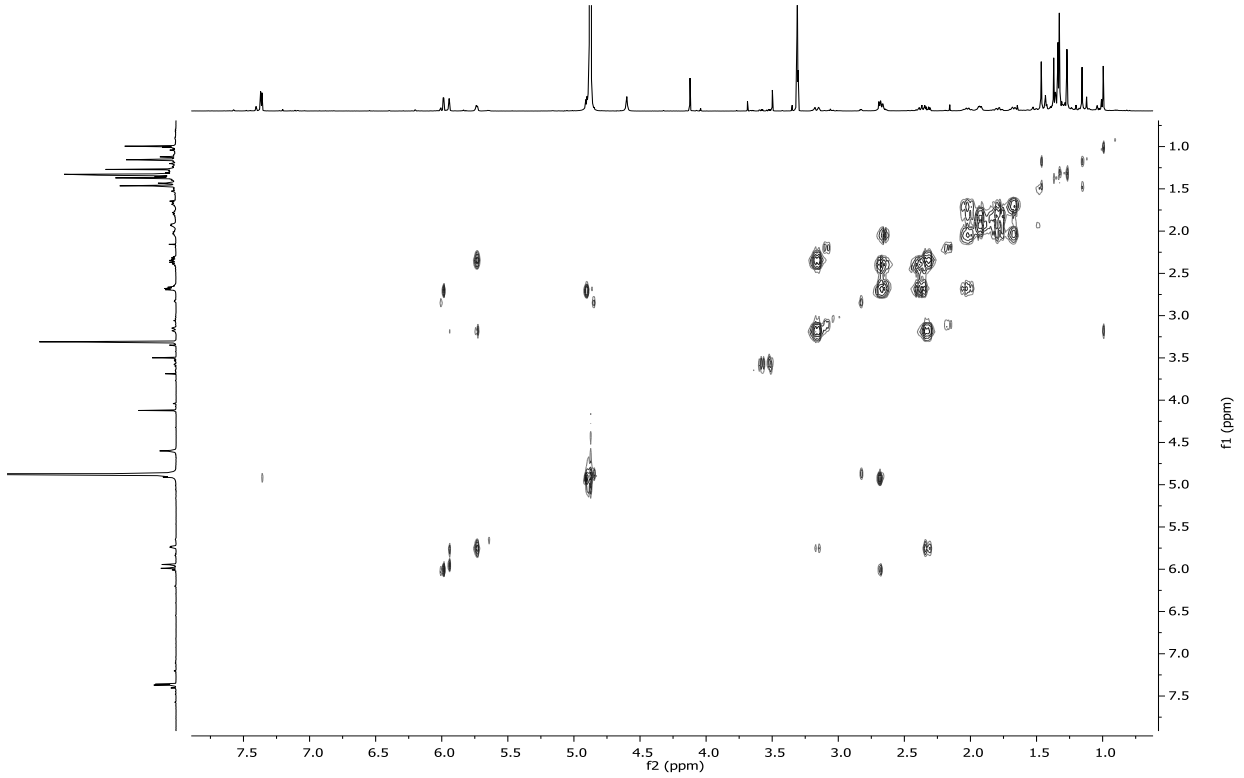

Figure S2.13. ^{1}H-^{1}H-COSY-NMR spectrum (600 MHz, MeOD-d_4) of shearinine M (**2**)

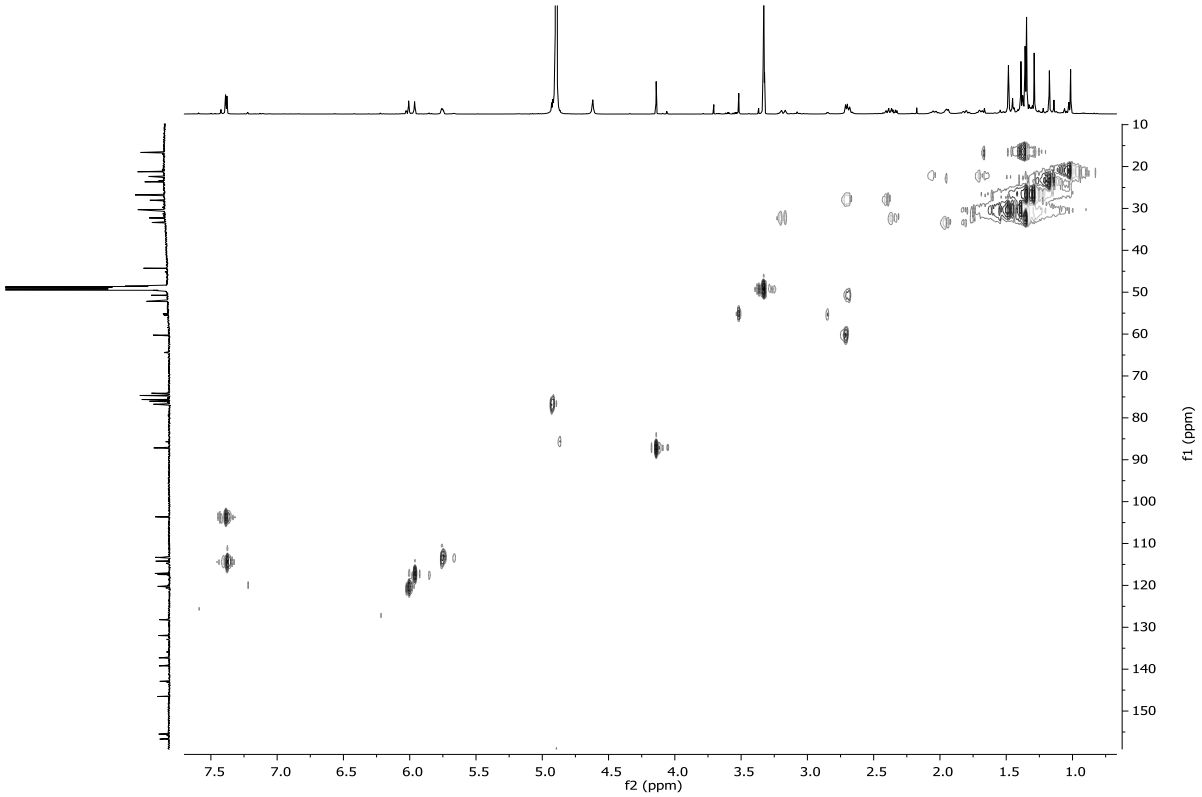

Figure S2.14. HSQC-NMR spectrum (600 MHz, MeOD-d_4) of shearinine M (**2**)

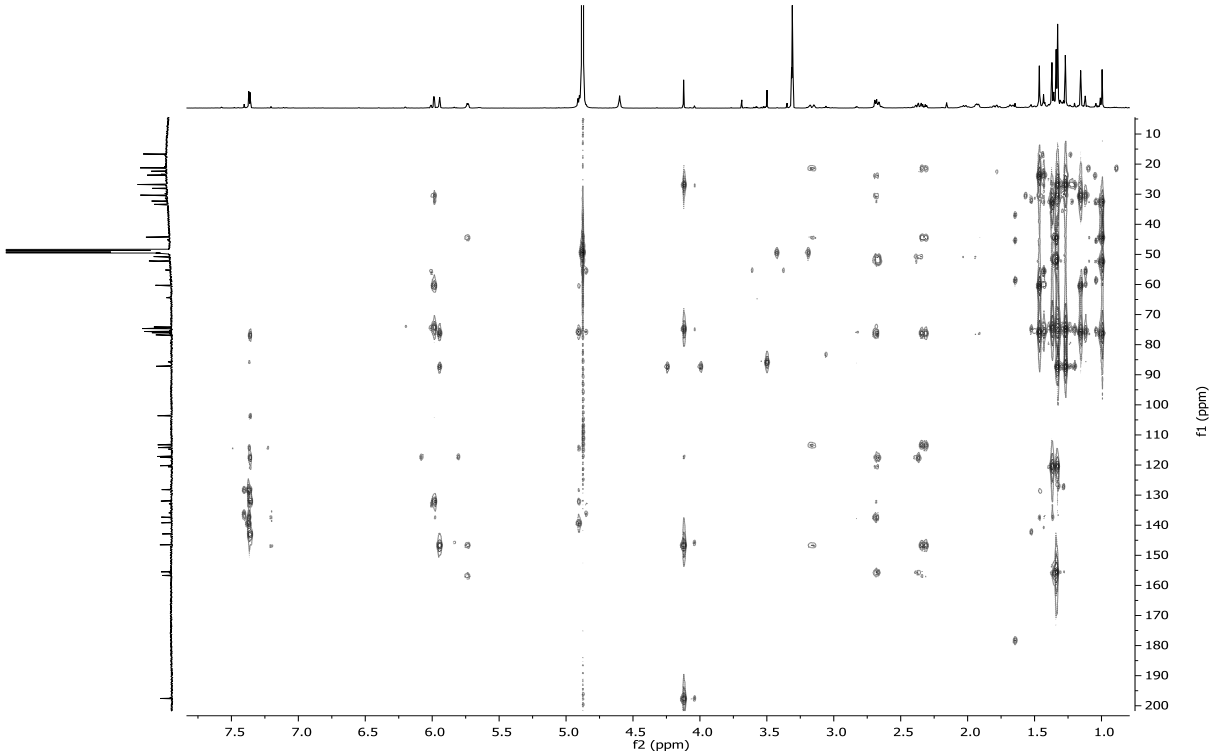

Figure S2.15. HMBC-NMR spectrum (600 MHz, MeOD-d_4) of shearinine M (**2**)

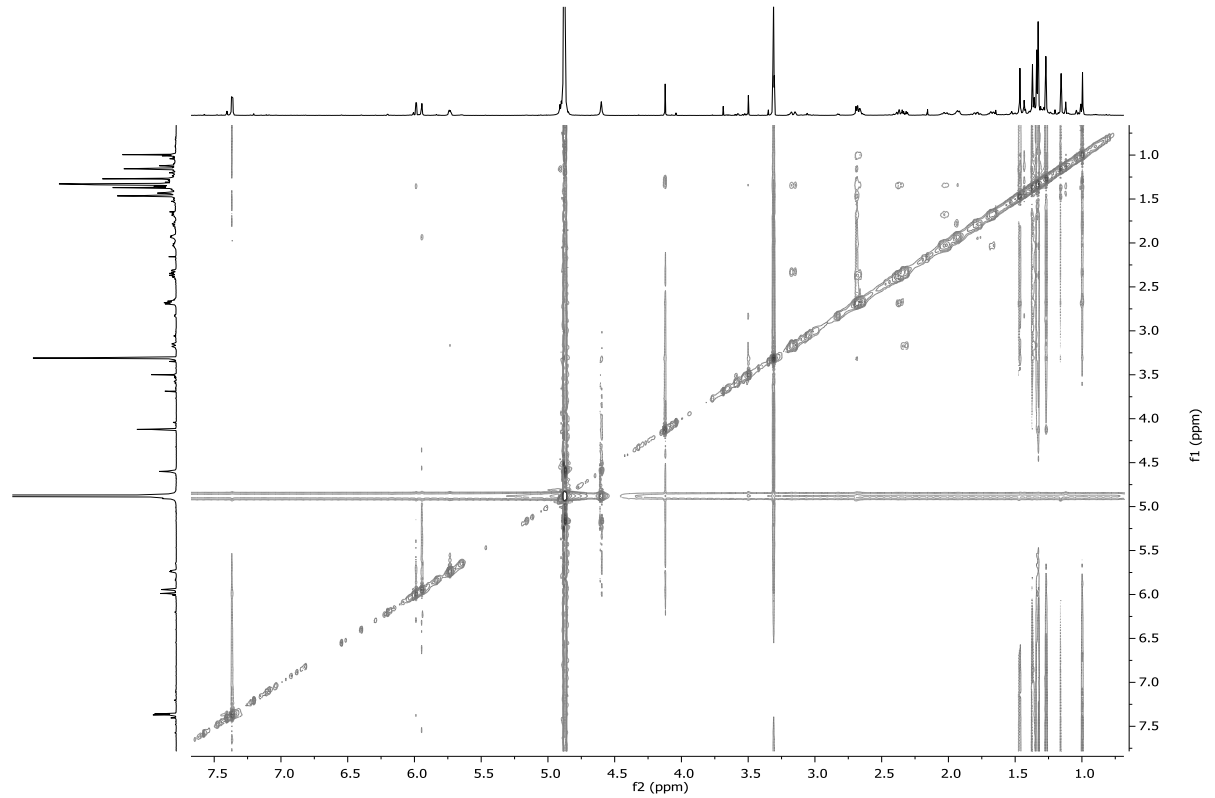

Figure S2.16. NOESY-NMR spectrum (600 MHz, MeOD-d_4) of shearinine M (**2**)

A)

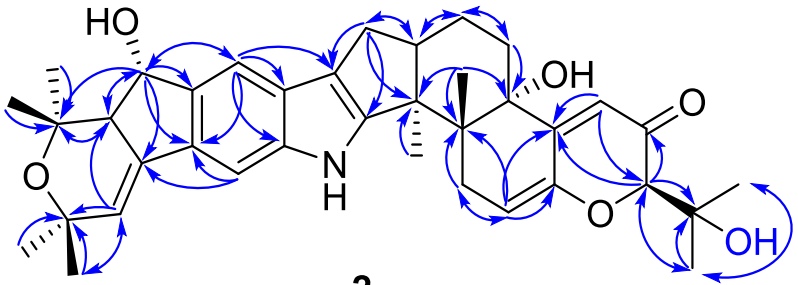

2

B)

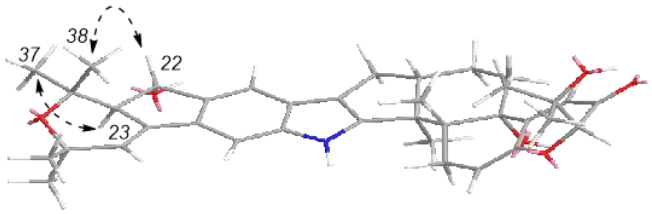

2

Figure S2.17. A) Key ^{1}H-^{1}H-Cosy and ^{1}H-^{13}C-HMBC correlations of shearinine M (**2**), B) Key NOESY correlations of shearinine M (**2**).

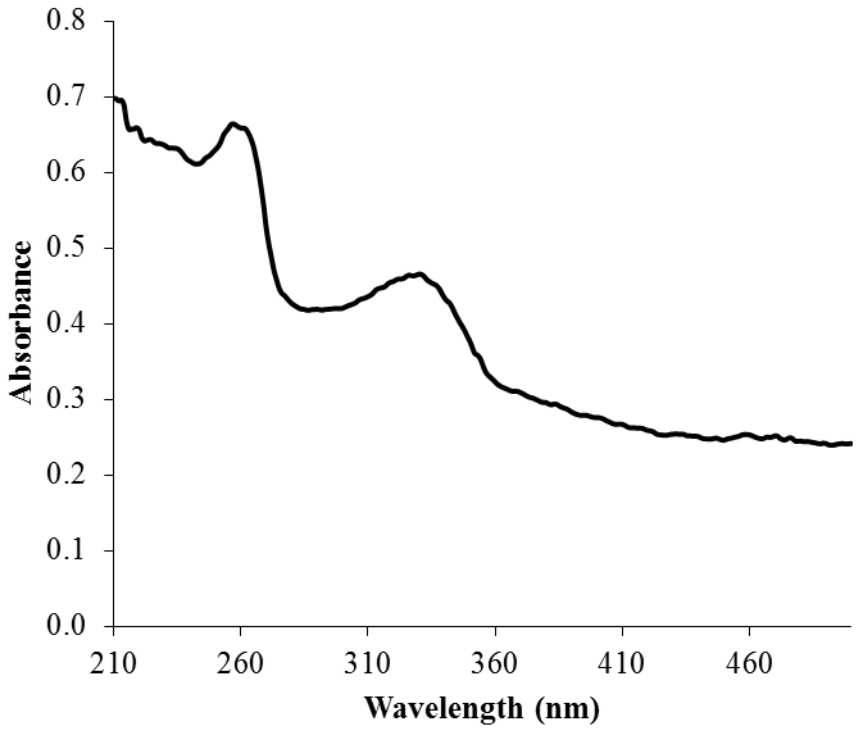

Figure S2.18. UV-Visible spectrum of the shearinine M (**2**) in methanol.

Structure elucidation of shearinine D (3)

1.45 mg, white amorphous powder.

^{1}H-NMR (600 MHz, MeOD-d_4) δ_H: 7.36 (1H, s, H-30), 7.35 (1H, s, H-20), 5.96 (1H, d, *J* = 2.9 Hz, H-27), 5.78 (1H, brs, H-11), 4.90 (1H, d, *J* = 5.3 Hz, H-22), 4.29 (1H, d, *J* = 1.3 Hz, H-9), 2.77-2.84 (1H, m, H-6a), 2.69 (1H, dd, *J* = 5.7, 2.9 Hz, H-23), 2.65 (1H, m, H-5a), 2.57-2.62 (1H, m, H-17a), 2.34 (1H, dd, *J* = 12.5, 10.4 Hz, H-17b), 2.01 (1H, m, H-15a), 1.95-1.98 (1H, m, H-14a), 1.92-1.95 (1H, m, H-5b), 1.86-1.92 (1H, m, H-6b), 1.71 (1H, m, H-14b), 1.63 (1H, m, H-15b), 1.46 (3H, s, H-39), 1.42 (3H, s, H-37), 1.38 (3H, s, H-36), 1.36 (3H, s, H-32), 1.33 (3H, s, H-40), 1.16 (3H, s, H-35), 1.16 (3H, s, H-33), 1.11 (3H, s, H-38).

^{13}C-NMR (150 MHz, MeOD-d_4) δ_C: 197.9 (C-10), 170.8 (C-12), 154.5 (C-2), 141.5 (C-31), 137.8 (C-28), 136.0 (C-21), 130.5 (C-29), 126.9 (C-19), 118.7 (C-27), 116.8 (C-11), 115.8 (C-18), 112.7 (C-20), 104.7 (C-7), 102.2 (C-30), 87.8 (C-9), 78.1 (C-34), 76.4 (C-13), 75.4 (C-22), 74.2 (C-24), 72.7 (C-26), 58.9 (C-23), 51.6 (C-3), 48.5 (C-16), 39.4 (C-4), 32.4 (C-14), 30.9 (C-40), 29.0 (C-39), 28.9 (C-36), 28.0 (C-6), 27.8 (C-37), 26.9 (C-5), 26.3 (C-17), 22.5 (C-33), 22.3 (C-35), 22.0 (C-38), 20.9 (C-15), 15.2 (C-32).

ESI-MS: m/z 598.4 $[M-H]^-$.

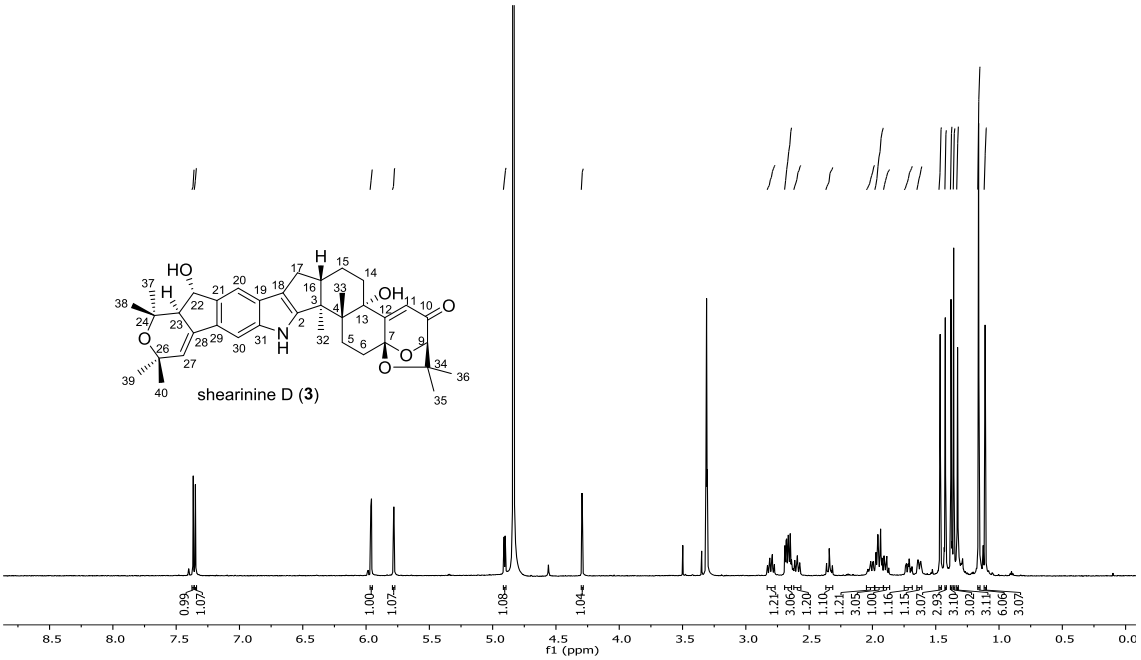

Figure S2.19. ^{1}H-NMR spectrum (600 MHz, MeOD-d_4) of shearinine D (**3**)

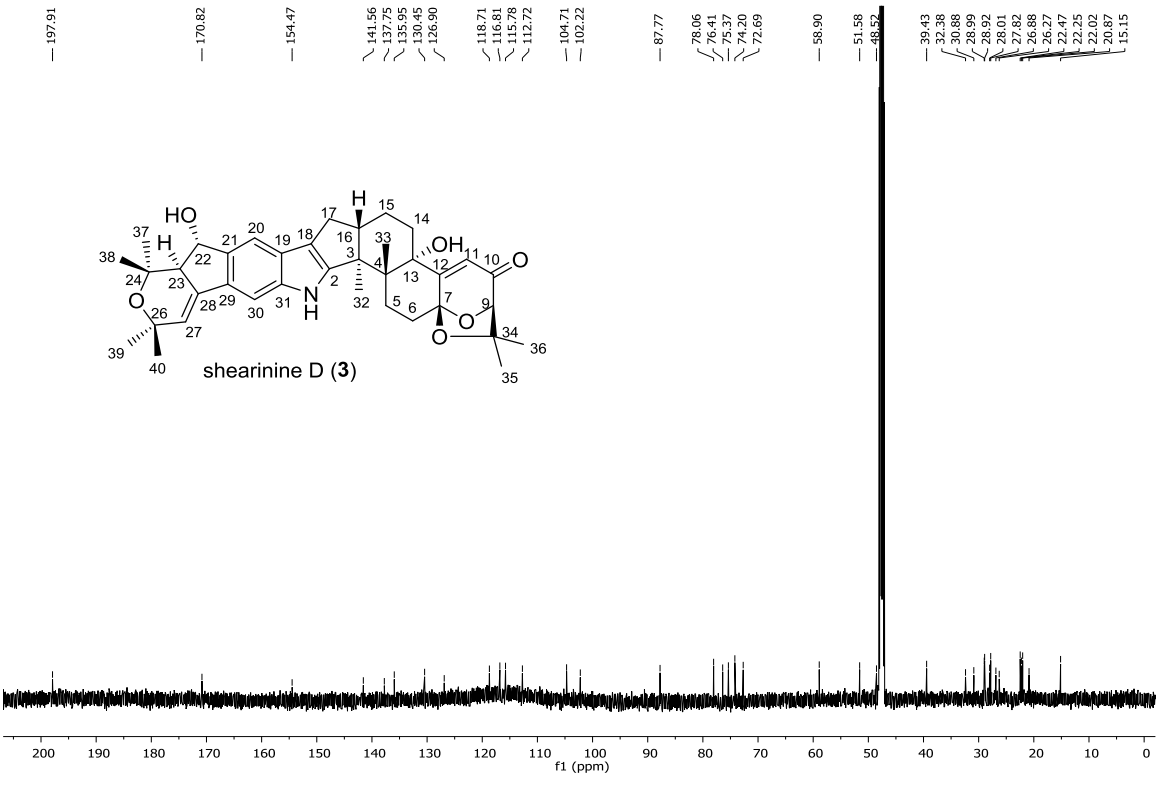

Figure S2.20. ^{13}C-NMR spectrum (150 MHz, MeOD-d_4) of shearinine D (**3**)

Structure elucidation of shearinine E (4)

1.30 mg, white amorphous powder.

^{1}H-NMR (600 MHz, MeOD-d_4) δ_H: 7.42 (1H, s, H-30), 7.35 (1H, s, H-20), 5.98 (1H, d, *J* = 2.8 Hz, H-27), 5.80 (1H, brs, H-11), 4.85 (1H, d, *J* = 5.2 Hz, H-22), 4.32 (1H, d, *J* = 1.3 Hz, H-9), 3.51 (3H, s, -CH_3), 2.85 (1H, dd, *J* = 5.6, 2.9 Hz, H-23), 2.77-2.82 (1H, m, H-6a), 2.67-2.71 (1H, m, H-5a), 2.61-2.67 (1H, m, H-17a), 2.40 (1H, dd, *J* = 12.3, 10.4 Hz, H-17b), 2.06-2.11 (1H, m, H-15a), 1.99-2.04 (1H, m, H-14a), 1.96-2.0 (1H, m, H-5b), 1.92-1.96 (1H, m, H-6b), 1.85-1.91 (1H, m, H-14b), 1.70-1.75 (1H, m, H-15b), 1.45 (3H, s, H-37), 1.44 (3H, s, H-36), 1.42 (3H, s, H-32), 1.37 (3H, s, H-39), 1.35 (3H, s, H-40), 1.21 (3H, s, H-33), 1.17 (3H, s, H-35), 1.13 (3H, s, H-38).

^{13}C-NMR (150 MHz, MeOD-d_4) δ_C: 197.9 (C-10), 170.8 (C-12), 155.1 (C-2), 141.8 (C-31), 135.1 (C-28), 134.4 (C-21), 131.4 (C-29), 126.9 (C-19), 119.0 (C-27), 116.8 (C-11), 115.8 (C-18), 113.2 (C-20), 104.7 (C-7), 102.4 (C-30), 87.7 (C-9), 84.4 (C-22), 78.0 (C-34), 76.4 (C-13), 74.2 (C-24), 72.8 (C-26), 54.0 (C-23), 53.7 (-OCH_3), 51.8 (C-3), 48.5 (C-16), 39.5 (C-4), 32.4 (C-14), 30.8 (C-40), 28.8 (C-39), 28.0 (C-6), 28.1 (C-37), 27.8 (C-36), 26.9 (C-17), 26.4 (C-5), 22.4 (C-33), 22.3 (C-35), 22.1 (C-38), 20.9 (C-15), 15.1 (C-32).

ESI-MS: m/z 612.4 $[M-H]^-$.

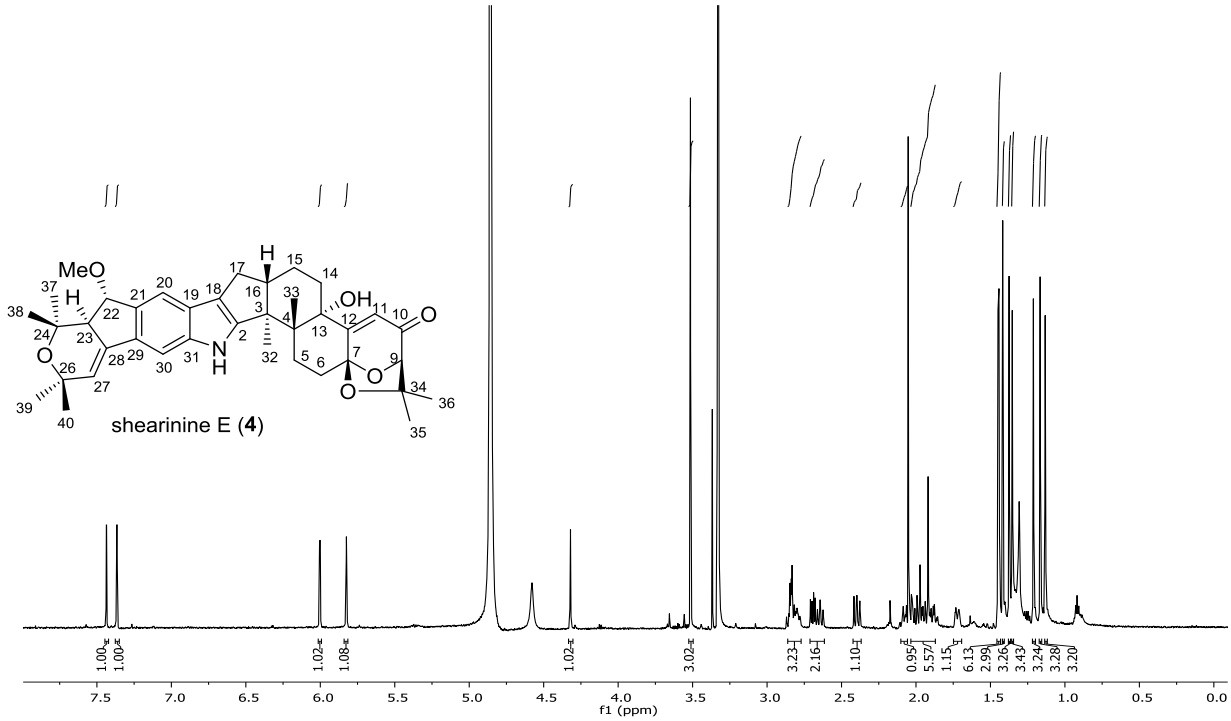

Figure S2.21. ^{1}H-NMR spectrum (600 MHz, MeOD-d_4) of shearinine E (**4**)

Structure elucidation of shearinine A (5)

1.25 mg, white amorphous powder.

^{1}H-NMR (600 MHz, MeOD-d_4) δ_H: 7.37 (1H, s, H-30), 7.14 (1H, s, H-20), 5.96 (1H, d, *J* = 2.9 Hz, H-27), 5.80 (1H, brs, H-11), 4.30 (1H, d, *J* = 1.3 Hz, H-9), 2.96 (1H, dd, *J* = 15.4, 9.2 Hz, H-22a), 2.74-2.78 (1H, m, H-23), 2.66-2.72 (1H, m, H-5a), 2.58-2.65 (1H, m, H-16), 2.53 (1H, dd, *J* = 15.4, 9.2 Hz, H-22b), 2.50 (1H, dd, *J* = 13.0, 6.8 Hz, H-17a), 2.20 (1H, dd, *J* = 12.4, 10.3 Hz, H-17b), 1.89-1.95 (1H, m, H-15a), 1.85-1.89 (1H, m, H-14a), 1.81-1.85 (1H, m, H-5b), 1.77-1.81 (1H, m, H-6b), 1.68-1.74 (1H, m, H-14b), 1.53-1.57 (1H, m, H-15b), 1.30 (3H, s, H-37), 1.25 (3H, s, H-32), 1.25 (3H, s, H-36), 1.21 (3H, s, H-39), 1.19 (3H, s, H-40), 1.05 (3H, s, H-33), 1.02 (3H, s, H-35), 0.99 (3H, s, H-38).

^{13}C-NMR (150 MHz, MeOD-d_4) δ_C:197.9 (C-10), 170.8 (C-12), 154.0 (C-2), 140.1 (C-31), 140.1 (C-29), 135.5 (C-28), 132.1 (C-21), 126.7 (C-19), 117.9 (C-27), 116.7 (C-11), 115.3 (C-18), 112.5 (C-20), 104.7 (C-7), 102.7 (C-30), 87.7 (C-9), 78.0 (C-34), 76.4 (C-13), 74.8 (C-24), 72.9 (C-26), 51.5 (C-3), 48.9 (C-23), 48.5 (C-16), 39.3 (C-4), 32.5 (C-22), 32.4 (C-14), 30.8 (C-40), 29.1 (C-39), 28.8 (C-36), 28.0 (C-37), 27.8 (C-6), 26.9 (C-5), 26.9 (C-17), 22.4 (C-33), 22.0 (C-35), 21.2(C-38), 20.9 (C-15), 15.1 (C-32).

ESI-MS: m/z 582.5 $[M-H]^-$.

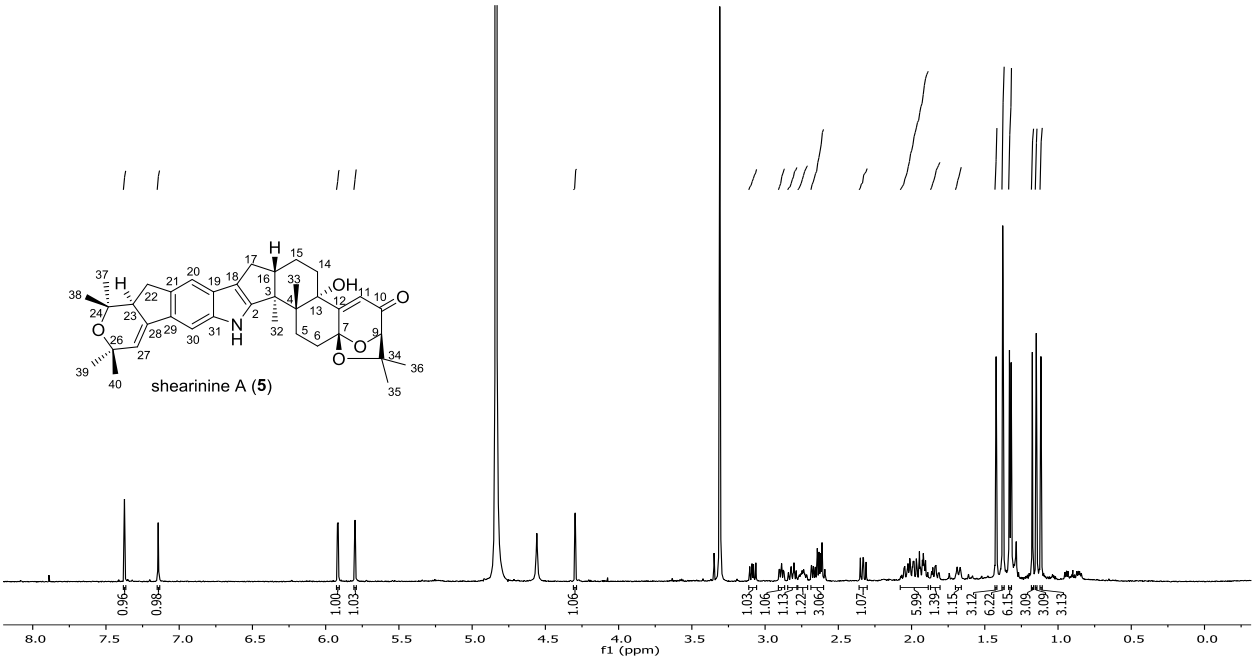

Figure S2.22. ^{1}H-NMR spectrum (600 MHz, MeOD-d_4) of shearinine A (**5**)

Structure elucidation of cycloarthropsone (6)

3.2 mg, greenish powder.

^{1}H-NMR (600 MHz, MeOD-d_4) δ_H: 7.18 (1H, dq, *J* = 15.6, 1.8 Hz, H-3), 7.09 (1H, d, *J* = 8.4 Hz, H-5), 7.03 (1H, d, *J* = 8.4 Hz, H-6), 6.39 (1H, dq, *J* = 15.6, 6.6 Hz, H-2), 1.88 (3H, dd, *J* = 6.6, 1.8 Hz, H-1), 1.53 (3H, s,H-12).

^{13}C-NMR (150 MHz, MeOD-d_4) δ_C: 202.4 (C-10), 159.9 (C-8), 143.3 (C-7), 131.1 (C-4), 128.9 (C-2), 126.6 (C-3), 125.3 (C-6), 118.8 (C-5), 116.6 (C-9), 104.7 (C-11), 22.2 (C-12), 18.8 (C-1).

ESI-MS: m/z 219.2 $[M-H]^-$.

UV (in MeOH): λ_{max} 235, 274 and 377 nm

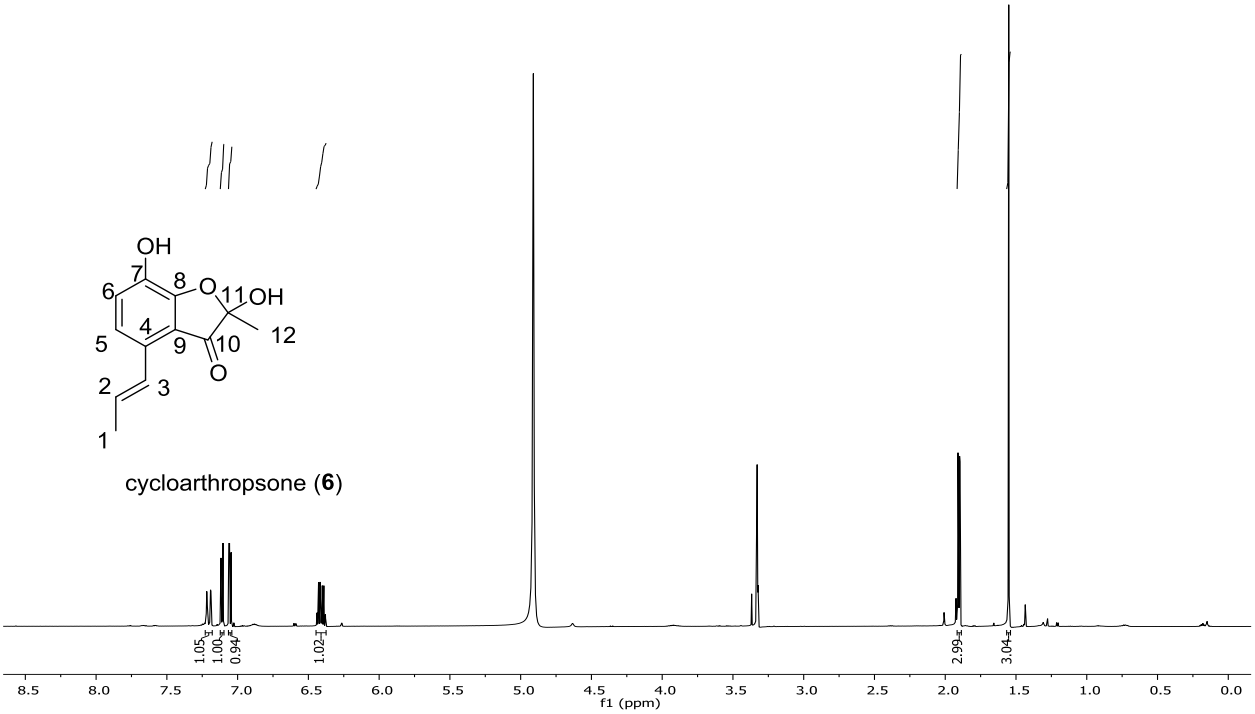

Figure S2.23. ^{1}H-NMR spectrum (600 MHz, MeOD-d_4) of cycloarthropsone (**6**)

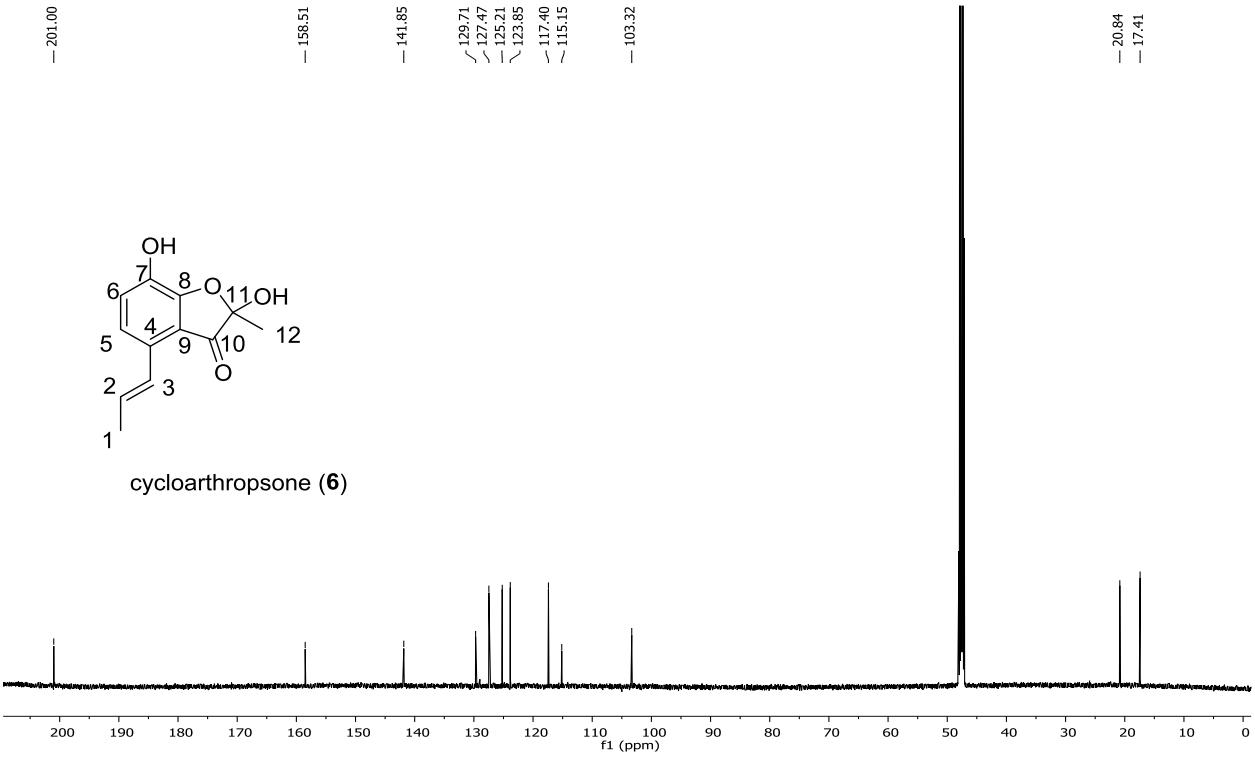

Figure S2.24. ^{13}C-NMR spectrum (150 MHz, MeOD-d_4) of cycloarthropsone (**6**)

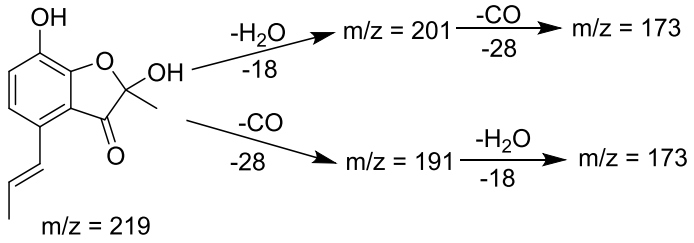

Figure S2.25: ESI-MS/MS fragmentation of the $[M-H]^-$ of cycloarthropsone (**6**)

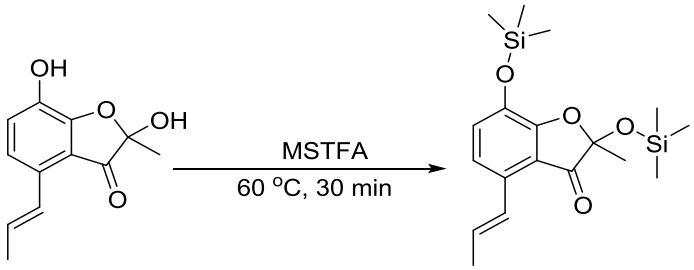

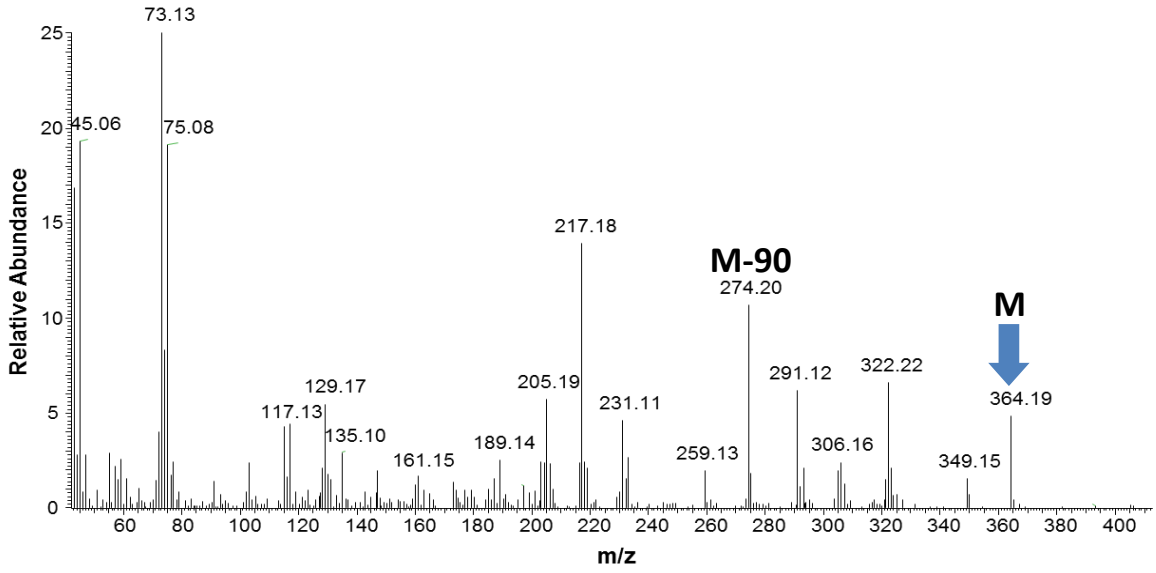

Figure S2.26. EI-MS (70 eV) of MSTFA derivatized cycloarthropsone (**6**)

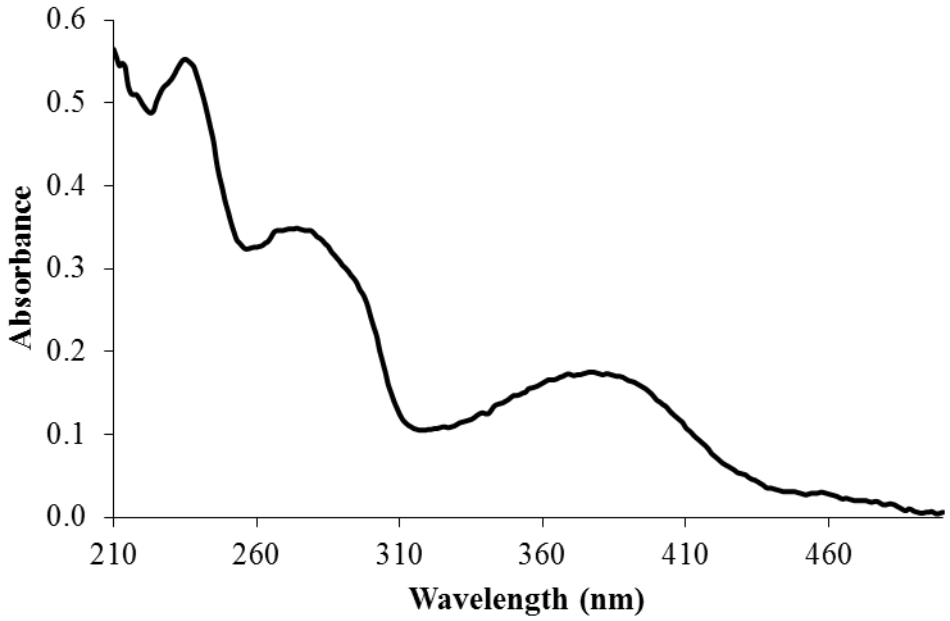

Figure S2.27. UV-Visible spectrum of the cycloarthropsone (**6**) in methanol.

Structure elucidation of emodin (7)

3.1 mg, orange needles or powder.

^{1}H-NMR (600 MHz, acetone-d_6) δ_H: 7.57 (1H, brs, H-5), 7.26 (1H, d, *J* = 2.4 Hz, H-4), 7.13 (1H, brs, H-7), 6.62 (1H, d, *J* = 2.4 Hz, H-2), 2.46 (3H, s, H-15).

^{13}C-NMR (150 MHz, acetone-d_6) δ_C: 191.2 (C-9), 182.5 (C-10), 168.1 (C-1), 166.4 (C-3), 162.2 (C-8), 149.2 (C-6), 136.6 (C-11), 134.4 (C-14), 124.8 (C-5), 121.4 (C-7), 114.7 (C-13), 110.6 (C-4), 109.8 (C-12), 108.9 (C-2), 22.0 (C-15).

ESI-MS: m/z 269.5 $[M-H]^-$.

UV (in MeOH): λ_{max} 216, 256, 308 and 461 nm.

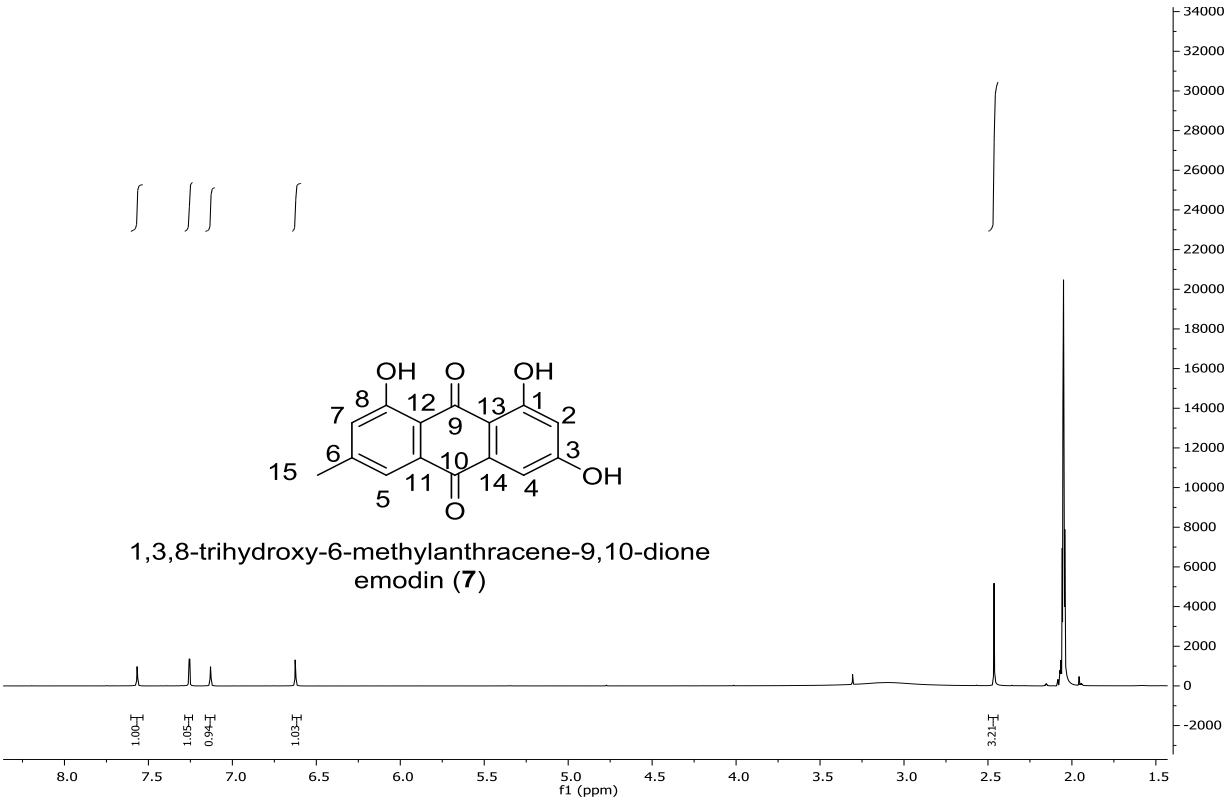

Figure S2.28. ^{1}H-NMR spectrum (600 MHz, acetone-d_6) of emodin (**7**)

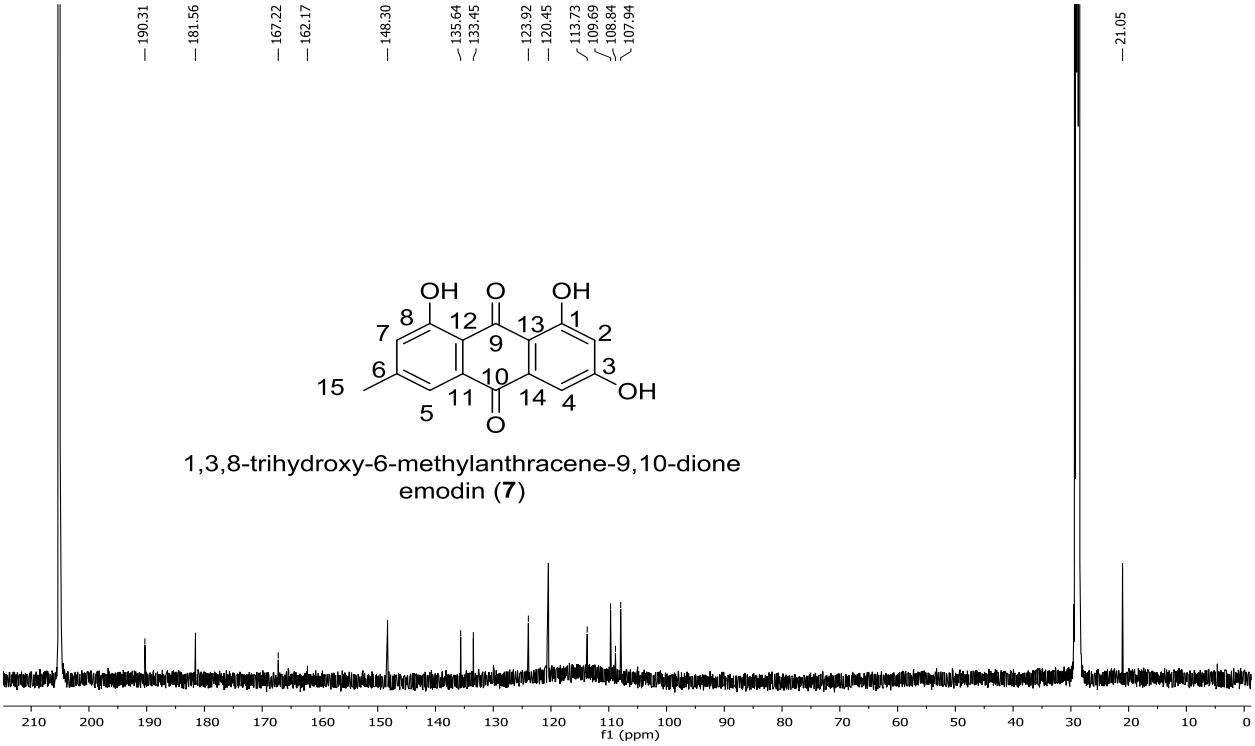

Figure S2.29. ^{13}C-NMR spectrum (150 MHz, acetone-d_6) of emodin (**7**)

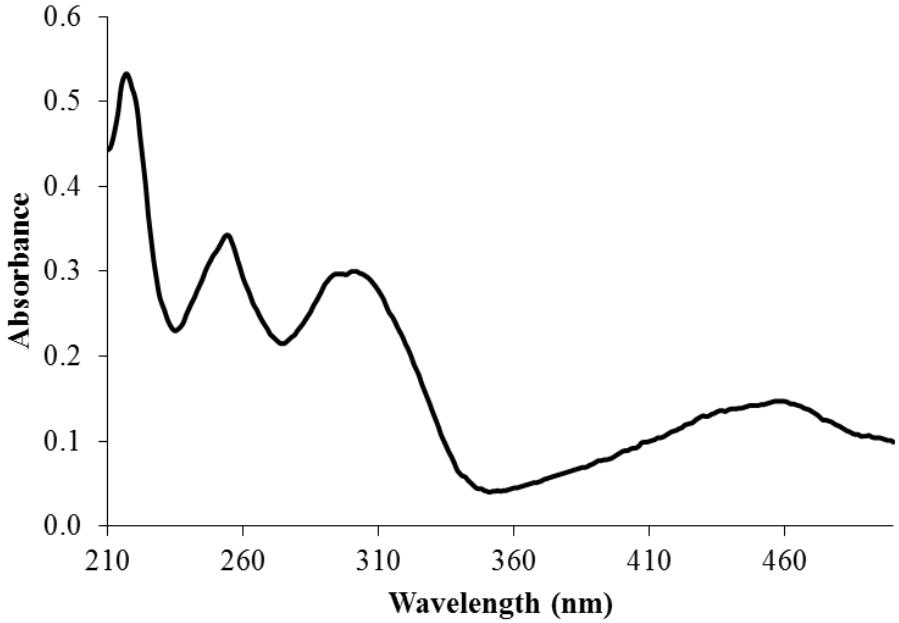

Figure S2.30. UV-Visible spectrum of the emodin (**7**) in methanol.

Comparison of secondary metabolite production of *E. weberi* and *E. aspergilloides*

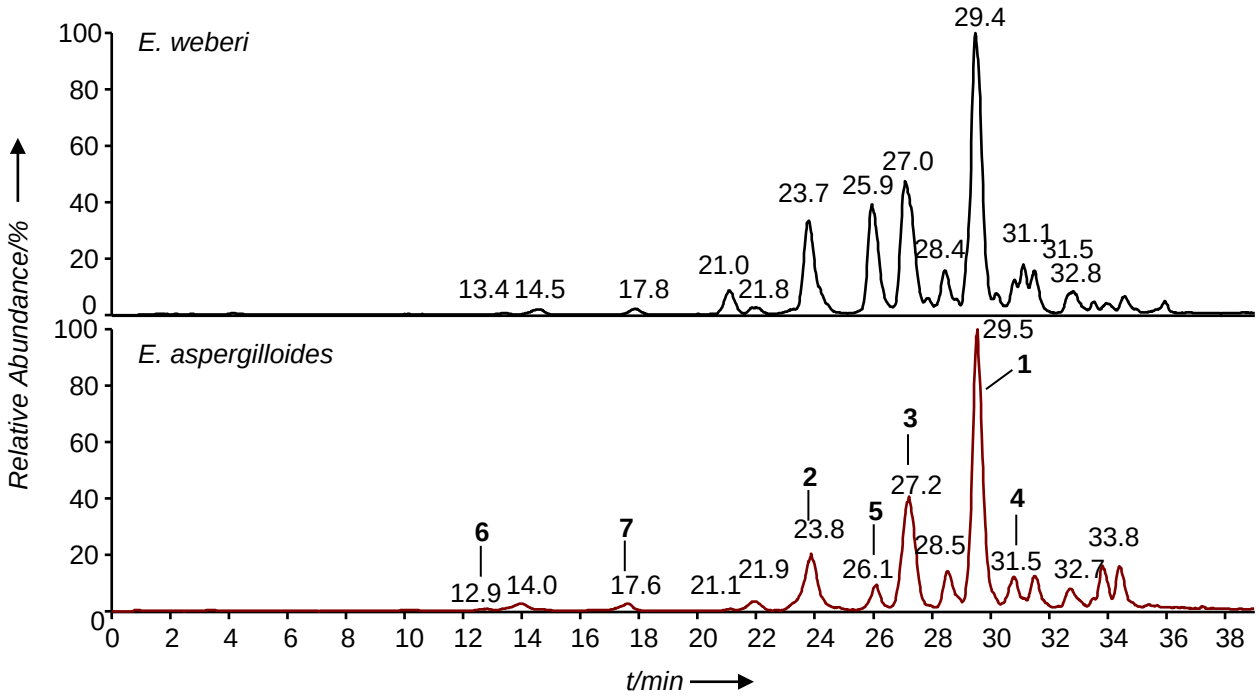

Figure S2.31: Comparison of LC-negative-ESI-MS base peak chromatograms of *E. weberi* and *E. aspergilloides* methanol extracts: (A) *E. weberi* and (B) *E. aspergilloides* exhibiting both peaks for shearinine L (**1**), shearinine M (**2**), shearinine D (**3**), shearinine E (**4**), shearinine A (**5**), cycloarthropsone (**6**), and emodin (**7**).

Agar diffusion assays

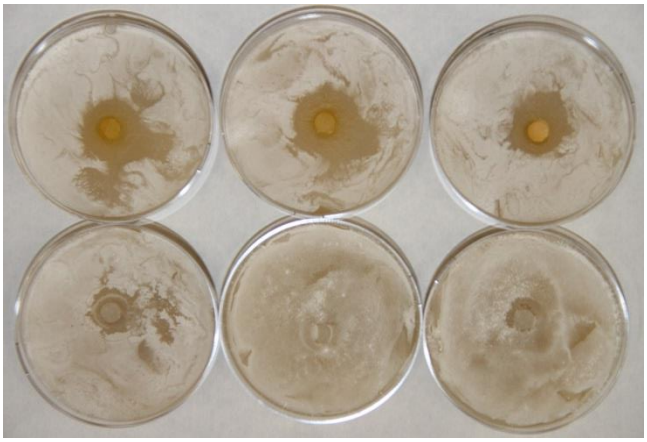

Figure S2.32: Agar diffusion assays with emodin (**7**) against *Streptomyces* sp. 28_1, on SFM agar plates (5.5 cm diameter) after 3d of growth: first row, 0.30 µmol emodin (**7**) on paper disk samples; second row, controls.

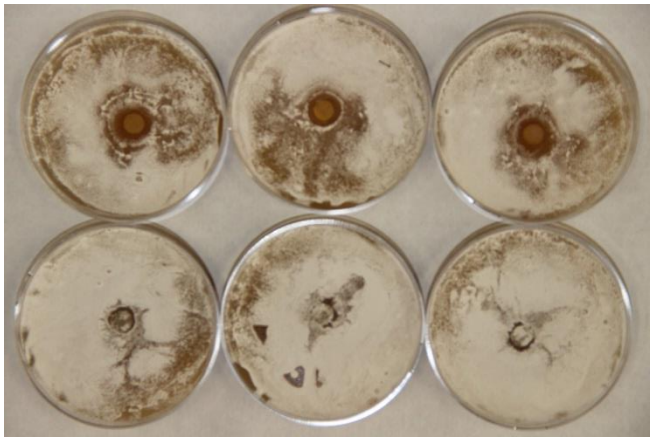

Figure S2.33: Agar diffusion assays with emodin (**7**) against *Streptomyces* sp. 26_3, on SFM agar plates (5.5 cm diameter) after 3d of growth: first row, 0.30 µmol emodin (**7**) on paper disks; second row, controls.

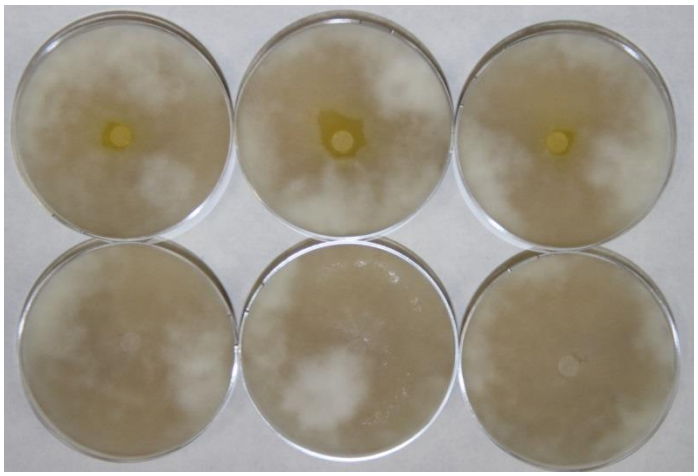

Figure S2.34: Agar diffusion assays with emodin (**7**) against *F. equiseti*, on SFM agar plates (5.5 cm diameter) after 3d of growth: first row, 0.30 µmol emodin (**7**) on paper disks; second row, controls.

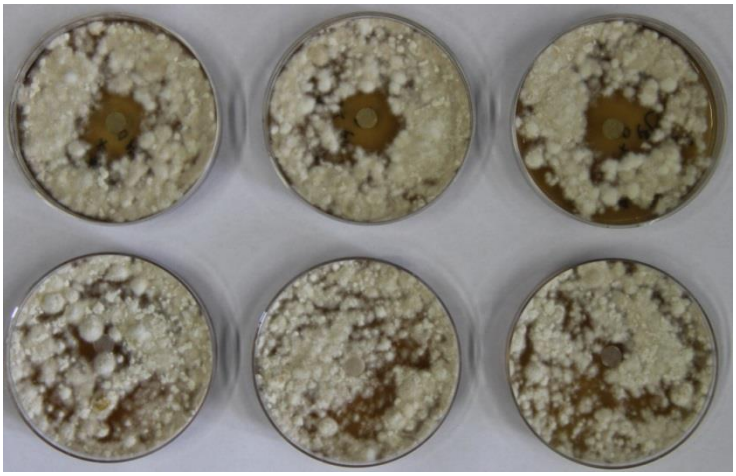

Figure S2.35: Agar diffusion assays with 0.66 µmol emodin (**7**) against *L. gongylophorus*, on PDA plates (5.5 cm diameter) after 18d of growth: first row, 0.66 µmol emodin (**7**) on paper disks; second row, controls.

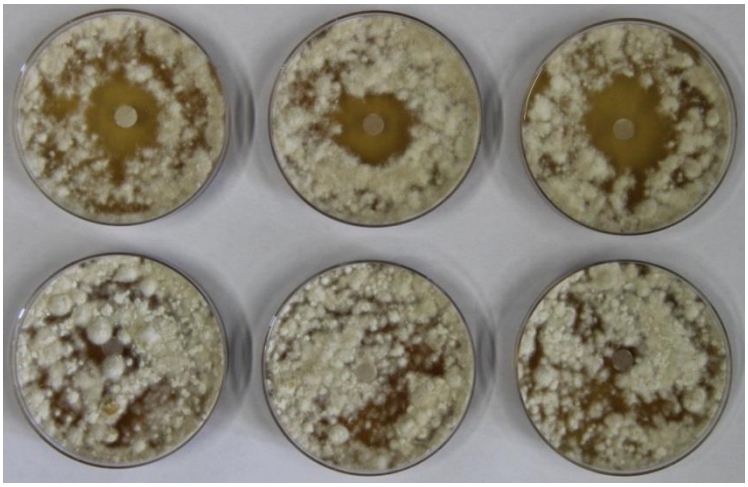

Figure S2.36: Agar diffusion assays with 0.82 µmol cycloarthropsone (**6**) against *L. gongylophorus*, on PDA plates (5.5 cm diameter) after 18d of growth: first row, 0.82 µmol cycloarthropsone (**6**) on paper disks; second row, controls.

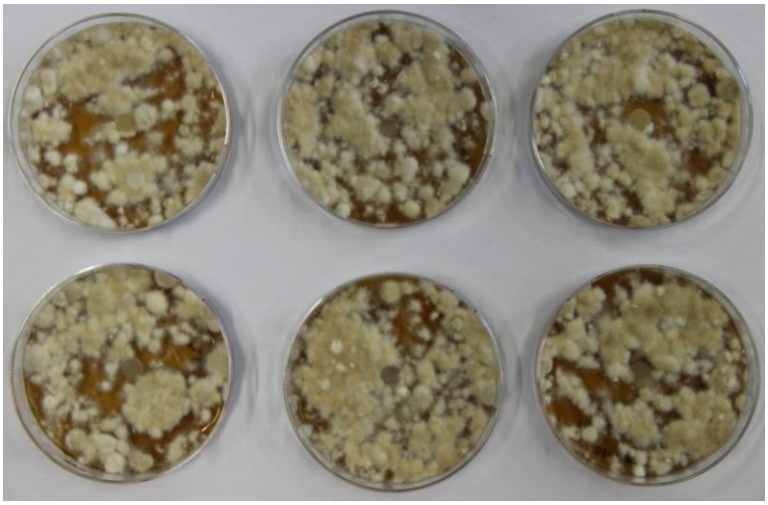

Figure S2.37: Agar diffusion assays with 0.31 µmol shearinine L (**1**) against *L. gongylophorus*, on PDA plates (5.5 cm diameter) after 18d of growth: first row, 0.31 µmol shearinine L (**1**) disk; second row, control.

Isolation and identification of *Leucoagaricus gongylophorous*

L. gongylophorus was isolated from the fungal garden of a *Acromyrmex octospinosus* nest (collected in Paratebueno, Medina, 4°23’38.4‘‘N 73°16’07.5‘‘W Colombia) and maintained at University of Kaiserslautern. Potato dextrose medium was used for the isolation of mycelium from the fungus. The small fungal garden parts were subcultured successively until pure isolates were obtained. Genomic DNA was prepared from the fungal mycelium and the 18*S* rDNA was PCR (amplified primers: (5'-TTTCCGTAGGTGAACCTGCG-3' and 5'-TTAAGTTCAGCGGGTAGTCCCAC-3'[1]) The PCR product was purified by gel electrophoresis, cloned using the pJET PCR cloning kit (Thermofisher). The purified plasmid was submitted to sequencing by MWG Eurofins. The sequence was 99 % identical to *L. gongylophorous* isolate Ae372 18*S* ribosomal RNA gene (Accession number KF571990.1).

Supporting Information

Chapter 3: Upon attack by the pathogenic fungus *Escovopsis weberi* the garden fungus of leaf-cutting ants *Leucoagaricus gongylophorus* releases 3-octanone that induces hygienic behavior

Basanta Dhodary[1], Benjamin Feth[2], Julia Schulz[2], Rainer Wirth[2], Dieter Spiteller[1]*

[1]*Chemical Ecology/Biological Chemistry, University of Konstanz, Universitätstrasse 10, D-78457 Konstanz, Germany.*
[2]*Plant Ecology and Systematics, Technical University Kaiserslautern, Erwin-Schrödingerstraße 13,* 67653 Kaiserslautern*, Germany.*

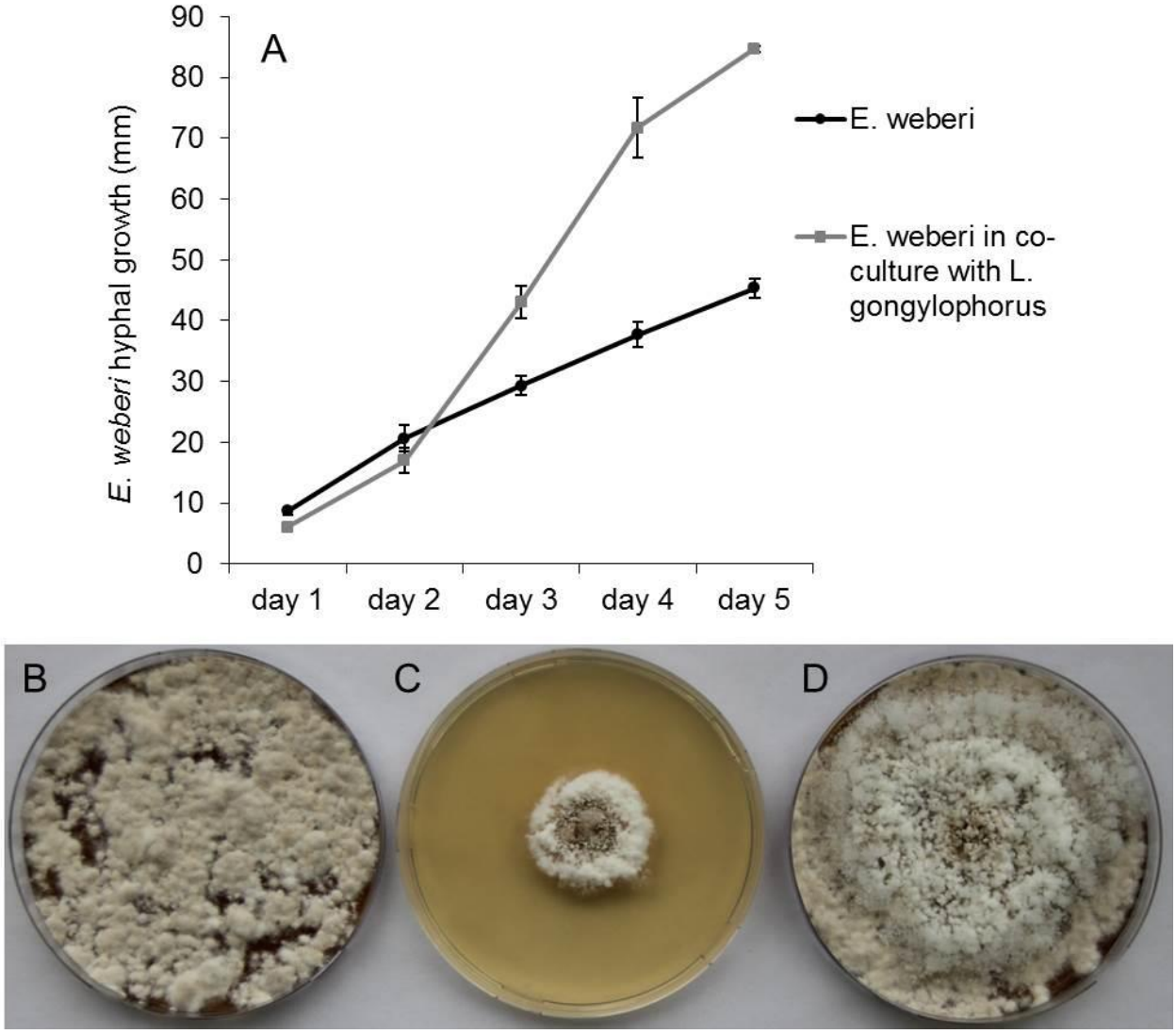

Figure S3.1: A) Growth curve of *E. weberi* alone and *E. weberi* in co-culture with *L. gongylophorus* on PDA agar plates (mean and standard deviation of mycelium diameter, n = 3). **B**) 18 d grown *L. gongylophorus* control on PDA agar plate. **C**) 4 d grown *E. weberi* control on PDA agar plate. **D**) 18 d grown *L. gongylophorus* infected with *E. weberi* for 4 d on PDA agar plate.

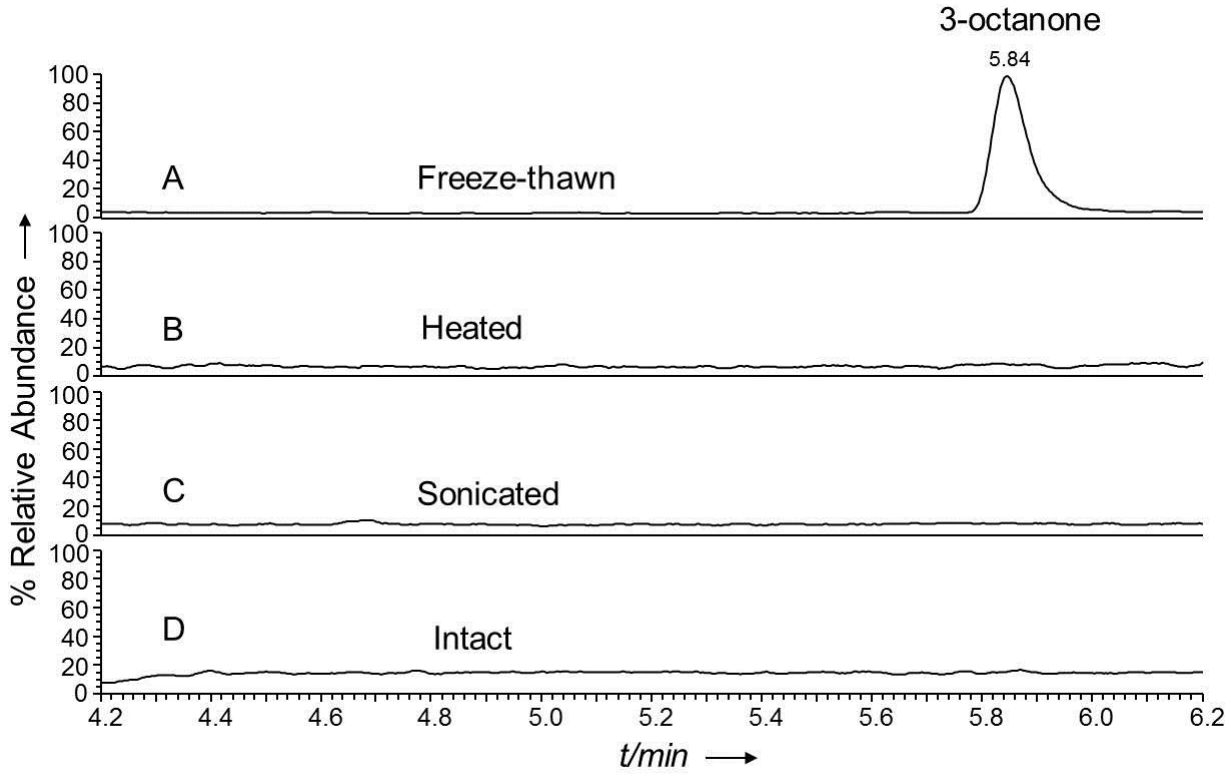

Figure S3.2: SPME-GC/MS analysis of volatiles formed by *L. gongylophorus* (12 d, grown on PDA agar plates, 5 mg mycelium). **A**) GC-MS profile after 30 min of freezing at -20^{o}C followed by 10 min of thawing at room temperature. **B**) GC-MS profile after heating at 80 °C for 30 min. **C**) GC-MS profile after sonication for 30 min. **D**) intact mycelium without any stress treatment.

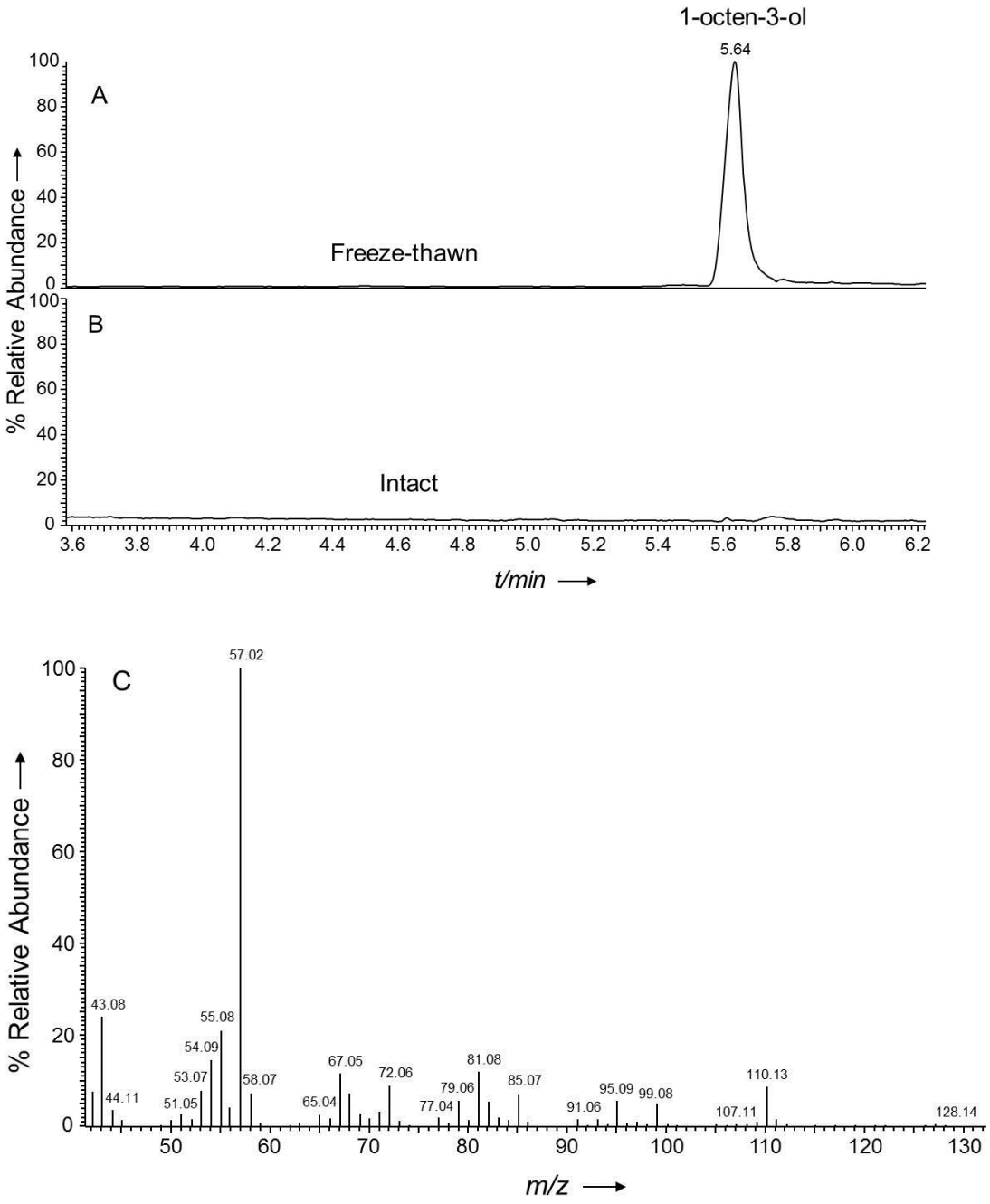

Figure S3.3: SPME-GC/MS analysis of volatiles formed by *E. weberi* (4 d, grown on PDA agar plates, 5 mg mycelium). **A**) GC-MS profile after 30 min of freezing at -20 °C followed by 10 min of thawing at room temperature. **B**) intact mycelium. **C**) EI-MS (70 eV) of 1-octen-3-ol.

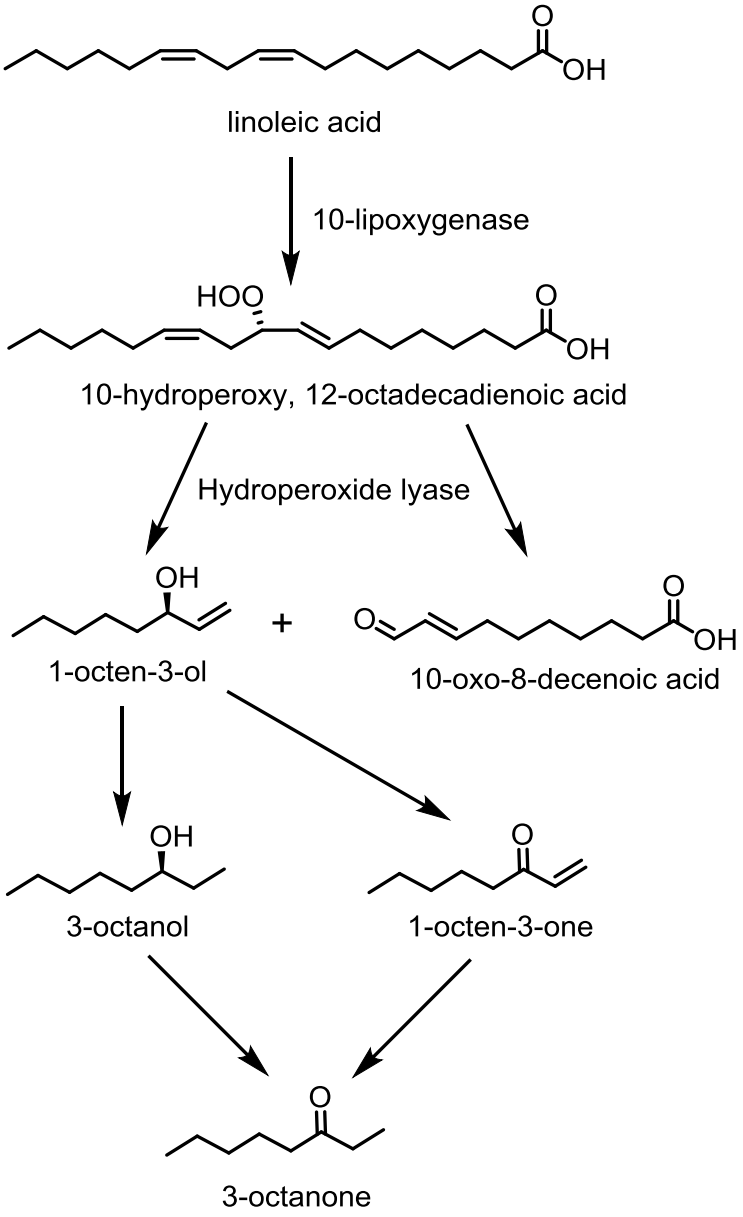

Figure S3.4: Scheme of the wound-activated biosynthesis of fungal C-8 oxylipin derivatives 1-octen-3-ol and 3-octanone from linoleic acid.

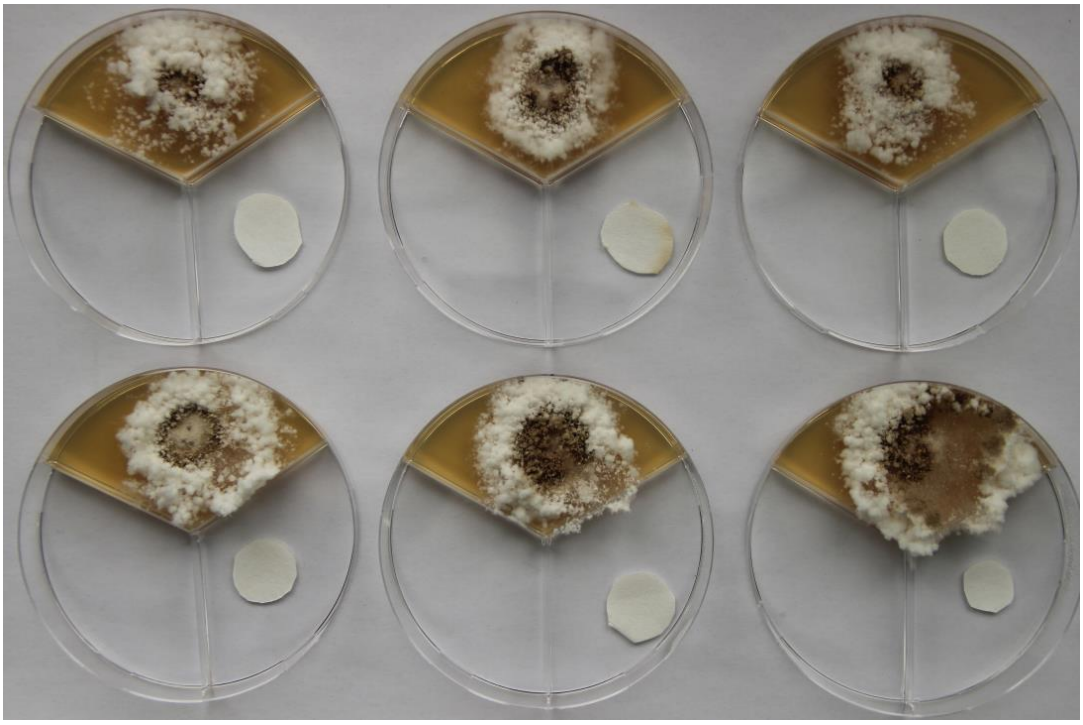

Figure S3.5: Testing 3-octanone for its potential antifungal properties against *E. weberi*: In a three compartment Petri dish *E. weberi* was cultivated in PDA medium for 4 d. In the second compartment a filter paper (1.5 cm diameter) was added. The third compartment was left empty. First row: 20 µL methanol as control on filter paper, second row: 6.3 µmol of 3-octanone dissolved in 20 µL of methanol on filter paper.

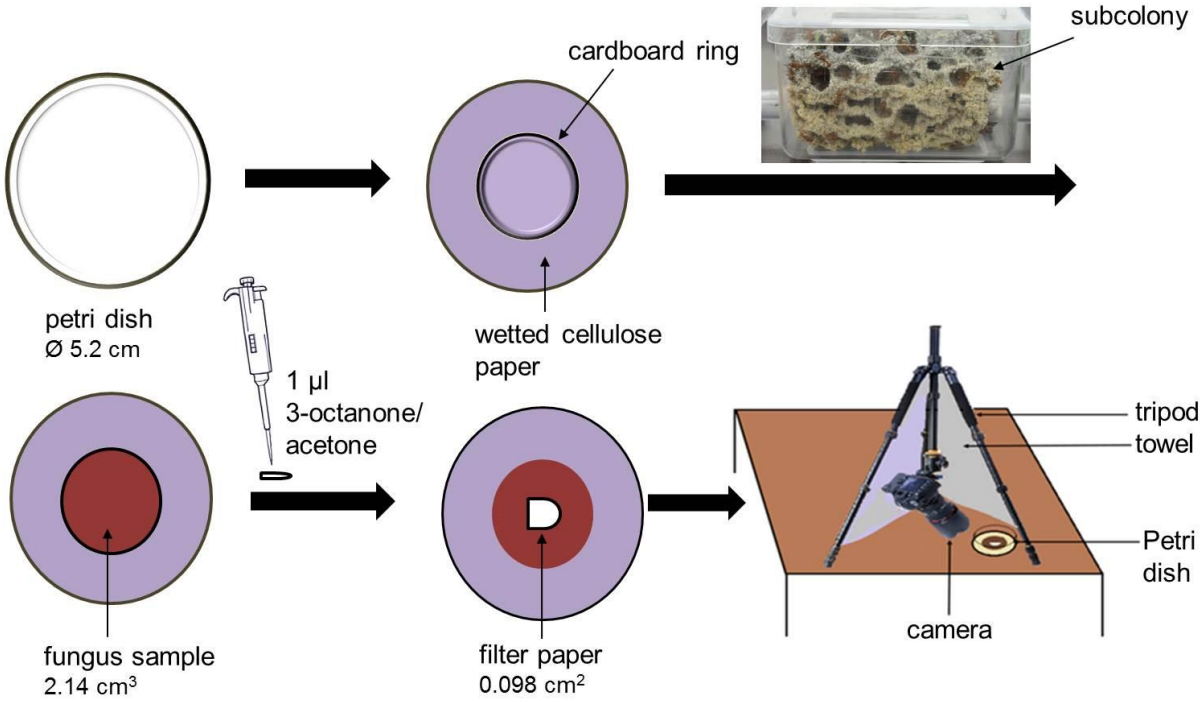

Figure S3.6: Scheme showing the workflow and experimental set-up analyzing the responses of *A. octospinosus* ant to 3-octanone.

Supporting Information

Chapter 4: Ammonia production by the *Streptomyces* sp. Av25_4 symbiont of the leaf cutting ant *Acromyrmex volcanus* strongly inhibits the growth of the pathogenic fungus *Escovopsis weberi*

Basanta Dhodary[1], Sören Radke[1], and Dieter Spiteller[1]*

[1]Chemical Ecology/Biological Chemistry, University of Konstanz, Universitätsstrasse 10, 78457 Konstanz, Germany.
*corresponding author

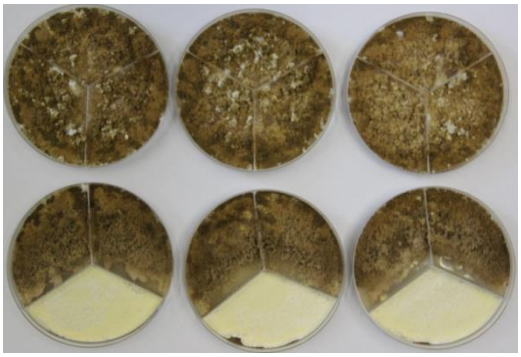

Av25_3

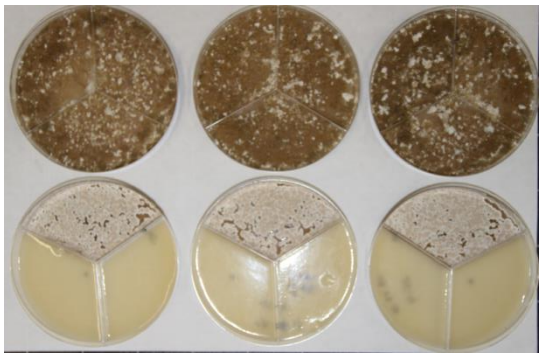

Av25_4

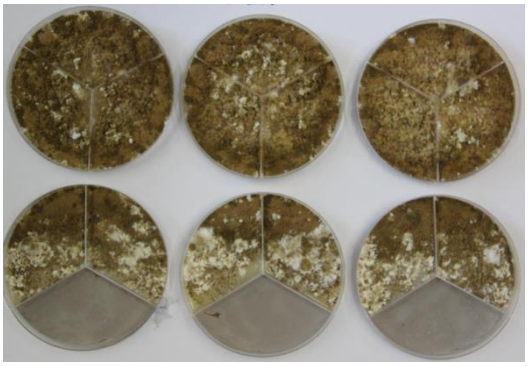

Av26_2

Av26_3

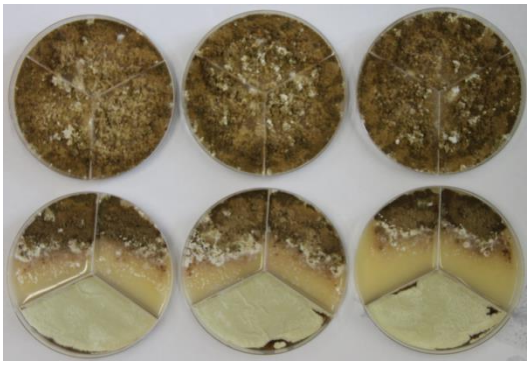

Av26_5

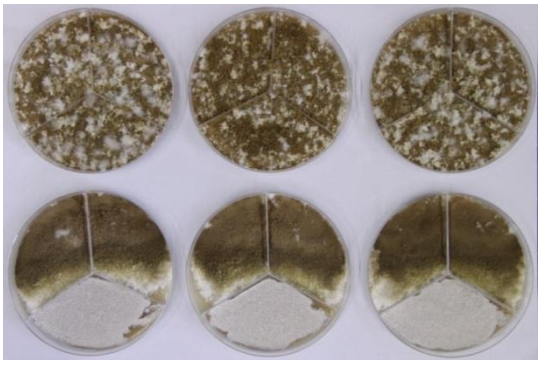

Av28_1

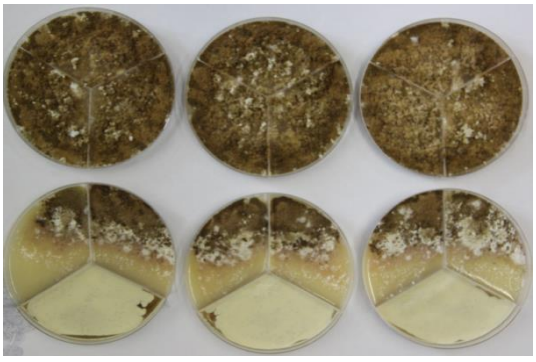

Av28_3

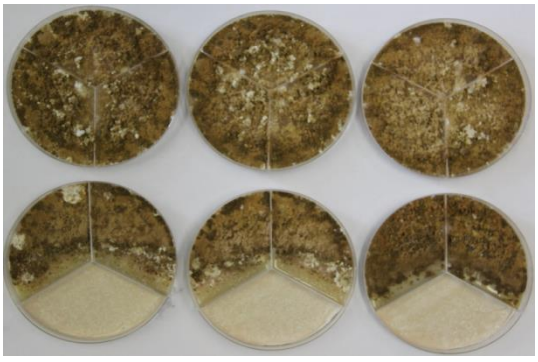

Av29_7

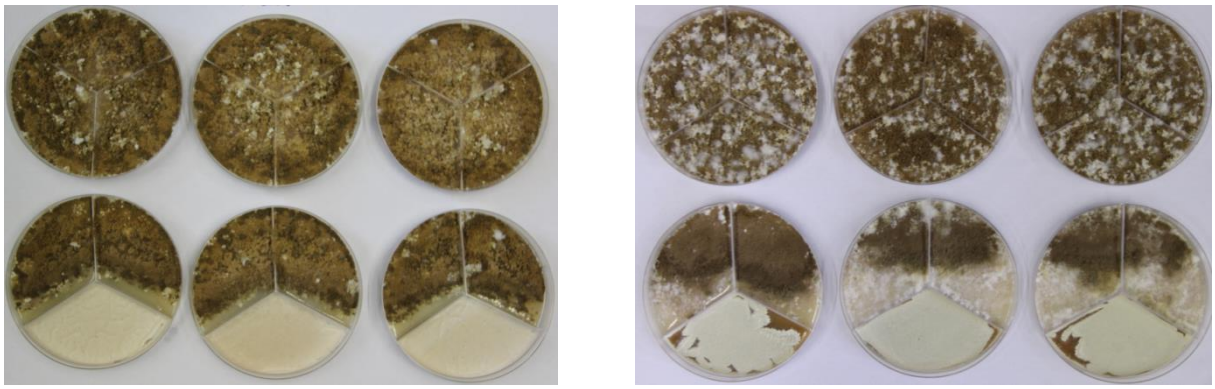

Av29_9 Ae32_2

Figure S4.1: Screening *Streptomyces* symbionts from leaf cutting ants for the production of volatile antifungal compounds that inhibit the growth of *E. weberi* using the three compartment petri dishes to only allow growth inhibition by volatile compounds. Each picture exhibits the bioassay for one Streptomyces symbiont after 10 day of incubation. Three replicates of *E. weberi* control plates (top row) and *E. weberi* co-culture plates (bottom row) are shown. The tested strains were: *Streptomyces* sp. Av25_3, *Streptomyces* sp. Av25_4, *Streptomyces* sp. Av26_2, *Streptomyces* sp. Av26_3, *Streptomyces* sp. Av26_5, *Streptomyces* sp. Av28_1, *Streptomyces* sp. Av28_3, *Streptomyces sp.* Av29_7, *Streptomyces* sp. Av29_9, and *Streptomyces* sp. Ae32_2.

Table S4.1. *Streptomyces* symbionts used to screen for volatiles with antifungal activity against *E. weberi*.

Strains	**Accession number**	**Isolated from**	**Complete growth inhibition of *E. weberi* mediated by VOCs**
Streptomyces sp. Av25_3	FJ490533	*A. volcanus*	No
Streptomyces sp. Av25_4	FJ490534	*A. volcanus*	Yes
Streptomyces sp. Av26_2	FJ490537	*A. volcanus*	No
Streptomyces sp. Av26_3	HM538453	*A. volcanus*	No
Streptomyces sp. Av26_5	FJ490538	*A. volcanus*	No
Streptomyces sp. Av28_1		*A. volcanus*	No
Streptomyces sp. Av28_3	FJ490540	*A. volcanus*	No
Streptomyces sp. Av29_7	FJ490541	*A. volcanus*	No
Streptomyces sp. Av29_9		*A. volcanus*	No
Streptomyces sp. Ae32_2	FJ490544	*A. echinatior*	No

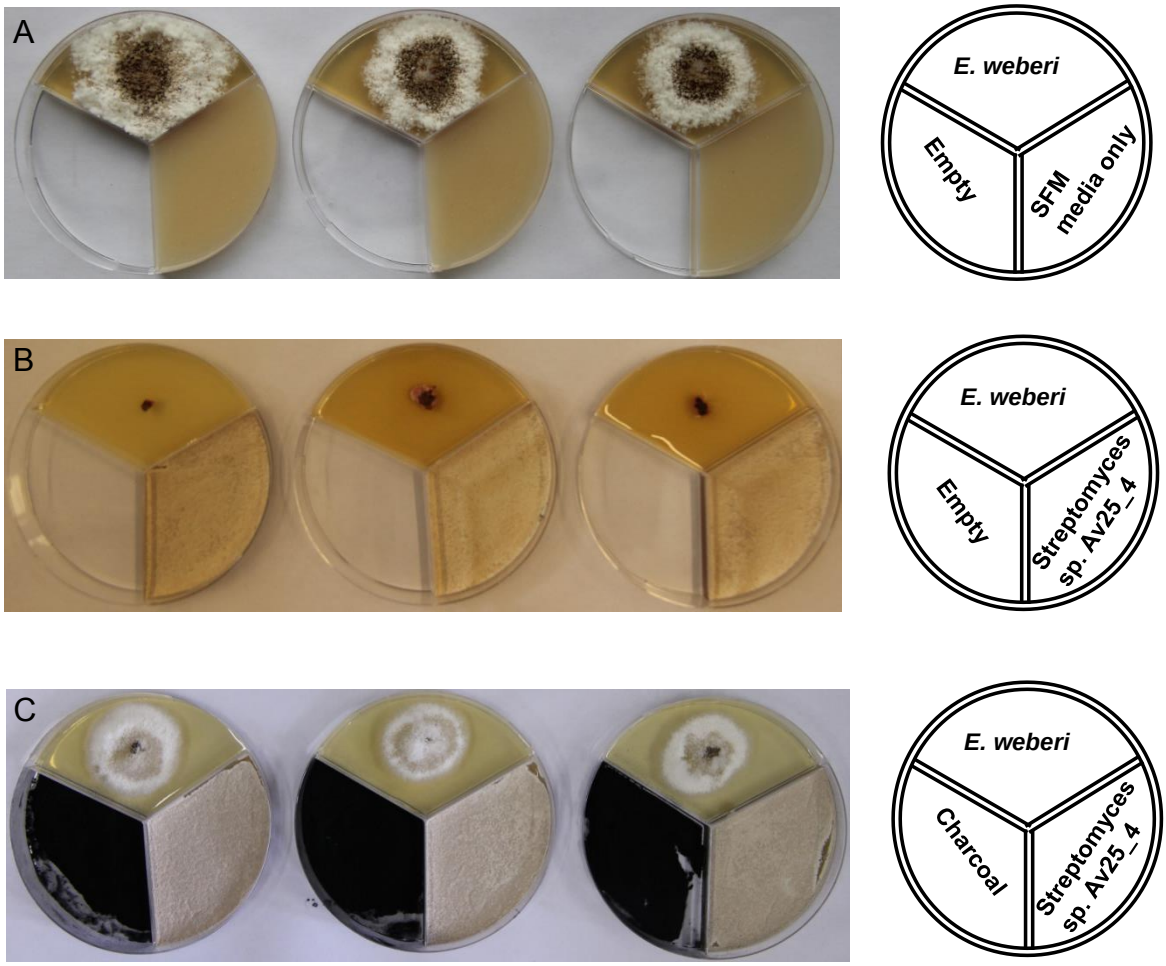

Figure S4.2: Three compartment bioassay to identify volatile compounds inhibiting the growth of *E. weberi*: **A**) agar plates with 4 d grown *E. weberi* in the second compartment, SFM medium in first compartment and empty third compartment. **B**) plates with 4d grown *E. weberi* in second compartment, 7 d grown *Streptomyces* sp. Av25_4 in the first compartment and empty third compartment. **C**) Agar plates with 4 d grown *E. weberi* in second compartment, 7 d grown *Streptomyces* sp. Av25_4 in first compartment and 2 g charcoal in third compartment. The presence of charcoal led to a reduced growth inhibition compared to the growth of the *E. weberi*/*Streptomyces* sp. Av25_4 co-culture.

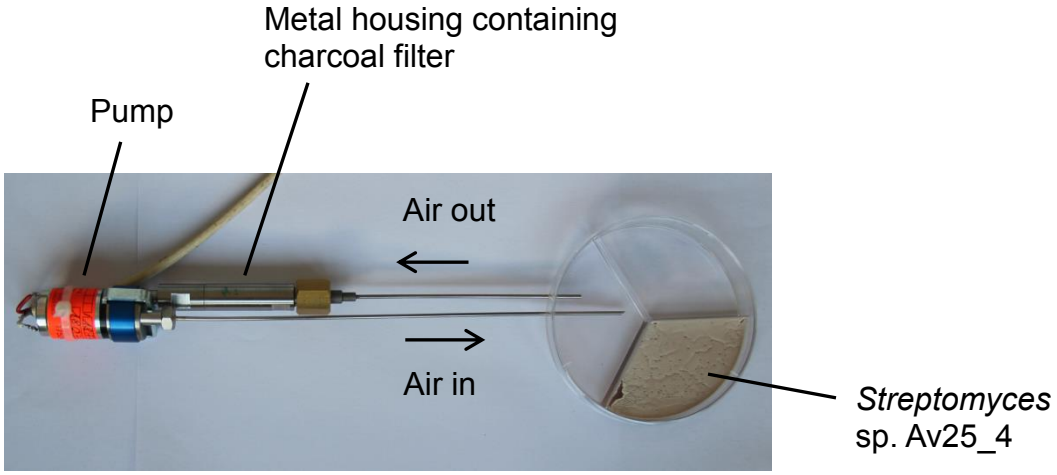

Figure S4.3: Collection of volatiles produced by *Streptomyces* sp. Av25_4 grown on SFM agar by using closed loop stripping.

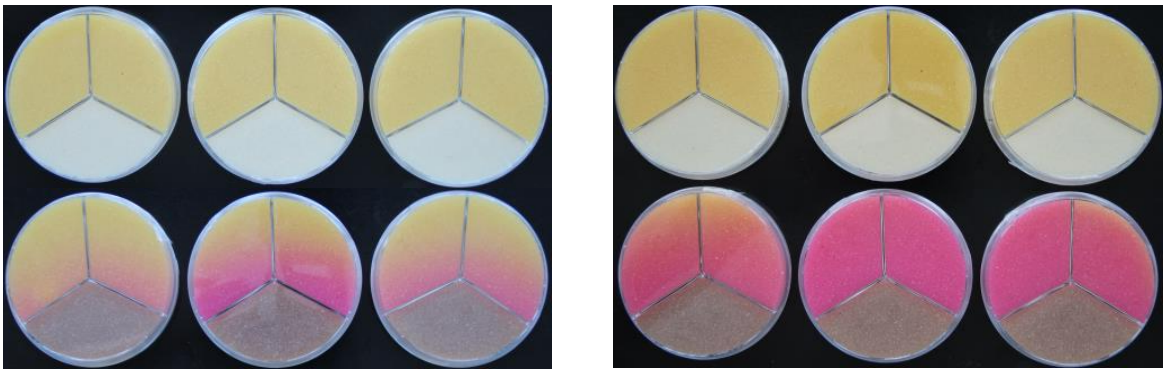

4 day

7 day

10 day

Figure S4.4: pH change revealed by the color change of the pH indicator phenol red (0.002 %) in the second and third compartment filled with SFM medium. Ammonia produced by *Streptomyces* sp. Av25_4 grown on first compartment induced the pH change in compartment 2 and 3. Top row: control plates with SFM agar in the first compartment and 0.002 % phenol red indicator in second and third compartment. Bottom row: plates with *Streptomyces* sp. Av25_4 growing in the first compartment and 0.002 % phenol red indicator in second and third compartment. Pictures were taken at day 4, 7 and 10. All samples and controls were performed in triplicate.

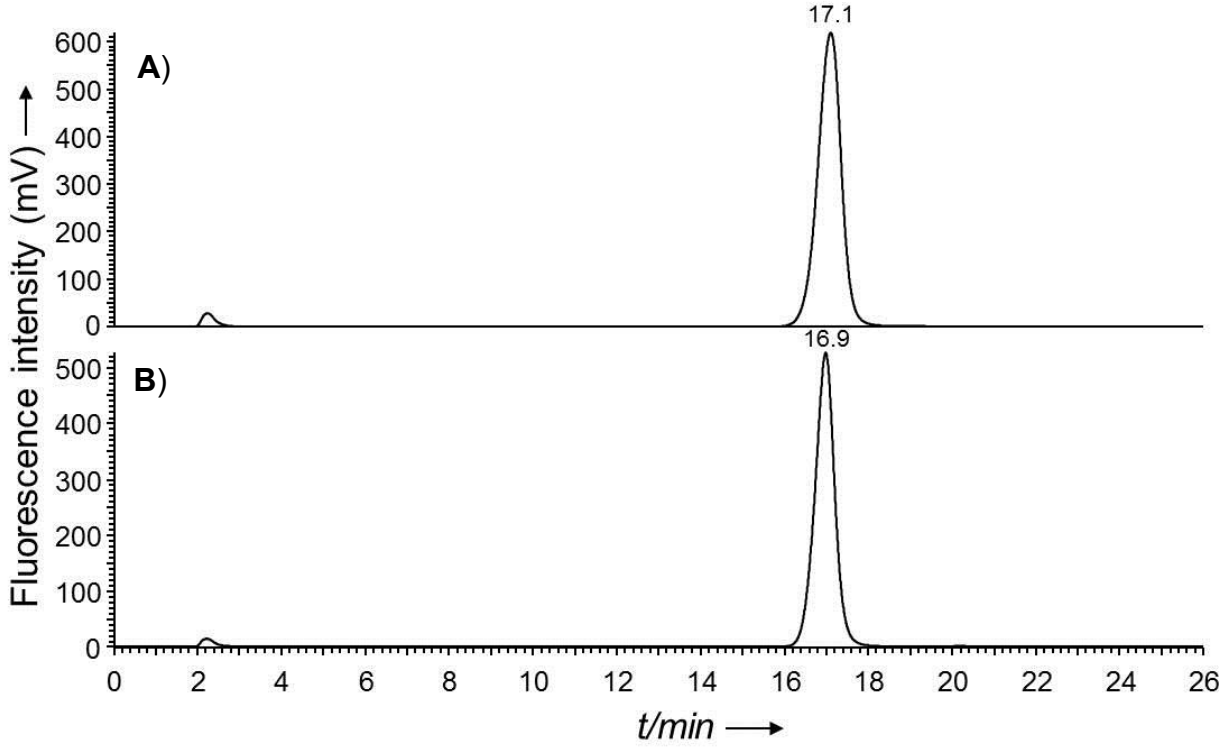

Figure S4.5: Identification of ammonia as pH changing principle using *ortho*-phthal-aldehyde derivatisation. Fluorescence signal measured for the identification of ammonia at excitation and emission wavelength of 360 nm and 420 nm for **A**) 7d grown *Streptomyces* sp. Av25_4 produced headspace volatiles **B**) 5 mM ammonia standard.

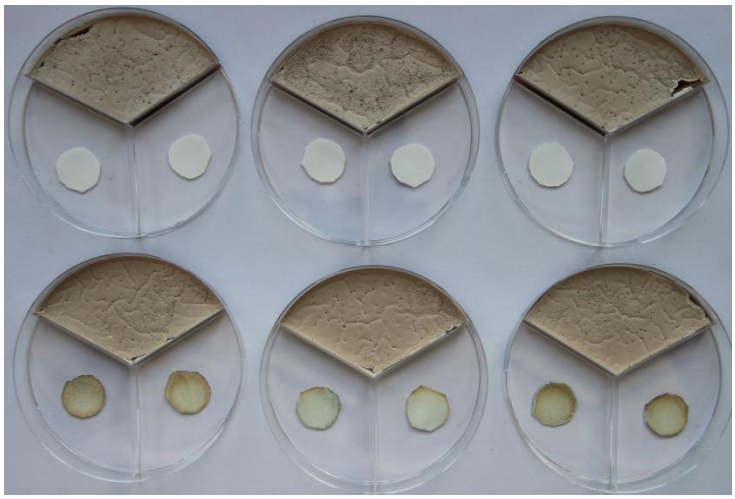

Expected color for
Positive control

Figure S4.6: Screening for HCN production. First row: plate with first compartment containing 10 d grown *Streptomyces* sp. Av25_4 and second and third compartment containing 1.5 cm dried filter paper disk soaked in chloroform (control). Second row: plate with first compartment containing 10 d-grown *Streptomyces* sp. Av25_4 and second and third compartment containing 1.5 cm dried filter paper disk soaked in 5 mg/ml of copper (II) ethyl acetoacetate and 4, 4'- methylenebis-*N*, *N*-dimethylaniline in chloroform.

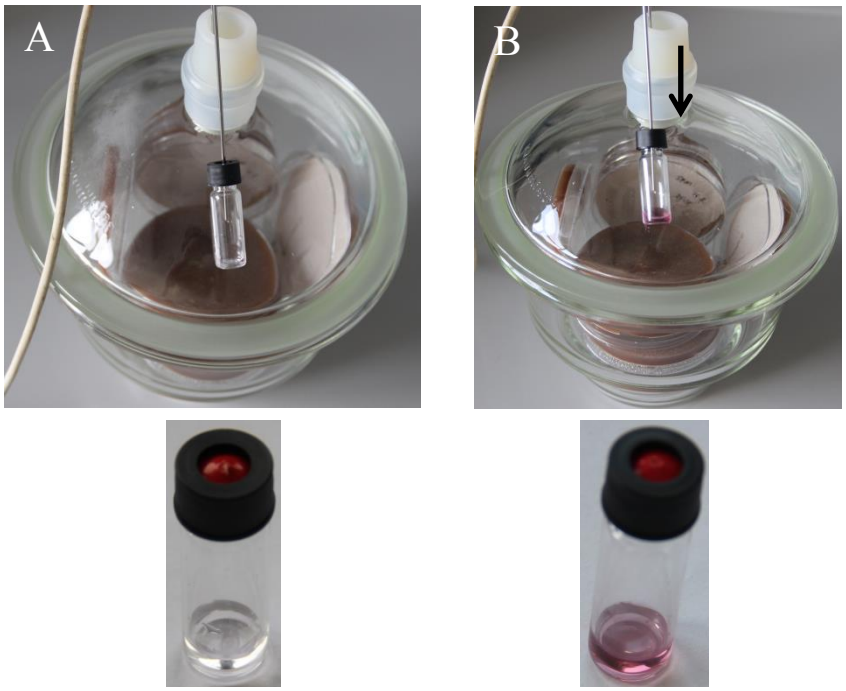

Figure S4.7: Detection of ammonia produced by *Streptomyces* sp. Av25_4 using a closed loop collection pump transferring the volatiles into the vial with the OPA derivatization reagent. **A**) Colorless derivatization solution before exposure to the volatiles in the headspace of the exsiccator filled with *Streptomyces* sp. Av25_4 agar plates. **B**) Reddish color after exposure of the derivatization reagent to the headspace volatiles indicating the formation of ammonia.

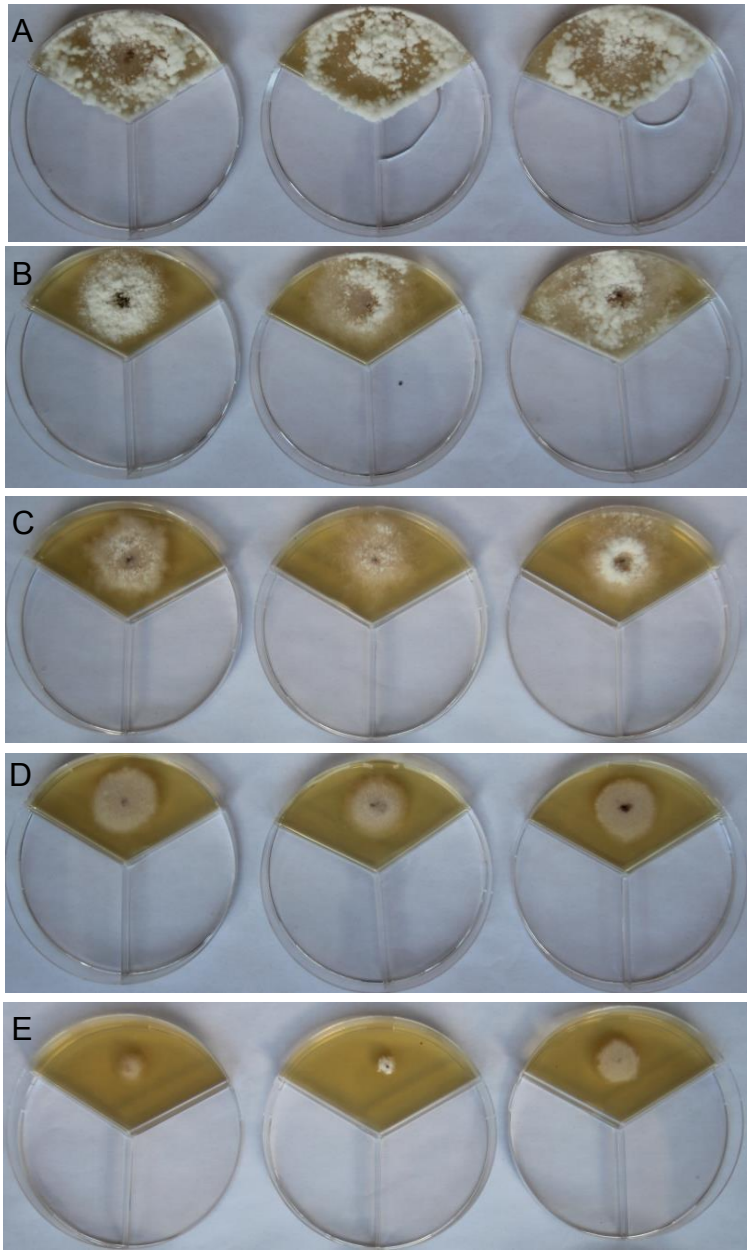

Figure S4.8: Three compartment Petri dish bioassay evaluating the effect of ammonia on *E. weberi* growth. The first compartment contains 4 d grown *E. weberi*, the second compartment contains 5 mL of sterile water or an ammonia solution in water. The third compartment was left empty. **A**) sterile water, **B**) 5 mM ammonia solution, **C**) 7 mM ammonia solution, **D**) 9 mM ammonia solution, and **E**) 11 mM ammonia solution.

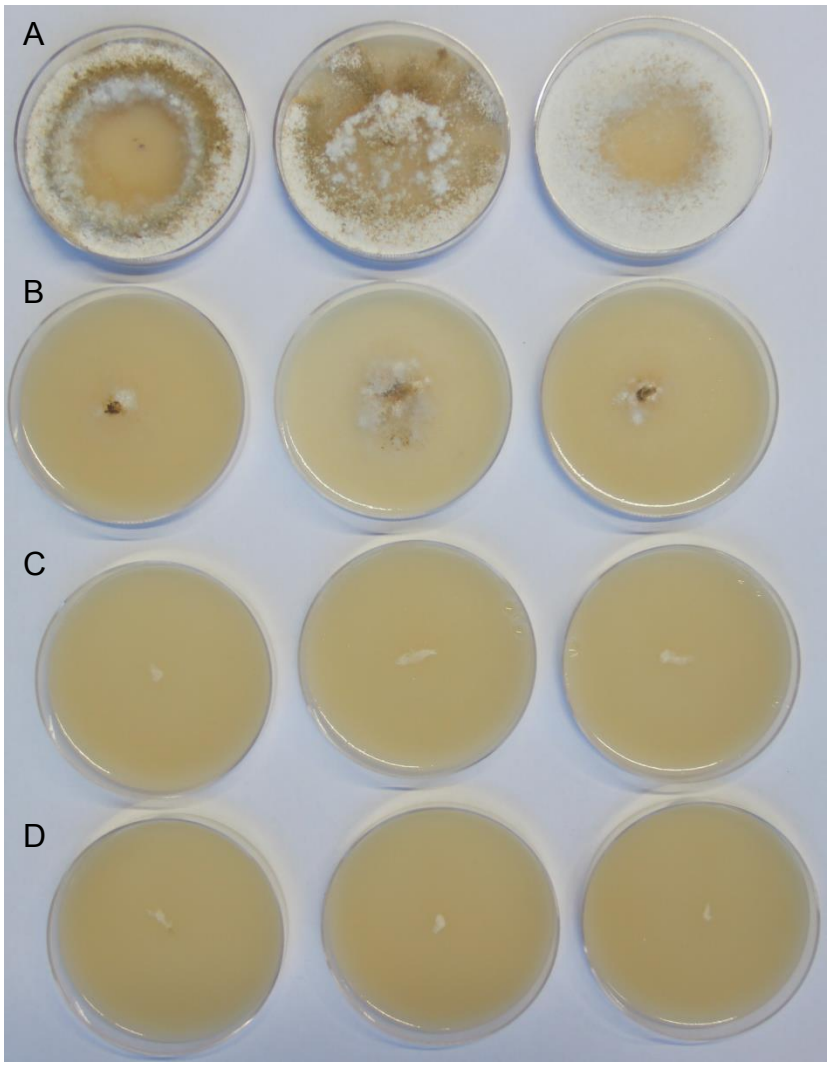

Figure S4.9: Growth of *E. weberi* on SFM agar plates at different pH adjusted with sodium hydroxide. **A**) untreated SFM agar plates (pH 6.2). **B**) SFM agar plates adjusted to pH 7.5. **C**) SFM agar plates adjusted to pH 8.0. **D**) SFM agar plates adjusted to pH 8.5.

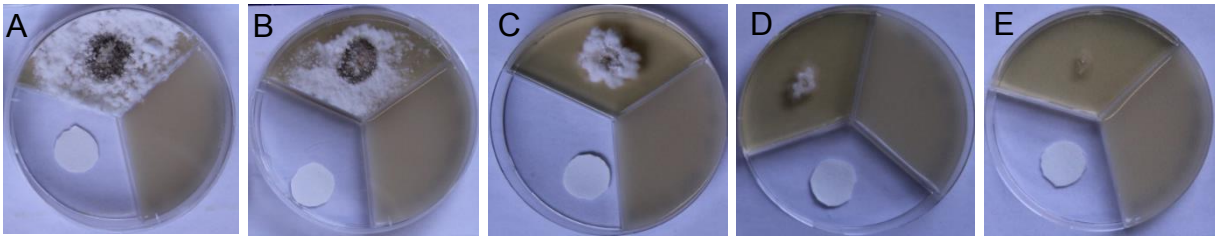

Figure S4.10: Three compartment petri dish bioassay evaluating the effect of benzaldehyde on *E. weberi* growth. The first compartment contains 4d grown *E. weberi*, the second compartment contains SFM medium only. The third compartment contain filter paper (1.5 cm diameter) with: **A**) 20 µL methanol only, **B**) 0.5 µmol benzaldehyde, **C**) 2 µmol benzaldehyde, **D**) 4 µmol benzaldehyde, **E**) 8 µmol benzaldehyde in 20 µL methanol.

Table S4.2: Inhibition of *E. weberi* at different concentrations of benzaldehyde in volatile bioassay (n=3).

Benzaldehyde	Inhibition
8 µmol/plate	89%
4 µmol/plate	73%
2 µmol/plate	66%
1 µmol/plate	0%
0.5 µmol/plate	0%

Table S4.3: Inhibition of *E. weberi* at different concentrations of nonanal in volatile bioassay (n=3).

Nonanal	Inhibition
14.5 µmol/plate	100%
11.6 µmol/plate	94%
7.3 µmol/plate	90%
3.5 µmol/plate	70%
2.3 µmol/plate	55%
1.7 µmol/plate	8%

Supporting Information

Chapter 5: *Pseudomonas* sp. Al1 from *Atta laevigata* leaf-cutting ants produces a variety of antibiotic peptides

Basanta Dhodary[1] and Dieter Spiteller[1]

[1]Chemical Ecology/Biological Chemistry, University of Konstanz, Universitätsstrasse 10, 78457 Konstanz, Germany.

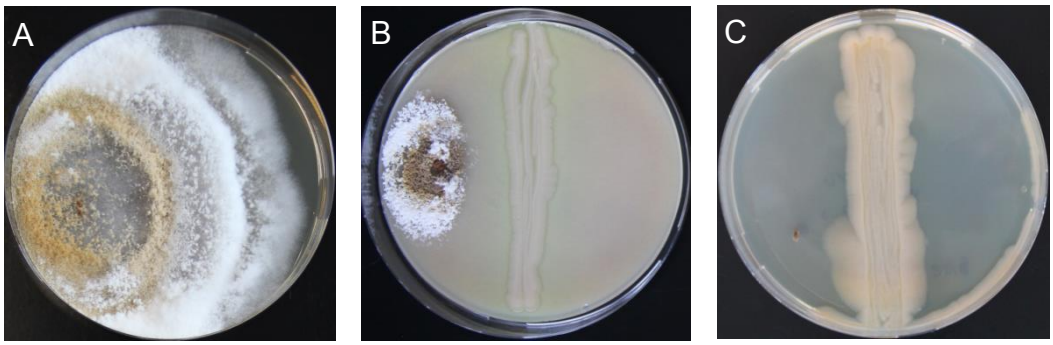

Figure S5.1: Confrontation bioassay of *Pseudomonas* sp. Al1 against *E. weberi* in different agar plate media. *Pseudomonas* sp. Al1 is in the middle of the agar plate and *E. weberi* was inoculated 1.5 cm apart from *Pseudomonas* sp. Al1. **A**) YEME medium: no antifungal effect, **B**) SFM medium: antifungal effect, **C**) PDA medium: antifungal effect.

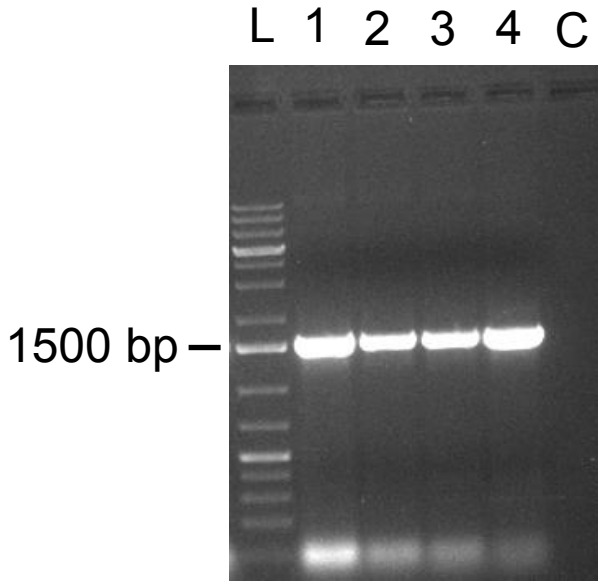

Figure S5.2: Agarose gel electrophoresis of PCR products of the 16S rDNA (ca. 1500 bp) of *Pseudomonas* sp. Al1. L represents 1 kb plus Gene Ruler (ThermoScientific) and C represents a negative control. 1-4 are replicates.

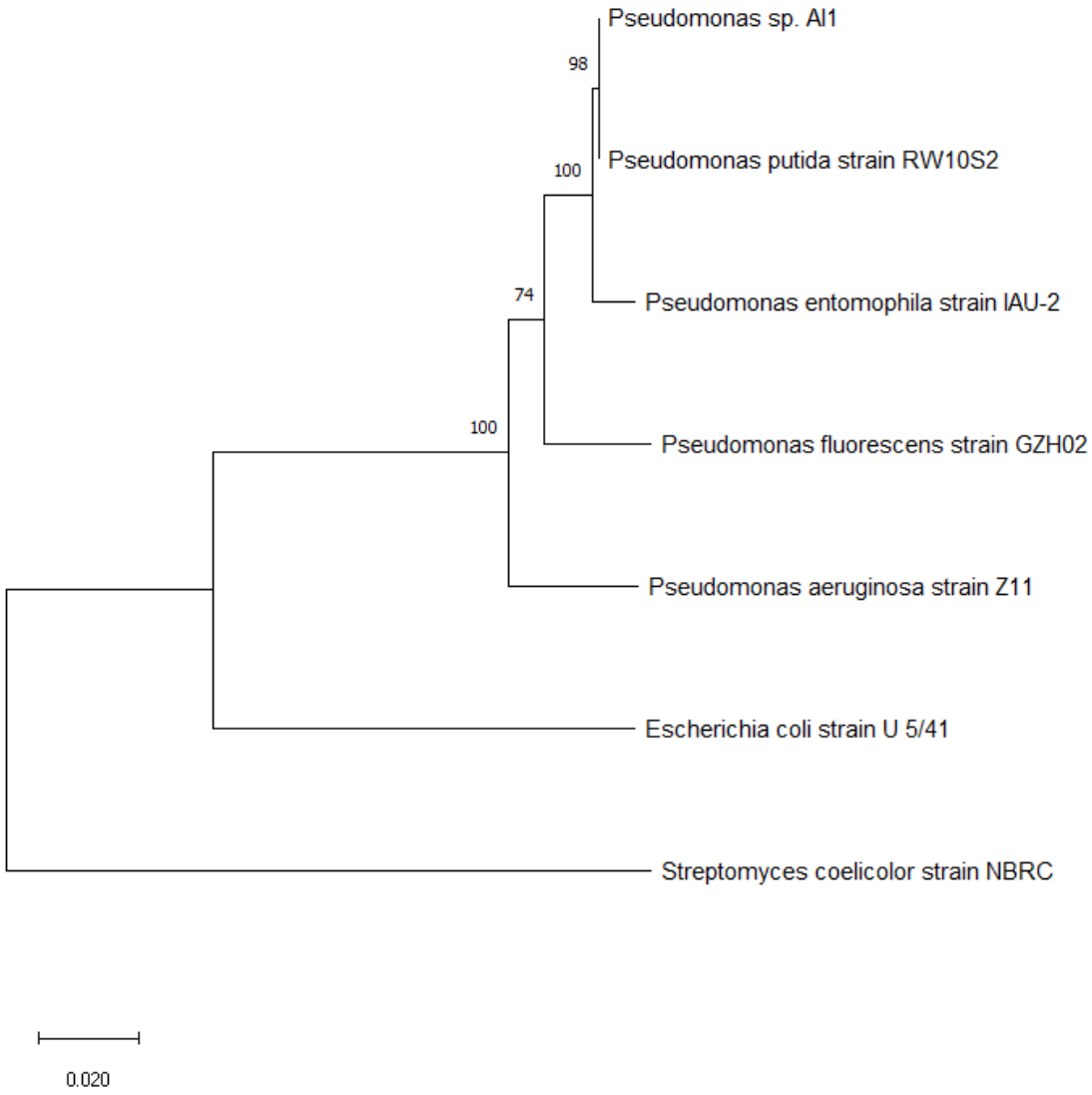

Figure S5.3: Neighbor-joining tree of *Pseudomonas* sp. Al1 compared with other previously identified *Pseudomonas* strains. *E. coli* strain U 5/41 and *Streptomyces coelicolor* strain NBRC represent outgroups. The scale bar represents 0.02 substitutions per nucleotide position. The % of replicate trees in which the associated taxa clustered together in the bootstrap test (500 replicates) is shown next to the branches. The tree is drawn to scale, with branch lengths in the same units as those of the evolutionary distances used to deduce the phylogenetic tree.

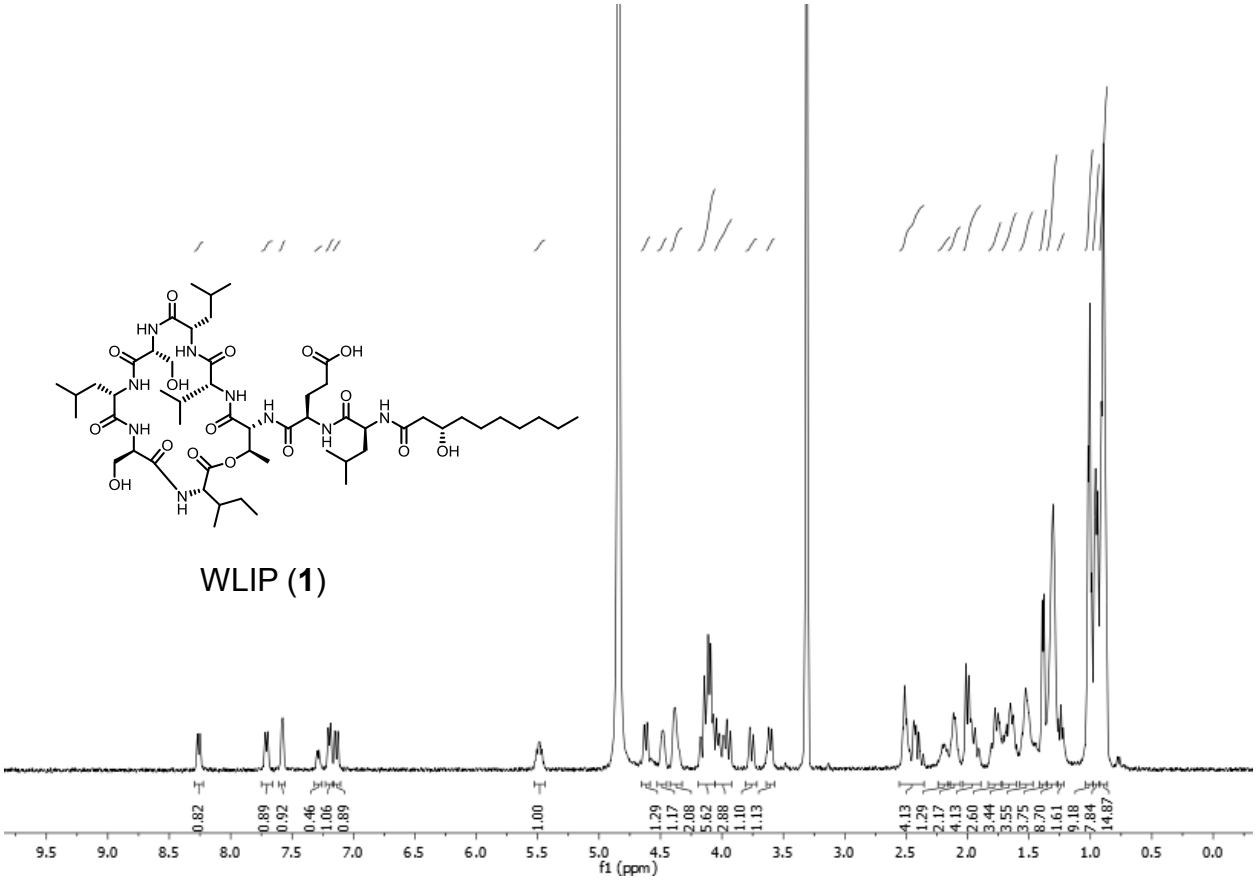

Figure S5.4: ^{1}H-NMR spectrum of WLIP (**1**) measured in MeOH-d4 (400 MHz).

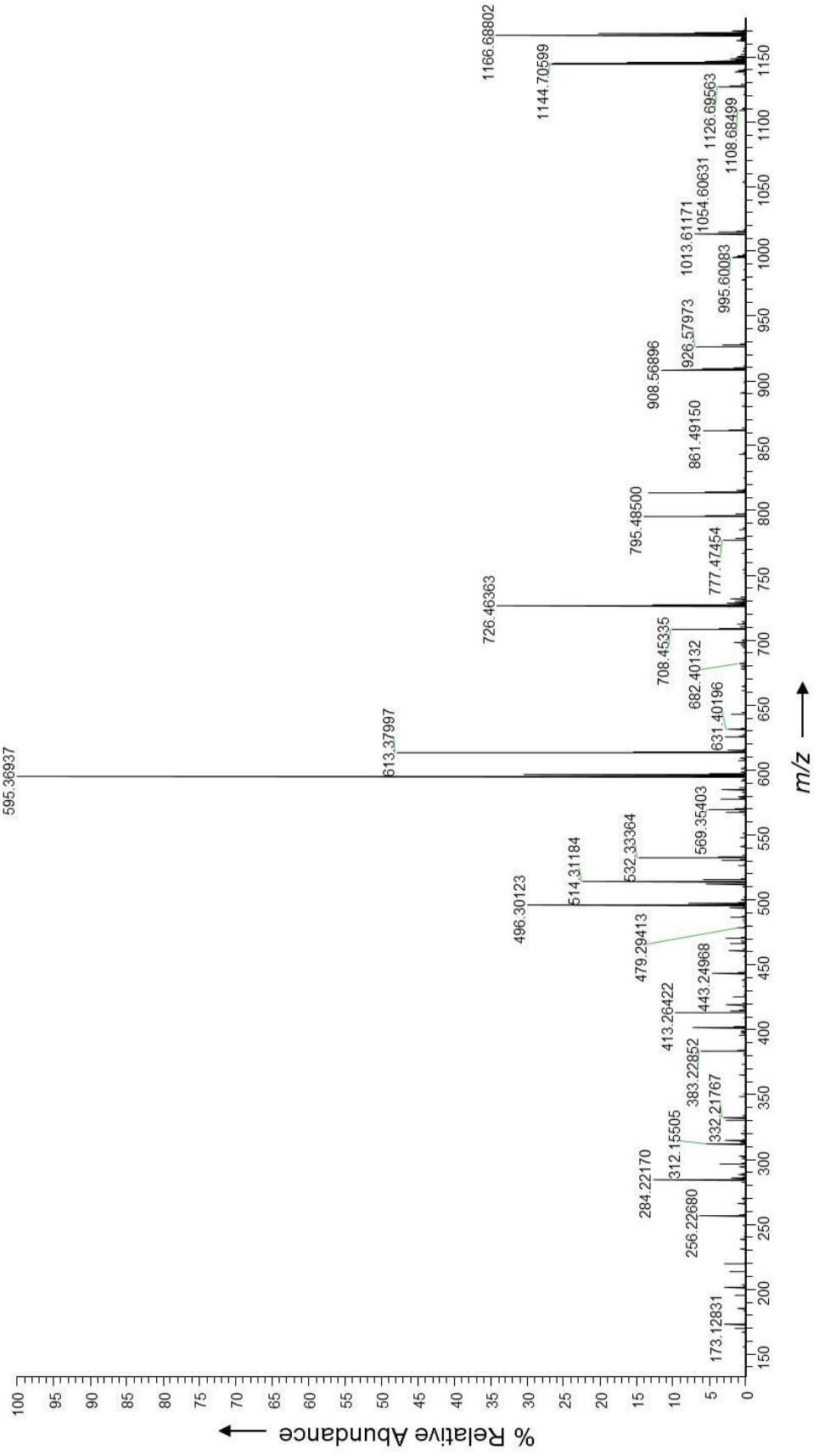

Figure S5.5: HR-ESI-MS/MS spectrum of linearized WLIP (**1a**)

Table S5.1: HR-ESI-MS/MS fragments of the $[M+H]^+$ ion of linearized massetolide H (**2a**)

Cleavage fragment	Calculated *m/z*	Observed *m/z*	Mass error (ppm)
b1	312.2533	312.2531	-0.64
y1	861.4927	861.4921	-0.70
b2	441.29591	441.2959	-0.02
y2	732.4501	732.4493	-1.09
b3	542.3435	542.3434	-0.18
y3	631.4025	631.4025	0.00
b4	641.412	641.4116	-0.62
y4	532.334	532.3338	-0.38
b5	754.496	754.4955	-0.66
y5	419.25	419.2498	-0.48
b6	841.5281	841.5273	-0.95
y6	332.218	332.2177	-0.90
b7	954.61216	954.6121	-0.06
y7	219.1339	219.1338	-0.46
b8	1041.6441	1041.6438	-0.29
y8	132.10191	132.1019	-0.08

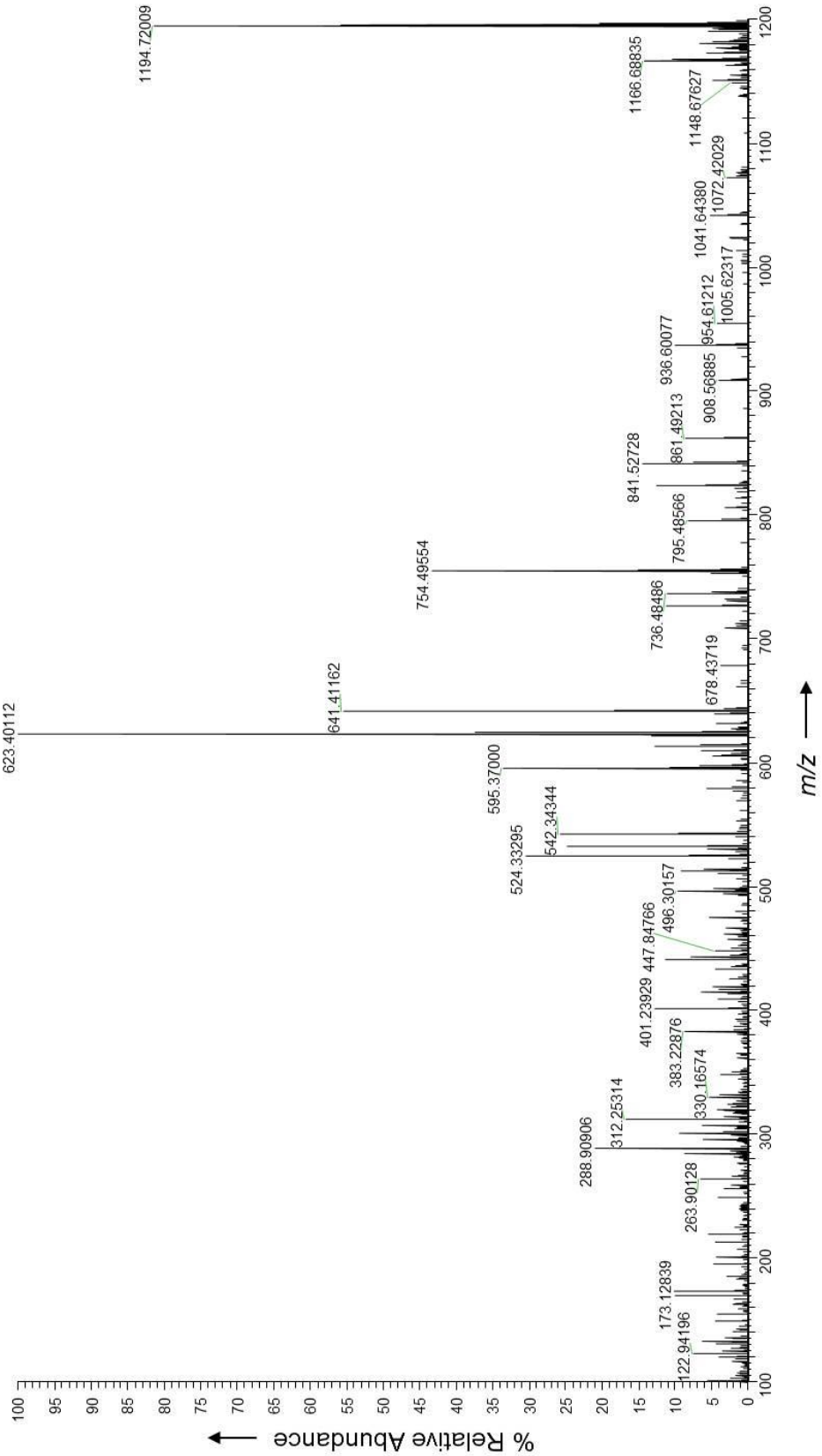

Figure S5.6: HR-ESI-MS/MS spectrum of the $[M+H]^+$ ion of linearized massetolide H (**2a**)

Table S5.2: HR-ESI-MS/MS fragments of the $[M+H]^+$ ion of linearized massetolide E (**3a**)

Cleavage fragment	Calculated *m/z*	Observed *m/z*	Mass error (ppm)
b1	284.222	284.2219	-0.35
y1	847.4771	847.4763	-0.94
b2	413.2646	413.2643	-0.48
y2	718.4345		
b3	514.3122	514.3123	0.19
y3	617.3868	617.3854	-2.27
b4	613.3807	613.3805	-0.33
y4	518.3184	518.3185	0.19
b5	726.4647	726.4641	-0.83
y5	405.2343		
b6	813.4968	813.496	-0.98
y6	318.2023	318.2022	-0.31
b7	926.5808	926.5803	-0.54
y7	205.1182	205.1183	0.49
b8	1013.6128		
y8	118.0862		

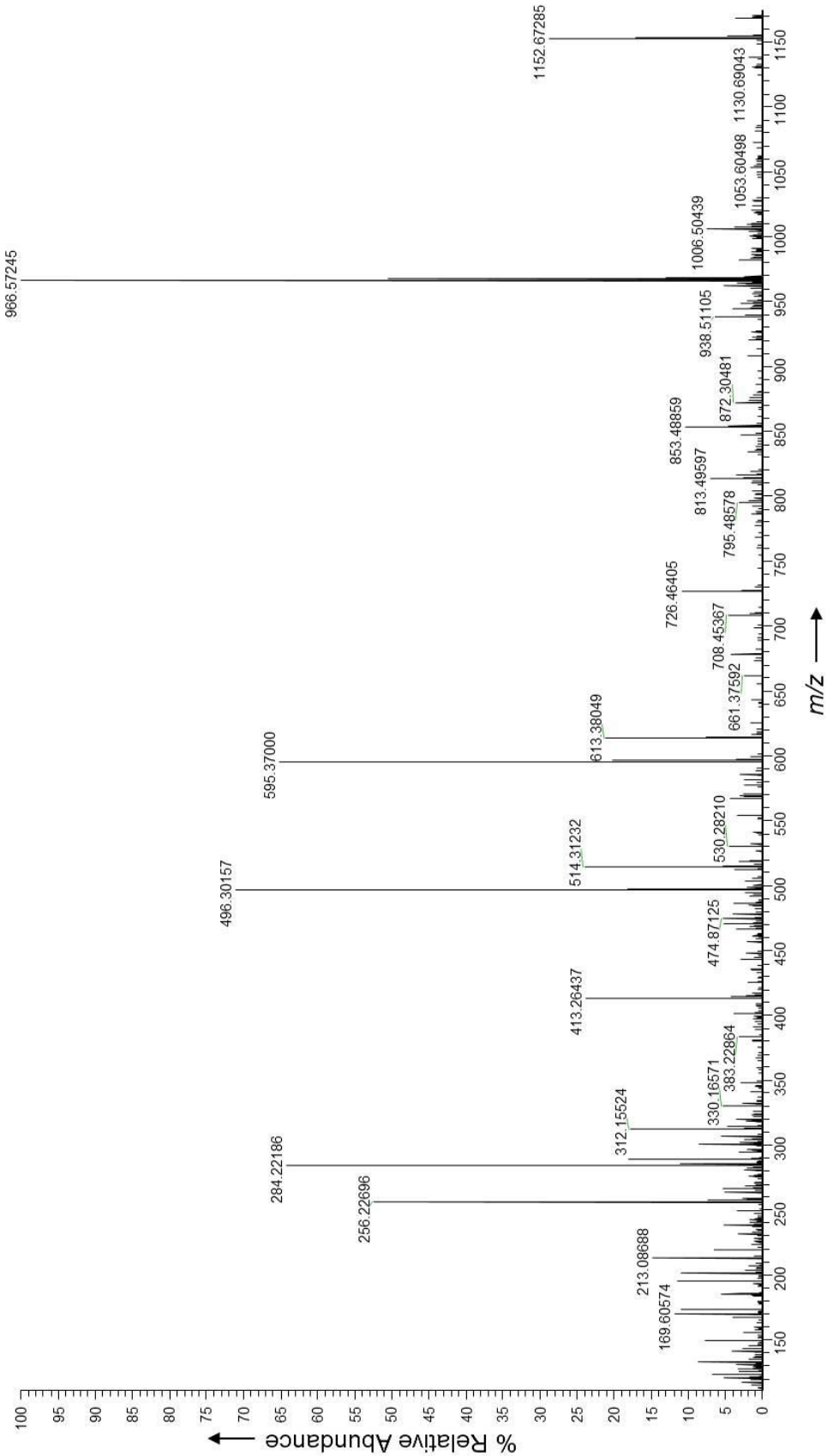

Figure S5.7: HR-ESI-MS/MS spectrum of the $[M+H]^+$ ion of linearized massetolide E (**3a**)

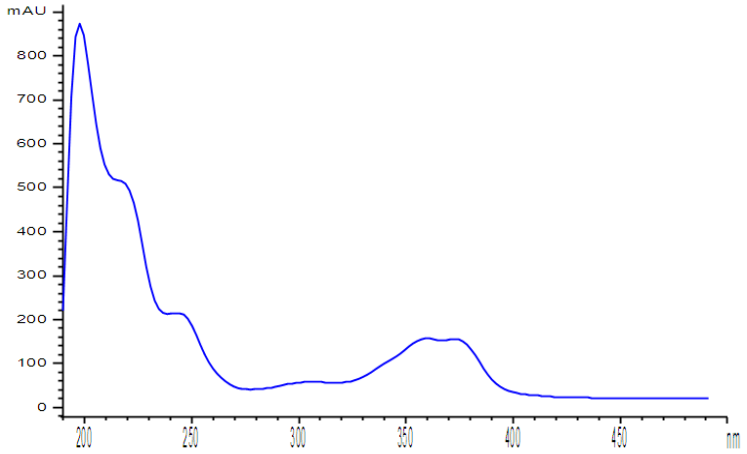

Figure S5.8: UV-VIS spectrum of the pyoverdine Pf 1547 (**4**)

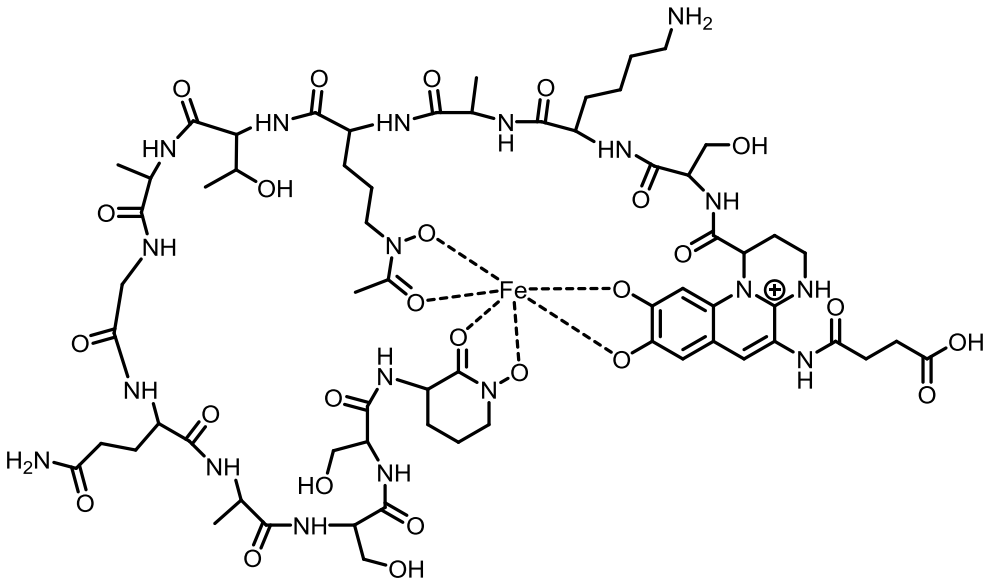

Figure S5.9: Ferri-proverdine Pf 1547 (**4**) complex charge of iron charge of oxygens

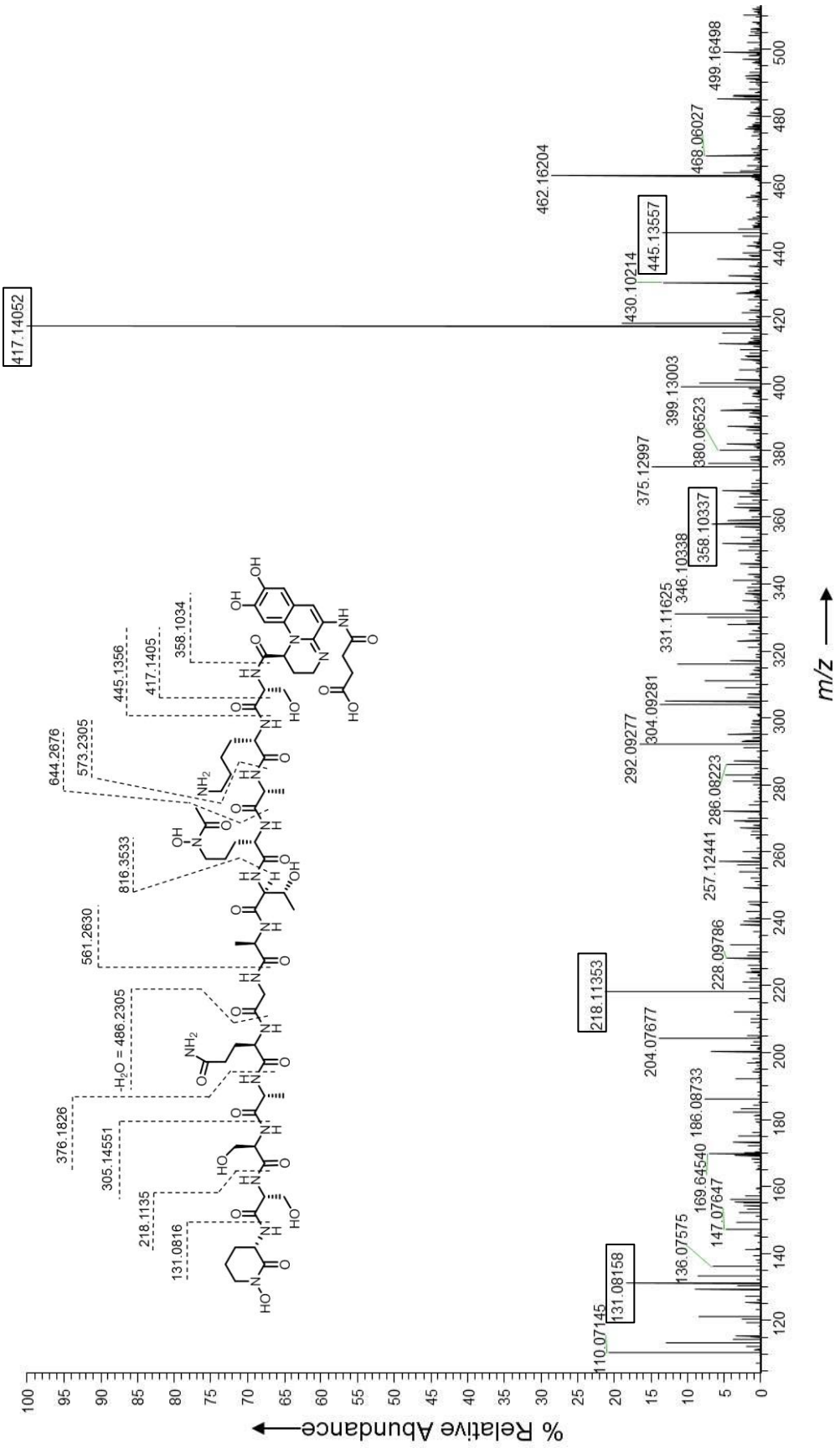

Figure S5.10: HR-ESI-MS/MS spectrum of the $[M+H]^+$ ion of pyoverdine Pf 1547 (**4**) (first part m/z 100-500 Da)

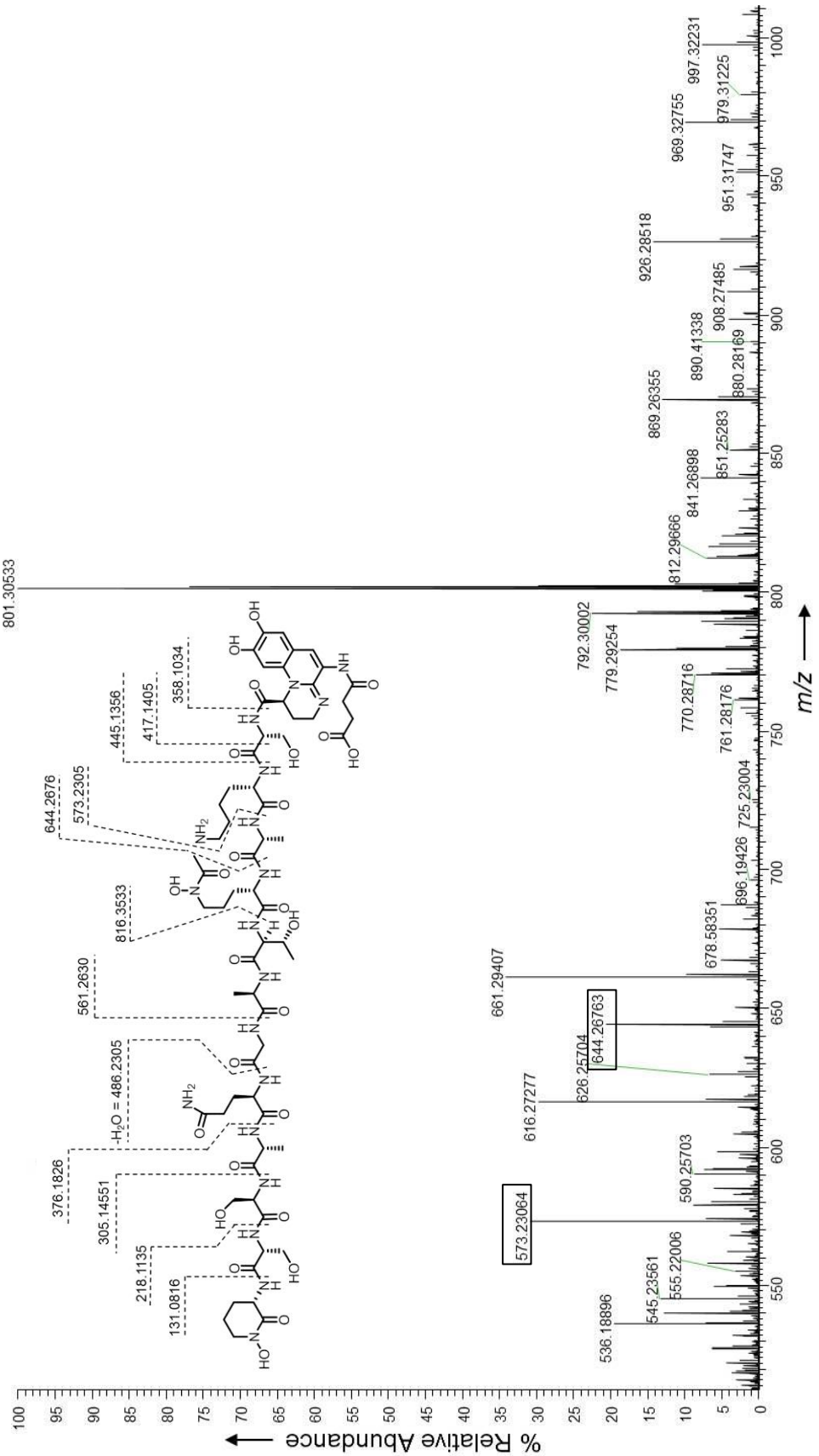

Figure S5.11: HR-ESI-MS/MS spectrum of the $[M+H]^+$ ion of pyoverdine Pf 1547 (**4**) (second part m/z 500-1000 Da)

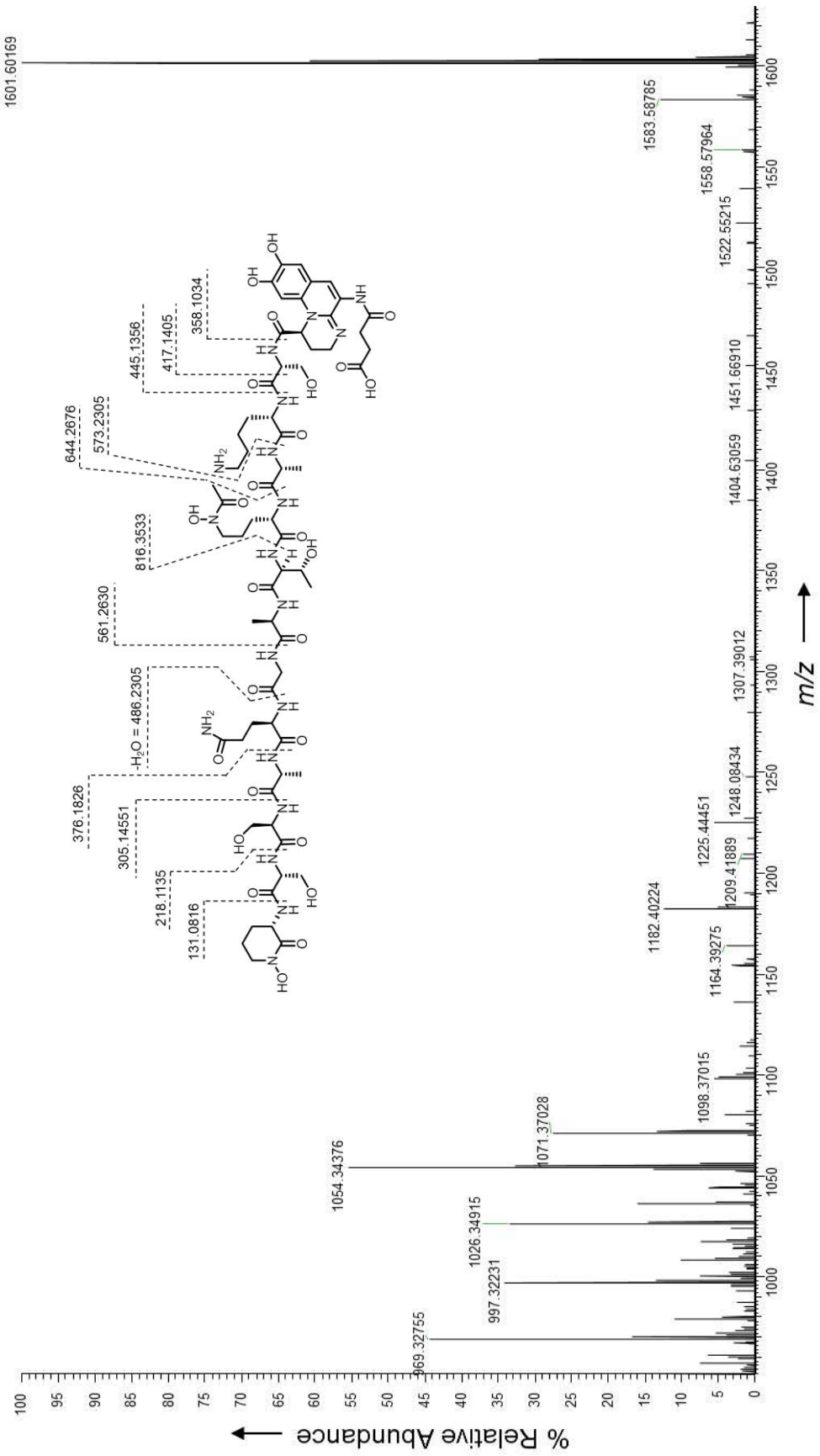

Figure S5.12: HR-ESI-MS/MS spectrum of the $[M+H]^+$ ion of pyoverdine Pf 1547 (**4**) (third part m/z 950-1650 Da)

Table S5.3: Amino acid composition and stereochemistry of pyoverdine Pf 1547 (**4**)

reference	bioinformatic analysis	Marfey analysis
D-Ser	D-Ser	D-Ser
L-Lys	L-Lys	-
D-Ala	D-Ala	D-Ala
L-AcOHOrn	L-AcOHOrn	-
L-Thr	L-Thr	L-Thr
D-Ala	D-Ala	D-Ala
Gly	Gly	Gly
D-Gln	D-Gln	D-Gln
D-Ala	D-Ala	D-Ala
D/L-Ser	L-Ser	L-Ser
D/L-Ser	D-Ser	D-Ser
L-cOHOrn	L-cOHOrn	-

Table S5.4: Marfey derivatization of standard amino acids and amino acids obtained from hydrolysis of pyoverdine Pf 1547 (**4**) (RT: retention time in min)

Amino acid	Reference amino acid RT after Marfey derivatization		Pyoverdine Pf 1547 (4) hydrolysis, amino acid after Marfey derivatization	
	L	D	L	D
Ser	19.81	20.33	19.95	20.53
Ala	27.37	31.32		31.48
Thr	21.19	25.50	21.36	
Gly	24.91	24.91	25.05	25.05
Gln	8.41	9.1		9.11

Table S5.5: Pyoverdine Pf 1547 gene cluster details identified in *Pseudomonas* sp. Al1 by genome mining

Locus tag	Coordinates	Size (nt)	Putative protein function
Alp6_235	236315 - 249268	12954	Putative NRPS: chromophore (4 modules)
Alp7_210	263119 - 278601	15483	Putative NRPS: peptide chain (4 modules)
Alp7_211	278603 - 289606	11004	Putative NRPS: peptide chain (3 modules)
Alp7_212	289606 - 301998	12393	Putative NRPS: peptide chain (3 modules)
Alp7_213	302011 - 310608	8598	Putative NRPS: peptide chain (2 modules)